



**HAL**  
open science

# Molecular mechanisms specifying Satb2/Ctip2-positive neurons in layer V of mouse somatosensory cortex and characterization of their morphology, connectivity, molecular profile and electrophysiological properties

Kawssar Harb

► **To cite this version:**

Kawssar Harb. Molecular mechanisms specifying Satb2/Ctip2-positive neurons in layer V of mouse somatosensory cortex and characterization of their morphology, connectivity, molecular profile and electrophysiological properties. Agricultural sciences. Université Nice Sophia Antipolis, 2014. English. NNT : 2014NICE4070 . tel-01387681

**HAL Id: tel-01387681**

**<https://theses.hal.science/tel-01387681>**

Submitted on 26 Oct 2016

**HAL** is a multi-disciplinary open access archive for the deposit and dissemination of scientific research documents, whether they are published or not. The documents may come from teaching and research institutions in France or abroad, or from public or private research centers.

L'archive ouverte pluridisciplinaire **HAL**, est destinée au dépôt et à la diffusion de documents scientifiques de niveau recherche, publiés ou non, émanant des établissements d'enseignement et de recherche français ou étrangers, des laboratoires publics ou privés.

Université de Nice-Sophia Antipolis  
Ecole doctorale SVS ED85  
Sciences-Vie-Santé

## THESE DE DOCTORAT

Pour obtenir le grade de

Docteur en Biologie de l'université de Nice-Sophia Antipolis

Spécialité: Interactions moléculaires et cellulaires

Soutenue par: Kawssar HARB

**Mécanismes moléculaires spécifiant les neurones positifs Satb2/Ctip2  
dans la couche V du cortex somatosensoriel chez la souris et  
caractérisation de leur morphologie, connectivité, profil moléculaire  
et propriétés électrophysiologiques**

**Molecular mechanisms specifying Satb2/Ctip2-positive neurons in  
layer V of mouse somatosensory cortex and characterization of their  
morphology, connectivity, molecular profile and electrophysiological  
properties**

Directrice de thèse: Michèle STUDER

**Préparée à l'iBV  
Soutenue le 17 Octobre 2014**

Jury:

Rapporteurs: Marta NIETO  
Fanny MANN

Directrice de thèse: Michèle STUDER

Président du jury: Thomas LAMONERIE

*I dedicate this thesis to  
my family and my fiancé, Ali  
for their support and endless love.*

*I love you all.*

# Acknowledgments

---

First of all I would like to thank my Ph.D supervisors Michèle Studer and Christian Alfano, for there guidance, support and encouragement during the four years of my Ph.D. Michèle, thank you for offering me the opportunity to work on this project, for all our fruitful discussions and advice during the four years.

Christian, I have enjoyed our many valuable discussions during these four years and I have learned a lot from you. I appreciate all your contributions of time and ideas to make my Ph.D experience productive.

I would like to thank all members of Studer group who helped or contributed to this work especially Elia Magrinelli and Mariel Pietri. The group has been also a source of friendship as well as good advice and collaboration. For the good times and fun we had, I'm especially thankful for Maria anna Di Bonito, Anna lisa Romano, Nadia Elganfoud, Audrey Touzot, josephine parisot, Michele Bertachi, Christian Alfano, Elia Magrinelli and Mariel Pietri.

I acknowledge Denis Jabaudon lab, and Laura Frangeul for the retrograde labeling experiments they provided at Geneva. For the morphological analysis, I thank Xavier Descombes, Franck Grammont, Nikita lukianets and Alexis Zubiolo. And I'm also thankful to the great help and facilities provided by Guillaume Sandoz lab and Céline Nicolas for the electrophysiological experiments.

I would like to thank all people who supplied me with essential antibodies, plasmids and brains: Silvia Arber from Basel University for the Er81 Antibody, Novitch Benett Lab, California, for the Bhlhb5 Antibody, Hsiao Huei Chen, Ottawa, for the LMO4 shRNA, Tao Sun from Cornell University for the P0 and P7 *LMO4 CKO* brains, Jane Visvader, Parkville, for the LMO4 Antibody and last but not least for Paola Arlotta from Harvard for the cdk5 IRES GFP plasmid.

Special thanks goes to Constance Hammond, and Edouard Pearlstein from Inmed Marseille for receiving me for a 2 months training on electrophysiology, whole cell patch clamp, which was very useful and important to get this work done.

I gratefully acknowledge the funding source that made my Ph.D. work possible. I was funded by the Lebanese CNRS for my first three years and by AFM for the fourth year.

During the last four years stay in Nice, my time was made enjoyable in large part due to the many friends and groups that I have met and became a part of my life, Hawraa, Habib, Janwa, Maha, Georges, Moustapha and Janah.

I am thankful to my uncle Hussein Harb for being the source of inspiration and enthusiasm since my childhood. I am grateful to my sister Hanan, who never stopped fulfilling my life with love, care and happiness, to her husband Moussa, to my sisters, brother and my parents in law. Thank you.

I am gratefully thankful to my fiancé Ali that was hand by hand with me during all my studies, and was always there for me in all hard and good situations, I am thankful to all your love, care and support. Without you, these 4 years would not have been possible.

I especially thank my mom and dad. My hard-working parents have sacrificed their lives for my sisters, brother and myself and provided unconditional love and care. I love them so much, and I would not have made it this far without their love, support and encouragement.

# *Abstract*

---

The mammalian cerebral cortex is subdivided into several tangential domains called functional areas, which are deputed to the elaboration of motor and sensory inputs, the selection and implementation of motor plans, and many other higher cognitive functions. Each functional area is constituted by six layers of projection glutamatergic neurons (PNs) with different morphologies, connectivity and molecular codes.

Several transcription factors specifying different subclasses of neurons, such as callosal neurons (CPN, which target the contralateral neocortical hemisphere) and subcerebral projection neurons (SCPN, e.g. corticopontine and corticospinal neurons) have been identified so far. *Fezf2* and *Ctip2* promote the specification of subcerebral PNs, whereas *Satb2* promotes callosal identity, mainly by repressing *Ctip2* transcription through the recruitment of the NURD complex to the *Ctip2* locus. However, little is known about the mechanisms specifying their features in a time- and areal-specific manner.

In this study I show that a population of cells co-expressing molecular markers of CPN and SCPN neurons, such as *Satb2* and *Ctip2*, becomes first specified in layers V and VI of rostro-medial mouse neocortex at perinatal stages and progressively increases between P0 and P21 in somatosensory areas. However, the mechanisms allowing co-expression of these two factors, as well as function and connectivity of *Satb2/Ctip2* co-expressing cells are still unknown. I found that in neocortices lacking COUP-TFI, a transcription factor modulating neocortical areal and cell-type specification, the number of *Satb2/Ctip2* co-expressing cells increases abnormally in layer V of the prospective primary somatosensory area. I demonstrated that LMO4 ectopic and premature expression of LMO4 in COUP-TFI mutant transgenic line de-represses *Ctip2* in *Satb2* positive cells by disturbing the assembly of the NURD complex at *Ctip2* locus. Moreover, by the use of a transgenic line expressing GFP in layer V neurons and of vital dyes, I analysed morphology, connectivity and electrophysiological activity of this hybrid class of neurons at postnatal stages of development. Together, my results have unravelled a novel molecular process specifying a new PN sub-population within layer V.

In conclusion, my study demonstrates that the co-expression of CPN and SCPN neuronal markers does not only characterize early phases of neuronal specification, but also defines neuronal subpopulation with different areal-specific features and developmental timing in the mammalian neocortex.

# Résumé

---

Le cortex cérébral des mammifères est divisé en plusieurs domaines tangentiels appelés des aires fonctionnelles, qui sont dévolues à l'élaboration des afférences motrice et sensorielles, la sélection et la mise en œuvre des plans moteurs, et d'autres fonctions cognitives supérieures. Chaque aire fonctionnelle est constituée par six couches de neurones de projections (PN) glutaminergiques avec différentes morphologies, connectivité et codes moléculaires.

Plusieurs facteurs de transcription spécifiant différentes sous-classes de neurones, comme les neurones calleux (CPN, qui ciblent l'hémisphère controlatéral du néocortex) et les neurones de projection sous-cérébraux (SCPN, par exemple les neurones corticopontines et corticospinaux) ont été identifiés à ce jour. *Fezf2* et *Ctip2* induisent la spécification des neurones sous-cérébraux, alors que *Satb2* induit l'identité calleuse, essentiellement en réprimant la transcription de *Ctip2* par le recrutement du complexe NURD au locus de *Ctip2*. Cependant, très peu est connu sur les mécanismes précisant leurs caractéristiques de manière temporelle et régionale.

Dans cette étude, je montre que la population de cellules co-exprimant des marqueurs moléculaires des neurones calleux et sous-cérébraux, comme *Satb2* et *Ctip2*, sont d'abord spécifiés dans les couches V et VI du néocortex rostro-médiale chez la souris au stades périnataux, et augmente progressivement entre P0 et P21 dans l'aire somatosensorielle. Cependant, les mécanismes qui permettent la co-expression de ces deux facteurs, ainsi que la fonction et la connectivité des cellules co-exprimant *satb2/Ctip2* sont encore inconnus. J'ai trouvé qu'en absence de COUP-TFI, un facteur de transcription modulant la spécification des aires fonctionnelles et des sous-types des cellules néocorticales, le nombre de cellules co-exprimant *Satb2* et *Ctip2* augmente fortement dans la couche V de l'aire somatosensorielle primaire éventuelle. J'ai démontré que l'expression ectopique et prématurée de LMO4 dans la lignée transgénique mutante pour COUP-TFI, de-réprime *Ctip2* dans les cellules *Satb2* positives en perturbant l'assemblage du complexe NURD au locus de *Ctip2*. En plus, par l'utilisation d'une lignée transgénique exprimant la GFP dans les neurones de la couche V et de colorants vitaux, j'ai analysé la morphologie, la connectivité et l'activité électrophysiologique de cette classe hybride de neurones à des stades de développement postnataux. Ensemble, mes résultats ont montré un nouveau mécanisme moléculaire spécifiant une nouvelle sous-population neuronale dans la couche V du cerveau.

En conclusion, mon étude a montré que la co-expression de marqueurs neuronaux calleux et sous-cérébraux ne caractérise pas seulement les premières phases de spécification neuronale, mais définit également une sous-population neuronale avec des caractéristiques régionales particulières et un calendrier de développement spécifique dans le néocortex cérébral.

# Table of Contents

---

## Introduction

<b>I. THE MAMMALIAN NEOCORTEX: ORIGIN AND FUNCTION.....</b>	<b>17</b>
<b>II. THE NEOCORTEX: GENERAL ORGANIZATION.....</b>	<b>17</b>
A. TANGENTIAL ORGANIZATION.....	17
B. RADIAL ORGANIZATION.....	19
C. THE FUNCTIONAL RELATIONSHIP BETWEEN CORTICAL AREAS AND THE THALAMUS.....	19
<b>III. NEOCORTICAL NEUROGENESIS AND RADIAL MIGRATION .....</b>	<b>20</b>
A. CELLULAR ORGANIZATION OF THE NEOCORTEX.....	20
B. PROGENITORS DIVERSITY AND CORTICOGENESIS .....	22
C. NEOCORTICAL "GLIA GUIDED" RADIAL MIGRATION.....	24
D. PROGENITOR LINEAGE COMMITMENT .....	26
<b>IV. GENETIC REGULATION OF NEOCORTICAL AREA MAPPING .....</b>	<b>28</b>
A. MORPHOGENS AND PATTERNING CENTERS.....	30
1. <i>Anterior neural ridge: Fgfs</i> .....	30
2. <i>Cortical hem: Bmps and Wnts</i> .....	32
3. <i>Antihem: Sfrp2, EGFs, Tgfa, Fgf15 and Fgf7</i> .....	32
4. <i>Ventral telencephalon: Shh</i> .....	33
B. GRADED EXPRESSION OF TRANSCRIPTION FACTORS.....	33
1. <i>Sp8</i> .....	34
2. <i>Pax6</i> .....	36
3. <i>Emx2</i> .....	37
4. <i>COUP-TFI</i> .....	37
<b>V. NEOCORTICAL PROJECTION NEURON SPECIFICATION AND DIVERSITY .....</b>	<b>39</b>
A. MAJOR SUBTYPES OF PROJECTION NEURONS WITHIN THE NEOCORTEX .....	40
1. <i>Callosal Projection Neurons (CPN)</i> .....	40
2. <i>Corticofugal Projection neurons (CFuPNs)</i> .....	45
a) Subplate neurons (SP).....	45
b) Corticothalamic neurons (CThPNs).....	45
c) Subcerebral projection neurons (SCPNs).....	46
3. <i>Corticostriatal projection neurons (CStrPN)</i> .....	48
B. NEOCORTICAL PROJECTION NEURON SPECIFICATION.....	49
1. <i>Corticofugal fate determination</i> .....	49
a) SCPN fate specification.....	49
(1) <i>Fezf2</i> .....	51
(2) <i>Ctip2</i> .....	53
(3) <i>Sox5</i> .....	54
(4) <i>Otx1</i> : A gene controlling the refinement and pruning of SCPN.....	54
b) Corticothalamic PN fate specification: .....	55
(1) <i>Fezf2, Ctip2 and Sox5</i> .....	55
(2) <i>Tbr1</i> .....	56
c) Callosal PN fate specification: .....	56
(1) <i>Satb2</i> .....	57
(2) Genes identifying distinct CPN subpopulations.....	60
(3) Genes involved in upper layer specification: <i>Brn</i> and <i>Cux</i> .....	62
<b>VI. NEOCORTICAL PROJECTION NEURON: CALLOSAL VERSUS SUBCEREBRAL AXON GUIDANCE CONTROL.....</b>	<b>62</b>
A. CALLOSAL PROJECTION NEURONS.....	62
B. SUBCEREBRAL PROJECTION NEURONS; AN EXAMPLE OF CSMN.....	66

<b>VII. TRANSCRIPTIONAL REGULATORS INVOLVED IN AREALIZATION AND CORTICAL SUBTYPE SPECIFICATION.....</b>	<b>68</b>
A. BASIC-LOOP-HELIX DOMAIN CONTAINING, CLASS B5 (BHLHB5).....	68
B. TBR1.....	69
C. LIM DOMAIN ONLY 4 (LMO4).....	70
1. <i>LMO4 structure and protein interactions</i> .....	70
2. <i>LMO4 in the developing and postnatal cortex</i> .....	74
a) LMO4 in early brain development.....	74
b) LMO4 has a dynamic and region-specific expression in the mouse developing cortex.....	74
c) LMO4 is a mediator of calcium activity.....	75
d) LMO4 in arealization.....	75
e) LMO4 in neuronal subtype specification.....	76
D. COUP-TFI.....	78
1. <i>COUP-TFI is involved in neurogenesis, gliogenesis and cell cycle control</i> .....	78
2. <i>COUP-TFI is required for the formation of commissural projections in the forebrain by regulating axonal growth</i> .....	80
3. <i>COUP-TFI promotes radial migration and proper morphology of callosal projection neurons by repressing Rnd2 expression</i> .....	81
4. <i>COUP-TFI regulates the balance between frontal/motor and sensory areas</i> .....	82
5. <i>Area-specific temporal control of corticospinal motor neuron differentiation</i> .....	83
<b>VIII. AIM OF THIS WORK.....</b>	<b>87</b>

## Materials and Methods

<b>I. MUTANT MICE AND GENOTYPING.....</b>	<b>90</b>
A. COUP-TFI FL/FL <sup>EMX1-CRE</sup> MOUSE LINE.....	90
B. THY1-EYFP LINE H:.....	93
<b>II. HISTOLOGICAL PROCEDURES:.....</b>	<b>93</b>
A. TISSUE PROCESSING.....	93
B. IMMUNOFLUORESCENCE ON CRYOSECTIONS.....	94
C. IMMUNOFLUORESCENCE ON VIBRATOME SECTIONS.....	95
D. RNA DIGOXIGENIN PROBES SYNTHESIS.....	96
E. WHOLE MOUNT <i>IN SITU</i> HYBRIDIZATION.....	97
<b>III. IMAGING AND MORPHOLOGICAL ANALYSES.....</b>	<b>98</b>
<b>IV. COUNTINGS.....</b>	<b>98</b>
<b>V. MOLECULAR BIOLOGY METHODS.....</b>	<b>99</b>
A. DNA EXTRACTION FROM MURINE TISSUE.....	99
B. PCDK5-LMO4-IRES-GFP PLASMID CONSTRUCTION.....	99
<b>VI. <i>IN UTERO</i> ELECTROPORATIONS.....</b>	<b>102</b>
<b>VII. CO-IMMUNOPRECIPITATION.....</b>	<b>103</b>
<b>VIII. CHROMATIN IMMUNOPRECIPIATION.....</b>	<b>104</b>
<b>IX. RETROGRADE LABELING.....</b>	<b>106</b>
<b>X. ELECTROPHYSIOLOGY ON ACUTE SLICES.....</b>	<b>107</b>
<b>XI. MOLECULAR AND MORPHOLOGICAL ANALYSIS OF RECORDED CELLS.....</b>	<b>107</b>
<b>XII. ELECTROPHYSIOLOGICAL ANALYSIS.....</b>	<b>108</b>

## Results

<b>I. CHARACTERIZATION OF A NEOCORTICAL POPULATION OF DOUBLE SATB2/CTIP2-EXPRESSING NEURONS IN NORMAL AND <i>COUP-TFI</i>-DEFICIENT CORTICES</b> .....	<b>110</b>
A. DOUBLE SATB2/CTIP2-EXPRESSING NEURONS ARE INCREASED IN LOWER LAYERS OF <i>COUP-TFI CKO</i> CORTICES.....	110
B. SATB2/CTIP2-POSITIVE NEURONS ARE MORE REPRESENTED IN THE MOTOR/FRONTAL AREA THAN IN THE SOMATOSENSORY REGION. ....	114
C. TANGENTIAL AND RADIAL INCREASE OF LMO4 EXPRESSION IN <i>COUP-TFI CKO</i> CORTICES.....	118
D. PROGRESSIVE INCREASE OF LMO4 EXPRESSION LEVELS IS CORRELATED WITH THE NUMBER OF SATB2/CTIP2-POSITIVE NEURONS IN THE POST-NATAL SOMATOSENSORY CORTEX.....	120
<b>II. A NOVEL MOLECULAR MECHANISM REGULATING CTIP2 EXPRESSION VIA CHROMATIN REMODELING</b> .....	<b>125</b>
A. THE WORKING HYPOTHESIS: LMO4 MIGHT INTERFERE WITH THE DEACETYLATION PROCESS ON THE CTIP2 LOCUS.....	125
B. INCREASED NUMBER OF DOUBLE LMO4/SATB2 AND LMO4/CTIP2-POSITIVE NEURONS IN <i>COUP-TFI CKO</i> BRAINS.....	127
C. INCREASED NUMBER OF TRIPLE LMO4/SATB2/CTIP2-POSITIVE NEURONS IN <i>COUP-TFI CKO</i> BRAINS.....	130
D. LMO4 DE-REPRESSSES CTIP2 TRANSCRIPTION BY BINDING HDAC1.....	133
E. LMO4 BINDS TO SKI: ANOTHER COMPONENT OF THE NURD COMPLEX.....	136
<b>III. <i>IN VIVO</i> ROLE OF LMO4 IN THE SPECIFICATION OF THE SATB2/CTIP2 LAYER V SUBPOPULATION IN THE SOMATOSENSORY CORTEX</b> .....	<b>140</b>
A. CORTICAL INACTIVATION OF LMO4 AFFECTS THE PERCENTAGE OF SATB2/CTIP2 LAYER V SUBPOPULATION.....	140
B. LMO4 OVEREXPRESSION PROMOTES THE NUMBER OF DOUBLE SATB2/CTIP2-POSITIVE CELLS IN LAYER V.....	143
C. LMO4 DOWNREGULATION RESCUES CTIP2 RADIAL EXPANSION IN <i>COUP-TFI CKO</i> MUTANT CORTICES.....	146
<b>IV. MOLECULAR, MORPHOLOGICAL, HODOLOGICAL AND ELECTROPHYSIOLOGICAL PROPERTIES OF THE SATB2/CTIP2 LAYER V NEURONAL POPULATION</b> .....	<b>151</b>
A. MOLECULAR CHARACTERIZATION OF THE DOUBLE SATB2/CTIP2-POSITIVE LAYER V NEURONS UNRAVELS TWO MAJOR SUBPOPULATIONS.....	151
B. SATB2/CTIP2-POSITIVE NEURONS IN LAYER V PROJECT TO SUBCEREBRAL AND CALLOSAL TARGETS.....	154
C. MORPHOLOGICAL ANALYSIS CONFIRMS DIFFERENCES BETWEEN SINGLE AND DOUBLE SATB2/CTIP2-POSITIVE LAYER V NEURONS.....	165
D. DISTINCT ELECTROPHYSIOLOGICAL PROPERTIES OF DOUBLE SATB2/CTIP2-POSITIVE NEURONS IN LAYER V.....	170

## Discussion

<b>I. SATB2/CTIP2 CO-EXPRESSION: NOT A TRANSIENT STATE BUT A PERMANENT CELL POPULATION</b> .....	<b>175</b>
<b>II. SATB2/CTIP2 CO-EXPRESSING NEURONS: A PREVIOUSLY UNCHARACTERIZED CELL POPULATION</b> .....	<b>175</b>
<b>III. ECTOPIC AND PRECOCIOUS EXPRESSION OF LMO4 IN <i>COUP-TFI CKO</i></b> .....	<b>176</b>

A.	LMO4 ALLOWS CTIP2 EXPRESSION IN SATB2-POSITIVE CELLS OF COUP-TF1 CKO BRAINS	176
B.	LMO4 BINDS TO HDAC1 AND DE-REPRESSSES CTIP2.....	178
<b>IV.</b>	<b>AREAL AND TEMPORAL DISTRIBUTION OF SATB2/CTIP2 POSITIVE NEURONS IN S1 CORTEX.....</b>	<b>179</b>
A.	LMO4 GAIN- AND LOSS-OF-FUNCTION.....	180
1.	<i>The majority, but not the totality of Satb2/Ctip2 co-expressing neurons decrease in the absence of LMO4 in layer V, unraveling a complementary compensatory mechanism.....</i>	<i>180</i>
2.	<i>Downregulation of LMO4 is sufficient to reduce the expansion of Ctip2 expression in layer V of COUP-TF1 mutant S1 cortices.....</i>	<i>181</i>
3.	<i>LMO4 overexpression anticipates the birth of Satb2/Ctip2 co-expressing neurons.</i>	<i>182</i>
<b>V.</b>	<b>TWO DISTINCT CELL POPULATIONS DIFFERING IN THEIR AXONAL PROJECTION, MOLECULAR CODE, MORPHOLOGICAL AND ELECTROPHYSIOLOGICAL PROPERTIES.....</b>	<b>183</b>
A.	MOLECULAR CHARACTERIZATION.....	183
B.	CONNECTIVITY.....	184
C.	ELECTROPHYSIOLOGY.....	186
D.	MORPHOLOGY.....	187

## Conclusion and Perspectives

<b>I.</b>	<b>TO COMBINE THE MORPHOLOGICAL AND ELECTROPHYSIOLOGICAL PROPERTIES WITH MOLECULAR MARKERS CHARACTERIZING THE TWO SUB-POPULATIONS OF SATB2/CTIP2 CO-EXPRESSING NEURONS.....</b>	<b>193</b>
<b>II.</b>	<b>TO DIRECTLY INVESTIGATE THE ROLE OF LMO4 ON THE SUBTYPE DIVERSITY AND AXONAL PROJECTIONS OF CORTICO-BRAINSTEM PROJECTION NEURONS..</b>	<b>193</b>
<b>III.</b>	<b>FURTHER MOLECULAR AND FUNCTIONAL CHARACTERIZATION OF SATB2/CTIP2 CO-EXPRESSING NEURONS.....</b>	<b>194</b>

# List of figures

---

Figure 1-Development of the mammalian forebrain.....	18
Figure 2-Sensory modalities reach the cerebral cortex through different thalamic nuclei.....	21
Figure 3-Neocortical projection neurons are generated in an 'inside-out' fashion by diverse progenitor types in the VZ and SVZ.....	23
Figure 4-Diverse populations of excitatory neuron progenitor cells in the mouse neocortex.....	25
Figure 5- Neocortical glia-guided radial migration.....	27
Figure 6-Graphical representations of the two main hypotheses on the mechanisms underlying formation of cortical areas.....	29
Figure 7-Patterning centers and graded transcription factors drive arealization of the neocortex.....	31
Figure 8- Summary of Intrinsic Genetic Mechanisms of Area Patterning and Mutant Phenotypes.....	35
Figure 9-Major Subtypes of Projection Neurons Within The Neocortex.....	41
Figure 10- Projection neuron diversity in the neocortex.....	43
Figure 11-Long-range axonal projections define two classes of Corticostriatal neurons.....	50
Figure 12- Competing molecular programmes direct differentiation of newly postmitotic projection neurons into one of three broad subtype identities.....	52
Figure 13- Satb2 protein interacts with both the Ctip2 promoter upstream region and histone deacetylase complex and controls chromatin remodeling.....	59
Figure 14- Ski associates with Satb2 and represses Ctip2 transcription in cortical neurons.....	61
Figure 15- Satb2- and Ctip2-dependent establishment of cortical connections.....	64
Figure 16- Key events in corticospinal tract guidance.....	67
Figure 17-Schematic representations of the human LMOs and LDB1.....	71
Figure 18-Schematic representations of LMOs in gene transcriptional regulation.....	73
Figure 19-Mechanisms underlying cortical thickening, expansion and lamination.....	79
Figure 20-Massive expansion of the Frontal motor area and posterior compression of primary sensory areas in COUP-TFI deficient cortex.....	84
Figure 21-Increased expression of molecular hallmarks of CSMN in corticofugal neurons of S1 cortex in COUP-TFI CKO mice.....	86

# List of Abbreviations

---

5-HT: 5-hydroxytryptamine  
A1: primary auditory  
AD: Alzheimer disease  
AHP: After Hyperpolarization  
Akt: protein kinase B  
ALS: amyotrophic lateral sclerosis  
ANR: anterior neural ridge  
AP: anteroposterior  
APV: D (-)-2-Amino-5-phosphonopentanoic acid  
ASD: autism spectrum disorders  
ATP: Adenosin tri-phosphate  
Auts2: autism susceptibility candidate 2  
BF1: Brain Factor 1  
Bhlhb5: Basic-loop-helix domain containing, class B5  
Bmps: bone morphogenetic proteins  
BPN: backward projection neurons  
BRCA1: Breast Cancer 1  
Brdu: Bromodeoxyuridine  
BSCs: bipolar shaped cells  
btd : Bttonhead  
Cadh8: cadherin 8  
CaM: calcium/calmodulin- dependent protein  
CAP1: cyclase-associated protein  
CAP1: cyclase-associated protein 1  
CBMN: corticobrainstem motor neurons  
CFuPN: corticofugal PNs  
ChIP: Chromatin immunoprecipitation  
Cited2: Cbp/p300-interacting transactivator  
CKO: conditional knock out  
CLIM: cofactor of LIM proteins  
CNS: central nervous system  
CoIP: Co-Immunoprecipitation  
CoP: commissural plate  
COUP-TFI : chicken ovalbumin upstream promoter transcription factor I  
COUP-TFI CKO: COUP-TF1 fl/fl<sup>Emx1Cre</sup>  
COUP-TFI: chicken ovalbumin upstream promoter-transcription factor 1  
CPN: callosal PNs  
CREB: cAMP response element-binding protein  
Crim1: Cysteine-Rich Motor Neuron 1  
CSMN: Corticospinal motor neurons  
CST: Corticospinal tract  
CStrPN: Corticostriatal PN  
CStrPNI: corticostriatal intratelencephalic  
CStrPNI: intralencephalic corticostriatal PN  
CTAs : corticothalamic afferents  
CTB: cholera toxin B subunit

CThPNs: Corticothalamic PNs  
Ctip2: COUP-TF1 interacting protein 2  
CTR: control  
Cux1: cut-like homeobox1  
Cux2: cut-like homeobox2  
DAP: Depolarizing afterhyperpolarization  
DCC: deleted in colorectal carcinoma  
DEAF1: deformed epidermal regulatory factor 1  
dLGN : dorsolateral geniculate nucleus  
DNQX: 6,7-Dinitroquinoxaline-2,3-dione  
DV: dorsoventral  
E: embryonic day  
Ebf2: early B-cell factor 2  
EC: entorhinal cortex  
EGFP: enhanced GFP,  
Egfs: epidermal growth factors  
Egr1: early growth response protein 1  
Emx CKOs: COUP-TF1fl/fl<sup>EmxCre</sup> mice  
Emx2: empty spiracles homeobox  
Eph: ephrin  
Er81: Ets-Related Protein 81  
ERK: Extracellular signal-regulated kinases  
ER $\alpha$  : Estrogen receptor  $\alpha$   
ES: embryonic stem  
ESC: embryonic stem cells  
ETS: E26 transformation-specific  
Etv1: ets variant 1  
Fezf2: fez family zinc finger 2  
Fgfs: fibroblast growth factors  
FI: Firing current  
Fog2: FOG family member 2  
Foxg1: Forkhead Box G1  
Foxp2: Forkhead box P2  
GABA:  $\gamma$ -aminobutyric  
GCSF: granulocyte colony-stimulating factor  
GCSF: granulocyte colony-stimulating factor  
GFAP: Glial fibrillary acidic protein  
h-COUP-TFI: human ortholog of COUP-TFI  
HDAC1: histone deacetylase 1  
HDACs: histone deacetylases  
Id2: inhibitor of DNA binding 2  
IGF1: Insulin like growth factor 1  
Igfbp4: insulin-like growth factor binding protein 4  
IL-6: interleukin 6  
IPC: intermediate progenitor cell  
IT: intratelencephalic  
IZ: intermediate zone  
KO: knock out  
LDB1: LIM domain binding protein 1  
Lhx: LIM/homeobox protein

LID: LIM interaction domain  
 LIM-HD: LIM homeodomain  
 LMO4 CKO: LMO4 flox fox<sup>Emx1 Cre</sup>  
 LMO4: Lim domain only 4  
 M1: primary motor  
 MAP: microtubule associated protein  
 MAPK: Mitogen-activated protein kinases  
 MARS: matrix attachment regions  
 MC<sub>c</sub>: caudal motor cortex  
 MC<sub>r</sub>: rostral motor cortex  
 MDGA1: MAM domain containing glycosylphosphatidylinositol anchor 1  
 MGv: ventral medial geniculate nucleus  
 mS1: motorized S1  
 MSCs: multipolar shaped cells  
 MSN: medium spiny neurons  
 MTA2: metastasis-associated 1 family, member 2  
 mVI: motorized sixth layer  
 NCAM: neural cell adhesion molecule  
 Ne: Nestin promoter  
 Nex CKOs: COUP-TF1fl/fl<sup>NexCRE</sup> mice  
 NFT: neurofibrillary tangles  
 NGN2: neurogenin 2  
 NMDA: N-Methyl-D-aspartate  
 Npn1: Neuropilin 1  
 NS: primary neurospheres  
 NuRD Nucleosome Remodeling Deacetylase  
 OSVZ: outer subventricular zone progenitor cell  
 Otx1: Orthodenticle homeobox 1  
 P: Postnatal day  
 Pax6: Paired box gene 6  
 PCR: Polymerase chain reaction  
 PI3K: phosphatidylinositol 3'-kinase  
 PLA: proximity ligation assay  
 PMBSF: posteromedial barrel subfield  
 PNs: projection neurons  
 POU: Pit-Oct-Unc domain TFs (Brn1 and Brn2)  
 PPAR $\gamma$ : peroxisome proliferation activated receptor- $\gamma$   
 Ppp1r1b: protein phosphatase 1, regulatory subunit 1B  
 PT: pyramidal tract  
 RA: retinoic acid  
 RGCs: radial glial cells  
 Rnd2: Rho family GTPase 2  
 Robo: Roundabout, Axon Guidance Receptor  
 ROR $\beta$ : RAR-related orphan receptor beta  
 Ryk: receptor-like tyrosine kinase  
 S1: primary somatosensory  
 SAGE: serial analysis of gene expression  
 Satb2: Special AT-Rich Sequence-Binding Protein 2  
 SCL: stem cell leukemia  
 SCPN: subcerebral PN

Sema: Semaphorin  
Sey: small eye  
Sfrp2: secreted frizeled related protein  
Shh: sonic hedgehog  
Sip1: SMN Interacting Protein 1-Delta  
Ski: ski sarcoma viral oncogene homologue  
Slit 2: Slit homolog 2  
SNPs: short neural precursors  
Sox5: SRY-box-containing gene 5  
SP: Subplate  
Sp8: trans acting transcription factor 8  
Stat3: Signal transducer and activator of transcription 3,  
SVZ: subventricular zone  
Tbr1: T-box brain protein 1  
TCA: thalamocortical afferents  
TFs: transcription factors  
Tgf $\alpha$ : Transforming Growth Factor  $\alpha$   
Tle4: transducing like enhancer of split 4  
Unc5C: Unc-5 Homolog C (C. Elegans)  
V1: primary visual  
VL: ventrolateral nucleus  
VPN: ventral posterior nucleus  
VZ: ventricular zone  
Wnts: vertebrate orthologs of drosophila wingless  
WT: wild type  
YAC: yeast artificial chromosome  
YFP: yellow fluorescent protein

# *Chapter I-Introduction*

---

## **I. The mammalian neocortex: Origin and function**

Early in embryonic development, the neural tube forms three major brain vesicles: the forebrain positioned at the anterior end, the midbrain and the hindbrain (**Figure 1**)[1]. The dorsolateral forebrain later evaginates to form the telencephalon and the diencephalon (thalamus/hypothalamus). Subsequently, the telencephalon is subdivided into ventral telencephalon, which gives rise to the striatum and the basal ganglia, and dorsal telencephalon, from which arises the cerebral cortex [1].

The cerebral cortex is the largest and the most complex structure of the mammalian brain, and more than any other brain structure, it has undergone the most dramatic changes during vertebrate evolution [2-4]. The cerebral cortex is subdivided into the neocortex, which is the largest region and unique to the mammalian forebrain, the archicortex (hippocampus) and the paleocortex (olfactory piriform cortex) [2-5].

The neocortex has acquired an increasing relevance during evolution, and is deputed to the elaboration of sensory and motor inputs. This structure represents the prevalent centre for the elaboration of peripheral inputs, and the seat of higher functions, such as memory, language and voluntary movements, and in humans, where it constitutes more than 80% of the total brain volume, it is responsible for thoughts and consciousness [2-4, 6, 7].

## **II. The neocortex: General organization**

### **A. Tangential organization**

In its tangential dimension, the neocortex is organized into “areas”, defined by Brodmann as the “organs of the brain” [8], which represent a partition of distinct neocortical functions among several tangential regions. In adult, the borders of these areas are sharply defined by differences in cytoarchitecture and chemoarchitecture, input and output connections, and pattern of gene expression [9-11].

The basic plan of the mammalian neocortex comprises four primary areas; three of these primary areas are sensory: the primary somatosensory (S1), visual (V1)

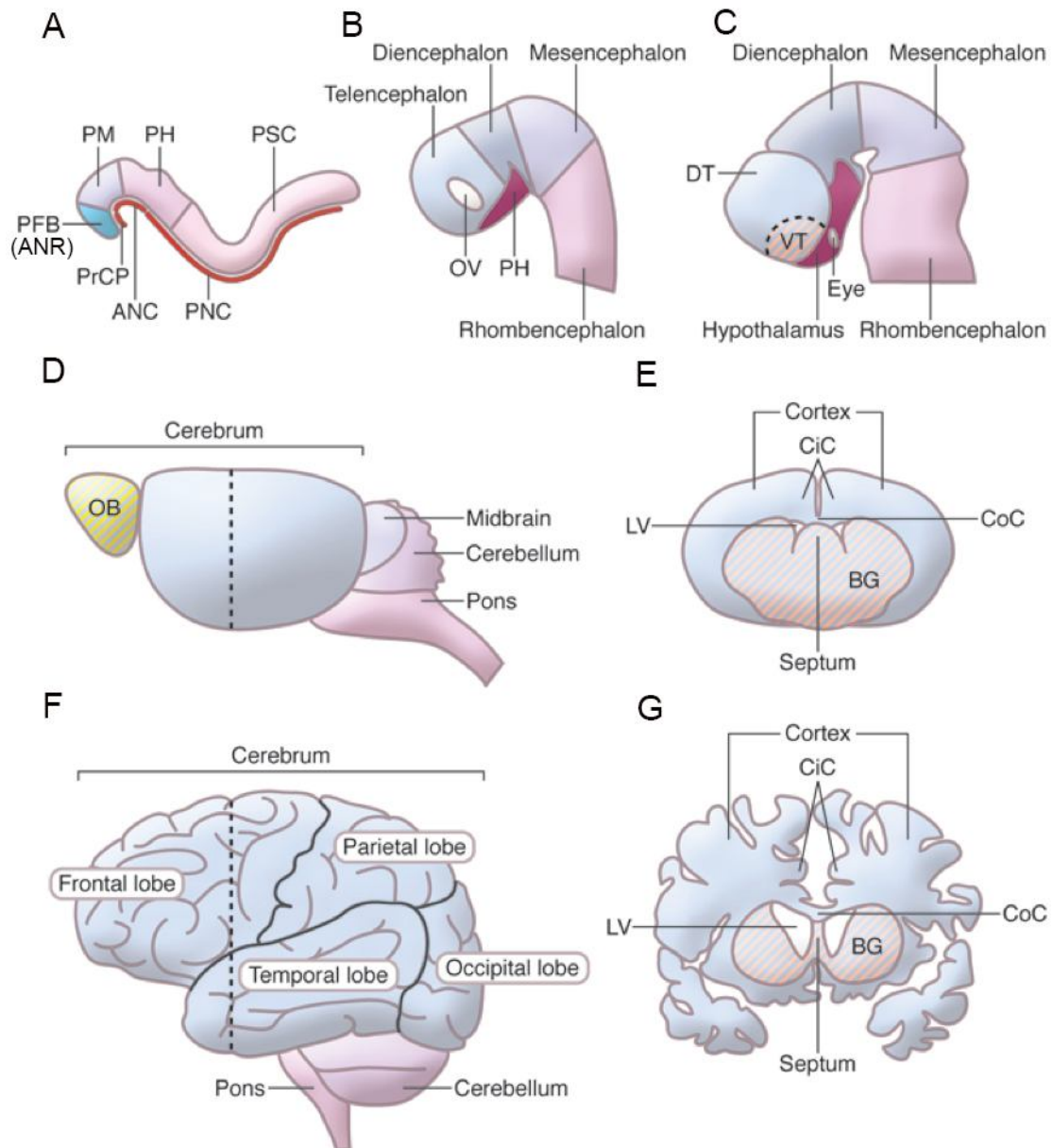


**Figure 1-Development of the mammalian forebrain.**

(A) At early somite stage (E8.5 for mouse; Carnegie Stage 10 (CS10) for human), the neural ectoderm has been specified into different regions along the anterior-posterior axis and the axial mesoderm is underlying the midline of the neural ectoderm. ANC, anterior notochord; PFB, prospective forebrain (or ANR: Anterior neural ridge); PrCP: prechordal plate; PH, prospective hindbrain; PM, prospective midbrain; PNC, posterior notochord; PSC, prospective spinal chord. (B) Neural tube closure occurs at around the 15-somite stage (E9.0 for mouse; CS11 for human). The forebrain gets further regionalized into telencephalon, diencephalon, and prospective hypothalamus (PH). OV, optic vesicle. (C) Approximately at E10.5 in the mouse or at CS14 in human embryos, the expanding telencephalon bifurcates dorsally to form the two hemispheres and gets patterned into dorsal telencephalon (DT) and ventral telencephalon (VT). (D and F) Lateral views of adult mouse (D) and human brain (F). OB, olfactory bulb. Black dashed lines in D and F indicate the location of coronal sections shown in E and G. (E and G) Coronal sections of adult mouse (E) and human brain (G). BG, basal ganglia; CiC, cingulate cortex; CoC, corpus callosum; LV, lateral ventricle (modified from [12]).

and auditory (A1), which process sensory information arriving respectively from the whole body, the eye (retina) and the inner ear (cochlea). The fourth primary area is motor (M1), which mainly controls voluntary movements [13].

Areal patterning will be presented in details in Chapter IV.

## **B. Radial organization**

The laminar organization of the neocortex is an important feature that differentiates it from other cortical structures. Each area is radially organized into six major “layers”, each containing a heterogeneous population of neurons, distinguished by their morphology, connectivity and function from those of other layers [9-11]. Each layer is generated according to an inside-out sequence. Early born neurons reside in deeper layers, while late born neurons reside in superficial layers [14]. Lower layer neurons (VI and V) project their axons to subcortical targets (striatum, thalamus, tectum, pons and spinal cord), while upper layer neurons (IV-II) establish cortico-cortical connections, or receive sensory and motor inputs from the thalamus [15]. Cellular organization of the neocortex, different types of progenitors, radial migration and different types of projection neurons will be discussed in chapters III and V.

## **C. The functional relationship between cortical areas and the thalamus**

One of the principal functions of the thalamus, originating from the diencephalon, is to receive sensory and motor afferents from peripheral systems, and to relay them to the main elaboration centre: the neocortex [3]. The dorsal thalamus has four principal thalamic nuclei that are functionally and topographically connected to the four primary cortical areas. This relationship between a primary cortical area and a nucleus in the dorsal thalamus is critical for both adult function and developmental differentiation of the areas [13].

The S1 receive thalamocortical afferents (TCA) from the ventral postero-medial nucleus (VPM), the V1 from the dorsolateral geniculate nucleus (dLGN) and the A1 from the ventral medial geniculate nucleus (MGv). TCAs will reach the fourth layer of the targeted sensory areas [16-18], while the motor area, which is connected to the ventrolateral nucleus (VL), receives TCAs in lower layer III [19-21]. In the

somatosensory area, TCA innervation of layer IV granular cells gives rise to the cortical barrels, which are constituted by columns of thalamocortical afferents surrounded by layer IV stellate (granule) cells. In turn targeted areas send corticothalamic afferents (CTAs) from layers V and VI to the respective thalamic nuclei [17, 18] (**Figure 2**).

### **III. Neocortical neurogenesis and radial migration**

#### **A. Cellular organization of the neocortex**

A prominent feature of the neocortex is its complex but well-organized cellular architecture. It contains an immense number of neurons, produced through extensive progenitor cell divisions during embryogenesis. These neurons are not randomly dispersed, but spatially organized into horizontal layers, essential for neocortical function. The formation of this laminar structure requires exquisite control of neuronal migration from the birthplace to the final destination in the cortex.

The main constituents of the neocortex are excitatory, inhibitory neurons and glial cells. The glutamatergic excitatory neurons represent the vast majority (70-80%) of neocortical circuit neurons and are responsible for generating the cortical output, while the  $\gamma$ -aminobutyric (GABA)-ergic inhibitory interneurons account for about 20% of cortical neurons, and provide a rich variety of inhibitions that shape the output of functional circuits [22]. Excitatory and inhibitory neurons convey and modulate motor and sensory inputs, favoring their integration and elaboration and, ultimately the implementation of motor plans. Thus, proper neocortical function critically depends on the production and positioning of a correct number of excitatory and inhibitory neurons, which largely occurs during embryonic stages.

In contrast, glial cells mainly constituted by oligodendrocytes, astrocytes and microglia are involved in a variety of functions including cell feeding, axon myelination, structural support and radial migration of neocortical projection neurons [22-24]. Moreover, oligodendrocyte precursor cells in the mammalian brain form synapses with neurons, suggesting an even greater degree of complexity in the interactions between neurons and oligodendroglia [25]. Glutamatergic and glial cells are born from common precursors (through neurogenic and gliogenic processes),

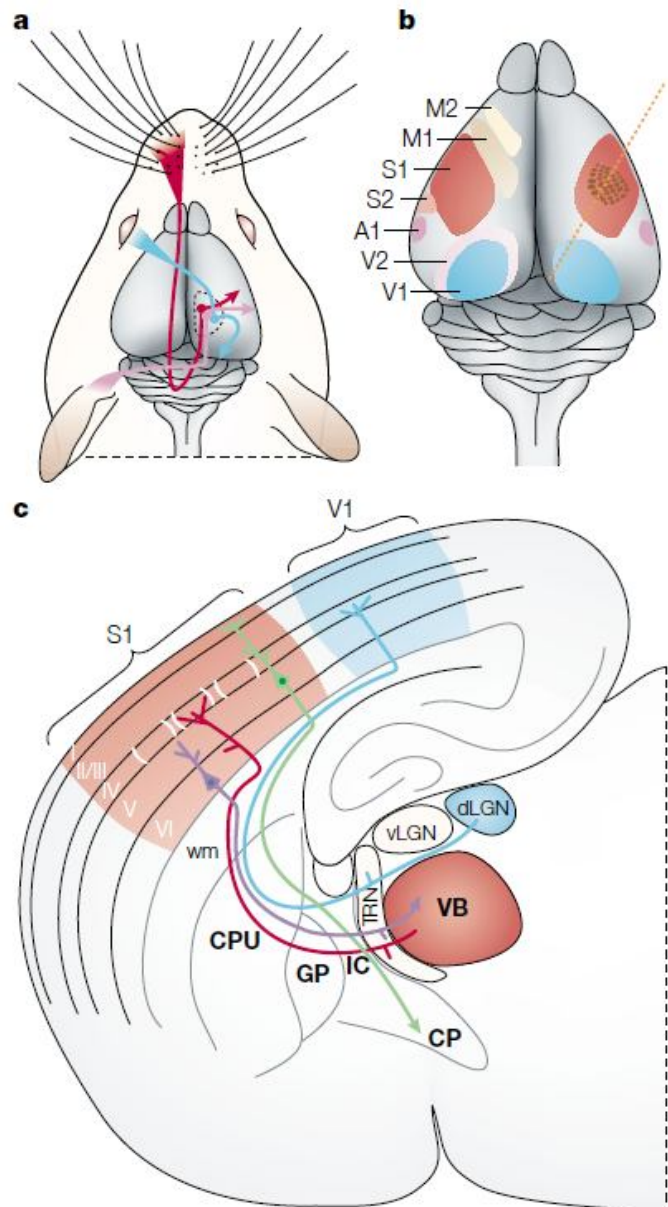


**Figure 2-Sensory modalities reach the cerebral cortex through different thalamic nuclei.**

a-Visual input from the retina (blue line) is relayed through the dorsal lateral geniculate nucleus (dLGN) to reach the visual cortex (V1, blue area in b). Somatosensory information from the whiskers (red line) reaches the ventrobasal complex (VB) through the brainstem, and is relayed to the barrel field of the primary somatosensory cortex (S1, red area in b). Acoustic information (purple line) arrives at the medial geniculate nucleus through numerous relays, and is then relayed to the primary auditory cortex (A1, purple area in b). b-The sensory and motor cortical areas of the mouse brain. Orange dashed line indicates plane of section in part c. c-Forebrain section, showing S1 and VB and the pathways that link them. The red line indicates the thalamocortical fibre running from VB to layer IV of S1 (red shading). The blue line indicates thalamocortical projections to the anterior segment of V1 (blue shading). Neurons in layer VI of the same area project to VB. Layer V extends projections to the cerebral peduncle (CP). White brackets in layer IV represent septa of barrels. CPU, caudate putamen; GP, globus pallidus; IC, internal capsule; M1, primary motor area; M2, secondary motor area; S2, secondary somatosensory cortex; TRN, thalamic reticular nucleus; vLGN, ventral lateral geniculate nucleus; WM, white matter (taken from [26]).

while excitatory and inhibitory neurons arise from different developmental lineages, and their progenitors are fully segregated in space [22-24]. Excitatory neurons are generated in the proliferative zone of the dorsal telencephalon and then migrate radially to constitute the future neocortex. Instead, inhibitory interneurons are produced in the proliferative zone of the ventral telencephalon and migrate tangentially to reach the neocortex [22].

In this section, I will present only glutamatergic cell specification and migration.

## **B. Progenitors diversity and corticogenesis**

Early in development, the telencephalic wall is composed of neuroepithelial cells (**Figures 3 and 4**). Most neuroepithelial progenitor cells undergo symmetric division; two neuroepithelial cells are produced at each division, expanding the population of founder cells. These neuroepithelial cells are multipotent, capable of generating radial glial cells (RGCs) and the first group of neurons in the neocortex [22, 27, 28]. Around embryonic day E9.5-E10.5 in the mouse, some neuroepithelial cells begin to differentiate into RGCs establishing the ventricular zone (VZ) [27]. RGCs are characterized by their radial bipolar morphology. They expand across the entire thickness of the developing neocortex with a long basal radial process pointing to the pial surface, and a short apical ventricular endfoot reaching the VZ surface, with their soma located in the VZ [29, 30]. RGCs divide symmetrically to self renew, and at later stages they undergo, alternatively, symmetric and asymmetric divisions to either self renew or generate neurons, respectively [31, 32]. RGC symmetric divisions give rise also to other two classes of progenitors: the intermediate progenitor cells (IPC) and the outer radial glia (or outer subventricular zone OSVZ progenitor cell), which reside between the upper VZ and the subventricular zone (SVZ) [31-35].

Intermediate progenitors have a multipolar morphology, and are not anchored to either the apical or basal surface. They act primarily as transit amplifying cells, undergoing limited proliferative divisions, and more often divide symmetrically to produce two neurons [27, 36-38]. The generation of neocortical neurons through IPCs increases the number of neurons produced by individual RGCs. Hence, it has been

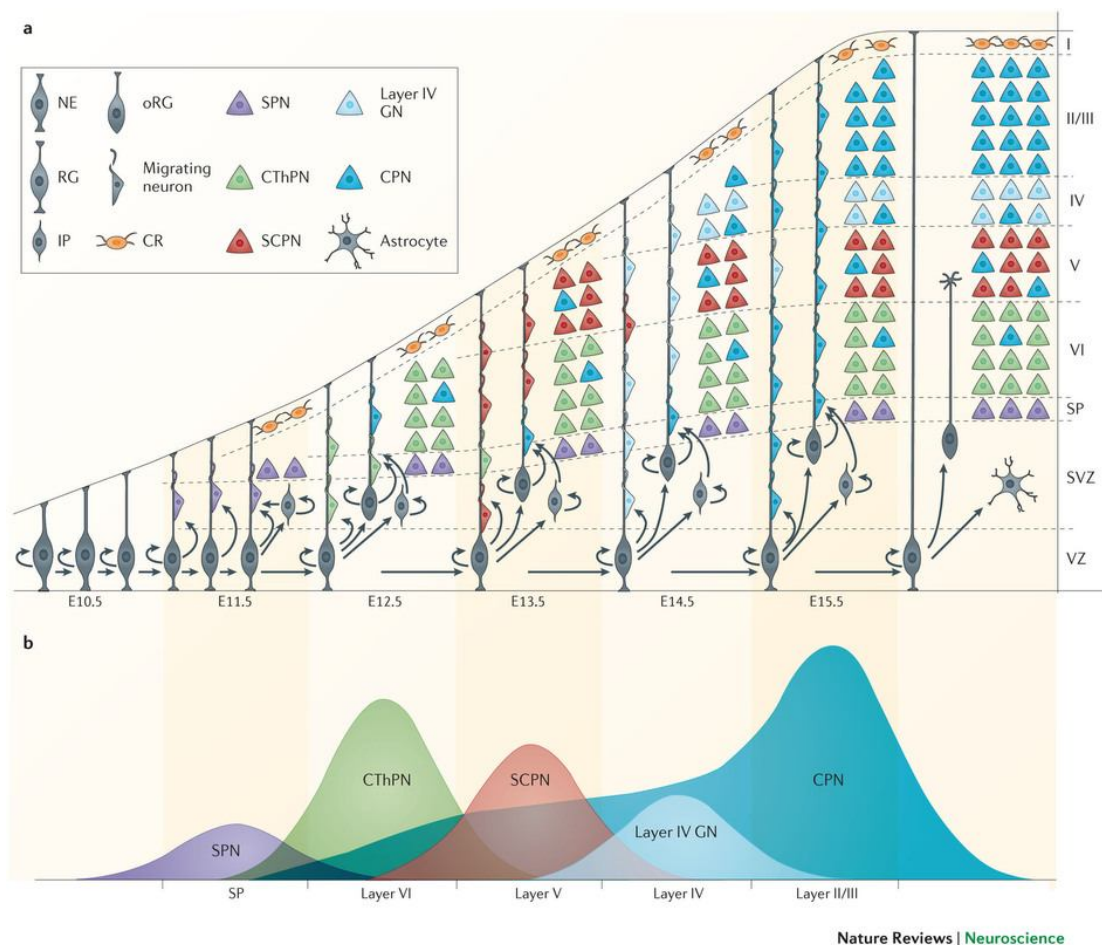


**Figure 3-Neocortical projection neurons are generated in an 'inside-out' fashion by diverse progenitor types in the VZ and SVZ.**

This schematic depicts the sequential generation of neocortical projection neuron subtypes and their migration to appropriate layers over the course of mouse embryonic development. **a** | Radial glia (RG) in the ventricular zone (VZ) begin to produce projection neurons around embryonic day 11.5 (E11.5). At the same time, RG generate intermediate progenitors (IPs) and outer RG (oRG), which establish the subventricular zone (SVZ) and act as transit-amplifying cells to increase neuronal production. After neurogenesis is complete, neural progenitors transition to a gliogenic mode, generating astrocytes and oligodendrocytes (not shown). Cajal–Retzius (CR) cells primarily migrate into neocortical layer I from non-cortical locations, whereas other projection neurons are born in the neocortical VZ and/or SVZ and migrate along radial glial processes to reach their final laminar destinations. **b** | Distinct projection neuron subtypes are born in sequential waves over the course of neurogenesis. The peak birth of subplate neurons (SPN) occurs around E11.5, with the peak birth of corticothalamic projection neurons (CThPN) and subcerebral projection neurons (SCPN) occurring at E12.5 and E13.5, respectively. Layer IV granular neurons (GN) are born around E14.5. Some callosal projection neurons (CPN) are born starting at E12.5, and those CPN born concurrently with CThPN and SCPN also migrate to deep layers. Most CPN are born between E14.5 and E16.5, and these late-born CPN migrate to superficial cortical layers. Peak sizes are proportional to the approximate number of neurons of each subtype born on each day. NE, neuroepithelial cell (taken from [39]).

postulated that the abundance of IPCs may contribute to the evolutionary expansion of the neocortex [40].

Outer radial glia have unipolar morphology, compared to RGCs, they retain only the basal process and lack the apical process [33, 41]. They undergo asymmetrical divisions to self renew and generate neurons [35, 42]. A very small population of outer radial glia was observed in the developing mouse neocortex [33, 43]. A fourth class of progenitors, that either possesses a short or lack the basal process reside in the VZ, they are termed as short neural precursors (SNPs). Most SNPs produce postmitotic neurons directly within the VZ [44, 45] (**Figure 4**).

Neocortical progenitors begin to produce glutamatergic projection neurons around embryonic day (E) 10.5. Earliest born neurons migrate away from the VZ to segregate from progenitors and form the preplate. Later born neurons migrate into the preplate, splitting it into the superficial marginal zone and the deeply located subplate and establishing the cortical plate between the two. The cortical plate which will give rise to the multilayered cortex, develops between them such that early born neurons populate the deep layers (layer VI, then layer V), and late born neurons migrate past them to progressively populate more superficial layers (layer IV, then layer II-III), establishing the six layered structure of the mature cortex in an “inside out” manner [46-49] (**Figure 3**).

### **C. Neocortical “glia guided” radial migration**

One of the major processes during cortical development is radial cell migration. After exiting the cell cycle, newborn projection neurons leave the VZ and migrate radially to give rise to the cortical plate, while starting their specification. During early stages of mammalian corticogenesis (E11-E13.5), newborn neurons leave the VZ by somal translocation. At this stage neurons inherit from their progenitors a process in contact with the pial surface, and use it as a puller, which progressively translocates the cell body towards the primordial cortical plate [36, 50-52]. Radial migration becomes more complex at late stages of corticogenesis (from E13.5), when neurons migrate along the glia scaffold generated by RGCs; this type of migration is called “glia guided”. Once moved from the VZ to the SVZ, the neurons adopt a multipolar shape, elongating and retracting thin neurites, and detach from the glia continuing their

migration both radially and tangentially with respect to the ventricular surface. Then, once they have reached the upper limit of the intermediate zone (IZ), they re-attach to the glia scaffold, adopt a bipolar shape, and enter the cortical plate [53, 54]. Finally, they contact the pial surface with their leading process, leave the glia scaffold, and move towards the pia by somal translocation. This last step of migration is critical for

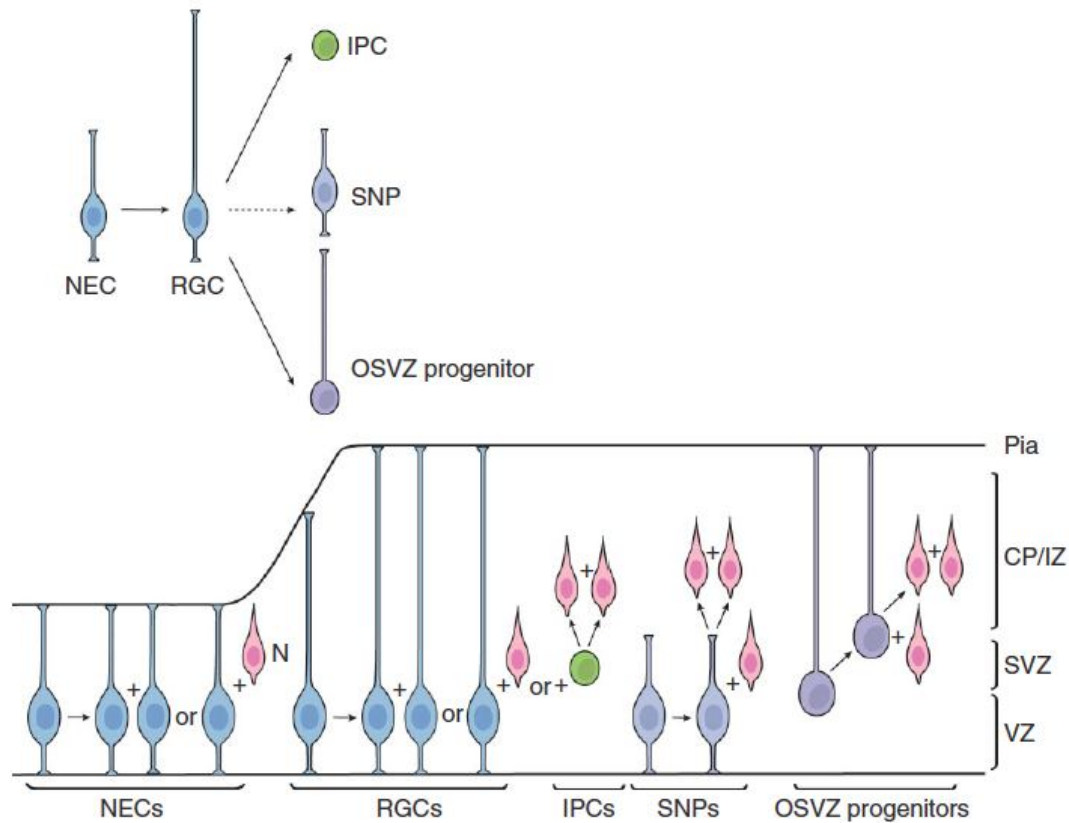


**Figure 4-Diverse populations of excitatory neuron progenitor cells in the mouse neocortex.**

During early brain development, neuroepithelial cells (NECs) are the major neural progenitors in the neocortex. NECs divide symmetrically to generate additional NECs, some of which give rise to the first group of neurons (N) through asymmetric division. As the developing brain epithelium thickens, NECs elongate and transit to radial glial cells (RGCs). RGCs can also divide symmetrically to expand the progenitor pool or asymmetrically to generate neurons either directly or indirectly through intermediate progenitor cells (IPCs), which generate neurons directly through symmetric division in the subventricular zone. It remains unclear how short neural precursors (SNPs) are generated. It is possible that they are generated from RGCs or they may be a distinct population originated directly from NECs. Most SNPs produce postmitotic neurons directly in the ventricular zone (VZ). Outer subventricular zone (OSVZ) progenitors likely originate from RGCs through oblique division, which leads to loss of the apical process and ascension of the nucleus toward the cortical plate/intermediate zone (CP/IZ). The minor population of OSVZ progenitors can also generate neurons through asymmetric division outside of the VZ (taken from [22]).

the inside-out order of layer formation, since it allows the incoming neurons to settle beyond their predecessors [51, 55] (**Figure 5**).

#### **D. Progenitor lineage commitment**

Neocortical progenitors generate the different subtypes of PN in sequential waves, however the lineages leading to specific neuronal subtypes remain largely unknown.

Two models have been proposed: the first model states that only one single lineage of progenitors exists and generates all subtypes of PNs, and the competence of a given progenitor to generate specific subtypes becomes progressively limited over the course of development [56-62]. The alternative model proposes that different independent fate restricted lineages of progenitors generate specific neuronal subtypes. In support to this latter model, a number of subtype specific transcription factors was shown to be expressed in progenitors, suggesting that distinct subsets of progenitors might be committed to generate specific classes of PNs. For instance, Fez family zinc finger 2 (Fezf2, also known as Fez1) is sparsely expressed in the proliferative zone during deep layer neurogenesis, and its postmitotic expression is specific to corticofugal PN [63-67]. See more details in chapter V.

Conversely, Cut-like homeobox 1 (Cux1) and Cux2 are expressed in the VZ and SVZ during upper layer neurogenesis, and its post-mitotic expression is specific to CPN, and other superficial layer neurons [68-70]. In favor of the second model, recent work has demonstrated that a subset of progenitors, positive for Cux2 and present from E10.5 corresponding to the earliest stages of corticogenesis, exclusively produces CPN and other superficial-layer neuron subtypes, and that early born neurons derived from the Cux2 lineage become deep layer CPN [71].

However, another recent paper [72] demonstrated that Fezf2-expressing radial glial cells (RGCs) exist throughout cortical development and sequentially generate all major projection neuron subtypes and glia. Moreover, this study showed that the vast majority of Cux2-positive cells in the VZ and SVZ are migrating interneurons derived from the subcortical telencephalon, and Cux2-positive RGCs generate both deep- and upper-layer projection neurons. Overall, this work identified Fezf2-positive radial glial cells as multipotent neocortical progenitors and suggests that determining whether laminar-fate-restricted RGCs exist since early stages of neurogenesis requires further investigation [72].

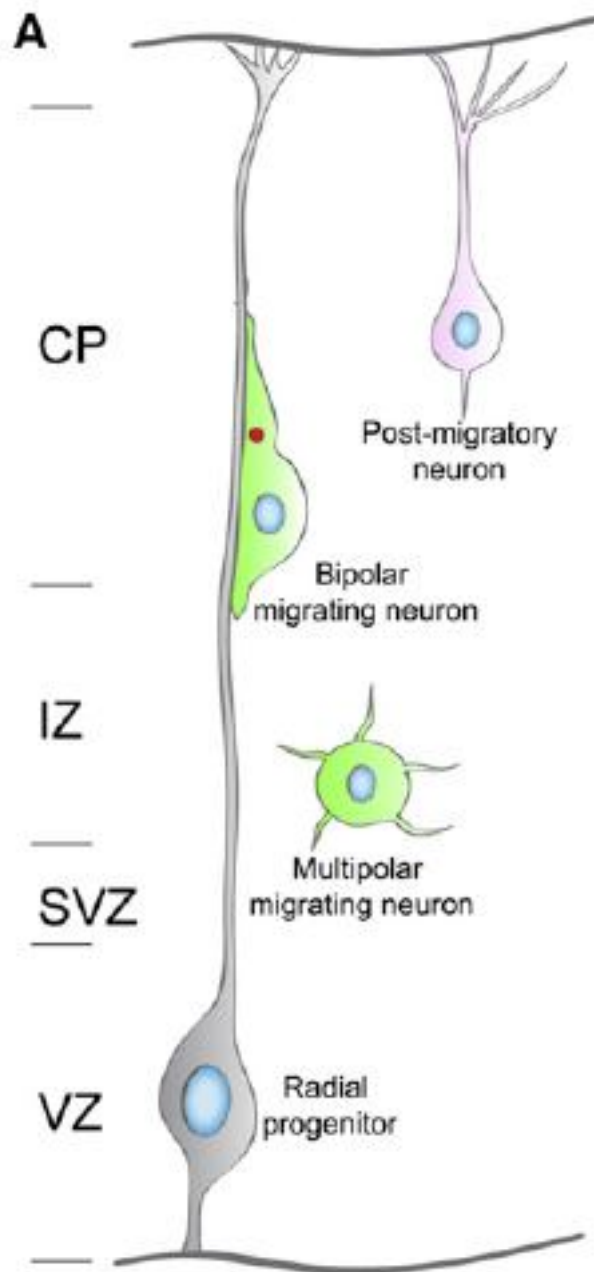


**Figure 5- Neocortical glia-guided radial migration.**

New neurons generated from radial progenitors undergo a transient multipolar migratory state in the SVZ and IZ prior to adopting a bipolar morphology and radial glial-guided migration to the cortical plate where they differentiate (modified from [73]).

#### **IV. Genetic regulation of neocortical area mapping**

As mentioned above, the neocortex has four primary areas; each of them is the cornerstone of clusters of functionally related areas that include scores of higher order areas prominently interconnected. Three of these primary areas are sensory, processing primary information from the whole body (S1), the inner ear/ cochlea (A1) and the eye/retina (V1), while the fourth primary area is motor (M1), controlling voluntary movements. Each area is innervated by thalamocortical afferents from distinct thalamic nuclei, establishing a topographical relationship between cortical areas and thalamic nuclei, which is crucial both for the development of functional areas and for adult brain functioning (**Figure 2**).

Neocortical areas form the basis for sensory perception, control our movements and mediate our behavior. Many features must be properly specified during arealization, not only the unique properties that determine an area function and interaction with other brain structures, but also the appropriate area size and positioning. Arealization of the neocortex is controlled by interplay between intrinsic mechanisms (genetic mechanisms that operate within the cortex), and extrinsic mechanisms (TCA innervation and relayed inputs) [13, 74]. Two hypotheses were proposed in this issue: the “protomap” versus the “protocortex” hypothesis (**Figure 6**). The protocortex hypothesis states that area pattern in the developing neocortex is extrinsically specified by the innervating thalamocortical afferents, and thus the naïve cortical primordium may be seen as a “tabula rasa” patterned by outside factors [75, 76]. In contrast, the protomap hypothesis proposed that neocortical areas are patterned by the interactions among several morphogens and transcription factors expressed by neuronal progenitors in different neocortical and allocortical (external structures to the neocortex) regions [77]. However, the truth lies in the middle, both extrinsic and intrinsic mechanisms are working in combination to regulate specification and development of neocortical areas. During early stages, before innervation by thalamocortical afferents, area identity is broadly established in the neocortex through intrinsic information in progenitors and postmitotic neurons, whereas at later stages, extrinsic input refines and sharpens these boundaries (**Figure 7**) [13, 74].

Neocortical areal patterning is controlled by a regulatory hierarchy beginning with morphogens secreted from patterning centers positioned at the boundaries of the dorsal telencephalon. These morphogens or signaling molecules establish, within

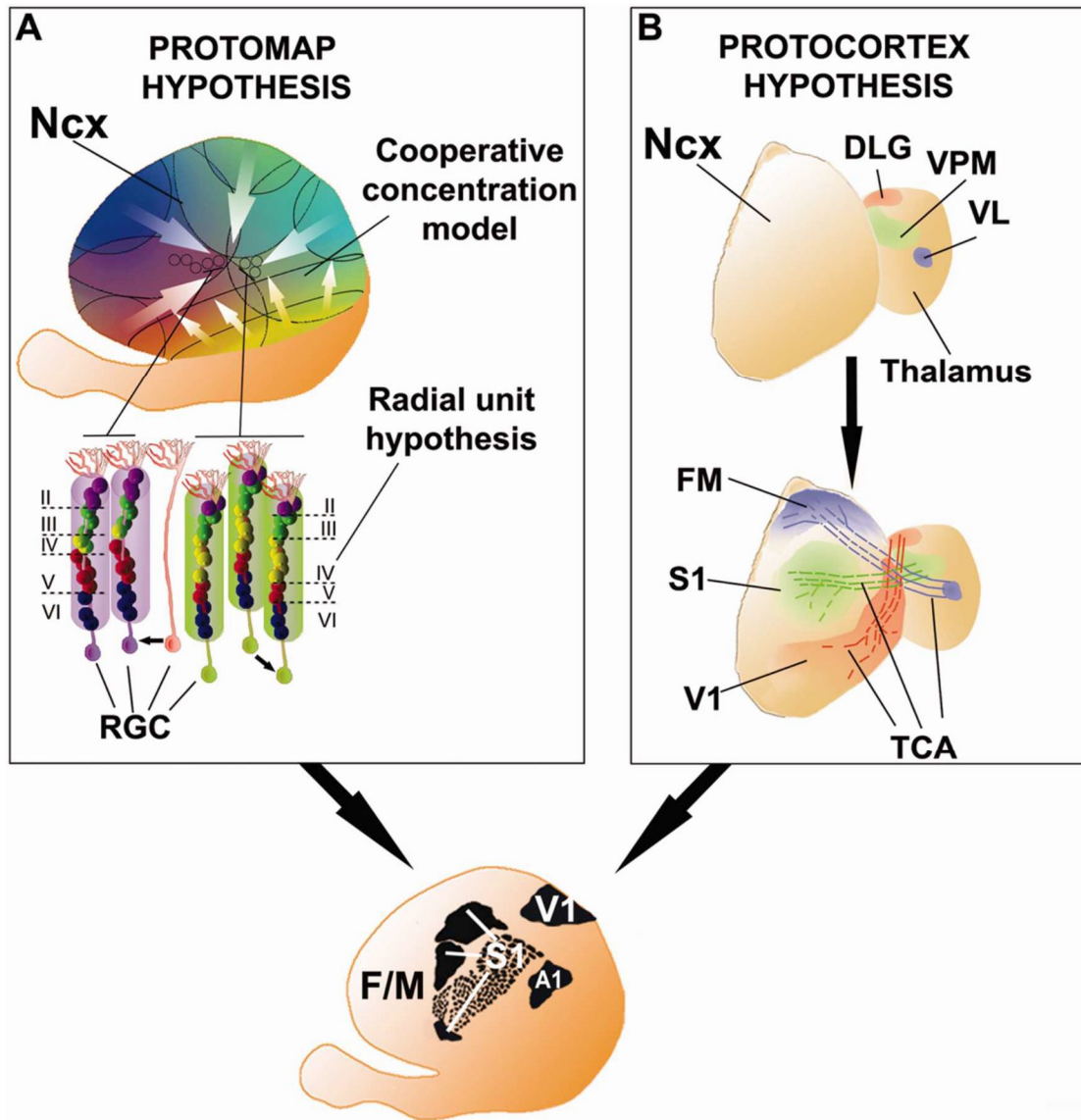


**Figure 6-Graphical representations of the two main hypotheses on the mechanisms underlying formation of cortical areas.**

A: The “protomap hypothesis” is mainly based on two models: the cooperative concentration model and the radial unit model. Various overlapping gradients of TFs and morphogens (represented in different colors) act synergistically and in a dose-dependent manner to define distinct neocortical domains. These signals control the specification of neuronal progenitors, which are committed to a given, areal-specific, neurogenetic program. Successively, these neuronal progenitors transfer both areal commitment and positional information to their offspring, giving rise to the peculiar cytoarchitecture and functional features of a given area.

B: The “protocortex hypothesis” states that the neocortex is like a tabula rasa until the arrival of TCA from distinct thalamic nuclei: the dorsolateral geniculate (dLG), the ventropostero medial (VPM), the VL. Abbreviations: F/M: frontal-motor areas; S1: primary somatosensory area; V1: primary visual area; A1: primary auditory area; Ncx: neocortex; RGC: radial glia cells (taken from [8]).

cortical progenitors, the differential graded expression of transcription factors that determine the areal identity of the neurons that will give rise to the cortical plate [13, 74].

### **A. Morphogens and patterning centers**

The early specification of cortical territories is controlled by a complex interaction between different morphogens, including fibroblast growth factors (Fgfs), sonic hedgehog (Shh), retinoic acid (RA), bone morphogenetic proteins (Bmps), vertebrate orthologs of *Drosophila* wingless (Wnts) and epidermal growth factors (Egfs) [8, 13, 74] (**Figure 7**).

Four telencephalic patterning centers appear to be involved directly or indirectly in cortical patterning. Two of them are directly involved in arealization: the commissural plate (CoP), which expresses Fgfs, and the cortical hem that releases Wnts and Bmps. The third patterning center is the antihem, producing Egfs (Neuregulin 1 and 3), Tgf $\alpha$ , Fgf7, and the Wnt antagonist secreted frizzled related protein (Sfrp2). The fourth patterning center is located in ventral telencephalon and in the ventral diencephalon (hypothalamus), expressing Shh (**Figure 7**) [8, 13, 74].

#### **1. Anterior neural ridge: Fgfs**

The anterior neural ridge (ANR), the anterior junction between neural and non-neural ectoderm, which becomes later through morphogenesis the CoP, is considered as an anterior patterning center. It begins to release Fgf8 at E8-E8.5, and shortly after Fgf15, 17 and 18 [8, 13, 74, 78]. Fgf8 and Fgf17 have been most implicated in arealization. They act by inducing ETS family of transcription factors, establishing the gradients of empty spiracles homeobox (Emx2) and chicken ovalbumin upstream promoter transcription factor I (COUP-TFI) within cortical progenitors [79-81]. Fgf8 and Fgf17 have crucial effects on area patterning, by altering TF levels, most probably through repression of COUP-TFI, Emx2, and other TFs [79-81]. However, there is a big debate between O'Leary and Grove whether Fgf8 controls Emx2 expression directly or indirectly. Other studies showed that Fgf8 controls the size of

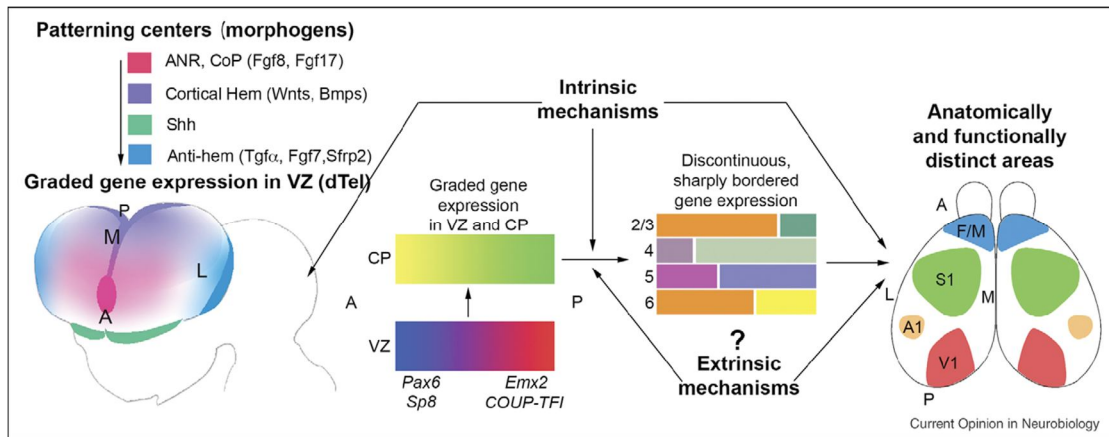


**Figure 7-Patterning centers and graded transcription factors drive arealization of the neocortex.**

The initial, tangential gradients of transcription factors (TFs) in the ventricular zone (VZ) are established by signaling molecules/morphogens secreted from telencephalic patterning centers, such as Fgf8 and Fgf17 from anterior neural ridge (ANR), which later becomes the commissural plate (CoP), and Wnts and BMPs from the cortical hem. The antihem is a putative patterning center identified based on its expression of secreted signaling molecules (e.g. Tgfa, Fgf7, Sfrp2, as well as Neuregulin1 and Neuregulin3) with known patterning functions. A fourth telencephalic patterning center is defined by the expression domains of sonic hedgehog (Shh) in ventral telencephalon, but it does not have defined roles in dorsal telencephalic (dTel) patterning. The graded expression of certain TFs, such as Pax6, Emx2, COUP-TFI, and Sp8, imparts positional or area identities to cortical progenitors which is imparted to their neuronal progeny that form the cortical plate (CP). The CP also initially exhibits gradients of gene expression that are gradually converted to distinct patterns with sharp borders. Coincident with this process, distinct cortical layers, and the anatomically and functionally distinct areas seen in the adult (M1, S1, A1, V1), differentiate from the CP. Genes that are differentially expressed across the cortex are often expressed in different patterns in different layers, suggesting that area-specific regulation of such genes is modulated by layer-specific properties, and questions the definition of area identity. Although the initial establishment of the graded gene expression in the embryonic CP is controlled by mechanisms intrinsic to the telencephalon, the more complex differentiation patterns established postnatally might be controlled in part by extrinsic mechanisms, for example, TCA input and the sensory activity that it relays from the periphery to the cortex (Taken from [74]).

both dorsal frontal cortex and ventral/orbital frontal cortex, while Fgf17 selectively controls the size of dorsal frontal cortex [82].

Overexpressing Fgf8 by *in utero* electroporation causes a caudal expansion of rostromedial areas [81, 83]. In contrast, Fgf8 reduction in hypomorphic mutants causes caudal areas of the neocortex to expand rostrally. A similar phenotype was observed by overexpressing the cytoplasmic domain of Fgf8 receptor Fgfr3C, which reduced rostral Fgf8 expression [79, 82].

A mutual inhibiting loop between Fgf8 and Bmp/Wnt signaling has been reported in different studies [80, 84-86]. In contrast, Shh, together with Noggin and chordin (two Bmps antagonists secreted by the ANR), favors Fgf8 expression presumably by inhibiting Wnt signaling [85, 87-95]. In turn, Fgf8 maintains Shh expression rostrally in a dose dependent manner [80].

## 2. **Cortical hem: Bmps and Wnts**

The cortical hem, which is a neuroepithelium extending from the medial cortex to the dorsal midline, expresses Bmps and Wnts [84, 96]. Very recently, important roles for the hem in dorsoventral and areal patterning have been revealed [97]. Hem ablation caused a reduction in the size of the dorsomedial cortex, whereas ventrolateral cortex was expanded rostrally. Moreover, hem ablation perturbed regional neocortical patterning. Genetically engineered mice lacking the hem showed an expansion of rostral neocortical domains, while caudal domains were diminished [97].

In addition, Lhx2 and Lhx5, two members of the LIM/homeobox protein (Lhx) class of Lim homeodomain proteins, have been shown to control the development of the cortical hem [98-101]. Lhx2 is expressed in the cortical VZ in a high posterior-medial to low anterior-lateral gradient. After repression of Bmp2 and Bmp4 in the roof plate, Lhx2 exhibits an abrupt decline in its posterior-medial expression, e.g. in the cortical hem [99]. In the absence of Lhx2 function, the neocortex is dramatically reduced in size, and proliferation is prematurely arrested [99-101]. Other studies in Lhx2 conditional knock out (KO) mice show that Lhx2 specifies cortical identity in a cell autonomous manner [102].

## 3. **Antihem: Sfrp2, EGFs, Tgfa, Fgf15 and Fgf7**

The anti-hem, located at the ventricular edge of the ventral pallium, is so called due to its opposite position with respect to the hem, and due to the production of Sfrp2, an antagonist of Wnt signaling [103]. However, the anti-hem releases also EGFs (Neuregulin 1 and 3), Transforming Growth Factor  $\alpha$  (Tgfa), Fgf15 and Fgf7.

No clear function has been found for the anti-hem in cortical patterning [74], but it is essentially absent in small eye (Sey) mutant mice lacking functional Paired box gene 6 (Pax6) protein, and therefore some of the major telencephalic defects observed in these mutants could be due to the absence of the anti-hem [104].

#### 4. **Ventral telencephalon: Shh**

The ventral telencephalon and the hypothalamic region of the ventral diencephalon produce high levels of Shh. It has been shown that Shh is involved in regional patterning of the forebrain [10, 84, 86, 88, 89, 93]. Gain- and loss-of-functions experiments show that Shh is involved in controlling levels of proliferation of neural progenitor cells along the entire central nervous system (CNS) including the neocortex [105, 106]. However, other studies have led to the proposal that Shh is not directly involved in areal patterning [10].

In conclusion, most of these signaling molecules act in a time- and dose-dependent manner to regulate proliferation, specification and survival of stem cells and neural progenitors. Some of them can even promote neurogenesis and differentiation. Their antagonizing effects influence, initially, the balance between cellular processes contributing to dorsoventral (DV) and anteroposterior (AP) patterning, and then the specification of neocortical domains [8]. However, among the different morphogens, the best described to date to play a clear cut role in cortical arealization belong to the Fgf family [8, 13, 39, 74] and, very recently, to the Wnt family and the other families of molecules expressed by the hem [97].

### **B. Graded expression of transcription factors**

Cortical morphogens and signaling molecules induce a graded expression of transcription factors (TFs) in ventricular zone progenitors. These TFs match the basic

criteria required for candidate genes in areal identity specification. They are regulatory genes, expressed in different AP and DV gradients by progenitors in the VZ, or in both the VZ and the SVZ. These characteristics allow for these transcription factors to act in a combinatorial manner across the cortical axes, which is essential to impart area identities.

Among these, four are expressed from early stages of development in the cortical primordium: Paired box gene 6 (Pax6) and empty spiracles homeobox (Emx2) are expressed in the VZ in reciprocal rostro-lateral to caudo-medial gradients, whereas *trans* acting transcription factor 8 (Sp8) and chicken ovalbumin upstream promoter transcription factor I (COUP-TFI) are expressed in reciprocal rostro-medial to caudo-lateral gradients (**Figure 8**).

In mice, the expression of these TFs begins at E8.0-E8.5 in the ventricular zone, and lasts, apart from Sp8, during the entire period of neurogenesis. Except for COUP-TFI, the expression of all these TFs is exclusively limited to the progenitor cells in the VZ. COUP-TFI is the only TF expressed in both mitotic and postmitotic cells [8, 13, 39, 74]

## 1. Sp8

Sp8 is a zinc finger transcription factor belonging to the family of *Bottonhead* (*btd*) homeotic genes. Its expression begins from E8.0 to E8.5 in the ANR, and from E9.5 in the cortical primordium, in a high antero-medial to low postero-lateral gradient. Sp8 is a direct transcriptional activator of *Fgf8* in the CoP [107]. Overexpression of *Fgf8* at E11.5 induces an ectopic expression of Sp8 indicating a reciprocal induction between these two genes [108, 109]. In vitro assays showed that Emx2 co-expresses with Sp8 in cortical progenitors but not in the CoP. Emx2 interferes with the ability of Sp8 to bind regulatory elements of *Fgf8* to induce its expression, explaining why Sp8 induces *Fgf8* expression only in the CoP but not within cortical progenitors [107].

Gain- and loss-of-function analyses by *in utero* electroporation, and the use of a conditional knock out ablating Sp8 specifically in the telencephalon (Sp8 fl/fl<sup>Foxg1-Cre</sup>),

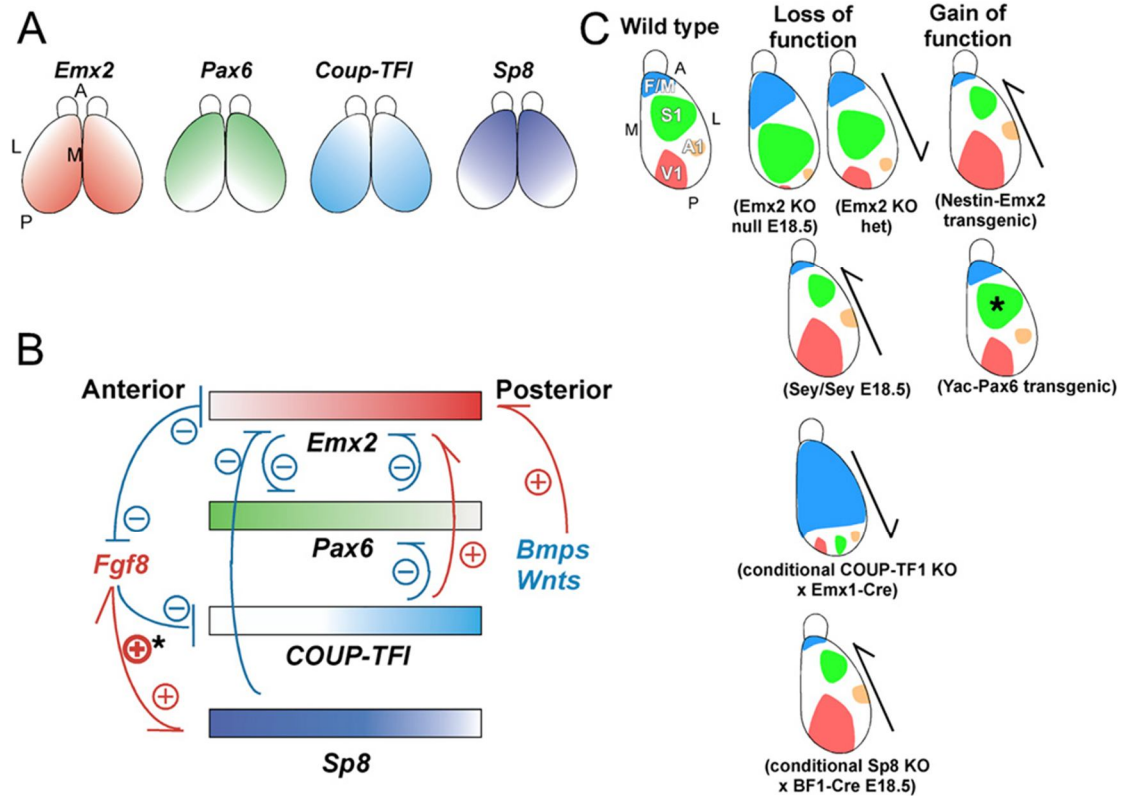


**Figure 8- Summary of Intrinsic Genetic Mechanisms of Area Patterning and Mutant Phenotypes.**

(A) Graded expression of *Emx2*, *Pax6*, *Coup-TFI*, and *Sp8* along anterior-posterior and lateral-medial axes. Key TFs for cortical area patterning show distinct graded expression patterns along anterior-posterior (A, P) and lateral-medial (L, M) axes. *Emx2* is expressed in a high P-M to low A-L gradient. *Pax6* expression pattern is opposite to that of *Emx2*, with a high A-L to low P-M gradient. *Coup-TFI* has a high P-L to low A-M gradient. *Sp8* is expressed in a high A-M to low P-L gradient. While the expression of *Emx2*, *Pax6*, and *Coup-TFI* is sustained in the VZ, *Sp8* expression is quickly downregulated around the onset of cortical neurogenesis.

(B) In the anterior signaling center, *Fgf8* establishes the low anterior-graded expression of the TFs *Emx2* and *COUP-TFI* by repression, and promotes the high anterior gradient of *Sp8* expression. *Fgf8* expression is also regulated positively by direct transcriptional activation by *Sp8* through its binding to *Fgf8* regulatory elements, and indirectly by *Emx2*, which represses the ability of *Sp8* to directly induce *Fgf8*. The asterisk marking the activation of *Fgf8* by *Sp8* indicates the only interaction that has been shown to be due to direct binding and transcriptional activation. Putative posterior signaling molecules *Bmps* and *Wnts*, expressed in the cortical hem, positively regulate the high caudal gradient of *Emx2* expression. Genetic interactions between TFs also participate in the establishment of their graded expression. For example, *Emx2* and *Pax6* mutually suppress each other's expression, *Coup-TFI* suppresses *Pax6* expression and enhances *Emx2* expression, and *Sp8* suppresses *Emx2* expression. Those changes to the expression patterns were identified in the knockout mice; thus, these interactions do not necessarily imply direct control of one TF on another. For instance, *Emx2* suppression by *Sp8* might be due to an enhancement of *Fgf8* expression, which in turn acts negatively on *Emx2* expression. +, positive interaction; -, negative interaction.

(C) Summary of all reports of loss-of-function or gain-of-function mice mutant for TFs that regulate area patterning. Reducing *Emx2* levels in the cortex of the heterozygote mutant mice results in posterior shifts of areas with shrinkage of V1, while overexpression of *Emx2* under the control of the nestin promoter shifts areas anteriorly. The small eye mutant without functional *Pax6* shows anterior area shifts. Unlike the *Emx2* transgenic mice, YAC transgenic mice of *Pax6* do not show area changes other than a slight, but significant, reduction in the size of S1 (asterisk). Loss of *COUP-TFI* in cortical progenitors transforms the fate of primary sensory areas into frontal/motor areas. The analysis of *Sp8* conditional knockout mice shows anterior shifts of gene markers (taken from [13]).

further unraveled the roles of Sp8 in areal patterning [107, 109]. Analyses of these mutant mice at E18.5 showed an anterior shift of cortical markers, suggesting that Sp8 specifies frontal/motor area identity. However, the use of the Foxg1-Cre line results in the deletion of Sp8 in the ANR/CoP. Since Sp8 is a direct activator of Fgf8 in the CoP, and is required for its maintenance, and since Fgf8 is involved in frontal/motor area specification it is not clear if Sp8 promote directly or indirectly frontal/motor identity. Moreover, Fgf8 negatively regulates the gradients of COUP-TFI and Emx2, thus it is not clear whether the regionalized marker shifts observed in the conditional knock out of Sp8 are mediated by the decrease of Fgf8 expression in the CoP, or by impairments in normal COUP-TFI and Emx2 gradients [107, 109]. However, a new work by Borello et al [110] using a binary transgenic system to express Sp8 throughout the mouse telencephalon in a temporally restricted manner, demonstrated a reciprocal cross-regulation between COUP-TFI and Sp8, and proposed that Sp8 promotes rostral and dorsomedial cortical development by repressing COUP-TFI and promoting Fgf signaling in pallial progenitors [110].

## 2. **Pax6**

Pax6 is a paired box domain TF. Its expression can be detected from E8.5 in the cortical primordium in a high anterior lateral to low posterior medial gradient, which correlates well with the neocortical neurogenic gradient [13, 77, 111, 112]. Pax6 is involved in controlling the balance between proliferation and neurogenesis. It is also involved in many other events, such as mediating the fate of neuronal precursors in the neocortex, and controlling the progression from apical to basal progenitors and orienting the mitotic spindle, which are at the basis of the neurogenic process [113-115]. Small eye (Sey) mutant mice, which lack a functional Pax6 protein, lack eyes and nasal structures, have major lamination defects and a cortex reduced by a third, in which TCA fail to reach the cortex [111, 116-118]. Moreover, analysis of areal-specific markers indicated a rostralization of sensory areas proposing Pax6 as a rostralizing agent [111, 116-118]. However, Pax6 overexpression using a YAC transgenic approach, reported no changes in areal patterning despite a partial reduction of the somatosensory area that can be explained by an induced pro-neurogenic and pro-apoptotic effects in response to increased Pax6 levels [119, 120].

The analysis of Pax6 conditional knock out (CKO) mice under the control of the cortical-specific *Emx1*-Cre promoter showed only few changes in arealization markers and no defects in TCA innervation. The only remarkable change was the shrinkage of the somatosensory area, while its position was not changed, suggesting a minor role for Pax6 in arealization [121]. Further analyses are required to explain these discrepancies and better define the role of Pax6 in areal patterning.

### 3. **Emx2**

*Emx2* is a homeotic genes belonging to the family of *Empty spiracles* TFs. It is expressed from E8.5 in the rostro-lateral neural plate, and later in the cortical primordium in a high caudo-medial to low rostro-lateral expression gradient [111, 112, 122]. *Emx2* promotes caudal cortical fate in a dose-dependent manner [111, 112, 122]. In *Emx2* mutants, sensory areas are shifted caudally and the V1 is reduced and mis-positioned at the most caudal portion of the cortex [111]. In contrast to the hypothesized role of *Emx2* through down-regulation of *Fgf8* expression, different genetic studies supported a direct role of *Emx2* in conveying positional information to cortical precursor cells [123-125]. Transgenic mice in which *Emx2* was overexpressed under the control of the Nestin promoter (*Ne-Emx2*) showed a rostral expansion of the V1 and a significant reduction of the postero-medial barrel subfield (PMBSF) of S1, which was shifted more rostrally. In these experiments, *Emx2* acted in a dose dependent manner in cortical patterning and had no effects on the morphology or the dimension of the neocortex [123]. In conclusion, *Emx2* is a crucial factor for V1 development, with a limited action on size and organization of the somatosensory area.

### 4. **COUP-TFI**

COUP-TFI is an orphan nuclear receptor that belongs to the steroid/thyroid hormone receptor superfamily, acting as a strong transcriptional repressor [126-130], but also as an activator [131-133]. COUP-TFI is involved in the temporal specification of neuronal precursor cells in the mouse neocortex [134]. COUP-TFI expression starts at E8.5 in anterior regions, and from E9.5, it is expressed in a high caudo-lateral to low rostro-medial gradient in the cortical primordium. In contrast to other TFs involved in

cortical arealization, COUP-TFI is the only TF among areal patterning genes, expressed in both mitotic and post-mitotic cells in the neocortex, with expression maintained in adult brains [8, 13, 135, 136].

First analyses in *COUP-TFI* constitutive *null* mutants, showed major defects in subplate and layer IV specification [137-139]. Moreover, TCAs fail to exit the internal capsule, and very few of them reach the subplate and the cortical plate. The cortices of these mutants showed a strong caudalization of sensory areas. However, since COUP-TFI is also expressed in the dorsal thalamus, and could be involved in the maturation of TCAs, these effects could not be assessed as a direct role for COUP-TFI in arealization or as a result of TCA innervation [137-139]. To overcome the potential effects of the TCAs, COUP-TFI was selectively ablated from the cortex using the *COUP-TFI<sup>fl/fl</sup><sup>EmxCre</sup>* mice (*Emx* CKOs). These mutant mice survive after birth to adulthood and TCAs invade the neocortex. In the absence of cortical COUP-TFI, rostral motor regions show an impressive caudal expansion at the expense of the caudal sensory areas, which are shrunken and shifted toward the occipital cortex [140] (see Chapter VII).

Another study from Tomassy et al, [134] showed that the parietal/somatosensory cortex acquired peculiar frontal/motor laminar organization in *COUP-TFI* conditional mutants, indicating a tangential (areal) and radial (laminar) control of COUP-TFI in neocortical organization. In these mutant mice, the expression of COUP-TFI interacting protein 2 (*Ctip2*), a TF involved in the specification of layer V subcerebral projection neurons [134], was considerably expanded in the fifth and sixth layers of the parietal cortex, considered as a “motorized” S1, while characteristic layer IV granule cells were lost [134] (see Chapter VII).

Some evidence suggests that COUP-TFI inhibits rostral fate and promotes caudal ones by out-competing with *Fgf8* signaling, which positively regulates *Mitogen-activated protein kinases* (MAPK). COUP-TFI interferes with MAPK signaling: the phosphorylation of the *Extracellular signal-Regulated Kinase* (ERK) (a main player in the MAPK cascade) is strongly affected in *D6/COUP-TFI* transgenic mice, which express ectopic high levels of COUP-TFI in the antero-dorsomedial region of the cortex [141, 142]. Accordingly, a consistent down-regulation of *Ets* genes (downstream targets of MAPK pathway) has been observed in these mice. This negative regulation of the *Fgf8* signaling can be mediated by *Sprouty 1* and *2*, which

are two inhibitors of the MAPK pathway positively regulated by COUP-TFI [141, 142]. Thus, COUP-TFI may interfere with Fgf8 rostralizing function by directly promoting Sprouty 1 and 2 transcription, supporting an active and direct role for COUP-TFI in the balance between rostral and caudal fate specification [141, 142]. The roles of COUP-TFI in areal patterning and neocortical projection neurons subtype specification will be presented in details in chapter VII.

Areal patterning is determined by the expression of mitotic and post-mitotic patterning genes such as Bhlhb5, Tbr1, LMO4 and COUP-TFI [143-146]. However, it is still unclear whether post-mitotic genes just refine area properties specified in progenitors or independently define areal features. A recent study from our group used genetic gain and loss-of function approaches to assess the roles of COUP-TFI at mitotic and post-mitotic levels. By comparing two transgenic lines, where COUP-TFI is ablated in all neocortical cells (*Emx CKOs*) and only in newborn cortical neurons *COUP-TFI<sup>fl/fl</sup><sup>Nex<sup>CRE</sup></sup>* mice (*Nex CKOs*), and by re-expressing the human ortholog of COUP-TFI (*hCOUP-TFI*) exclusively in post-mitotic neurons of *COUP-TFI KO*, we showed that COUP-TFI post-mitotic expression is necessary and sufficient to drive sensory area specification. Moreover, this study demonstrate that ectopic post-mitotic overexpression of COUP-TFI in rostral cortical regions reprograms frontal/motor areal features into sensory ones indicating that areal patterning is a more plastic process than previously expected (Alfano et al, 2014 under revision).

## **V. Neocortical projection neuron specification and diversity**

The organization of the mammalian neocortex into only six histologically distinct layers belies an extraordinary diversity of neuronal subtypes. Individual phenotypic characteristics, such as dendritic morphology, electrophysiological properties and projection patterns have been used in the past to classify projection neurons (PNs). Nowadays, the commonly used characteristic to group neocortical neurons is by the target of their axons, because “hodology”, defined as the path followed by axons to reach their targets [39], is centrally related to projection neuron function. Moreover, the establishment of appropriate projections requires successful execution of

developmental and molecular programs. As previously mentioned, the absence of COUP-TFI function, an important areal patterning gene, results in both areal and laminar alterations in the neocortex. Other genes such as LMO4, Bhlhb5, and Tbr1 are also involved in neocortical arealization and subtype specification of neocortical projection neurons (details will be discussed in chapter VII) [143-146]. Thus, it is becoming increasingly clear, that specification of PN subtypes and area identity are two related and highly dependent processes.

PNs progressively acquire area and subtype identities, and their development can be followed along three different axes: time, subtype differentiation and area differentiation. Therefore, genetic programs operate in establishing boundaries in n-dimensional “identity space” among different PNs subtypes, and different neocortical areas [39].

### **A. Major subtypes of projection neurons within the neocortex**

Within the broad class of neocortical PNs, many subtypes exist with distinct connectivity, soma laminar location and gene expression patterns. Classified by hodology, there are three basic subtypes of cortical PNs: Commissural callosal PNs (CPN), Associative PNs and corticofugal PNs (CFuPN) (**Figures 9 and 10**).

#### **1. Callosal Projection Neurons (CPN)**

CPN are interhemispheric commissural pyramidal neurons, whose myelinated axons make up the corpus callosum, the largest white-matter tract in the placental mammalian brain, which connects the two cerebral hemispheres. The corpus callosum is not unique in its ability to connect the two neocortical hemispheres, since the anterior and the hippocampal commissures also cross the forebrain midline, but the corpus callosum is the only fiber tract devoted solely to integrate information from the two cortical hemispheres. Thus CPN play a key role in the high level complexity of cognition and associative behavior [147-149].

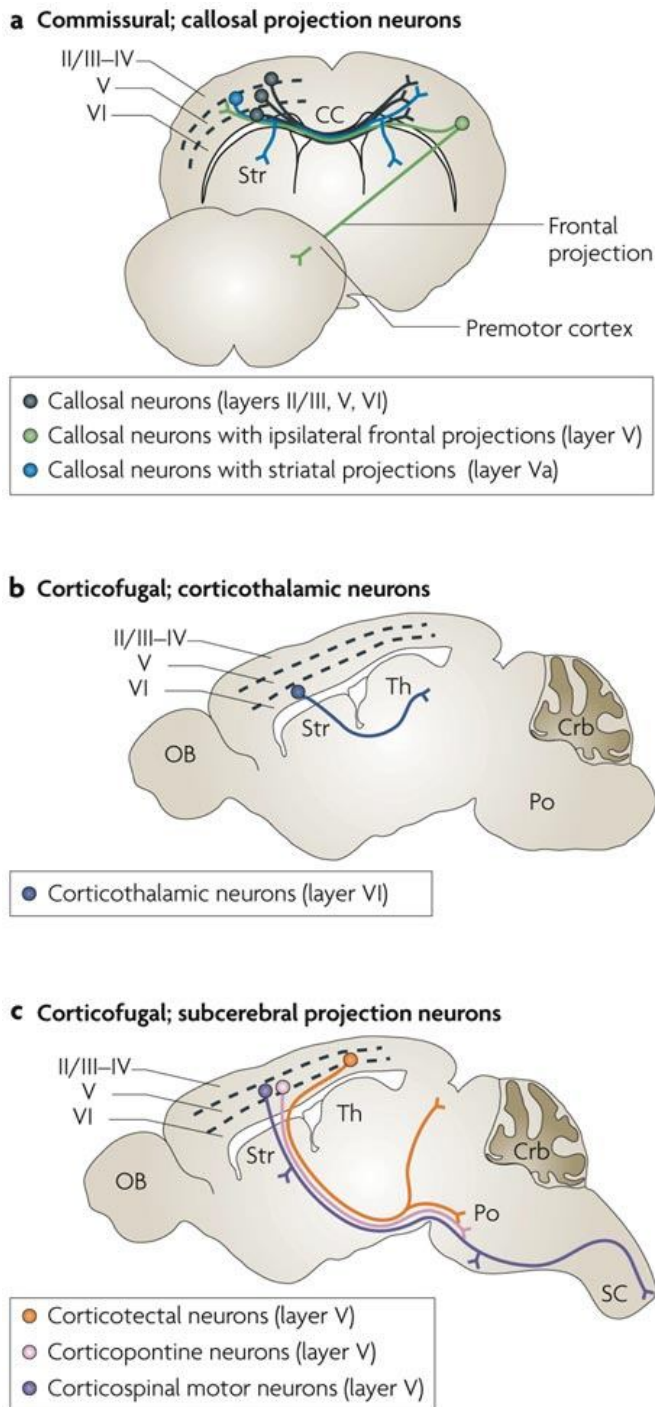


**Figure 9-Major Subtypes of Projection Neurons Within The Neocortex.**

Classified by hodology, there are three basic classes of cortical projection neuron: associative, commissural and corticofugal. Below are some principal subtypes:

Commissural: Callosal projection neurons. Projection neurons of small to medium pyramidal size that are primarily located in layers II/III, V and VI, and extend an axon across the corpus callosum (CC) (panel a). At least three major types of callosal neuron can be classified. These maintain: single projections to the contralateral cortex (black); dual projections to the contralateral cortex and ipsilateral

or contralateral striatum (blue); and dual projections to the contralateral cortex and ipsilateral frontal cortex (green). These never project axons to targets outside the telencephalon. Str, striatum.

Corticofugal (subcortical): Corticothalamic neurons. Projection neurons primarily located in cortical layer VI, with a smaller population in layer V, that project subcortically to different nuclei of the thalamus (Th) (panel b).

Subcerebral projection neurons. Also referred to as type I layer V projection neurons (panel c). These include pyramidal neurons of the largest size, which are located in deep-layer V and extend projections to the brainstem and spinal cord. neuron subtypes. Among them:

Corticotectal neurons (orange) are located in the visual area of the cortex and maintain primary projections to the superior colliculus, with secondary collateral projections to the rostral pons (Po).

Corticopontine neurons (pink) maintain primary projections to the pons.

Corticospinal motor neurons (purple) are located in the sensorimotor area of the cortex and maintain primary projections to the spinal cord, with secondary collaterals to the striatum, red nucleus, caudal pons and medulla. Many other subtypes of subcerebral projection neuron exist that send axons to different areas of the brainstem or have different combinations of collaterals, but are not depicted here for simplicity. Crb, cerebellum; OB, olfactory bulb; SC, spinal cord (Taken from [15]).

Abnormalities in CPN can lead to cognitive deficits. The absence of CPN in humans is associated with defects in abstract reasoning, problem solving and generalization. CPN dysgenesis is one of only few reproducibly identified pathologies in autism spectrum disorders (ASD), with reduced corpus callosum relative to the overall brain volume [150-156].

CPNs are more abundant than CFuPN and comprise the largest class of commissural neurons in placental mammals. CPNs are a heterogeneous population of neocortical neurons, with respect to their birthdate, final laminar destinations and distinct projections patterns. Their cell bodies principally reside in layers II-III (approximately 80% in rodents), layer V (approximately 20% in rodents) and to a lesser extent in layer VI [147-149]. In mice, layer VI CPN are born at embryonic day E12.5, layer V CPN are born around E13.5, and superficial layers CPN are born from approximately E15.5 to E17.5 [15, 148, 157].

CPN axons innervate their target in the contralateral hemisphere in a homotopic manner; thus, the location of a CPN within the cortex defines the target of its axon [36, 158, 159]. In addition to homotopic interhemispheric projections extended by all CPN, subpopulations of CPN can be defined by the variety of long-range dual axonal projections. Subpopulations of CPN send dual projections to contralateral or ipsilateral striatum (intralencephalic corticostriatal PN; CStrPNi). In

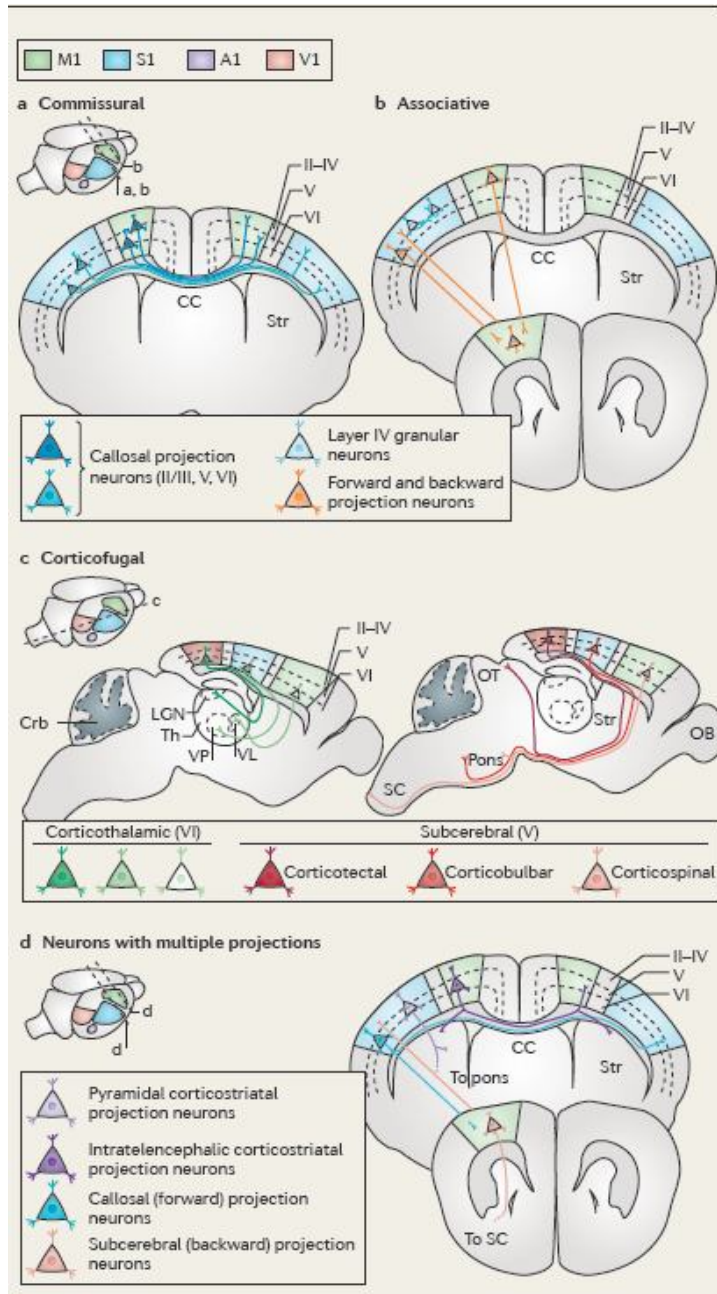


**Figure 10- Projection neuron diversity in the neocortex.**

Projection neurons are broadly classified according to whether they extend axons within one cortical hemisphere (associative projection neurons), across the midline to the contralateral hemisphere (commissural projection neurons) or away from the cortex (corticofugal projection neurons). Importantly, neurons of a given subtype residing in different cortical areas (motor, somatosensory, visual and auditory) project to anatomically and functionally distinct targets.

Most commissural projection neurons cross the midline through the corpus callosum (CC) — these are called callosal projection neurons (CPN) — whereas a smaller population of these neurons cross through the anterior commissure (see the figure, part a). CPN reside primarily in layer II/III, with fewer residing in layers V and VI, and extend axons to mirror-image locations in the same functional area of the contralateral hemisphere, enabling bilateral integration of information.

Present in all cortical layers, associative projection neurons include short-distance intrahemispheric projection neurons, which extend axons within a single cortical column or to nearby cortical columns (such as layer IV granular neurons) and long-distance intrahemispheric projection neurons, which extend axons to adjacent or distant cortical areas (such as forward and backward projection neurons; see the figure, part **b**).

Corticofugal projection neurons include corticothalamic projection neurons (CThPN), which reside in layer VI, and subcerebral projection neurons (SCPN), which reside in layer V (see the figure, part **c**). CThPN extend axons to specific thalamic nuclei: motor cortex (M1) CThPN establish connections with the ventral lateral (VL) and ventral anterior nuclei, somatosensory cortex (S1) CThPN with the ventral posterior (VP) nucleus and visual cortex (V1) CThPN with the lateral geniculate nucleus (LGN). SCPN extend axons to different primary targets in the brainstem and spinal cord (SC). In general: M1 SCPN project to the SC (corticospinal motor neurons) and brainstem motor nuclei (cortico-brainstem motor neurons); S1 SCPN project to the trigeminal principal sensory nucleus and dorsal column medullary nuclei (corticobulbar projection neurons); and visual cortex SCPN project to the optic tectum (OT) (corticotectal projection neurons). Neurons that send projections to multiple targets (see the figure, part **d**) can sometimes be classified into more than one of these categories. Examples include CPN with frontal projections, which extend axons to the contralateral hemisphere and to the ipsilateral frontal cortex; SCPN with backward projections, which extend axons to subcerebral targets and to the ipsilateral caudal cortex; and intratelencephalic corticostriatal projection neurons, which extend projections to the contralateral hemisphere and to the ipsilateral striatum (Str). Other neurons that project to multiple targets, such as pyramidal corticostriatal projection neurons, can be classified into only one category. A1, primary auditory cortex; Crb, cerebellum; OB, olfactory bulb; Th, thalamus (taken from [39]).

caudal neocortical regions, subpopulations of CPN send dual projections to contralateral or ipsilateral S1 (Backward PN; BPN), and rostrally, to contralateral or ipsilateral frontal areas (Frontal PN; FPN) [160-162].

CPN with a single contralateral projection reside in layer II, III, layer V and to a lesser extent in VI, whereas CPN with dual projections reside preferentially in deep layers of the neocortex [160]. For instance, CStrPNi reside almost exclusively in layer Va [161]. While deep layer CPN have long distance dual axonal projections, superficial layer CPN participate in local circuitry within cortical columns. Ipsilaterally, superficial layer CPN send collaterals to pyramidal neurons in layers II-III, V and VI. Thus, in addition to their role in integrating two homotopic regions of the neocortical hemispheres, CPN are also responsible for functional association and integration among different neuronal types in ipsilateral and contralateral hemispheres [163].

CPN establish exuberant projections early in development, with maximum number of dual projections at postnatal day 8 (P8) [160, 164, 165]. These dual projections are progressively refined until P21, through activity-dependent

mechanisms [164, 165]. Finally, CPN arose relatively recently in evolution, since they first appeared in placental mammals. Their broad laminar distribution not only reflects a broad time window of generation, but also suggests preferential expansion of this neuronal population throughout evolution [147, 148]. Indeed, a large portion of CPN with known heterotopic long-range dual-projecting axons reside in deep neocortical layers, suggesting that deep-layer CPN might have been co-opted from existing populations of CFuPN, during evolution, to project not only to subcerebral targets but also to cortical ones to connect and integrate the two neocortical hemispheres [148].

## **2. Corticofugal Projection neurons (CFuPNs)**

In contrast to CPN, CFuPNs send their axons away from the cortex. CFuPNs can be further subdivided into subplate and corticothalamic neurons, which form together the subcortical PNs and project to the thalamus, and subcerebral projection neurons, which extend their primary axons to targets in the midbrain, hindbrain and spinal cord [148, 166]. These distinct subtypes of cortical projection neurons are born in a tightly orchestrated sequence and reside in distinct laminar locations in the neocortex [15, 167]. Subcortical and subcerebral projection neurons are confined to deep cortical layers (layers V, VI, and subplate). CFuPNs are exclusively generated during the first few days of murine neocortical development.

### **a) Subplate neurons (SP)**

Subplate neurons are born around E11.5 in the mouse. They form the deepest cortical layer, the subplate, and send pioneering subcortical projections toward the thalamus, forming the first corticofugal tract [168, 169]. Although subplate and corticothalamic PNs share the same targets, these two neuronal subtypes have distinct functions and fates. In most species, SP neurons die postnatally, but they are thought to play a critical developmental role in instructing corticothalamic and thalamocortical connectivity [168, 170].

### **b) Corticothalamic neurons (CThPNs)**

Corticothalamic PNs are born around E12.5. Contrary to subplate neurons, CThPNs

persist throughout life in layer VI and establish permanent connections between the cortex and the sensory and motor thalamic nuclei. As previously mentioned, all cortical areas receive thalamic input and send projections to the thalamus [171], through reciprocal connections formed by TCA and CTA, representing a highly integrated processing unit that dynamically regulates thalamic transmission of peripheral information for cortical processing [172]. CThPNs reside in layer VI with a smaller population in layer V. TCA and CTA contribute to form the internal capsule (IC), a large axonal highway, which also comprises output subcerebral axons proceeding toward the cerebral peduncle and the pyramidal tract [15, 173, 174].

Layer VI CThPN innervate thalamic nuclei depending on their tangential identity, projecting to the first order thalamic nuclei from which they receive sensory input. Thus, CThPN from the V1 project to the dLGN, while CThPN from S1 innervate the VPM, CThPN from A1 project to the MGv and CThPN from the M1 project to the VL [175-178]. These CTA form numerous glutamatergic synapses on the distal dendrites of the relay cells, modulating their activity and gating pathways that transmit peripheral information. Layer VI CTAs send also collaterals to the reticular thalamic nucleus, generating an inhibitory circuit modifying the activity of relay cells [172, 179, 180]. In addition, collaterals from layer V corticobulbar and corticospinal motor neurons send inputs to higher order thalamic nuclei (pulvinar group, mediodorsal thalamic group and lateral posterior nucleus), through glutamatergic synapses on matrix cells. Higher order thalamic nuclei, in turn, project excitatory fibers to the upper and lower layers of the corresponding cortical areas distributing cortico-cortical information, and integrating different cortical areas into a global synchronized network [172, 181].

### **c) Subcerebral projection neurons (SCPNs)**

SCPNs are born around E13.5 [157]; SCPNs migrate to the deeper layer V and its production ceases after E14.5 [15, 166]. Even if all SCPNs share a common laminar position and are born within the same developmental time frame, they are quite diverse and include several unique subtypes.

Cortico-Spinal Motor Neurons (CSMN) are large pyramidal neurons that reside in sensory and motor areas and extend their primary axons to the spinal cord, with some secondary collaterals to the striatum, red nucleus, caudal pons and medulla.

Instead, Corticopontine PNs extend a primary axon to hindbrain targets in the pons and medulla. Finally, Corticotectal PNs reside mainly in the visual cortex and extend their primary axon to the superior colliculus in the midbrain [15, 66, 166]. All SCPN normally extend a primary axon through the internal capsule and the pyramidal tract to the spinal cord (inappropriate connections are later pruned) such that subcerebral PNs in the sensorimotor cortex project to the caudal pons and spinal cord, while those in the visual cortex project to the rostral pons and superior colliculus [182-184]. Since SCPN have a common pattern of initial development, it is not surprising that many transcription factors regulating their early specification and differentiation are co-expressed in their distinct subtypes. The most well studied subtype of SCPNs is the CSMN, whose molecular, physiological and morphological features have been extensively characterized [185, 186].

CSMNs are of great interest because they control voluntary movements in humans; their degeneration is a key factor in motor neuron degenerative diseases, including amyotrophic lateral sclerosis (ALS). CSMN injury contributes centrally to the loss of motor function following spinal cord injury [66, 149]. Among the different subcerebral axonal tracts, the corticospinal tract is one of the longest longitudinal projections in the vertebrate central nervous system, and the major output from the motor cortex connecting the cerebral cortex to the spinal cord [185, 186].

CSMNs extend their axons ipsilaterally via the internal capsule, descending to the cerebral peduncle, through the midbrain and hindbrain, until they reach the most caudal part of the hindbrain, where most of them, cross the midline dorsally toward the contralateral side, and form the pyramidal decussation. They further project in a region containing the dorsal funiculus in rodents, and innervate neurons located in the spinal gray matter. Some of them do not decussate in the medulla, but continue downward in the ventral funiculus and decussate just prior the spinal gray matter. The complete trajectory reaches a maximum level of gray matter spinal cord innervation at P14 in mice. Then, this connectivity is gradually refined in the following weeks. Once fully developed, it allows the execution of precise voluntary movements [187-191].

Layer V neocortical PN, callosal or subcerebral, send collaterals either ipsilaterally or contralaterally to the striatum; therefore, they are considered as corticostriatal projection neurons.

### 3. **Corticostriatal projection neurons (CStrPN)**

Corticostriatal PN project from the neocortex to ipsilateral or contralateral striata, and are the cortical efferents of the corticobasal ganglia circuitry. Connectivity between cortex and striatum is directional; cortex connects mono-synaptically to the striatum, while the striatum communicates only indirectly to the cortex, via polysynaptic downstream circuits.

Corticostriatal projections are crucial components of forebrain circuitries, and are widely involved in motivated behavior, cognitive and motor functions, which include for instance, action selection, motor control, sequence learning and habit formation [192-194]. CStrPN are clinically important since their injury and degeneration are implicated in the pathophysiology of several neurological disorders. They are the cortical population that predominantly degenerates in the Huntington's disease. Their impairment contributes to multiple forms of cerebral palsy [195-202].

CStrPNs are formed by two distinct classes of neurons: The intratelencephalic IT-type CStrPNs (CStrPNi) project to targets within the telencephalon. They have the unique attribute of being both corticofugal because they project to the striata bilaterally, and callosal because their axons cross the midline. They possess dual callosal and corticofugal anatomic and molecular characteristics, suggesting that they might be evolutionary "hybrids" with both callosal and corticofugal features [203]. They are located in layer Va of the neocortex. In mice, they are born between E12.5 and E14.5; they can be distinguished from pure callosal around P3-P4 when they first invade the contralateral striatum [203]. In addition to CStrPNi, there is another population of subcerebral projection neurons (corticospinal and related corticobrainstem) that sends axon collaterals to the ipsilateral striatum, the co called pyramidal tract-corticostriatal projection neurons (PT-CStrPN). PT-CStrPN are only restricted to layer Vb [193, 194, 203]. Finally, it is important to recall that CStrPN are either IT or PT but not both (**Figure 11**).

PT-type and IT-type are neurochemically, morphologically and electrophysiologically distinct pyramidal neuron types [204]. For example, PT-type neurons are larger than IT-type in the rat cortex. These two neuronal populations also differ in their dendritic arborization. While PT-type have a prominent apical dendrite, that ascends and branches profusely in layer I of the cortex, IT-type are more slender and their arborization in layer I is sparser [193].

Moreover, PT-type and IT-type neurons have different electrophysiological activity, they convey distinct signals to the striatum. For instance, PT-type neurons in primates are three to four times more rapid than IT-type [161, 205-208]. In addition, in the motor cortex, PT-type fire during movement, while IT-type fire in relation to movement planning [206, 208, 209]. There is growing evidence, that imbalance between the two classes of CStrPN, the intratelencephalic (IT) versus pyramidal tract (PT), is an etiological factor of neurodevelopmental, neuropsychiatric and motor disorders, including autism, amyotrophic lateral sclerosis, obsessive-compulsive disorder, schizophrenia, Huntington's and Parkinson's diseases and major depression (Reviewed in [194]).

## **B. Neocortical projection neuron specification**

### **1. Corticofugal fate determination**

SCPNs and CThPNs are closely related subtypes of CFuPN, residing in deep layers of the neocortex and are sequentially generated early in corticogenesis. Substantial plasticity exists in the specification of these two subtypes, and in the absence of critical molecular controls, each of them can expand at the expense of the other (**Figure 12**).

#### **a) SCPN fate specification**

A relevant work by Arlotta et al [66] have led to the identification of genes controlling SCPN specification, in particular CSMN, by purifying CSMN at distinct stages of development, and comparing their gene expression to two other neuronal populations: callosal and corticotectal PNs. This work identified Ctip2, Fezf2, SRY-box-containing gene 5 (Sox5), Orthodenticle homeobox 1 (Otx1), Ets-Related Protein

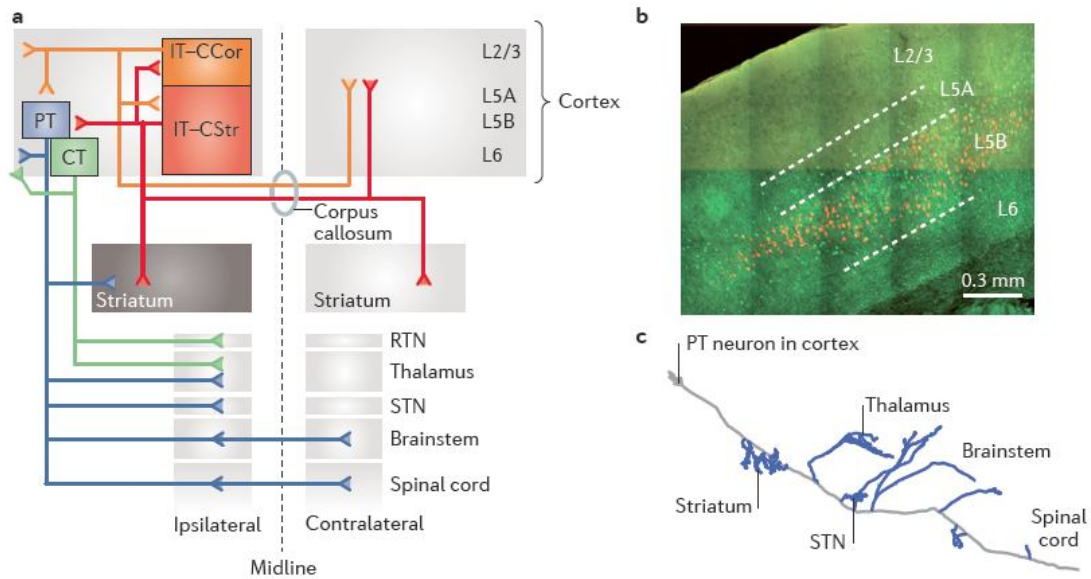


**Figure 11-Long-range axonal projections define two classes of Corticostriatal neurons.**

**a** | pyramidal tract (PT) neurons (blue) project to ipsilateral striatum, thalamus, subthalamic nucleus (STN) and many brainstem and spinal cord regions. PT neurons also project to contralateral brainstem and spinal cord. Intratelencephalic (IT) neurons project ipsi- or bilaterally (via corpus callosum) within the cerebral hemispheres to cortex (IT-C-Cort orange), and many IT neurons also project to striatum (IT CStr; red). The ipsilateral striatum (black) is unique in receiving CStr input from both IT and PT neurons. Layer 6 (L6) corticothalamic neurons (CT; green) project subcortically only to thalamus and its reticular nucleus (RTN). **b** | retrogradely labeled spinally projecting PT neurons and callosally projecting IT-CStr neurons in mouse motor cortex. IT (green) and PT (orange) neurons are intermingled in L5B, but are not double labeled. **c** | Single PT neuron's axon is multiprojectional sending branches to many subcortical areas (blue) (taken from [194]).

81 (Er81), insulin-like growth factor binding protein 4 (Igfbp4), cysteine rich transmembrane BMP regulator 1 (Crim1) and many others [66] as SCPN specific genes. Later, the roles of some of these genes were investigated, and it was revealed their crucial involvement in SCPN specification. Diverse studies have shown that the specification and differentiation of SCPN are directed by a combinatorial code of TFs including Fezf2, Ctif2 and SRY-box-containing gene 5 (Sox5).

(1) *Fezf2*

*Fezf2* is a zinc finger TF, crucial for SCPN specification; it is expressed by a subset of progenitors during deep layer PN generation and is expressed at high levels by all post-mitotic subcerebral PNs throughout adulthood [63-67, 210]. In the absence of *Fezf2* function, in null mutant mice, the entire population of layer V pyramidal subcerebral PN is absent. Moreover, expression of SCPN specific genes is lost, and there are no projection neurons from the cerebral cortex to either the spinal cord or brainstem [65, 67]. Importantly, without *Fezf2*, neocortical progenitors still produce similar numbers of layer V neurons [65, 210], however, using a *Fezf2* mutant with a human placental alkaline phosphatase inserted at the *Fezf2* locus, the authors demonstrated that these neurons adopt CPN-like properties, by extending axons across the midline via the anterior commissure, and expressing the CPN-specific molecular marker Special AT-rich sequence-binding protein 2 (*Satb2*) [211], a critical factor in the specification of CPN identity [150, 212]. In addition, more neurons in layer V display electrophysiological characteristics typical of CPNs [65, 210]. In contrast, superficial-layer pyramidal neurons are born correctly and appear normal [65, 210]. Therefore, *Fezf2* does not affect the ability of progenitors to generate layer V glutamatergic neurons, it likely acts in directing the specification, and defining characteristics of SCPN. Moreover, *Fezf2* appears to repress *Satb2* expression, directly or indirectly, repressing thereby callosal identity. Furthermore, misexpression of *Fezf2* by *in utero* electroporation causes layer II/III CPN to redirect their axons towards a broad set of subcerebral targets, including brainstem, spinal cord but also thalamus [65, 67, 211, 213]. These data further support the involvement of *Fezf2* not only in the specification of SCPNs, but also in determining general CFuPN identity (as it will be discussed below).

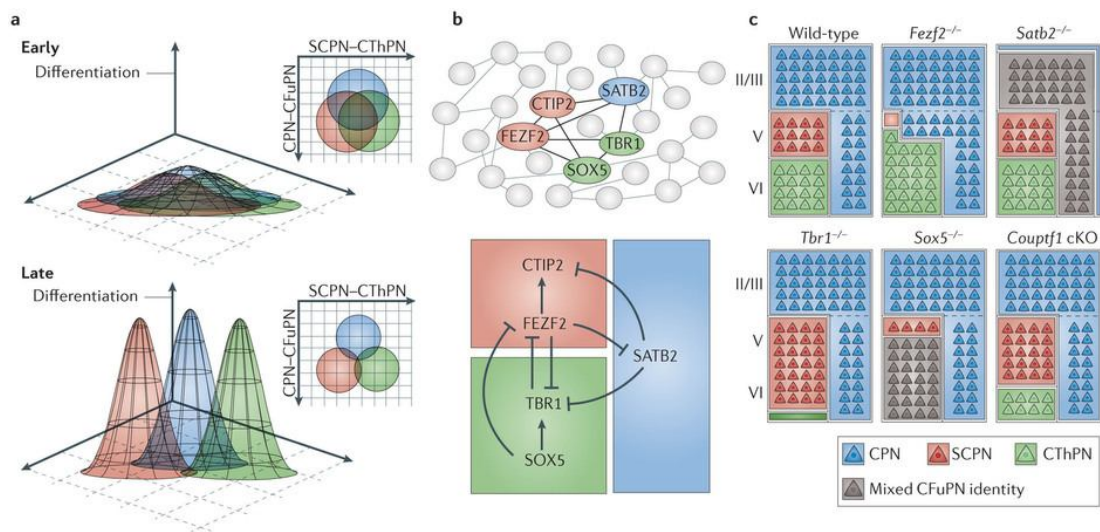


**Figure 12- Competing molecular programmes direct differentiation of newly postmitotic projection neurons into one of three broad subtype identities.**

**a** | The subtype identities of postmitotic projection neurons are depicted within a theoretical  $n$ -dimensional ‘subtype space’ in which individual subtype identities (as defined by gene expression, morphology, dendritic structure, projection patterns, physiology and other characteristics) occupy distinct coordinates. Boundaries between these identities, which prevent neurons of one subtype from taking on characteristics of another subtype, are established by the action of cross-repressive molecular controls. One boundary exists between neurons specified as subcerebral projection neurons (SCPN) and those specified as corticothalamic projection neurons (CThPN), and another exists between corticofugal projection neurons (CFuPN) (SCPN and/or CThPN) and callosal projection neurons (CPN). Early in corticogenesis, undifferentiated neurons have largely overlapping subtype identities (top). As development proceeds, neurons differentiate and subtypes become more distinct from each other (bottom). **b** | Known molecular controls form key nodes of an elaborate transcriptional network, which is only beginning to be elucidated (top). Arrows indicate known cases of genetic or transcriptional activation or repression, and further interactions and molecular controls remain to be identified (bottom). **c** | Changes in expression of these key regulators can cause boundaries between subtypes to shift, with neurons partially or completely acquiring features characteristic of other subtypes. In some mutants (for example, *Satb2*-null (*Satb2*<sup>-/-</sup>) and *Sox5*<sup>-/-</sup>), neurons acquire CFuPN identity generally rather than a well-defined CThPN or SCPN identity. The boundaries between CFuPN and deep-layer or superficial-layer CPN (represented by dashed lines) may shift independently of one another. *Couptf1* cKO, chicken ovalbumin upstream promoter transcription factor 1-conditional-knockout (*Couptf1*<sup>fl/fl</sup>; *Emx1-Cre*) mice; CTIP2, COUP-TF-interacting protein 2; FEZF2, fez family zinc finger 2; SATB2, special AT-rich sequence binding protein 2; SOX5, SRY-box containing protein 5; TBR1, T-box brain protein 1 (taken from [39]).

A second set of genes controls later aspects of SCPN development, possibly acting downstream of *Fezf2*. The most studied and, probably, one of the most important members is *Ctip2*.

(2) *Ctip2*

*Ctip2* (also known as *Bcl11b*) is a zinc finger transcription factor that acts as a transcriptional repressor [214, 215]; it begins to be expressed at high level in all post-mitotic SCPNs, once they reach the cortical plate [66]. *Ctip2* is a major downstream effector of *Fezf2*, in regulating the extension of axons toward subcortical targets [211]. *Ctip2* is not expressed in layer V of *Fezf2 null* mutant mice and it can rescue the axonal phenotype of *Fezf2* mutants [211].

*Ctip2* is a crucial regulator of subcerebral axon extension and collaterals refinement [66, 211]. In *Ctip2* mutant mice, SCPN are still born and migrate to layer V, however they exhibit defects in fasciculation, outgrowth and pathfinding. SCPN axons fail to reach the spinal cord, as they are misrouted in the forebrain; they rarely reach the pons and never reach the pyramidal decussation [66]. Moreover, reduced *Ctip2* expression in heterozygous mice results in a defective pruning of transient projections to the spinal cord from SCPN residing in the somatosensory cortex, further demonstrating different roles for this TF at different levels of expression [66].

Interestingly, *Ctip2* also controls proper differentiation of striatal medium spiny neurons (MSN), and the organization of their patch matrix, which is traversed by CSMN axons. *Ctip2* controls also the expression of a set of axons guidance signals by MSN, suggesting an additional non-cell autonomous function for *Ctip2* in CSMN axon growth and fasciculation [216]. All these data identified *Ctip2* as a crucial regulator of SCPN axon extension and their collaterals refinement.

Although *Ctip2* activation by *Fezf2* is critical for SCPN development, several transcriptional controls over CPN, CThPN and subplate development, including *Satb2* [150, 212], *Sox5* [166] and COUP-TFI [134], operate at least in part by repressing *Ctip2* expression, suggesting that *Ctip2* is a critical target for transcriptional regulation during the development of neocortical PNs.

(3) *Sox5*

*Sox5* is a TF belonging to the SRY-box-containing gene family. *Sox5* is expressed at high levels in layers V, VI and subplate in all CFuPNs, and is lacking in almost all CPNs [166, 217]. *Sox5* controls the sequential generation of CFuPN subtypes, including subplate cells, CThPNs and SCPNs, by repressing high level expression of SCPN genes, such as *Fezf2* and *Ctip2*, until the generation of subplate and CThPN is concluded, and preventing premature generation of SCPN during early stages of corticogenesis [166]. It has been shown that *Sox5* directly represses *Fezf2* expression by binding to an enhancer element required for *Fezf2* expression in the forebrain [218]. To support its role in specifying CFuPN identity, ectopic *Sox5* expression in upper layer neurons prevented them from extending axons across the corpus callosum, and stimulated the extension of corticofugal axons [166].

*Sox5* loss-of-function causes a striking overlap among the three principal CFuPN subtypes. In *Sox5 null* cortices, subplate neurons aberrantly develop molecular hallmarks and connectivity of SCPN, while SCPN axons show pathfinding defects, including extensive defasciculation in the midbrain and formation of an accessory subcerebral tract that projects through the external capsule, suggesting that *Sox5* is crucial to control SCPN timing of generation, and connectivity [166, 217].

(4) *Otx1: A gene controlling the refinement and pruning of SCPN*

Another key TF known to function in the choice of final SCPN targets is *Otx1*, which is a homeodomain TF, expressed in putative deep-layer progenitors in the VZ, and exhibiting a decreasing level of expression in the VZ during the generation of superficial-layer neurons [63, 219]. As deep-layer PN mature, *Otx1* localization shifts from the cytoplasm to the nucleus [219, 220]. Post-natally, *Otx1* is expressed by 40-50% of layer V SCPN primarily within the visual cortex, while it is completely absent from CPN [219]. In the absence of *Otx1* function, defects in corticotectal PN development are observed. Corticotectal PNs maintain collaterals to the spinal cord and caudal pontine nuclei, which are normally pruned during late stages of their differentiation [219]. This indicates that *Otx1* has a later role in SCPN development

than *Fezf2* and *Ctip2*, possibly in controlling the refinement and pruning of axonal collaterals.

**b) Corticothalamic PN fate specification:**

(1) *Fezf2, Ctip2 and Sox5*

Similar to layer V SCPN, the fate of layer VI CThPN is at least in part specified by the expression of *Fezf2*, *Ctip2* and *Sox5*. *Fezf2* and *Ctip2* are expressed at lower levels by layer VI CThPNs and subplate neurons [63-67, 210]. In *Fezf2 null* mice, CThPN and subplate neurons appear to be disorganized, and a number of specific CThPN genes including protein phosphatase 1, regulatory subunit 1B (*Ppp1r1b*), transducing like enhancer of split 4 (*Tle4*) and Forkhead box P2 (*Foxp2*), fail to be expressed [65, 210]. This strongly indicates that low level of *Fezf2* expression by CThPN and subplate neurons is necessary for precise differentiation of these populations, and that the level of *Fezf2* protein is directly linked to its function, and exerts different functions in distinct neuronal populations in a dose-dependent manner.

Moreover, in the absence of *Fezf2* function, the expression of the T-box brain protein 1 (*Tbr1*), a transcription factor crucial for CThPN development, expands into presumptive layer V, and many of these *Tbr1*-positive cells project to the thalamus, (whereas others are converted to CPNs as discussed above). Thus, *Fezf2* specifies SCPN identity at least in part by repressing CThPN fate.

*Sox5* regulates the differentiation of the three CFuPN subtypes; it is normally expressed by layer V SCPN, layer VI CThPN and subplate neurons and seems to control the timing of generation of layer V SCPNs by repressing *Ctip2* in layer VI and subplate [166, 217]. It was hypothesized that *Sox5* acts in combination with different expression levels of *Tbr1* and *Ctip2* in controlling the specific identities of layer VI and subplate neurons [166]. In *Sox5 null* mice FOG family member 2 (*Fog2*) and *Ctip2*, respectively expressed by CThPNs and SCPNs, are co-expressed by a single population of neurons with mixed SCPN and CThPN features (indicating imprecise differentiation), whereas corticothalamic projections are severely compromised [166, 217].

Another Key TF having a key role in the molecular mechanisms regulating the development of layer VI CThPNs and subplate neurons is Tbr1.

(2) *Tbr1*

Tbr1 is a T-box TF, highly expressed in subplate and layer VI postmitotic neurons during early corticogenesis [221]. Tbr1 expression is highest in the rostral cortex, but it seems to specify layer VI neurons along the whole cortex [221]. Genetic manipulations have shown that Tbr1 is necessary for the differentiation of layer VI and preplate neurons. In *Tbr1 null* mice, indeed, the subplate is morphologically indiscernible, subplate specific genes fail to be expressed and CTAs are absent. Moreover, layer VI neurons that would normally develop into CThPNs express aberrantly high levels of *Fezf2* and *Ctip2*, and other SCPN specific genes, and they project to the spinal cord, [143, 221-224]. In addition, Tbr1 misexpression in layer V neurons suppresses *Fezf2* expression and prevented layer V neurons from extending axons to subcerebral targets [223, 224]. Thus, Tbr1 gene acts in opposition to *Fezf2* and *Ctip2* to specify CThPN identity. In support of this, Tbr1 directly binds to *Fezf2* locus and represses its activity in layer VI CThPNs to restrict the birth of the corticospinal projections to layer V. Hence, Tbr1 functions, at least in part, by preventing SCPN specification in layer VI [223, 224].

c) **Callosal PN fate specification:**

CFuPNs share a sort of developmental boundary with CPNs, since a subpopulation of CPNs resides in deep layers (V and VI), which are generated during the same temporal window. From the time CFuPN and CPN axons exit the cortical plate, they follow dramatically divergent trajectories, one away from the cortex and the other toward the midline [39, 225]. Thus, some critical controls over CFuPN and CPN development largely function by repressing molecular programs that would instruct the alternative fates. Because the majority of CPN reside in superficial layers, the first known molecular controls over CPN generation and development were laminar specific genes.

(1) *Satb2*

Special AT-Rich Sequence-Binding Protein 2 (*Satb2*) was the first identified key regulator of CPN specification. *Satb2* is a DNA binding TF, showed to bind AT-rich DNA sequences [226-228]. *Satb2* is expressed by a subset of neurons in all cortical layers, with a prominent expression in layers II-V, but not in SVZ progenitors [150, 212, 226]. It is expressed at high levels by CPNs, and probably also by associative neurons throughout cortical layers [150, 212].

Two independent laboratories inactivated *Satb2* in the mouse and characterized its cortical phenotype [150, 212]. In *Satb2 null* mice, almost no axons cross the corpus callosum, even though establishment of the midline appears normal. Instead, some neurons expressing *Satb2* in normal conditions project towards the spinal cord and brainstem [150, 229]. Moreover, absence of *Satb2* function leads to a loss or a severe reduction of genes characteristic to CPN, including *Cdh10*, *Dkk3*, *Sip1* and *Cux1*. In contrast, upper layer neurons in these mice express high levels of *Ctip2*, and a number of other genes typical of SCPN, including *Clim1*, *Cdh13* and *Grb14* [150, 212]. Furthermore, ectopic *Satb2* expression markedly reduces the number of *Ctip2*-expressing cells and alters the projections of deep layer neurons [150, 212]. These data showed that *Satb2* is required for CPN specification by repressing *Ctip2* expression.

It is known that *Satb* TFs regulate gene expression by binding AT-rich sequences of matrix attachment regions (MARs), promoting higher-order chromatin organization and facilitating long range interactions between enhancers and promoters [150, 212, 227, 228, 230-232]. Chromatin Immunoprecipitation (ChIP) experiments demonstrated that *Satb2* protein binds to the upstream regulatory region of *Ctip2*, both *in vitro* and *in vivo*. Co-Immunoprecipitation (CoIP) experiments revealed that *Satb2* interacts with the members of the Nucleosome Remodeling Deacetylase (NURD) complex, such as Histone Deacetylase 1 (HDAC1, belonging to a class of enzymes involved in deacetylation of hyperacetylated histone tails leading to compaction of protein and transcriptional repression [233]) and the Metastasis-Associated 1 family member 2 (MTA2), in the developing cortex. Moreover, *Satb2* deletion leads to the hyperacetylation of the *Ctip2* locus and reduces HDAC1 and MTA2 levels at this locus (**Figure 13**). Thus, *Satb2* is required to recruit the NURD complex to the *Ctip2* locus. The NURD complex in turn deacetylates histones in the vicinity, converting the

chromatin to an inactivate state. This indicates that Satb2 downregulates Ctip2 expression via the assembly of a NURD chromatin-remodeling complex at the Ctip2 locus [212, 232].

Moreover, the transcription co-regulator sarcoma viral oncogene homologue (Ski) has been shown to be a critical component of the repressor complex recruited by Satb2 to initiate HDAC1-dependent chromatin remodeling [234]. Ski protein is expressed in distinct subtypes of neocortical progenitor cells from E10.5 and in projection neurons. In upper layers, Ski and Satb2 are largely co-expressed, while in deep layers the percentage of Ski-positive cells that express Satb2 is lower. Interestingly, *Ski null* mice mimic the phenotype shown by *Satb2-null* mice. In the

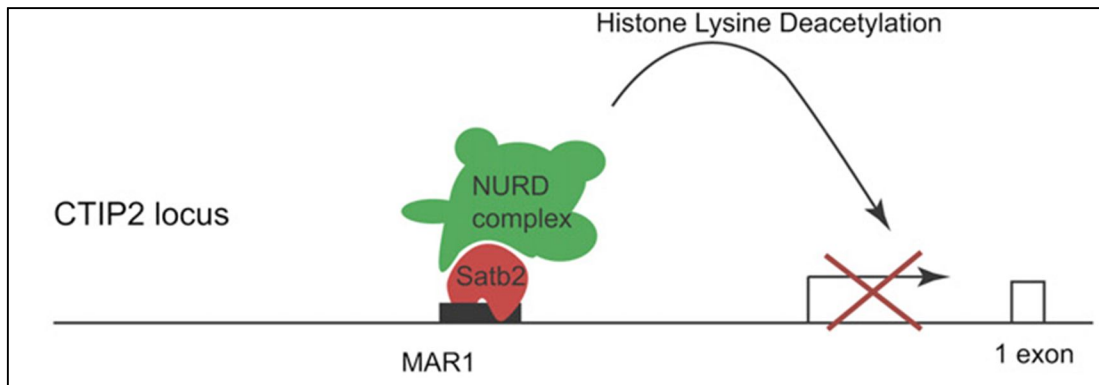


**Figure 13- Satb2 protein interacts with both the CtIP2 promoter upstream region and histone deacetylase complex and controls chromatin remodeling.**

Model of Satb2 function in the cortical lamination. Satb2 is required to assemble NURD chromatin remodeling complex on CtIP2 locus. This induces deacetylation of histones and inactivation of CtIP2 expression (modified from [212]).

absence of Ski, CPNs redirect their axons to subcerebral targets similarly to *Satb2 null* mice. In the absence of Ski, upper layer Satb2-positive neurons ectopically express Ctip2, and other deep layer-specific genes, such as *Clim1*, *Ldb2* and *Cdh13*, but not *Fezf2*, suggesting that Ski-deficient CPNs acquire some but not all SCPN characteristics.

In addition, the expression of CPN specific genes (such as including *Lmo4*, *Cdh10* and *Ptn*) was also up-regulated upon loss of Ski, revealing further changes in the regulation of CPN genetic program. Finally, ChIP, Co-IP, antibody based proximity ligation assay (PLA), and luciferase reporter transfection essays demonstrated that, although Satb2 directly binds to MAR sequences in the Ctip2 locus and recruits MTA2 independently of Ski, this latter factor is essential for attracting HDAC1, thereby allowing the NURD complex to form properly, and enabling the Satb2-containing protein assembly to act as an inhibitory complex [234] (**Figure 14**).

## (2) *Genes identifying distinct CPN subpopulations*

A study from Molyneaux and colleagues [70] defined a set of genes that identify and molecularly categorized distinct populations of CPN during embryonic and post-natal development. On the one hand, they showed that genes highly expressed at early stages of CPN development (before E18.5 in mouse), such as *Inhba*, *Btg1*, *Frmd4b*, *Epha3* and *Ptn*, likely act during neuronal subtype specification, differentiation, migration or initial axonal extension. On the other hand, they suggested that genes with expression that rises and falls at mid-stages of CPN development such as *Cpne4*, *Tmtc4*, *Nnmt*, *Cav1*, *Nectin-3* and *Chn2*, might function at the time when CPN have already crossed the midline, and are extending toward specific targets. Finally, they reported that genes expressed in late CPN development, such as *Plexin-D1*, *Gfra2*, *TcrB* and *Dkk3*, might function in final stages of CPN maturation and their axonal refinement during adulthood [70]. In addition to a temporal classification, this work identified CPN genes specific to most CPN in all layers including *Lpl*, *Hspb3*, and *Cited2*, and others discriminating between lower layers CPN, including *Plexin D1*, *Gfra2*, *Tcrb* and *Dkk3*, and upper layers including *Inhba*, *Limch1*, *Cpne4*, *Tmtc4* and *Btg1* [70].

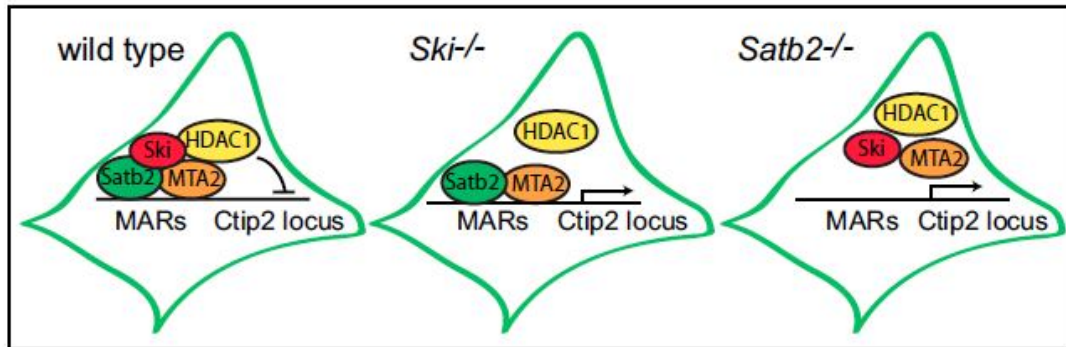


**Figure 14- Ski associates with Satb2 and represses Ctip2 transcription in cortical neurons.**

Model for Ski function at the Ctip2 locus in callosal projection neurons. Ski is required to assemble a functional NuRD repressor complex containing Satb2, MTA2, and HDAC1 at MAR sites in the Ctip2 locus. In the absence of Ski, Satb2 still binds the regulatory DNA sequences together with MTA2, but recruitment of HDAC1 is impaired. In the absence of Satb2, the NuRD complex is not assembled. Thus, Satb2 and Ski play specific roles in the formation of a functional NuRD complex, and individual loss of these factors prevents transcriptional repression of Ctip2 in callosal projection neurons. Modified from [234].

(3) *Genes involved in upper layer specification: Brn and Cux*

The POU domain TFs Brn1 (Pou3f3) and Brn2 (Pou3f2) expressed in superficial layers promote the birth of upper layer neurons. In Brn1 and Brn2 double mutants, superficial layer pyramidal neurons are not generated [235, 236].

Moreover, TF Cut-like homeobox 1 and 2, Cux 1 and Cux2 are expressed in SVZ cells and in their progeny in layers II-IV [68, 69]. The analysis of Cux2 knockout (KO) animals revealed Cux2 function in SVZ formation, as it promotes cell cycle exit of SVZ cells [237]. Moreover, Cux1 and Cux2 also regulate dendrite branching, spine development and synapse formation specifically in layer II/III CPNs [237]. Since most CPNs lie in superficial cortical layers, Brn and Cux genes could be involved in controlling their generation.

## **VI. Neocortical projection neuron: Callosal versus Subcerebral axon guidance control**

Neocortical neurons form connections through specific and predetermined trajectories in the brain in response to several guidance cues present in the environment.

These guidance factors determine the direction of neocortical axons to different cortical or subcerebral targets. Neurons express specific combinations of receptors for secreted ligands, mediating either a chemoattractive or chemorepulsive response.

### **A. Callosal projection neurons**

A wide diversity of developmental processes regulates the midline crossing of callosal axons. When they are still migrating to the cortical plate, CPNs send axons away from the cortex. They are in part guided by guidance factors such as Semaphorin (Sema) 3A, which repels axons away from the cortical marginal zone [238]. Once they reach the intermediate zone, callosal axons turn toward the midline rather than projecting laterally as corticofugal axons do. This key decision point is regulated by the action of Sema3A [239]. Then, CPN axons approach the midline in a ventral trajectory through the cingulate cortex and abruptly turn to cross the midline at the corticoseptal boundary. This process is initiated by pioneering axons from the cingulate cortex that begin the process of midline crossing and act as pioneers for neocortical CPN axons

and guide them most probably by providing a structural framework to follow by direct axon-axon contact [240-244]. This process is mediated by Neuropilin 1 (Npn1) [245, 246], which is also expressed by cingulate pioneering axons and has been shown to be involved in corpus callosum formation [246-248].

It has been also shown that Netrin-1 initially attracts callosal pioneering axons, but it is not attractive for neocortical callosal axons [249]. Instead, Netrin-1 attenuates slit-roundabout axon guidance receptor (Robo) repulsion in pre-crossing callosal axons to allow them to cross the midline of the developing brain [247].

Once arrived at the midline, callosal axons are guided by midline glial structures such as the glial wedge and the indusium griseum, by neurons in the subcallosal ring [250], and by short-range guidance molecules of the ephrin (Eph) family [251]. The glial wedge is a bilaterally symmetrical glial structure that releases a cocktail of repulsive molecules, such as Slit homolog 2 (Slit2), Draxin, and Wnt 5A preventing the ventral growth of CPN axons into the septum [252-258]. While, the indusium griseum, which is a region of the hippocampus constituted by neurons and glia positioned dorsally to the corpus callosum and expressing slit2, acts as a dorsal repulsive barrier for CPN axons [253].

Upon encountering the contralateral glial wedge, CPN axons turn dorsally to enter the contralateral cingulate cortex and extend into the contralateral cortex toward their homotopic regions. This mechanism is still largely unknown; although it has been proposed that callosal axons follow the trajectory of the radial glia as they extend their axons to appropriate targets [245]. Finally, the pattern and maintenance of CPN projections is likely to be sculpted by activity-dependent mechanisms [259]. When callosal axons fail to cross the midline, they remain ipsilateral and form probst bundles, which are longitudinal axon fascicles, product of callosal axon misguidance [149].

Even if adhesion molecules and axon guidance receptors are well studied, the relationships between transcription factors and these effectors that determine the terminal differentiated state of a neuron are mostly unknown. A recent study showed the contribution of Unc-5 Homolog C (*C. Elegans*) (Unc5C) and deleted in colorectal carcinoma (DCC) in the corpus callosum formation. But most importantly, the authors demonstrated that these two Netrin-1 receptors are directly repressed by Satb2 and Ctip2, respectively [260].

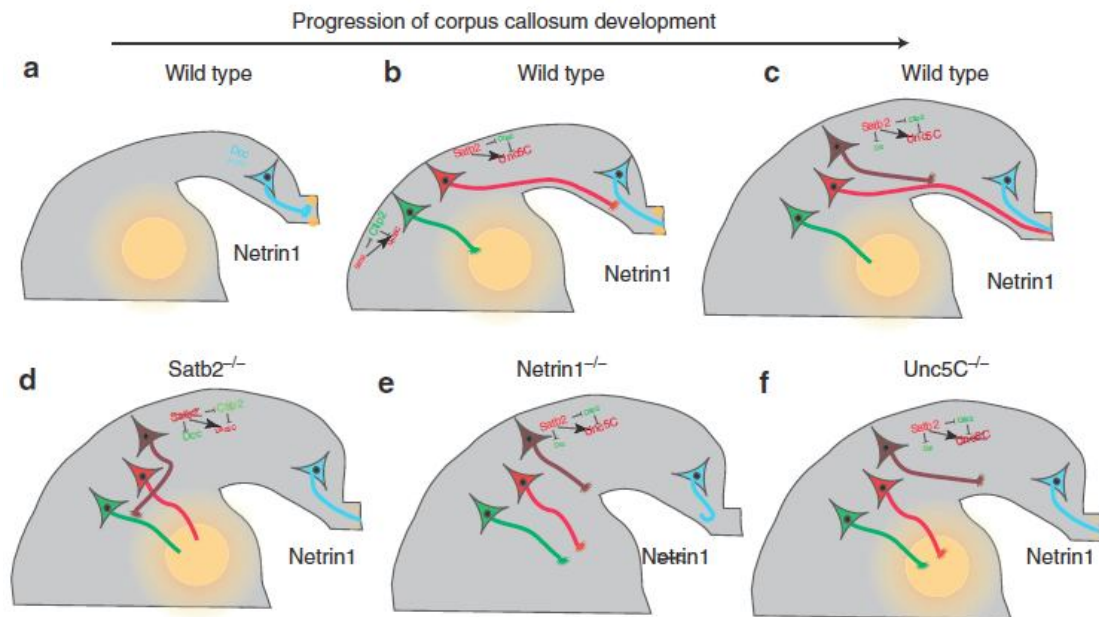


**Figure 15- Satb2- and Ctip2-dependent establishment of cortical connections.**

(a) During early corticogenesis, cingulate neurons with high DCC expression form the pioneer axons for the CC. These axons respond to midline Netrin1 and are attracted towards the Netrin1 source. (b) Later, when Layer V cells start projecting medially, Satb2 represses Ctip2, thereby promoting Unc5C expression. These Unc5C axons are repelled by the Netrin1 source in the internal capsule and thus turn towards the midline. Corticofugally projecting neurons, however, express high Ctip2 and thus repress Unc5C. In addition, the lack of repression of DCC by Satb2, promotes high DCC levels in these neurons. Thus, these axons are attracted towards the internal capsule (c). Despite expressing high levels of Unc5C and low levels of DCC, upper layer neurons are not dependent on these molecules and instead either follow the deep layer callosal pioneer axons or are dependent on other axon guidance molecules. (d–f) Represent the scenario in the Satb2, Netrin1 or Unc5C mutants, respectively. In each of the mutants, the lack of an Unc5C-Netrin1 interaction causes a misrouting of deep layer callosal axons to subcortical targets (from [260]).

As aforementioned, *Satb2* and *Ctip2* have been shown to orchestrate important and mutually exclusive genetic programs to establish corticocortical versus corticofugal connections. Whereas *Satb2* is indispensable for the formation of the corpus callosum, *Ctip2* is required for the fasciculation and pathfinding of subcerebral projection neurons [66, 226]. In normal development, *Satb2* overrides the *Ctip2* driven molecular pathway in order to establish interhemispheric projections instead of corticofugal ones [150, 212].

*Unc5C* and *DCC* act as receptors for the secreted ligand *Netrin1*, mediating either a chemorepulsive (*Unc5C-DCC* together) or a chemoattractive (*DCC* alone) response [261-264]. While *Unc5C* expression was downregulated in *satb2* mutants, *DCC* expression was upregulated [260]. This study showed that the negative regulation of *Unc5C* and *DCC* by *Ctip2* and *Satb2*, respectively, mediates a differential response of neocortical axons to *Netrin1*. Using *Satb2* and *Ctip2* compound and double mutants, and by overexpression and down-regulation by *in utero* electroporation, the authors revealed the roles of *Unc5C* and *DCC* in corpus callosum formation. High levels of *Unc5C* expression, and low levels of *DCC* expression, instruct neurons to project through the corpus callosum, since in the absence of either *Unc5C* or *Netrin1*, callosal axons misproject to subcortical targets mimicking the effect of *Satb2* deletion. In contrast, inactivation of *Ctip2* or *DCC*, or the restoration of *Unc5C* in *Satb2* mutants can partially restore the corpus callosum formation. Moreover, *DCC*-positive cingulate axons act as pioneers for the corpus callosum. The authors suggested a scenario where the source of *Netrin1* is the internal capsule, which attracts *Unc5C*-negative/*DCC* positive axons while repelling *Unc5C* positive/*DCC* negative axons. Hence, callosal projecting deep layer neurons require higher levels of *Unc5C* and lower levels of *DCC*, whereas low levels of *Unc5C* and high levels of *DCC* instruct neurons to project subcortically (**Figure 15**).

Since none of the rescue experiments performed after E14.5 lead to the formation of a corpus callosum the control of *Satb2* and *Ctip2* over callosal and corticofugal connectivity seems to be dependent on *Unc5C* and *DCC* only in deep layer neurons, while upper layer neurons are dependent on other molecular pathways. Hence, it is likely that deep layer neurons act in a cell autonomous manner in deciding between callosal and subcortical fates [260].

## B. Subcerebral projection neurons; an example of CSMN

In rodents, spinal cord innervation by corticospinal tract (CST) starts relatively late in development, and occurs almost entirely at postnatal stage. Concurrently with axonal outgrowth through the spinal cord, the topographic organization of the motor cortex does not achieve its final configuration before three weeks after birth [149].

Similar to the CPN, the forefront of the developing CST is composed of a small number of pioneering axons, while the majority of axons follow as tightly fasciculated bundles. The tract remains fasciculated the entire developmental period, and defasciculate only when the axons have entered the spinal cord where they spread out, at the precise level where they connect with their respective targets in the spinal gray matter [149]. The trajectory of the CST axons results from a combination of various guidance factors acting at different choice points along its journey (**Figure 16**).

Early axonal guidance cues are likely to be common between all corticofugal PN subtypes. Initially, the axons growth is directed ventrally from the cortical plate into the intermediate zone at E12.5. The coordinated expression of chemoattractive *Sema3C* and chemorepellent *Sema3A*, via the interaction with *Npn-1* and *Npn-2* receptors on the axons is involved in this step [265]. Moreover, *Sema3A* signaling might involve the cell adhesion molecule *L1* as a part of the receptor complex with *Npn-1*, during early cortical growth [266, 267]. Diffusible *Netrin-1* coming from the underlying ganglionic eminences provides a chemoattractive gradient for early subcortically projecting axons in the IZ [268, 269]. After turning away laterally from the midline, the axons extend through the intermediate zone toward the pallial-subpallial boundary. Once inside the internal capsule, corticospinal axons separate from the corticothalamic axons and enter the cerebral peduncle. At this level, *Slit1* and *Slit2* contribute to the maintenance of the dorsoventral positioning of the corticofugal axons within the internal capsule, and prevent their growth toward and across the midline [254]. Both *Slit* receptors, *Robo1* and *Robo2* are expressed in developing cortical axons, since in their double mutants a massive number of axons abnormally cross the midline [257].

The axons pass then through the midbrain to the ventral pons. By birth, they reach the caudal region of the medulla where the majority decussate at the junction with the spinal cord [185, 190]. The *Netrin1* signaling through *DCC* and *Unc5* [270],

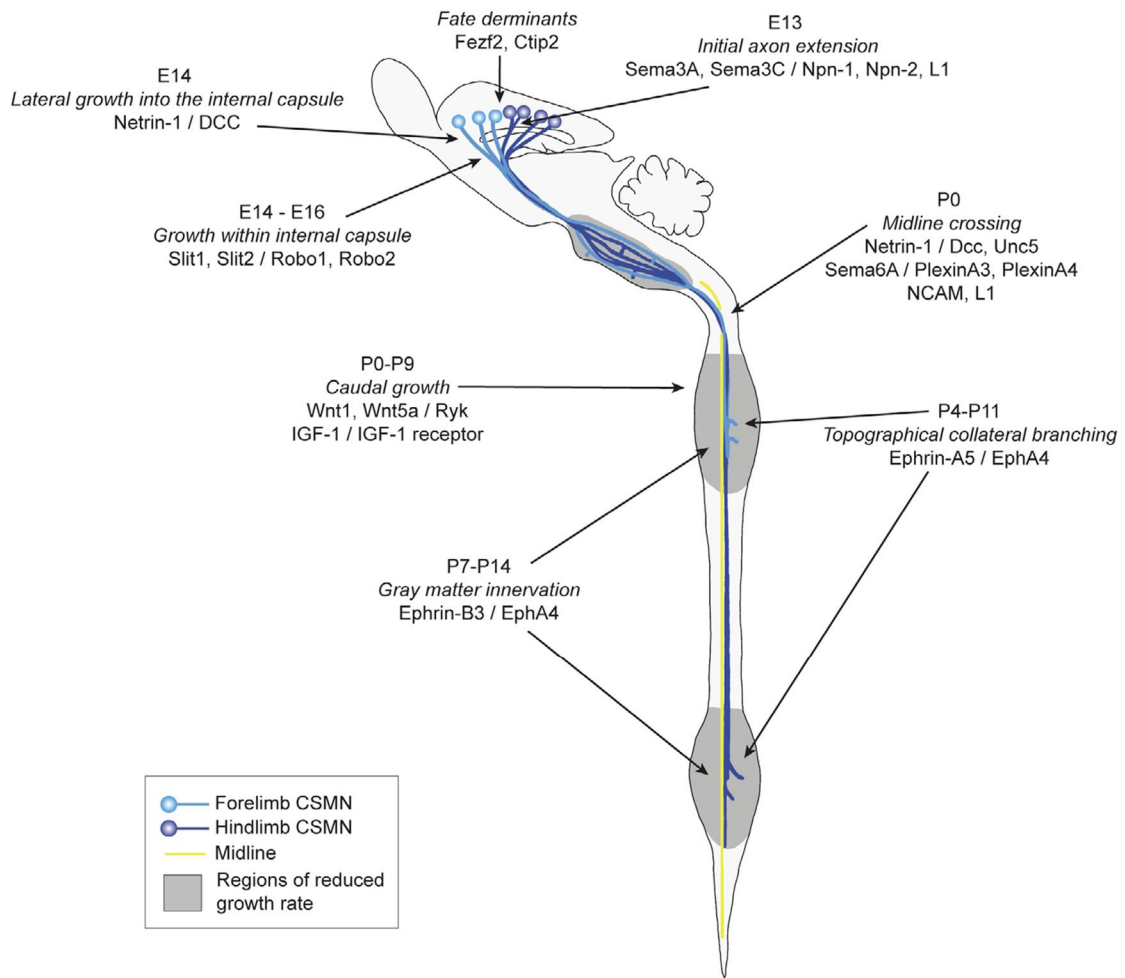


**Figure 16- Key events in corticospinal tract guidance.**

Schematic representation of the rodent corticospinal projection (in blue) from the motor cortex to the spinal cord gray matter, indicating the major guidance events at the different developmental stages and showing the regions of reduced growth rate where axons branch (taken from [149]).

the cell adhesion molecule L1 [271-273], and the neural cell adhesion molecule (NCAM) [274] are involved in the decision to cross the midline and in the correct guidance of the CST through the medulla. While Netrin1 is acting on CST growth at the level of pioneer axons, NCAM and L1 regulate the pathfinding of the following axons by regulating interactions among themselves and with pioneer axons [275]. More recently, Sema6A-PlexinA3/A4-mediated repulsion has been shown to be involved in driving CSMN axons toward the midline where they undergo decussation [276, 277]. After crossing the midline, CSMN axons project caudally in the dorsal funiculus of the spinal cord [191]. These axons express the Insulin like growth factor 1 (IGF1) receptor and the receptor-like tyrosine kinase (Ryk) receptor. The presence of IGF1 and a decreasing gradient of Wnt1 and Wnt5a [278, 279] in the neonatal gray matter surrounding the dorsal funiculus help to direct these axons down toward the lumbar levels of the spinal cord.

Following its descent, each CSMN axon must exit the dorsal funiculus at a discrete location along the spinal cord and make topographically specific connections with the target neuron in the dorsal horn. At this level EphA4 and ephrin-A5 are involved in the proper exit of axons to reach their targets [280, 281].

## **VII. Transcriptional regulators involved in arealization and cortical subtype specification**

Post-mitotic regulators transform continuous gradients of positional information inherited from progenitors into sharp areal boundaries, instruct the formation of motor and sensory maps and direct projection neurons to acquire areal-specific phenotypic characteristics [39]. To date, only few of such controls have been identified: the Basic-loop-helix domain containing, class B5 (Bhlhb5), Lim domain only 4 (LMO4), Tbr1, and possibly COUP-TFI.

### **A. Basic-loop-helix domain containing, class B5 (Bhlhb5)**

Bhlhb5 starts to be expressed in the cortical plate at E12.5, and is maintained in post-mitotic neurons all along corticogenesis. From E15 onwards, Bhlhb5 is expressed in a high-caudomedial to low-rostralateral gradient. After birth, its expression becomes

progressively restricted to layers II-V of the primary sensory areas (somatosensory, visual and auditory).

Absence of *Bhlhb5* does not produce a severe areal shift, but rather induces faint changes in the morphology of sensory areas. The V1 is slightly increased and the boundaries of the S1 barrels become faintly discernible. Moreover, the thalamocortical inputs appear to be more diffuse, and some area-specific genes such as *LMO4* are aberrantly expressed. This suggests that *Bhlhb5* refines the shape and boundaries of somatosensory and caudal areas [144].

Notably, the sensorimotor region, which has a crucial function in the control of voluntary movements in rodents and contains the highest percentage of CSMN resulted mispecified in *Bhlhb5* mutants [15, 144]. *Bhlhb5* is strongly expressed in CSMNs of sensorimotor cortex and corticotectal PNs of the occipital cortex. In *Bhlhb5 null* mutants, CSMN failed to send their axons to the spinal cord and together with corticotectal PNs showed a reduced expression of SCPN markers such as *S100A10*, *MucrySTALLIN* and *Crim1*, indicating a role for *Bhlhb5* in their specification [144].

## **B. Tbr1**

*Tbr1*, which has been discussed above as a critical control over CThPN subtype identity, contributes also to area identity acquisition and is expressed mostly in rostral areas of the cortex. *Tbr1* mutants lack TCA innervation to the CP and, although they die at birth, regional and laminar markers indicated a rostral shift of their caudal areas, suggesting a role for *Tbr1* in arealization [143]. Moreover, *Fgf17*, its variant 1 (*Etv1*) and *Sprouty1*, which are downstream targets of *Fgf8*, are increased in *Tbr1* mutants at E12.5, suggesting that normally, *Tbr1* negatively regulates *Fgf8* signaling [143]. Since *Tbr1* is expressed in newborn neurons and not in progenitors [221, 282], this negative regulation could be a post-mitotic feedback exerted on mitotic compartment [8]. Finally, *Tbr1* has been shown to have a direct transcriptional control on the expression of the frontal marker autism susceptibility candidate 2 (*Auts2*) further confirming the role of *Tbr1* in frontal area development [283]. Interestingly, mutations in the *Auts2* locus were found in cases of Autism and mental retardation [283, 284].

### C. LIM domain only 4 (LMO4)

Given the important and various roles of LMO4 and its central role in my work, a more detailed description for LMO4 structure and different aspects of its function will be presented in this section.

#### 1. LMO4 structure and protein interactions

LMO4 belongs to the subclass of LIM domain only (LMO4) of nuclear transcription co-regulators [285]. The LMO subclass of LIM proteins is characterized by a LIM domain, which is a highly conserved cysteine-rich zinc finger-like motif that was found in a variety of nuclear and cytoplasmic proteins, and functions as a docking site for the assembly of multi-protein complexes [286, 287]. The LIM domain does not directly bind the DNA; instead LIM domain proteins function by mediating protein-protein interactions [288, 289]. The LMO subclass of LIM proteins is characterized exclusively by the presence of two tandem LIM domains [285]. Therefore, they regulate gene expression by acting as “linker” or “scaffolding” proteins thanks to their LIM domains, and thus, they are involved in the formation of multi-protein complexes of DNA-binding factors, and transcriptional regulatory proteins [288-290].

LIM proteins represent a very conserved subclass, found in species ranging from *Caenorhabditis elegans*, *Drosophila*, and zebrafish to humans [291-295]. Four LMO4 proteins have been so far identified (LMO1-LMO4) (**Figures 17**). LMO4 is the most recently described member, and was isolated as an interacting protein of Ldb1, also known as NLI or cofactor of LIM proteins (CLIM) [291, 296-298]. LMO4 is the most divergent member of the LMO proteins, and shows a wide expression in embryonic and adult tissues throughout development and adulthood, whereas the other 3 members (LMO1-LMO3) are more restricted to specific tissues.

LMO proteins function essentially as transcriptional co-regulators, mediating protein-protein interactions of various transcription factors or chromatin remodeling proteins. They were initially proposed as negative regulators of LIM homeodomain (LIM-HD) transcription factors [299-303]. However, mounting evidence indicate that they are also able to activate transcription by nucleating the assembly of complexes with TFs, such as stem cell leukemia (SCL) and GATA [299, 304, 305]. Therefore,

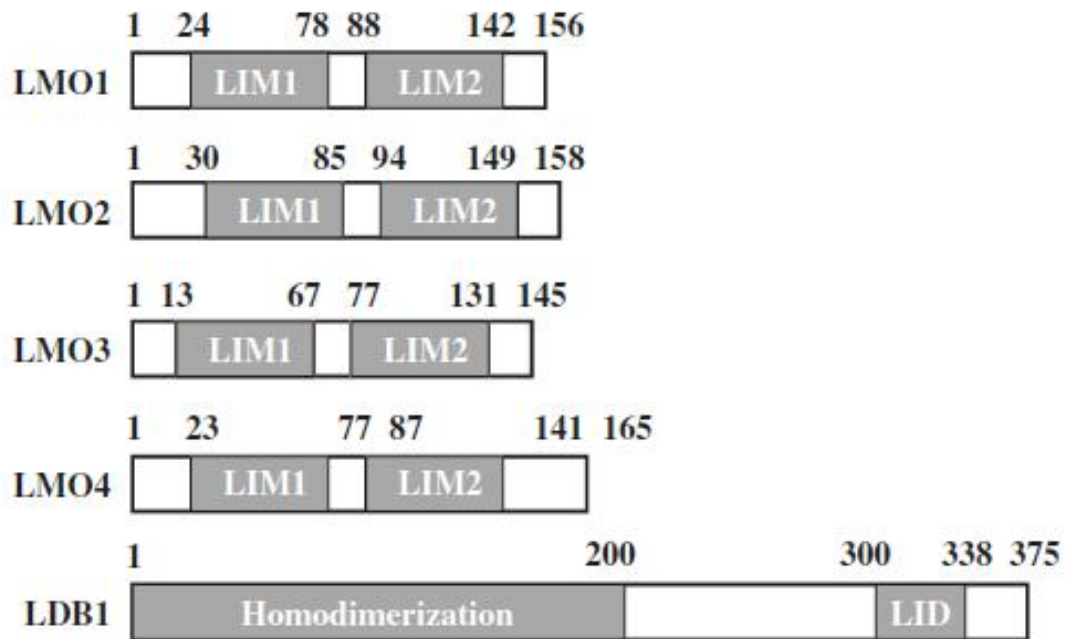


**Figure 17-Schematic representations of the human LMOs and LDB1.**

The first LIM domain (LIM1) and the second LIM domain (LIM2) of four LMO proteins are indicated. The homodimerization domain and the LIM interaction domain (LID) of LDB1 are also indicated (Taken from [306]).

LMO proteins control transcription both negatively and positively depending on the cell context and their binding partners (**Figure 18**).

LMO4 is a 165 amino acid protein broadly expressed in human tissues, and playing important roles in several developmental systems, including epithelial, mammary, ear and neural development [297, 307-312]. However, it also acts as a mammary oncoprotein and is overexpressed in more than 50% of primary breast tumors [313], squamous cell carcinomas of the oral cavity [314], and primary prostate cancer [315]. Overexpression of LMO4 markedly reduces epithelial cell differentiation, implicating it as an oncogene [313, 316].

LMO4 was found to interact with several kinds of proteins. It binds to the ovarian tumor suppressor protein Breast Cancer 1 (BRCA1) and inhibits its transcriptional activity in yeast and mammalian cells [317]. LMO4 is also a binding partner of the basic helix-loop-helix protein (HEN1) [318] involved in hematopoiesis and specifically expressed in the developing nervous system [319]. Furthermore, LMO4 interacts with the peroxisome proliferation activated receptor- $\gamma$  (PPAR $\gamma$ ) required for neuron protection in ischemic injury. It interacts also with deformed epidermal regulatory factor 1 (DEAF1), a DNA binding protein that interacts with regulatory sequences and modulates transcriptional outcome [297]. Finally, LMO4 can also associate with other proteins, including the repulsive guidance molecule A receptor Neogenin in human SH-SY5Y cells, in human NTERA neurons, and in embryonic rat cortical neurons [320], the cAMP response element-binding protein (CREB) complex, the glycoprotein 130 subunit, a common receptor subunit for interleukin 6 (IL-6) type cytokines [321] and the transcription modulator Cbp/p300-interacting transactivator (Cited2) [322].

Interestingly, LMO4 was found *in vivo* to bind to the Estrogen Receptor  $\alpha$  (ER $\alpha$ ) and MTA1 by establishing a multi-protein complex constituted by LMO4, ER $\alpha$ , MTA1 and histone deacetylases (HDACs) [323]. Similarly to MTA2 (see above), MTA1 is also part of the NuRD complex and functions by recruiting HDACs. In physiologic conditions LMO4 was identified as an important component of the NuRD complex, which act as a potent repressor of ER $\alpha$ , a ligand-dependent TF controlling a variety of essential physiologic and developmental processes [323]. Another study revealed that LMO4 associates with HDAC2, and enhances granulocyte colony-stimulating factor (GCSF)-induced Stat3 signaling in mice

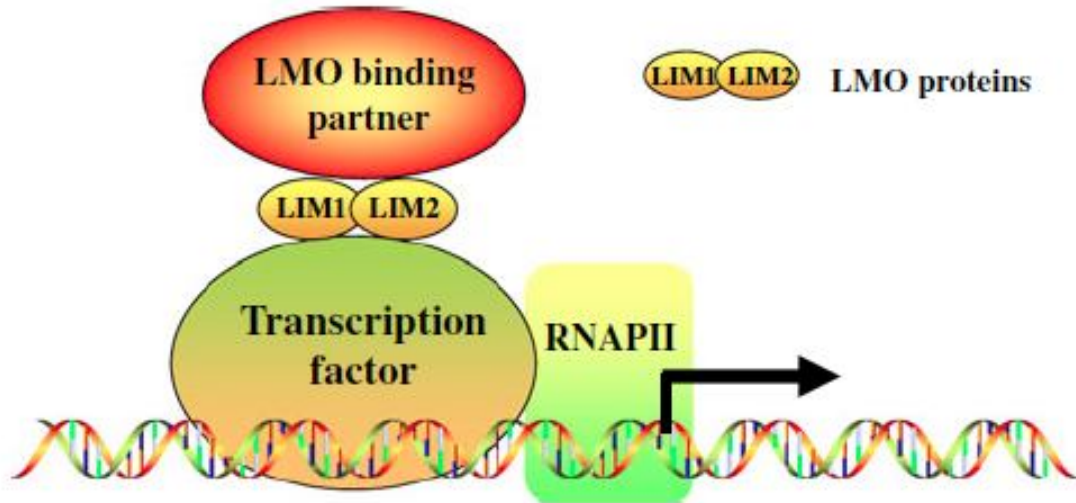


**Figure 18-Schematic representations of LMOs in gene transcriptional regulation.**

LMOs regulate gene transcription by functioning as “linker” or “scaffolding” proteins through their LIM domains and are involved in the formation of multi-protein complexes of DNA-binding factors and transcriptional regulatory proteins. ‘RNAPII’ means RNA polymerase II (taken from [306]).

cortical neurons, in part by sequestering HDAC2 [324]. Overall, LMO4 seems to bind primordially to HDAC1 and 2 to modulate positively or negatively the transcription of target genes.

## 2. **LMO4 in the developing and postnatal cortex**

### a) **LMO4 in early brain development**

In mice, targeted disruption of LMO4 gene led to embryonic lethality. Most *LMO4 null* mice die during embryogenesis. Even though few of them are born, they usually die within hours [325]. LMO4 mutation results in exencephaly for a significant percentage of pups, whereas others show overall normal brain morphology [308, 309, 311, 325]. It is not clear whether the closure defect in the dorsal brain is caused by abnormal neural crest development or abnormal brain formation [325].

LMO4 has been shown to act as an activator of neurogenin 2 in the developing cortex [326]. The proneural protein neurogenin 2 (Ngn2) is a key TF in regulating neurogenesis in the vertebrate cortex [327, 328], and promotes radial migration of neocortical neurons, at least in part, by direct transcriptional activation of the small GTP-binding protein, Rho family GTPase 2 (Rnd2) [329]. It was shown that LMO4 and NLI can bind to Ngn2 forming a multi-protein transcriptional complex, and promoting Ngn2-mediated transactivation of neuronal and cortical-specific genes. In addition, *Tbr2* and *NeuroM*, which are targets of Ngn2 and markers of neuronal commitment, as well as *Rnd2* and early B-cell factor 2 (*Ebf2*), expressed in post-mitotic neurons, showed a significant reduced expression in the *LMO4 null* cortex. Overall, LMO4 promotes the acquisition of cortical neuronal identities by forming a complex with Ngn2 and subsequently activating Ngn2 target genes [326].

### b) **LMO4 has a dynamic and region-specific expression in the mouse developing cortex**

Onset of cortical LMO4 expression starts at E12.5, where LMO4 is detected in the preplate, and in the striatum [325]. At E15.5, LMO4 expression is detected in the cortical SVZ and in the hippocampus. At P0, LMO4 is mostly expressed in post-mitotic neurons of the cortical plate [145, 325]. At this stage, the expression of LMO4 is mainly localized in the anterior and posterior cortical regions, corresponding to motor and visual cortices, respectively, but not in the parietal region, which

corresponds to the future somatosensory areas. After P0 LMO4 expression progressively increases in layers III/IV of the somatosensory regions, and at P10 LMO4 is expressed from lower to upper layers of the parietal cortex [325]. This dynamic and region-specific expression of LMO4 during critical periods for areal specification and neuronal subtype differentiation suggests that this factor may play important roles in these processes.

**c) LMO4 is a mediator of calcium activity**

LMO4 was identified as an effector of calcium activity, driving transcription in response to calcium influx in cortical neurons [146]. Calcium influx occurs through voltage-sensitive calcium channels and *N-Methyl-D-aspartate (NMDA)* receptors, and LMO4 activation involves calcium/calmodulin-dependent protein (CaM) kinase IV and microtubule associated protein (MAP) Kinase, acting downstream of synaptic stimulation by calcium influx [146]. The first LIM domain of LMO4 favors CREB-mediated transcription, and disruption of both its LIM domains impairs activation of LMO4 function by calcium influx [146].

Furthermore, LMO4 is a mediator of calcium activity not only in cortical neurons, but also in different brain structure including the hippocampus [330] and the hypothalamus [331].

**d) LMO4 in arealization**

In the study identifying LMO4 as a mediator of calcium-related transcriptional activity in cortical neurons [146], it was used an *LMO4 conditional KO* mice under the control of the *Nex* promoter [146]. In these *conditional KO* mice expressing LMO4 only in postmitotic cells, the barrels of the primary somatosensory area were poorly differentiated, smaller than normal ones and blurred [146]. Moreover, these mutants showed an affected distribution of thalamocortical afferents, which do not segregate into distinct columns or give rise to smaller columnar units suggesting that LMO4 loss does not prevent thalamocortical projections from reaching the cortex but does affect their patterning in the cortex [146]. These defects in thalamocortical connections were similar to defects reported after conditional deletion of the NMDA receptor [332]. Since the authors showed that NMDA receptor activation regulates

LMO4 dependent transcription, they hypothesized that the effects of NMDA receptor on barrel formation were at least in part mediated by LMO4. Thus, activity dependent regulation of LMO4-mediated transcription plays an important role in the patterning of thalamocortical connections [146].

The role of LMO4 in arealization was studied by the mean of other LMO4 conditional Kos: one expressing Cre under the control of the *Nestin* promoter, which deletes LMO4 in the central nervous system, and another under the control of the *Emx1* promoter deleting LMO4 selectively in the cortex. Both CKOs showed a less severe phenotype concerning the barrel field and thalamocortical connections. LMO4 deletion caused a rostral shift of cortical regional markers such as cadherin 8 (Cad8), inhibitor of DNA binding 2 (Id2) and EphrinA5 and its receptor EphA7. However, the relative position of the posteromedial barrel subfield (PMSF) did not shift rostrally or caudally. But the shape of the PMSF was altered, with a clear shrinkage of its structure [325]. However thalamocortical and corticothalamic connections were not affected, even if the innervation of thalamic axons in the mutant cortices was not as clear as controls, implying that LMO4 deletion affects the strength of synaptic connections. Moreover, LMO4 ablation caused behavioral abnormalities related to sensorimotor functions [325]. In summary, LMO4 defines the shape of functional areas in developing cortices and regulates sensory motor control [325].

#### **e) LMO4 in neuronal subtype specification**

It was previously stated that the refinement of subtype identity is a progressive mechanism. While mature deep-layer neurons exhibit strikingly divergent patterns of gene expression and axonal projection, newborn postmitotic neurons often extensively co-express transcription factors that later become restricted to different subtypes [39].

In this regard, it has been shown that LMO4 and the cofactor of LIM proteins (Clim1) progressively delineate cortical PN subtypes during mouse cortex development [333]. Among layer V cortical PNs, callosal and subcerebral neurons progressively adopt distinct and complementary patterns of LMO4 and Clim1 expression. However, during early differentiation steps at E15.5, LMO4 and Clim1 co-localize and are expressed in both presumptive SCPN and CPN in layer V. During mid to late differentiation (from P0 to P6), when layer V PN axons have reached their specific

targets, this overlapping expression of LMO4 and Clim1 gradually diminishes. In this phase LMO4 expression becomes specific for CPNs, while Clim1 is confined to layer V SCPNs. This is confirmed by molecular analysis. At P6 LMO4 is excluded from the majority of Ctip2 expressing neurons, while all Satb2 expressing neurons in layer V express LMO4. In contrast, Clim1 is expressed in nearly all Ctip2 expressing neurons. However, a subpopulation of neurons maintains co-expression of LMO4 and Clim1, possibly reflecting ongoing neuronal maturation, or alternatively, highlighting a distinct subpopulation of layer V PNs [333]. Thus, cortical PN identity is progressively refined throughout embryonic and postnatal neuronal differentiation [333].

A more recent report showed that LMO4 and Bhlhb5 have a striking complementary expression patterns in the motor cortex postnatally [145]. The authors divided the motor cortex into rostral motor cortex (MC<sub>r</sub>) characterized by a high LMO4 expression and absence of Bhlhb5 expression, and a caudal motor cortex (MC<sub>c</sub>) characterized by a high Bhlhb5 expression and absence of LMO4. Thus, LMO4 labels the MC<sub>r</sub> containing regions controlling facial, neck and forelimb movements, and is excluded from MC<sub>c</sub> containing regions controlling trunk and hindlimb movement [145]. This study partially contradict previous conclusions from the same group [333]. Indeed, although LMO4 is expressed in CPNs and lacking in CSMNs of the MC<sub>r</sub>, it is also highly expressed by cortico-brainstem motor neurons (or CBMNs, a subpopulation of SCPNs) residing in layer Va (upper layer V). Moreover, most dual backward PNs (or BPNs, sending a projection backward to the sensory cortex and the other toward either cortical or subcortical targets) are largely restricted to the LMO4 expressing MC<sub>r</sub>.

In the absence of LMO4 function the molecular MC<sub>r</sub>/MC<sub>c</sub> boundary was not impaired, however the molecular identity of neurons in MC<sub>r</sub> was more homogeneous, and rostral layer Va SCPN aberrantly project to the spinal cord instead of the brainstem. Moreover, many BPNs projecting either callosally or subcerebrally fail to send a second backward projection [145]. Overall, this study demonstrated that LMO4 is a central developmental control over the diversity of motor cortex PN subpopulations, establishing their area specific identity and specialized connectivity [145].

## D. COUP-TFI

COUP-TFI controls the tangential (areal) and radial (laminar) neocortical specification (**Figure 19**). Moreover, COUP-TFI has been shown to be involved in different aspects of forebrain development, from neuronal migration to neurogenesis, gliogenesis and the formation of commissural projections.

### 1. COUP-TFI is involved in neurogenesis, gliogenesis and cell cycle control

In the developing CNS, subtypes of neurons and glial cells are generated according to a temporal sequence defined by cell-intrinsic mechanisms that function at progenitor level.

A study by Naka et al [334] showed that knocking down COUP-TFI and COUP-TFII in neurospheres (NS) obtained from mice embryonic stem cells (ESC) delays the onset of gliogenesis. The time of neurogenesis was prolonged to the third stage of NS, while in normal conditions gliogenesis starts at the second generation of NS.

Furthermore, the knock-down of COUP-TFI and COUP-TFII in the cerebral cortex leads to an increase of early born neurons and to the production of neurons at the expense of glia cells, suggesting that COUP-TFs impinge on progenitor cell neuropotency.

Analysis of the promoter of Glial fibrillary acidic protein (GFAP), which is an important molecule for glia cell specification in COUP-TFI/II knocked-down cells revealed an altered methylation pattern, indicating that COUP-TFI promote gliogenesis through epigenetic modifications. However, COUP-TFI and II appeared to be necessary but not sufficient to induce gliogenesis, suggesting that they limit the neurogenic temporal window rather than promoting gliogenesis [334].

In this context, another study by our group [142] has investigated the role of COUP-TFI in neurogenesis and laminar fate using a gain-of-function mouse model overexpressing COUP-TFI in the neocortex under the promoter of the *mDach1* gene (D6/COUP-TF1 transgenic mice) and *COUP-TFI KO* mice. This study showed that COUP-TFI influences dorso-ventral patterning of the cortex and promotes cell cycle exit and neural differentiation. In addition, this study demonstrated that COUP-TFI

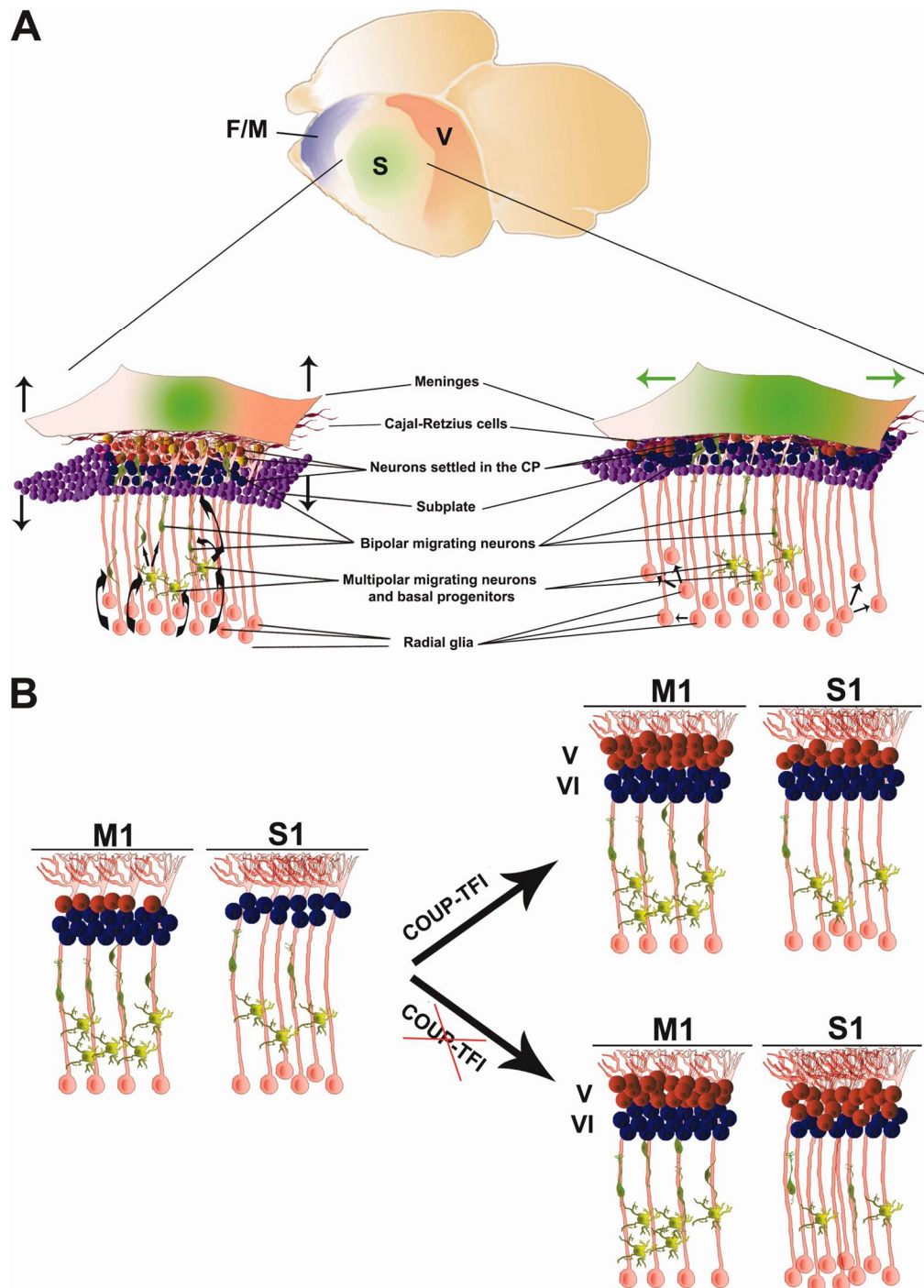


**Figure 19-Mechanisms underlying cortical thickening, expansion and lamination.**

A: Schematic representation of an embryonic mouse brain delineating the prospective frontal/motor (F/M), somatosensory (S), and visual (V) areas. According to the radial unit hypothesis, newborn neurons receive positional information from their progenitors. During neurogenesis, the thickening of a given area or areal region (bottom left represents a cortical section) will increase (black arrows), while an increment of the self-renewing progenitor pool will lead to area surface expansion (bottom right, green arrows). B: Schematic representation of the hypothetical function of the areal patterning gene COUP-TFI in the specification of layer VI in primary motor (M1) and somatosensory (S1) areas. When COUP-TFI (which is highly expressed in parietal and occipital neocortical regions) is active, it delays the onset of the layer V (red) specification program in S1 area, where neurogenesis proceeds slower than in M1. As a result layer VI (blue) of S1 acquires approximately the same thickness of that of M1, while layer V results thinner in S1 compared to M1. When COUP-TFI is ablated, it fails to repress layer V program in S1, which in turn expands its layer V neuronal pool at the expense of layer VI neurons (taken from [8]).

regulates the balance between early and late born neurons, and provides evidences that COUP-TFI coordinates these processes through modulating Mapk/Erk, phosphatidylinositol 3'-kinase (PI3K)/ protein kinase B (Akt) and  $\beta$ -catenin mediated Wnt signaling [142]. The Mapk/Erk pathway is involved in the G1- to S-phase transition of cell cycle in different systems [335]. Similarly,  $\beta$ -catenin, a downstream effector of Wnt signaling controls in a dose dependent manner, the duration of the G1 phase in neuronal precursors of the cortical midline [336]. While a short G1 promotes proliferation, a prolonged G1 phase promotes cell responsiveness to intrinsic and extrinsic signals, which trigger the neurogenic program in mammals (reviewed in [337]).

## **2. COUP-TFI is required for the formation of commissural projections in the forebrain by regulating axonal growth**

COUP-TFI is expressed in the major developing commissural neurons. In the absence of COUP-TFI function, fibers of the three commissures, the corpus callosum, the hippocampal commissure and the anterior commissure project aberrantly and fail to cross the midline in COUP-TFI *null* mutants [338].

In COUP-TFI mutants callosal projections fail to decussate and stop abruptly at the midline. They form aberrantly oriented fibres, known as Probst bundles. Moreover, hippocampal commissure fails to cross the midline, and shows the presence of ventrally oriented thick ectopic bundles [338]. However, the anterior commissure was thicker [338]. In summary, in the absence of COUP-TFI, all the major forebrain commissures show abnormalities along the antero-posterior and the dorso-ventral axes.

Moreover, COUP-TFI deficient hippocampal neurons have a defect in neurite outgrowth and show an abnormal axonal morphology (REF). These defects could be due to the altered expression of various cytoskeletal molecules involved in axon guidance and neuronal migration in the absence of COUP-TFI function, such as the two microtubule-associated proteins regulating microtubule dynamics, MAP1B and MAP2, the member of the Rho GTPases family Rnd2, and the cyclase-associated protein 1 (CAP1) known to regulate actin dynamics. Overall, this study provides strong evidence that COUP-TFI is intrinsically required for proper axonal outgrowth in the developing forebrain [338].

### 3. **COUP-TFI promotes radial migration and proper morphology of callosal projection neurons by repressing Rnd2 expression**

As mentioned in chapter II, the inside-out pattern of corticogenesis was made possible by the appearance of glia-guided migration [3, 339]. While early born neurons give rise to the preplate and lower layers by somal translocation [50, 51], upper layer neurons follow a more complex migration pattern (see Chapter II).

The small Rho-GTPase Rnd2 is involved in the regulation of multipolar shaped cell (MSC) to bipolar shaped cell (BSC) transition, and BSC migration during mid-late stages of corticogenesis [329, 340]. Rnd2 expression is high in multipolar shaped cells and is downregulated in the upper IZ where BSCs attach to the glia and migrate to the cortical plate. Thus, precise transcriptional control of Rnd2 activity is required for proper radial migration [341].

A study from our group, demonstrated a role of COUP-TFI in promoting radial migration of upper layer callosal neurons by repressing Rnd2 expression [341]. In the absence of COUP-TFI function, newborn upper layer neurons in the presumptive somatosensory cortex were properly specified but abnormally positioned, suggesting their abnormal migration. The analysis of COUP-TFI mutants showed an increased number of MSCs and a defective cell transition from the IZ to the cortical plate. Normally, the highest percentage of BSCs is found in the upper IZ and the CP, however mutant BSCs were mainly located in the IZ, indicating that although they adopt a bipolar morphology, COUP-TFI<sup>-/-</sup> neurons fail to reach the cortical plate. This indicated that COUP-TFI is required for both the transition from multipolar to bipolar shape and the intrinsic migratory property of BSCs within the IZ and cortical plate during radial migration of upper layer neuron.

This study also revealed that COUP-TFI and Rnd2 have opposite expression gradients in migrating neurons. COUP-TFI KO brains Rnd2 expression expanded caudally and labeled abnormally migrating neurons. Moreover, COUP-TFI was demonstrated to negatively regulate Rnd2 expression in migrating post-mitotic cells favoring newborn neurons to reach the cortical plate. However, the rescue of correct levels of Rnd2 in COUP-TFI mutant brains partially recovered the balance between MSCs and BSCs and strongly promoted BSCs migration to the cortical plate.

In addition, acute inactivation of COUP-TFI in single newborn neurons strongly delayed the formation of the corpus callosum. Moreover, Satb2-positive

callosal neurons normally having a branched apical dendrite and complex apical tufts in layer I, showed after cell autonomous inactivation of COUP-TFI an altered morphology of their tufts, which barely reached the marginal zone. Moreover their dendrite branching was also strongly altered. Restoring correct levels of Rnd2 rescued the proper contact of these neurons with the pial surface, their apical tuft complexity in layer I and finally their dendritic branching. Overall this work demonstrated a cell autonomous role for COUP-TFI in migration, axonal pathfinding and dendritic arborization of CPNs, and indicated that fine-tuning of Rnd2 levels by COUP-TFI during radial migration favors CPN maturation [341].

#### 4. **COUP-TFI regulates the balance between frontal/motor and sensory areas**

COUP-TFI role in area patterning was suggested by its high caudolateral to low rostromedial expression gradient in the progenitors of the VZ, and later in their neuronal progeny in the cortical plate [138, 342]. As previously mentioned, COUP-TFI roles were studied by our group using genetically engineered mice to inactivate COUP-TFI expression selectively in the cortex [140]. These mice were generated to overcome the complications raised by constitutive loss of COUP-TFI. Indeed, COUP-TFI constitutive knockout mice die after birth, before areas can be defined, and analyses were therefore limited to regional markers and connections between the cortex and the thalamus [138]. Moreover, the interpretations of these analyses were complicated due to the robust expression of COUP-TFI in forebrain structures that are critical for cortical development, such as the dorsal thalamus and the ganglionic eminences [338, 342, 343].

*COUP-TFI CKO* (*COUP-TFI flox/flox<sup>Emx1-Cre</sup>*) animals, instead, were viable and fertile [140]. To assess COUP-TFI role in arealization, the position of the somatosensory areas and thalamocortical axons were analyzed by Serotonin (5-HT) immunostaining, which revealed that each primary sensory area in COUP-TFI CKO mice are strikingly reduced in size and are aberrantly positioned at the occipital edges of the cortex. These primary sensory areas maintained their positions relative to one another along the mediolateral cortical axis, but not along the rostrocaudal axis. Although S1 was substantially reduced in size and caudally shifted, its barrel-like pattern was still identifiable by serotonin staining, but the barrels were smaller than in

control brains (**Figure 20**). Accordingly, layer IV neurons were caudally shifted as revealed by Nissl staining and molecular markers specific to layer 4 demonstrating that basic mechanisms sculpting barrels in S1 are not completely lost in COUP-TFI CKO, even though S1 is much smaller and ectopically positioned. But, since primary sensory areas are shifted caudally, most of the neocortex, in these mice, shows a lower density of Nissl stained cells in layer IV and a reduced expression of layer IV markers, which is a characteristic of frontal/motor areas. Finally, topographic shift of cortical areas was paralleled by a shift in thalamocortical connectivity.

In addition to this caudal shift of sensory areas, Cadherin 8 (Cadh8), which is a cell adhesion protein labeling the rostral motor domains, showed a remarkable caudal expansion covering almost the entire cortical hemisphere, with the exception of the region corresponding to the shrunken primary sensory areas (**Figure 20**). Similarly, frontal markers analyses including Id2, Fezf2 and Tbr1 indicate a caudal expansion of frontal/motor areas in COUP-TFI CKOs. DiI and DiA labeling in frontal and parietal cortices showed that most projections targeted either the ventrolateral thalamic nucleus, which is normally connected only to the frontal/motor area, or the cerebral peduncle, suggesting that corticothalamic and corticofugal projection neurons of the S1 area adopted the identity of motor area PNs. In summary, the molecular, cytoarchitectural and hodological features of frontal areas expanded massively to parietal and caudal regions of the neocortex after ablation of COUP-TFI (**Figure 20**).

All together, these data indicate a role for COUP-TFI in specifying both layer properties that are unique for different sensory areas, and the positional information that controls development of a precise connectivity network between cortex and dorsal thalamus. Thus COUP-TFI might be involved in repressing frontal/motor area identities along its expression domains in parietal and occipital cortices [140].

## **5. Area-specific temporal control of corticospinal motor neuron differentiation**

The adult primary motor cortex contains a large number of CSMNs and has a thick layer V, while the somatosensory area is characterized by a thick layer IV, where the neurons receiving relayed sensory inputs are located [182]. CSMNs are generated at a higher rate in the developing motor cortex than in sensory areas in mice [344]. A recent study from our group showed that COUP-TFI CKO mice, in accordance with

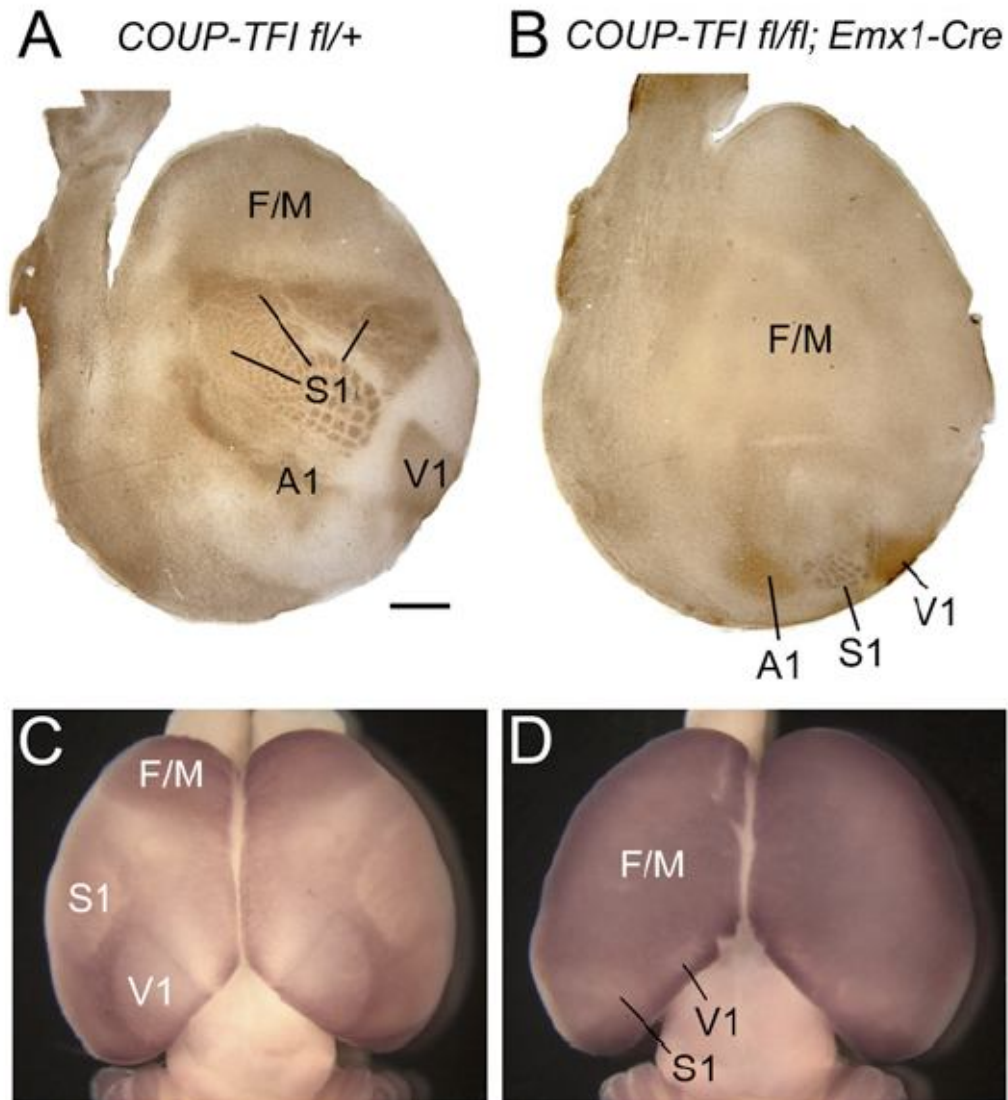


**Figure 20-Massive expansion of the Frontal motor area and posterior compression of primary sensory areas in *COUP-TFI* deficient cortex.**

(a and b) Serotonin (5HT) immunostaining on tangential sections through layer IV of flattened cortices of P7 control (*COUP-TFI fl/+*) and conditional mutant (*fl/fl; Emx1-Cre*) cortices. Anterior is to left, and medial to the top. (a) Serotonin staining reveals primary sensory areas, including primary somatosensory (S1), visual (V1), and auditory (A1) areas, by marking area-specific TCA axon terminations. (b) In *COUP-TFI fl/fl, Emx1-Cre* conditional mutant brains, the primary sensory areas are much smaller than in controls and are compressed to ectopic positions at the posterior pole of the cortical hemisphere. The barrelfield of the ectopic S1 retains its characteristic patterning but is substantially reduced in size and caudally shifted, while a reduced V1 is located medial and a reduced A1 lateral to the miniature S1 barrelfield. (c and d) In situ hybridization for *Cad8* on whole mounts of P7 wild-type (+/+; *Emx1-Cre*) and homozygous conditional mutant (*COUP-TFI fl/fl; Emx1-Cre*) brains uniquely marks the frontal/motor areas (F/M). The F/M areas substantially expand following selective deletion of *COUP-TFI* from cortex. The reduced ectopic primary sensory areas (V1, S1) can be identified by small domains of diminished *cad8* expression in posterior cortex (Taken from [74]).

previously described areal impairments, show also a F/M-like laminar organization of the parietal cortex.

Analyses of CSMN markers in the frontal and parietal region of COUP-TF1 CKO, called from now on motorized S1 (mS1), showed that *Fezf2* and *Ctip2* were dramatically increased in layers VI and V of the mS1 [134]. *Ctip2* was strikingly increased in the upper sixth layer of the mS1, and other area specific markers known to be expressed in layer V neurons of the M1, such as Cysteine-Rich Motor Neuron 1 (*Crim1*), *FOXP2* and insulin-like growth factor binding protein 4 (*Igfbp4*), were expressed by layer V neurons of the mS1 (**Figure 21**). Thus, in the absence of COUP-TF1 function, the number of neurons expressing high levels of F/M-specific markers in layer V and VI of the motorized S1 is dramatically increased.

Interestingly, the caudal shifted S1 and V1 in COUP-TF1 CKO express a comparable level of *Ctip2* expression with respect to their counterparts in WT animals. Therefore, COUP-TF1 acts in an area restricted manner on the differentiation of the two main classes of corticofugal deep layer neurons, the corticothalamic and the corticospinal motor neurons [134, 140].

In addition, *FOXP2/Tbr1* and *Ctip2* that are normally expressed in distinct subsets of neurons in layers VI and V respectively, with only rare cells co-expressing both *FOXP2* and *Ctip2* or *Tbr1* and *Ctip2*, showed increased co-localization in COUP-TF1 CKO. This indicates an abnormal acquisition of mixed corticothalamic and CSMN identity by corticofugal neurons. Moreover, altered balance between *Fezf2/Ctip2*, that were increased in layer VI and *Tbr1* expressing cells was observed since E13.5 and persists at E16.5 when the generation of CFuPN is terminated, indicating that COUP-TF1 is normally involved in determining CSMN versus CThPN identity since early stages of corticogenesis. Thus, in S1 cortex, COUP-TF1 normally represses a CSMN differentiation program during generation of layer VI corticothalamic neurons and in the absence of its function, presumptive CThPN display cardinal molecular features of CSMN differentiation.

Correspondingly, fluorogold retrograde labeling in the cerebral peduncle showed that SCPNs, which are confined to layer V in S1, were expanded to the layer VI of mS1 where abnormally high *Ctip2* expressing cells were located. Additional retrograde labeling from the spinal cord reveals that these abnormal SCPN of the motorized layer VI are able to successfully send axonal projections to more caudal targets in the cervical spinal cord. Instead, in the mS1 layer V, genuine CSMNs that

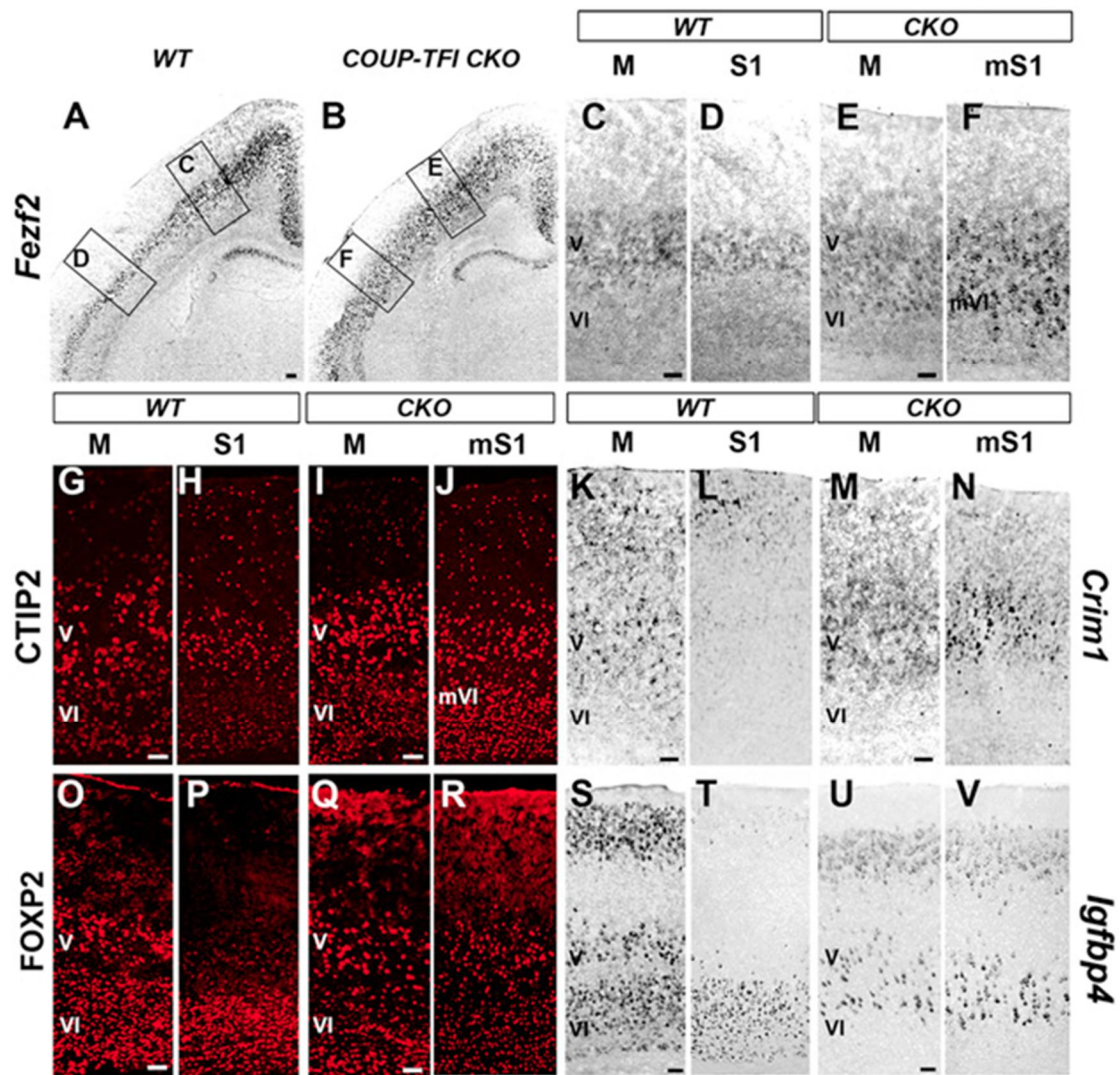


**Figure 21-Increased expression of molecular hallmarks of CSMN in corticofugal neurons of S1 cortex in COUP-TFI CKO mice.**

(A and B) Coronal sections and (C–V) higher magnification views of frontal (M) and parietal (S1/mS1) cortices of WT and COUP-TFI CKO P8 brains indicate abnormal expression levels of the CSMN markers Fezf2 (A–F), CTIP2 (G–J), Crim1 (K–N), FOXP2 (O–R), and Igfbp4 (S–V) in layer V and radial expansion of these markers toward superficial layer VI (mVI) in mS1 of COUP-TFI CKO cortices. Note that expression of FOXP2 is reduced (Q and R) and expression of Igfbp4 is abolished (U and V) in layer VI in both areas of COUP-TFI CKO cortices (taken from [134]).

abnormally express high levels of *Fezf2*, *Ctip2*, *FOXP2* and *Tbr1* fail to reach the spinal cord, limiting their axonal projections to the cerebral peduncle. Thus, abnormal expression levels of CSMN-specific control genes in presumptive CThPN initiate central features of CSMN differentiation, including spinal cord axonal targeting, whereas the transcriptional dysregulation in genuine CSMNs in the absence of COUP-TF1 function results in abnormal differentiation of this cell population.

The effects of the increase in motor area size, and the reassignment of the corticospinal connectivity to layer VI corticothalamic neurons were tested by different behavioral tests aimed to evaluate the sensorimotor function. These tests demonstrated that even in the presence of relatively preserved corticospinal connectivity, the altered areal and temporal specification of CSMN critically impairs the function of the cortical neuronal networks controlling skilled motor behavior. These mis-specified neurons in layer VI of the mS1 may not be integrated into appropriate cortical motor neuronal networks, and therefore are unable to contribute to fine motor control.

Overall, COUP-TFI seems to precisely control the areal and temporal specification of CSMNs during corticogenesis, and might thus regulate the number of CSMNs in sensory areas by negatively regulating the CSMN differentiation program [134].

## **VIII. Aim of this work**

As previously described, in the absence of COUP-TF1 function, in S1 cortex, layer VI neurons that would normally differentiate into CThPN, prematurely and abnormally differentiate as CSMNs and send their axons to all segmental levels of the spinal cord. However, COUP-TF1 deficient neurons in layer V, expressing abnormally high levels of *Fezf2*, *Ctip2*, *FOXP2*, *Tbr1*, *Crim1* and *Igfbp4* and showing an abnormally increased number of neurons co-expressing corticothalamic and corticospinal markers *FOXP2/Ctip2* and *Tbr1/Ctip2* are abnormally differentiated. These genuine CSMN neurons reach the cerebral peduncle, but fail to project to the spinal cord, resulting in impaired fine motor skills in COUP-TF1 CKO adult mice [134].

The initial aim of my project was to unravel the molecular mechanisms underling the abnormal differentiation of layer V neurons in COUP-TFI mutants. As a

first approach, I checked the expression of the two molecular controls regulating the differentiation of the two main populations of layer V neurons: callosal and subcerebral PNs in the S1 of WT and COUP-TFI mutant cortices. Given the increase in *Fezf2* and *Ctip2* expression observed in COUP-TFI CKOs, a decrease in *Satb2* expression was expected. However, *Satb2* expression did not decrease in COUP-TFI mutants, but was even increased in layer Vb, and more surprisingly, a remarkable increase in the number of *Satb2/Ctip2* co-expressing neurons was observed in COUP-TFI mutants. I observed that a population expressing these two mutually exclusive markers, normally representing 4% of layer V neurons at P0, increases dramatically in COUP-TFI mutants to represent 18% of layer V neurons and 8% of layer V neurons. Since *Satb2/Ctip2* co-expressing neurons constitute a previously uncharacterized cell population, I aimed to investigate the molecular mechanisms allowing *Satb2* and *Ctip2* co-expression, and the temporal and areal distribution of these cells. Moreover, by the use of molecular markers, vital dyes, and biochemical and electrophysiological approaches I tried to unravel the specific features of *Satb2/Ctip2*-positive cells. Thus, overall, my work was aimed to characterize a novel and previously uncharacterized cell population at molecular, hodological, electrophysiological and morphological levels.

## *Chapter 2: Materials and Methods*

---

## I. Mutant Mice and genotyping

### A. COUP-TFI fl/fl<sup>Emx1-Cre</sup> mouse line

To assess the intrinsic role of COUP-TFI in cortical area patterning, our group generated a conditional cortex specific COUP-TFI KO mouse line, *COUP-TFI fl/fl*<sup>Emx1 Cre</sup> (COUP-TFI CKO) [140].

The generation of this mouse line was described in Armentano et al, 2007 [140] (**Figure 1**). Homozygous COUP-TFI<sup>fl/fl</sup> animals are viable and fertile and mated to the *Emx1-IRES-cre* mouse line, which has been shown to drive site-specific recombination in dorsal pallium from E10.5. Mice homozygous for COUP-TFI<sup>fl/fl</sup> and heterozygous for *Emx1-IRES-cre* were named COUP-TFI fl/fl<sup>Emx1Cre</sup> (COUP-TFI CKO). Mice heterozygous for COUP-TFI<sup>fl/fl</sup> (fl/+) and heterozygous for *Emx1-IRES-cre*, and Mice heterozygous or homozygous for COUP-TFI<sup>fl/fl</sup> (fl/+ or fl/fl) without an *Emx1-IRES-cre* allele were considered as controls. COUP-TFI CKO mice are viable and fertile and show cortex specific inactivation, as assessed using a COUP-TFI antibody [140] (**Figure 2**).

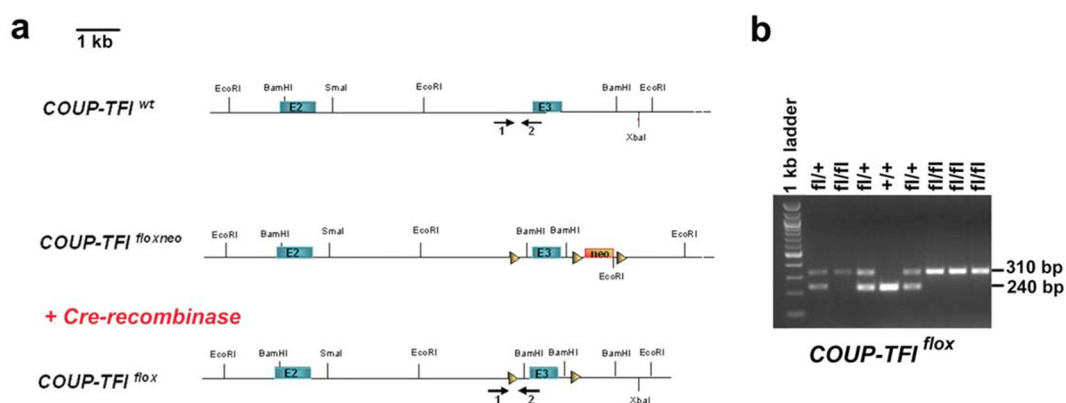


**Figure 1-Generation of COUP-TFI CKO mice.**

(a) To generate the COUP-TFI<sup>fl/fl</sup> allele in embryonic stem cells (ES), the *Cre-recombinase* was electroporated in ES clones heterozygous for the COUP-TFI<sup>fl/neo</sup> allele and excised the neomycin (neo) cassette. Triangles indicate the presence of *LoxP* sites. E2, exon2; E3, exon3. (b) PCR genotyping on wild type (+/+), heterozygous (fl/+) and homozygous (fl/fl) mice using the primers indicated in (a) as black arrows. Taken from [140].

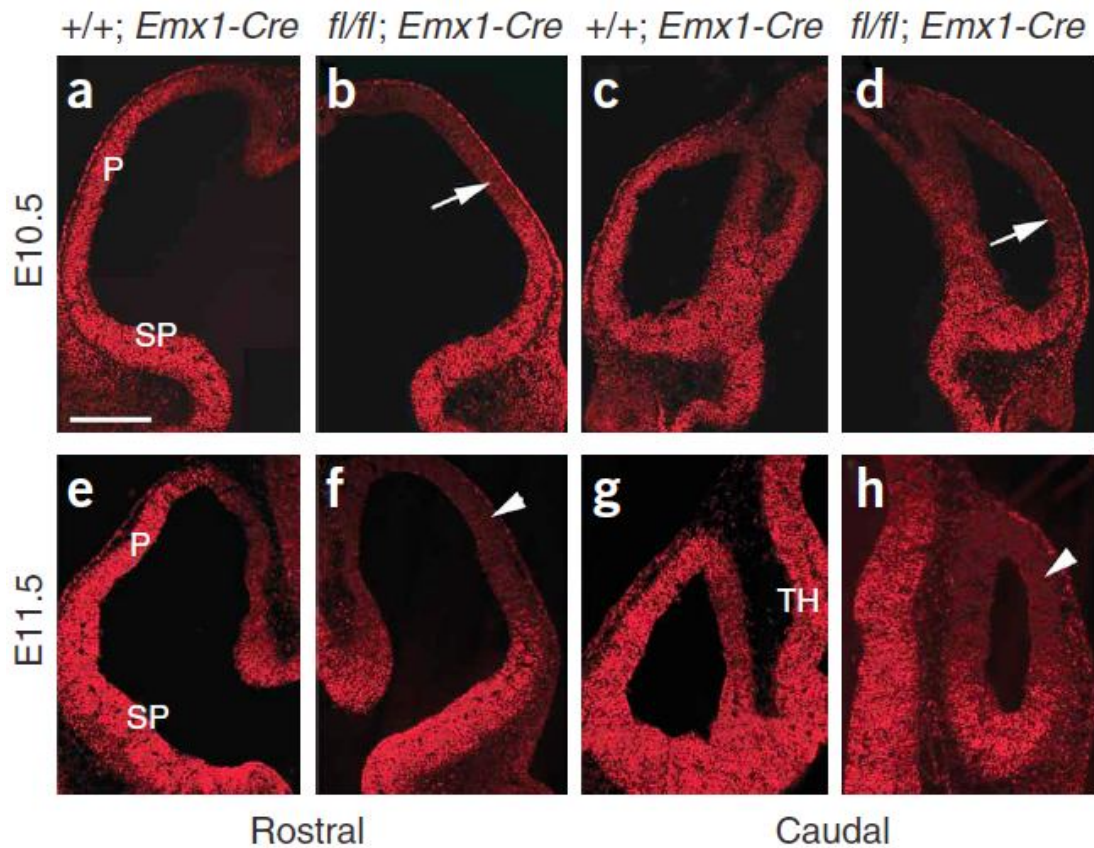


**Figure 2-Cortex-specific inactivation of COUP-TFI in COUP-TFI *fl/fl* *Emx1Cre* mice**

(a–h) Coronal sections at rostral and caudal levels of control (+/+; *Emx1Cre*) and COUP-TFI*fl/fl**Emx1Cre* (*fl/fl*; *Emx1Cre*) embryos, at the stage indicated on the left, and immunostained with an antibody to COUP-TFI. Note that a few COUP-TFI–positive cells were still present at E10.5 (arrows in b,d) in the pallium (P), whereas no pallial cells expressed COUP-TFI at E11.5 (arrowheads in f and h). Staining in the subpallium (SP) and thalamus (TH) was not affected (f,h), confirming a cortex-specific inactivation of COUP-TFI (Taken from [140]).

COUP-TFI *fl/fl*<sup>*Emx1-Cre*</sup> mouse line was genotyped by Polymerase Chain Reaction (PCR). For each sample, two different reactions were made in order to test the presence of the floxed COUP-TFI allele, and the allele containing Cre recombinase. All reactions were prepared using the Green Taq (PROMEGA), which is a mix containing the enzyme and the proper buffer in a 2x concentration. To genotype the COUP-TFI locus, three primers were used (at a concentration of 1µM) to verify the presence of the third exon and of the flox sequences in the COUP-TFI genomic sequence. The forward primer (ARM531) anneals to a sequence upstream of the third exon (and is used with a double concentration compared to the other two primers to maintain stoichiometric proportions), whereas EX351 anneals to the third exon sequence and ARM 402 to a site, which is downstream of the floxed exon. Their

sequences are: ARM531 (5' CTGCTGTAGGAATCCTGTCTC 3'), ARM402 (5' AAGCAATTTGGCTTCCCCTGG 3') 1μM and EX351 (5' AATCCTCCTCGGTGAGA 3') 1μM. The amplicon corresponding to the *wt* is 250bp fragment, while the one corresponding to the floxed COUP-TFI allele is a 350bp fragment. Thus, the genotype of heterozygotes (*fl/+*) gives rise to 2 fragments of 250 and 350bp. The PCR amplification program used to amplify the COUP-TFI alleles was the following:

94°C – 7'  
 94°C – 45'' }  
 60°C – 45'' } 35x  
72°C – 1' }  
 72°C – 7'

In order to genotype the *Emx1-Cre* allele the primers used were designed to amplify a fragment of DNA within the CRE-recombinase sequence: CRE1 (5' CAGGATATACGTAATCTGGC 3') and CRE4 (5' CACGGGCACTGTGTCCAGACCA 3'). The obtained amplicon corresponds to a fragment of 200bp. To control the quality of the PCR reaction and DNA samples, two primers were also run to amplify a fragment of β-actin. The primers sequences are the following: CCRmL (5' CAACCGAGACCTTCCTGTTC 3') and CCRmR (5' ATGTGGATGGAGAGGAGTCG 3'). The product of this reaction corresponds to a 250bp fragment. The program used for these PCR is the following:

94°C – 7'  
 94°C – 1' }  
 60°C – 45'' } 32x  
72°C – 30'' }  
 72°C – 7'

All the reactions were done in a total volume of 10μl using 1μl (100ng-500ng) of the genomic DNA solution and 9μl of the following master mixes:

Mix for COUP-TFI floxed	Volume used	Mix for Cre recombinase	Volume used	Mix for β - actin	Volume used
ARM531	2μl 10μM	CRE1	1μl 10μM	CCRmL	1μl 10μM
ARM402	1μl 10μM	CRE4	1μl 10μM	CCRmR	1μl 10μM
EX351	1μl 10μM				

H <sub>2</sub> O	1μl	H <sub>2</sub> O	3μl	H <sub>2</sub> O	3μl
Green Taq	5μl 2x	Green Taq	5μl 2x	Green Taq	5μl 2x

### B. Thy1-eYFP line H:

Thy1-eYFP line H mice [345] were obtained from Jackson Labs and bred in our institute's animal facility. Genotyping was performed by PCR using the primers Thy1.fw (5' TCTGAGTGGCAAAGGACCTTAGG 3') annealing to the Thy1 promoter sequence, and eYFP.rev (5' CGCTGAACTTGTGGCCGTTTACG 3') annealing to the eYFP sequence [345]. The presence of this allele gives an amplicon of 400 bp. Samples included all the animals expressing the transgene, presumably both homo- and heterozygous individuals.

The reaction was done in a total volume of 10μl using 1μl (100ng-500ng) of the genomic DNA solution and 9μl of the following master mix:

Mix for thy1 YFP	Volume used
Thy1	1μl 10μM
YFP	1μl 10μM
H <sub>2</sub> O	3μl
Green Taq	5μl 2x

## II. Histological procedures:

### A. Tissue processing

Brains were collected from postnatal P0, P7 or P21 mice after perfusion with paraformaldehyde (PFA) 4%, in order to fix the tissue and remove as much blood as possible from the brain to avoid its intrinsic fluorescence and the phosphatases that could interfere with the histologic analysis. After dissection the brains were fixed with PFA 4% at +4°C in gentle rocking, for 2 hours, followed by 3 washes in PBS, 10' each.

## B. Immunofluorescence on cryosections

After PFA fixation, brains were gradually equilibrated in PBS sucrose 10%, 20% and 30%. Sucrose traces were removed by washing the brains in Optimal Cutting Temperature (OCT), in which they were embedded and frozen. Brains were then stored at -80°C until cutting.

Samples were cut with a leica cryostat, at a thickness of 20 µm. Slices were collected on polarized slides (Thermo Scientific), and were stored at -80°C until usage.

Before immunofluorescence the slides were incubated in Unmasking Buffer (Sodium citrate 85mM, pH6.0) and boiled twice (first time for 15'' and the second time just brought to the boiling point after changing the buffer), for antigen retrieval.

The slides were cooled in ice 10' and washed 3 times 10' in PBS, before incubating them 1h at RT with the blocking solution (PBS 0.3% Triton and 10% Goat Serum or New Born Calf Serum in case one of the primary antibody is made in goat) to block all the sites that would aspecifically bind antibodies. After blocking, slides were incubated ON at +4°C with primary antibodies diluted in 200 µl/slide of PBS 0.3% Triton and 3% Goat or New Born Calf Serum. The primary antibodies used were the following:

Antibody	Host animal	Working concentration	Incubation	source
Anti-Satb2	Mouse	1:20	ON at 4°C	abcam
Anti-Ctip2	Rat	1:300	ON at 4°C	abcam
Anti-Ctip2	Rabbit	1:500	ON at 4°C	abcam
Anti-Sox5	Rabbit	1:300	ON at 4°C	Gentaur
Anti-Ski	Rabbit	1:50	ON at 4°C	Santa Cruz biotechnology
Anti-LMO4	Rat	1:500	ON at 4°C	Donated by Jane Valsvader lab, Parkville, Australia
Anti-Er81	Rabbit	1:1000	ON at 4°C	Donated by Silvia Arber lab, Basel, Switzerland
Anti-Bhlhb5	Guinea pig	1:500	ON at 4°C	Donated by Benett Novitch lab, California, Lois Angeles

After incubation with primary antibodies, slides were washed 3 times in PBS 10' each, and then they were incubated 2 hours at room temperature with the secondary antibodies diluted as for primary antibodies. The secondary antibodies used were the following:

Epitope	Working concentration	Incubation conditions	Host animal	Source
Rabbit FC 350	1:300	2h R.T.	goat	Life Technologies
Rabbit FC 488	1:300	2h R.T.	goat	Life Technologies
Rabbit FC 594	1:300	2h R.T.	goat	Life Technologies
Guinea pig FC 488	1:300	2h R.T.	goat	Life Technologies
Guinea pig FC 594	1:300	2h R.T.	goat	Life Technologies
Rat FC 488	1:300	2h R.T.	goat	Life Technologies
Rat FC 594	1:300	2h R.T.	goat	Life Technologies
Mouse FC 488	1:300	2h R.T.	goat	Life Technologies
Mouse FC 594	1:300	2h R.T.	goat	Life Technologies

After the incubation with the secondary antibodies slides were washed 3 times in PBS (10' each), and mounted with Vectashield medium with or without DAPI (clinisciences).

### C. Immunofluorescence on vibratome sections

After fixation in PFA 4% and PBS washes, brains were embedded in 4% agar, and 200  $\mu\text{m}$  thick slices were cut with a leica vibratome (VT1000S) at +4°C. Slices were incubated in blocking solution (PBS 0.3% triton, 3% Bovin calf serum (BSA) and 10% goat or new born calf serum) ON at +4°C in gentle rocking. Then, primary antibodies diluted in 500  $\mu\text{l}$ /well of PBS 0.3% triton, 3% BSA and 3% goat or new born calf serum were carried out ON at +4°C followed by long PBS washes at room temperature, 1 hour each. Primary antibodies used were:

Antibody	Host animal	Concentration	Incubation	Source
Anti-Satb2	Mouse	1/80	ON at 4°C	Abcam
Anti-GFP	Rabbit	1/1000	ON at 4°C	Molecular Probe
Anti-Ctip2	Rat	1/500	ON at 4°C	abcam
Anti-Ctip2	Rabbit	1/500	ON at 4°C	abcam
Anti-Sox5	Rabbit	1/300	ON at 4°C	Gentaur
Anti-LMO4	Rat	1/500	ON at 4°C	Donated by Jane Valsvader lab, Parkville, Australia
Anti-Er81	Rabbit	1/1000	ON at 4°C	Donated by Silvia Arber lab, Basel, Switzerland
Anti-Bhlhb5	Guinea pig	1/500	ON at 4°C	Donated by Benett Novitch lab, California, Lois Angeles

Secondary antibodies diluted as primary antibodies were then added ON at +4°C.

Secondary antibodies used were:

Epitope	Working concentration	Incubation conditions	Host animal	Source
Rabbit FC 488	1:500	ON at 4°C	goat	Life Technologies
Rabbit FC 594	1:500	ON at 4°C	goat	Life Technologies
Rabbit FC 633	1:500	ON at 4°C	goat	Life Technologies
Guinea pig FC 488	1:500	ON at 4°C	goat	Life Technologies
Guinea pig FC 594	1:500	ON at 4°C	goat	Life Technologies
Guinea pig FC 633	1:500	ON at 4°C	goat	Life Technologies
Rat FC 488	1:500	ON at 4°C.	goat	Life Technologies
Rat FC 594	1:500	ON at 4°C	goat	Life Technologies
Rat FC 633	1:500	ON at 4°C	goat	Life Technologies
Mouse FC 488	1:500	ON at 4°C	goat	Life Technologies
Mouse FC 594	1:500	ON at 4°C	goat	Life Technologies
Mouse FC 633	1:500	ON at 4°C	goat	Life Technologies

Slices were washed again as previously described after primary antibodies, and mounted on slides with Vectashield medium with or without DAPI (clinisciences).

#### D. RNA digoxigenin probes synthesis

Plasmid containing the open reading frame (ORF) of LMO4 was linearized using a restriction enzyme (BamHI) that cut the plasmid in a single site positioned at the 5' of the ORF. The reaction was carried with 15µg of plasmids, 5µl of the correspondent 5x buffer and 3µl of the enzyme (Ozyme) in H<sub>2</sub>O for 2 hours in a total volume of 50 and verified in gel electrophoresis. The linearized plasmid was then purified on MicroSpin (Roche) columns using the protocol provided by the manufacturer. The transcription of RNA probes was carried using 1µg of linearized DNA in a 20µl mix containing 2µl of transcription buffer 10x (Roche), 2µl of Dig labeling Mix (Roche), 1µl of RNAase inhibitor (Roche) and 2µl of the RNA polymerase Sp6 for 2h at +37°C. Then, 2µl of DNAase (Roche) were added and the mix was left at +37°C for other 30' to destroy the linearized DNA in the solution. DNase action was stopped adding 2 µl of EDTA 25mM. Probes were then precipitated at -80°C for 30' by adding 100µl H<sub>2</sub>O, 10µl LiCl 4M and 300µl of Ethanol 100% to the mix. To separate precipitated RNA, the mix was centrifuged 15' at 20000 g at +4°C. The pellet was

then washed in 100µl ethanol 70% and re-centrifuged at the same speed. RNA was air-dried to remove ethanol, and then re-suspended in 40 µl of sterile H<sub>2</sub>O.

### **E. Whole mount *In situ* hybridization**

Sample preparation: After PFA fixation, brains were progressively dehydrated in ethanol 25%, 50%, 75% and 100% in PBS-tween 0.1% by washing 2 times in each solution for 10' at +4°C. Brains were stored at -20°C in pure ethanol and then progressively rehydrated to PBS-tween 0.1% before usage.

Hybridization: Brains were treated with H<sub>2</sub>O<sub>2</sub> 0.5% in PBS-Tween 0.1% for 1h at RT. Then, brains were washed twice with PBS-Tween 0.1% and incubated with Proteinase K 10µg/ml in PBS-Tween 0.1%, for 30'. After brief rinse in PBS-Tween 0.1% the brains were post-fixed with P.F.A. 4%, glutaraldehyde 0.1% in PBS-Tween 0.1% for 20' in ice and in gentle rocking. Then, the brains were washed 5' in PBS-Tween 0.1% and incubated in hybridization buffer (Formamide 50%, SSC 1.3X, EDTA 5mM, 2%, 50µg/ml, CHAPS 0.5%, Tween 2%, Yeast RNA 50µg/ml, in H<sub>2</sub>O) first 10' at RT, then pre-hybridized 1h at +70°C. Probes were diluted in the same hybridization buffer up to a concentration of 200ng/ml, hybridization was carried out at +70°C over night.

Antibody incubation: The excess of probes was washed with hybridization buffer twice for 5' and then 30' at +70°C, then the brains were equilibrated in a mix of 50% TST (NaCl 0.5M, Tris HCl pH7.5 0.01M, Tween 0.1% in H<sub>2</sub>O) and 50% hybridization solution at +70°C, then in 100% TST at RT for 10'. To eliminate unbound RNA, brains were incubated 30' in RNAase A 10µg/ml solution in TST at RT, then samples were washed in TST for 10' at RT, in hybridization buffer for 10' at RT, and then twice in hybridization buffer for 30' at +65°C. Brains were equilibrated in B1 buffer (Maleic acid 100 mM, NaCl 150 mM in H<sub>2</sub>O) (four washes: 5', 5', 10' and 1h) at RT. The blocking was done with the B2 buffer (20% sheep serum in B1 buffer) for 1h at RT and followed by incubation with the α-Dig-U-AP antibody (ROCHE) (diluted to 1/2000 in B1 2% sheep serum) ON at +4°C. This antibody

recognizes the digoxigenin of the riboprobes and it is conjugated to an Alkaline Phosphatase.

Revelation of the signal: The excess of antibody was removed from brains by washing them in B1 buffer at RT first for 5', then twice for 1h, and finally for 2 days changing the buffer every day. Before the revelation, brains were incubated twice for 20' in B3 buffer (Tris HCl 100mM, MgCl<sub>2</sub> 50mM, NaCl 100mM, Tween 0.1% in H<sub>2</sub>O) at RT. Revelation was performed using NBIT-BCIP (SIGMA) 0.2% tween as a substrate of alkaline phosphatase giving a blue precipitate where the Digoxigenin antibody bound hybridized riboprobes. The reaction was left going either at RT or at +4°C until the signal reached the proper intensity. After a time varying from 1 to 3 days the reaction was stopped washing 3 times the hybridized brains with PBS-tween 0.1% for 10'.

De-staining process: during the revelation, aspecific precipitate may impinge on the quality of the signal. The de-staining process removes some precipitate increasing the quality of the signal. All the following passages were performed at RT for 1h in gentle rocking. They consist in equilibrating brains in a mix of 50% methanol and 50% PBS-Tween 0.1%, followed by 3 washes in methanol 100%, and an equilibration in a mix of B.A.B.B. (Benzyl alcohol 33%, Benzoin benzoate 67%) and 50% methanol, finally followed by washes in B.A.B.B. for several days until brains reach a good quality of the signal. De-staining process was stopped by inverting all previously described steps. Samples were stored at +4°C in PBS (0.1% tween, 0.1% PFA).

### **III. Imaging and Morphological analyses**

Images of immunostained cryosections were taken using the LEICA DM6000 microscope, while images of immunofluorescences carried out on thick vibratome sections were taken using the Zeiss 710 confocal microscope. Images from optical and confocal microscopes were then processed using Photoshop and Zen-lite 2012, respectively. Finally, images for Whole Mount I.S.H. were acquired using a Leica Spot microscope.

### **IV. Countings**

Countings were done manually. Images of coronal sections taken in the somatosensory area (S1BF) or in Motor area (M1) were divided in 6 bins, at P0, going from layer VI to the pia. Bins 1 and 2 represent layer VI, bins 3 and 4 represent layer V, while bins 5 and 6 represent the upper layers. At P7, cortical thickness is increased; the radial surface of analyzed brain regions was thus divided in 10 bins allowing to count cells from layer VI to layer I (1-10). Bins 1, 2 and 3 represent layer VI, bins 4, 5, and 6 represent layer V, and bins 7-10 represent upper layers. The correspondence between bins and layers was determined analyzing the expression of specific laminar markers such as *Ctip2*, *Satb2*, *Cux1* and others. Counting of single or double labeled cells were normalized to the total number of DAPI cells in each bin. To compare the counting performed on different sections to analyze triple colocalizations, the counting was performed on cortical images with a constant width of 600 $\mu$ m.

## **V. Molecular biology methods**

### **A. DNA Extraction from murine tissue**

To genotype animals, earmarks of P21 weaned mice were collected and used for the extraction of genomic DNA, while for sacrificed postnatal pups, DNA was extracted from the tip of the tail. Tissue lysis was performed by 2 hours incubation at +58°C, in agitation, in 500 $\mu$ l of lysis buffer (50mM Tris pH 7.5, 100mM EDTA pH8, 100mM NaCl, 1% SDS, 0.2 $\mu$ g/ $\mu$ l Proteinase K). DNA was extracted with an equal volume of isopropanol added and mixed by inversion. Samples were centrifuged for 5' at 20000 g. DNA pellet was washed with 1ml of Ethanol 70%, followed by a centrifugation for 2' at 20000 g. DNA was air-dried and resuspended in an appropriate volume of H<sub>2</sub>O (70  $\mu$ l for earmarks and 500  $\mu$ l for tails) at 37°C with agitation for 1 hour. DNA was stored at 4°C until usage.

### **B. pCDK5-LMO4-IRES-GFP plasmid construction**

The LMO4 ORF was amplified using available cDNA, previously synthesized in the lab starting from RNA extracted from P0 cortices, and the following primers: MluI-

Lmo4.fw (5'GGACGCGTTGAGAGCAGCTC3') and MluI-Lmo4.rev  
(5'GGACGCGTTTCTGCATTACTC3')

PCR program was as follows:

95°C – 5'  
 95°C – 30'' }  
 60°C – 30'' } 35x  
 72°C – 45'' }  
 72°C – 8'

These primers were designed with an MluI restriction cassette at their 5' end, which allowed digesting the amplified Lmo4 sequence with MluI on both sides (3' and 5'). After purifying the PCR product using the QIAGEN PCR Purification Kit (following manufacturer's protocol) LMO4 amplicon was digested as follows:

Mix for MluI digestion	Volume used
DNA	28µl 150 ng/µl
Buffer 3	5µl 10x
H <sub>2</sub> O	14µl
MluI (BioLabs)	3µl 10u/µl

After 2h at 37°C the digested LMO4 ORF was purified again using QIAGEN Gel Purification Kit (following manufacturer's protocol) and cloned in the expression vector to be used for *in utero* electroporations. The expression plasmid was previously used in another study to overexpress Fezf2 sequence in post-mitotic cells of the cortex [213], and contains the Cdk5 promoter (upstream of the polylinker), which drives the expression of cloned genes together with an IRES-GFP sequence (**Figure 3**). The IRES sequence allows GFP expression from the polycistronic RNA resulting from CDK5-driven transcription, which contains at the 5' end the sequence of interest and at the 3' end the GFP ORF. To clone MluI digested LMO4 ORF in this plasmid, CDK5-IRES-GFP was digested with the same enzyme and the same protocol described above. However, after digestion and Gel purification, the plasmid ends

were dephosphorylated using Calf Intestinal Phosphatase (CIP, BioLabs) to avoid empty plasmid closure during ligation:

Dephosphorylating Mix	Volume used
DNA	44µl 20 ng/µl
Buffer 3	5µl 10x
CIP (BioLabs)	1µl 5u/µl

The mix was left 1h at 37°C, then another µl of CIP was added and the mix was left again for 1h at 37°C. Dephosphorylated plasmid was then precipitated as previously described and re-suspended in 10 µl of sterile water. The digested LMO4 ORF was then cloned in the expression vector by ligation in a 1:5 stoichiometric ratio between the plasmid (6kb) and the insert (600 bp), respectively, as follows:

Ligation mix 1:2 ratio	Volume used
Plasmid	1µl 94 ng/µl
Insert	1µl 47 ng/µl
Ligase buffer	2µl
T4 DNA Ligase (Biolabs)	1µl 10u/µl
H <sub>2</sub> O	15µl

As a control, a mix was prepared containing solely the digested plasmid without the insert. The reaction was left ON at 16°C and then precipitated as previously explained and re-suspended in 10µl of sterile water. Two µl of the ligation were then electroporated in XL1Blue bacterial cells and the cells were re-suspended in 1 ml of LB medium and left shaking at 160 rpm for 1h at 37°C. 100µl of electroporated growing cells were then plated on LB-Agar solid medium and left ON at 37°C. The day after single colonies were picked and left growing in 5 ml LB + Ampicilline

(10mg/ml dil. 1:10000) at 160 rpm ON at 37°C. These minipreps were then processed using QIAGEN Miniprep Kit (according to the manufacturer's protocol) and the extracted plasmid (pCDK5-LMO4-IRES-GFP) was sequenced to verify the presence and orientation of the insert using the following primer: pCDK5C.fw (5'-AGGACTAAACGCGTCGTGTCC-3'). Positive clones were amplified by maxiprep (in 400 ml LB + Amp) and purified using Endofree Maxiprep Kit of QIAGEN (according to manufacturer's instructions) to avoid the presence of endonucleases in the DNA used for *in utero* electroporations.

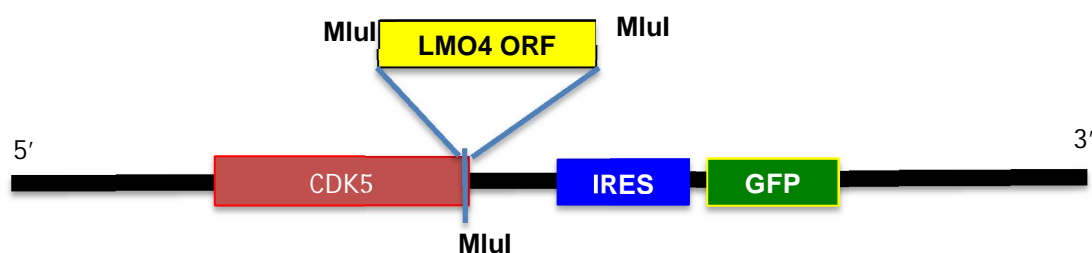


**Figure 3- Schematic of cdk5 LMO4 IRES GFP**

## **VI. *In utero* electroporations**

*In utero* electroporations were performed as previously described in [346] with some modifications as follows:

The DNA mix to inject in embryonic brains was prepared as follows: DNA 1mg/ml, 2 µl FASTGREEN (Sigma) in a total volume of 20 µl reached by adding sterile water. E13.5 pregnant mice were anesthetized with Ketamine/Xylazine. After shaving and cleaning the abdomen with 70% ethanol, a 3-cm midline laparotomy was performed, and the uteri were extroflexed. For DNA microinjection, 75-mm glass capillary tubes (Drummond Scientific, Broomall, PA) were used and pulled with a micropipette puller P-97 (Sutter Instrument, Novato, CA) under the following conditions: pressure, 500; heat, 800; pull, 30; velocity, 40; time, 1. The pulled capillaries were filled with DNA mix and broken at 60 µm external diameter by pinching with forceps. One microliter of DNA solution was injected into the lateral ventricle (**Figure 4**) using a Femtojet microinjector (Eppendorf). The dorsal surface of the telencephalon was visible through the uterine wall by illuminating with a fiber-optics light source (**Figure 4**). Square electric pulses were delivered at a rate of one pulse per second to embryos through the uterus by holding them with forceps-type electrodes CUY650P3

(NEPAGENE, Japan) (**Figure 4**), while the uterus was kept wet by dropping saline (prewarmed at 37°C) between the electrodes. Four electric pulses (37V, 50 ms each) were delivered by using a NEPA21 electroporator (NEPAGENE, Japan). Then, the uterine horns were repositioned in the abdominal cavity. The abdominal wall and skin were sewed up with surgical sutures. Finally, operated mice were peritoneal injected with Gentamicin 10 µg/ml and Ketofen 50 µg/ml (Sigma) to prevent infections and decrease post-operative pains, respectively.



**Figure 4- *In utero* Electroporation**

(A) Schematic representation of a micropipette and electrodes. (B) DNA injection into an E15.5 mouse embryo in utero, illuminated with a fibre-optics light source. (C) Electroporation by holding the embryo through the uterus with forceps-type electrodes. Arrows indicate a micropipette for DNA injection (B) and electrodes (C). Scale bar, 5 mm.

## VII. Co-Immunoprecipitation

Co-Immunoprecipitation was performed as described in [212] with some modifications. Postnatal day one (P1) pups were anesthetized with ketamine/xylazine, perfused with cold PBS and decapitated. Cerebral cortices were dissected and nuclear proteins were purified using the NE-PER kit from Pierce (Thermo scientific) according to the manufacturer's instructions. Nuclear proteins were dialyzed against buffer D (20% glycerol, 20mM HEPES (pH=7.9), 100mM KCl, 0.2mM EDTA, 0.5mM DTT, 0.5mM PMSF, all from Sigma-Aldrich) for 2 hours, changing the buffer after 50 minutes at +4°C, in 3500 Molecular Weight Cut-Off Slide-A-Lyzer Mini Dialysis Units (Fisher scientific). For pre-clearing, 50µg of the nuclear extracts were incubated with 100 µl Protein A Sepharose 50% bead slurry (sigma aldrish) in 400 µl of total volume with constant, slow rotation for 1 hour at 4 °C, prior to being pelleted by centrifugation at 10,000 g for 10 minutes at 4°C. The precleared nuclear extracts

were then immunoprecipitated with 2 µg of anti-Satb2 antibody (mouse monoclonal, abcam) or anti-LMO4 antibody (rat monoclonal, donated by Jane Visvader lab, Australia) or a control antibody (anti-Brdu, mouse monoclonal, sigma) for 2 hours. Immunocomplexes were captured by adding 100 µl of Protein A Sepharose bead slurry. After one additional hour of rotation at 4 °C, the bound fraction was separated by pulse centrifugation. The beads were washed three times with 1 ml of ice-cold washing buffer: 1x Phosphate Buffered Saline (PBS) containing 0.1% Igepal (sigma). After the last wash, the beads were re-suspended in 2x loading buffer containing 0.1M DTT and lithium dodecyl sulfate sample buffer (sigma). Samples were denatured at +99 °C for 10 minutes, centrifuged at 10,000 g for 5 minutes at room temperature, and subjected to SDS 10% polyacrylamide gel-electrophoresis using Biorad reagents and Mini-Protean tetra cell (Biorad) for protein electrophoresis. After the electrotransfer (Trans-Blot<sup>®</sup> SD Semi-Dry Transfer Cell, Biorad), proteins were identified by immunoblotting with the following antibodies: anti HDAC1 (rabbit polyclonal, Millipore, 1/500), anti-Ski (rabbit polyclonal, santa cruz biotechnology, 1/100), anti-Brdu (mouse monoclonal, sigma (1/500)), anti-Satb2 (mouse monoclonal, abcam, 1/80), anti LMO4 (rat monoclonal, donated by Jane Vasvader lab, Australia (1/500)) and anti-β-actin (rabbit polyclonal, abcam, 1/500). Biotinylated secondary antibodies (anti-rabbit biotinylated, Vector (1/500), and anti-mouse biotinylated, Vector (1/500) a,d anti-rat biotinylated, Vector (1/500)) were then added and followed by the ABC kit (Vector laboratories). Immunoblots were visualized using SuperSignal West Pico Chemiluminescent Kit (Thermo scientific) with LAS 3000.

## **VIII. Chromatin immunoprecipiation**

Cortices from P1 controls and *COUP-TFI CKO* mutant mice (4 pups for each genotype) were dissected in HBSS, washed with DMEM, centrifuged at 500g for 1 min and fixed in PFA 1% for 10'. Cortices were then washed twice in 10 ml chilled Cell Wash buffer (20mM HEPES pH7.4, 150mM NaCl, 125mM Glycine, PMSF 0.2 mg/ml).

Samples were lysed in a lysis buffer (20mM HEPES pH7.4, 1mM EDTA, 150mM NaCl, 1%SDS, 125mM Glycine, PMSF 0.2 mg/ml).

Tissues were homogenized and membranes were fractured to obtain nuclei using a glass potter connected to an electric drill until homogenate becomes clear. Homogenized tissues were then resuspended in sonication buffer (20mM HEPES pH7.4, 1mM EDTA, 150mM NaCl, 0.4% SDS, PMSF 0.2mg/ml) in a total volume of 1200  $\mu$ l, and then divided into 4 aliquots for each genotype and sonicated 6 times for 5 seconds at 10 $\mu$ m amplitude. Aliquots were then centrifuged at 14000g and transferred to a new eppendorf leaving debris in old ones. 1,2ml of SDS Dilution Buffer (20mM HEPES pH7.4, 1mM EDTA, 150mM NaCl, 1% Triton X100, PMSF 0.2mg/ml) was added to the supernatants that were then incubated overnight at 4 °C with 3  $\mu$ g of the following antibodies: HDAC1 (rabbit polyclonal antibody, Millipore), H4K12 (rabbit polyclonal, Abcam), a control antibody (anti-GFP, rabbit polyclonal, Molecular probe) and no antibody. Another aliquot of simple sonication buffer was also added (MOCK) and used as a control (No DNA, No antibody).

Then 50  $\mu$ l of protein A sepharose beads were added to each sample. The samples were subsequently incubated with constant rotation for 3 hours at 4 °C. Samples were centrifuged and supernatant was only collected from the No-antibody aliquot and used as input control. The beads were washed 3 times for 5' at RT with 900 $\mu$ l of Chilled Washing Buffer A (20mM HEPES pH7.4, 1mM EDTA, 500mM NaCl, 0.8% Triton X100, 0.1% SDS, PMSF 0.2mg/ml), 3 times with chilled Washing Buffer B (20mM HEPES pH7.4, 1mM EDTA, 250mM LiCl, 0.5% NP40, 0.5% Deoxycholate, PMSF 0.2mg/ml) and 3 times with chilled TE (20mM Tris pH8.0, 1mM EDTA, PMSF 0.2mg/ml). After the final wash, the precipitated protein-DNA complexes were eluted by incubation with the Elution Buffer (50mM NaHCO<sub>3</sub>, 1mM EDTA, PMSF 0.2mg/ml) for 1 hour at room temperature. After centrifugation, the supernatants were incubated overnight at 65 °C to reverse the cross-linking. DNA was then extracted with phenol/chloroform, and precipitated with (1/9V NaAC, 1  $\mu$ l glycogen and 2.5 V Ethanol 100%) ON at -20°C. After 20k g centrifugation, the DNA pellet was washed with Ethanol 70% and resuspended in 20  $\mu$ l of MQ H<sub>2</sub>O.

0.5  $\mu$ l of DNA from each sample was used to perform a PCR for semiquantitative analysis of the ChIP experiment. Primers for Ctip2 locus were used as in [212]. PCR was carried out for 27 cycles, annealing temperature was 60°C. Ctip2 locus primer sequences are as follows: 8 direct 5'- GCTTGGACTCAGTGTACCTC C-3', 8 reverse 5'-CAAGAAAGCACACACCGAGA-3', 5 direct 5'- CCCGTACTCGTAGCCATCTC- 3', 5 reverse 5'-

CAAAGTCTGGAAGCGTCTCCT-3'.

The PCR products were separated on 2% agarose and bands were visualized with SYBR-Safe DNA stain (Invitrogen) and a FUJI 3000 LAS intelligent dark box equipped with a CCD camera.

## **IX. Retrograde labeling**

For retrograde labeling, mice pups were anesthetized by hypothermia at postnatal day 2 (P2). Pups were placed on a stereotaxic apparatus and callosal projecting neurons in the somatosensory cortex were retrogradely labeled via 92 nl injections of Alexa Fluor 488-conjugated cholera toxin subunit B (1 mg/ml; Invitrogen). Coordinates (in mm) were: AP:  $+1.2$ ; and ML: 1.3 from the lambda; DV:  $-0.2$  from the pial surface. Subcerebral injections, into the pons or spinal cord, were performed under ultrasound guidance (Vevo 660, VisualSonics), via 92 nl injections of Alexa Fluor 555-conjugated cholera toxin subunit B (1 mg/ml; Invitrogen). Mice were perfused with 4% formaldehyde and brains were collected at P7.

For retrograde labeling of corticospinal motor neurons (CSMN), corticospinal tracts (CST) of deeply anesthetized postnatal day 2 (P2) pups were visualized using a Vevo 770 ultrasound backscatter microscopy system (Visual Sonics) at cervical vertebral level 1 (C1) to C2. 92 nl injections of Alexa Fluor 555-conjugated cholera toxin subunit B (1 mg/ml; Invitrogen) were injected bilaterally into the CST using a Drummond Nanoject II. Mice were perfused and brains were collected at P7.

For retrograde labeling of corticobrainstem motor neurons (CBMN), descending subcerebral projection tracts of deeply anesthetized P2 pups were visualized using a Vevo 770 ultrasound backscatter microscopy system (Visual Sonics) at the midbrain-hindbrain junction. 92 nl injections of Alexa Fluor 555-conjugated cholera toxin subunit B (1 mg/ml; Invitrogen) were deposited bilaterally into the CST using a Drummond Nanoject II. Mice were perfused and brains were collected at P7.

Dual retrograde labeling of CBMN and CPN was performed with Red Retrobeads or Green IX Retrobeads (Lumafuor Inc) respectively at P2 and P3 as described for single retrograde labeling. Pups were perfused and brains were collected at P7.

## **X. Electrophysiology on acute slices**

Thy1-eYFP-H mice (23–28 days) were anesthetized with isoflurane, and decapitated. The dissected brain was vibratome cut to prepare 300  $\mu\text{m}$ -thick coronal slices. The slices were recovered in a holding chamber for 1 h at 37°C in oxygenated artificial cerebrospinal fluid (ACSF) composed as follows: 126mM NaCl, 3mM KCl, 2mM MgSO<sub>4</sub>, 1mM NaH<sub>2</sub>PO<sub>4</sub>, 25mM NaHCO<sub>3</sub>, 2mM CaCl<sub>2</sub>, and 10mM sucrose. Slices were transferred to a thermo-regulated recording chamber and continuously perfused with oxygenated ACSF containing the following synaptic blockers: 50 $\mu\text{M}$  2-amino-5-phosphonovaleric acid (APV), 20 $\mu\text{M}$  6,7-dinitroquinoxaline-2,3-dione (DNQX), and 50 $\mu\text{M}$  picrotoxin. Visually guided whole cell patch-clamp recordings were made using near-infrared differential interference contrast microscopy. Recording pipettes (with a resistance of 4-7 M $\Omega$ ) were filled with an intracellular solution composed as follows: 20mM KCl, 100mM Kgluconate, 10mM HEPES, 4mM Mg-ATP, 0.3mM Na-GTP, 10mM Na-phosphocreatine, and 0.1% biocytin. Recordings were performed on layer V cells of primary somatosensory cortex using an AxoPatch 200B amplifier (Axon Instruments, Foster City, CA), filtered at 10 kHz and were not corrected for liquid junction potentials. Data were collected on a DELL PC using custom clampfit software. Analyses of recorded responses were performed using Mini Analysis software.

## **XI. Molecular and morphological analysis of recorded cells**

Clamped cells were filled with biocytin through the recording pipette and fixed 4 hours in 4% PFA. To visualize labeled cells and recognize their molecular code, acute brain slices were rinsed in PBS, and incubated ON in PBS with 0.3% Triton-X, 3% BSA and 10% goat serum at +4°C. Then, the slices were incubated in primary antibodies diluted in PBS with 3% goat serum, 3% BSA and 0.3% triton ON at +4°C. Used primary antibodies were anti-Satb2 (1:80) mouse (abcam) and anti Ctip2 (1:500) rabbit (abcam). Slices were washed many times for 1 hour each, and biocytin was detected with Texas Red Avidin D (1:500; Vector Laboratories), whereas Satb2 and Ctip2 primary antibodies were detected by the use of Alexafluor anti-mouse far red 633 (life technologies) and anti-rabbit blue 350 (life technologies) secondary fluorescent antibodies (1:300). Avidin and secondary antibodies were diluted as in the same solution used for primary antibodies ON at +4°C. Immunolabeled slices were

mounted on polarized slides (Thermo Scientific) using Vectashield without DAPI (clinisciences). Images were taken using a zeiss 710 confocal microscope, and colocalization of biocytin filled cells with Satb2 and Ctip2 was analyzed using zen lite 2012 software.

## **XII. Electrophysiological analysis**

Electrophysiological analyses were done as in Hattox et al, 2007 [347]:

We plotted the relationship between the amount of injected current and the firing frequency. To calculate the initial slope of the firing current (FI) ratio, we analyzed responses of cells to threshold currents injected to generating action potentials and their responses to two times the threshold current. The difference in the number of action potentials in the two traces was divided by the difference in current levels. To capture the slower phase of spike frequency adaptation, which may represent a biologically separate process from fast adaptation, we defined the adaptation ratio as the ratio between the third interspike interval and the last one. This adaptation ratio was analyzed using responses recorded injected two times the threshold current. To calculate action potential characteristics, including firing threshold and afterpotentials, we analyzed responses of cells to threshold currents for generating action potentials. Firing threshold is calculated as the interpolated membrane potential at which  $dV/dt$  equals 20 V/s. To measure post spike potentials, we searched for minimum values within 50 ms of the spike and maximum values within 70 ms of this minimum. If the minimum value is more hyperpolarized than both the action potential threshold and the measured maximum value, the fast afterhyperpolarization (fAHP) amplitude is defined as the difference between the firing threshold and the average membrane potential in a small time window about the minimum value. The depolarizing afterpolarization (DAP) amplitude is the difference between the fAHP minimum and the average membrane potential in a small time window about the maximum value.

## *Chapter 3: Results*

---

## **I. Characterization of a neocortical population of double *Satb2/Ctip2*-expressing neurons in normal and *COUP-TFI*-deficient cortices**

### **A. Double *Satb2/Ctip2*-expressing neurons are increased in lower layers of *COUP-TFI* CKO cortices**

Previous work from our lab has shown that deep cortical layer neurons of the somatosensory (S1) area are abnormally specified in the absence of COUP-TFI function. Layer VI neurons express high levels of *Fezf2* and *Ctip2* (two genes involved in the specification of layer V subcerebral projection neuron or SCPN [39]) and aberrantly project to the spinal cord [134]. Mutant layer V cortico-spinal motor neurons (CSMN), instead, abnormally express both SCPN and corticothalamic projection neuron (PN) markers, and their axons are stalled in the cerebral peduncle failing to reach the spinal cord [134]. This could be due to a switch of fate of *COUP-TFI* CKO CSMN.

To investigate about the genetic mechanisms leading to this abnormal differentiation of layer V neurons and the increase in the number of *Fezf2* and *Ctip2* positive cells, I started to assess the expression and distribution of several cortical-specific genes in coronal sections of P0 mutant cortices and compared them with control brains of littermates. In particular, I focused my attention on two major transcription factors, *Satb2* and *Ctip2*, normally involved in the specification of two distinct subpopulations of layer V, callosal and subcerebral PNs. It has been reported that, normally, *Satb2* binds to MAR sequences on the *Ctip2* promoter, and recruits the NURD complex and histone deacetylase 1 (HDAC1) to directly repress *Ctip2* expression [150, 212]. *Ctip2* immunolabeling confirmed a radial expansion layer V neurons in the presumed somatosensory area of COUP-TFI mutant cortices [134] (**Figure 1 A, C**). The observed increase in *Ctip2*-positive cells (**Figure 1 C, D and E**) suggested a decreased number of *Satb2*-positive cells in mutant lower layers. On the contrary, the number of *Satb2*-positive cells was nearly unaltered and even increased in layer Vb of COUP-TFI CKO (**Figure 1 C', D' and F**). Importantly, the analysis of mutant cortices revealed an unexpected increase in the number of neurons co-expressing high levels of *Satb2* and *Ctip2*, which are mutually exclusive in normal conditions (**Figure 1 C'', D'' and G**). In P0 mutant cortices, indeed, the percentage of double

Satb2/Ctip2-expressing neurons constitutes  $18 \pm 1.8\%$ , and  $8 \pm 0.5\%$  of the total layer V and VI neurons, respectively, while these percentages stand at around  $4 \pm 0.3\%$  in layer V and  $0.35 \pm 0.01\%$  in layer VI of control brains ( $P= 0.002$  in layer V and  $P=0.0003$  in layer VI) (**Figure 1 G**). Together, my data unraveled a non-well characterized neuronal population in P0 somatosensory cortices, expressing two mutually exclusive genes, Satb2 and Ctip2, normally involved in the specification of two divergent PN subtypes, callosal and subcerebral. This cell population is remarkably increased in lower layers of COUP-TFI CKO P0 cortices. The aim of my work is to characterize this neuronal population at molecular, hodological, morphological and electrophysiological levels.

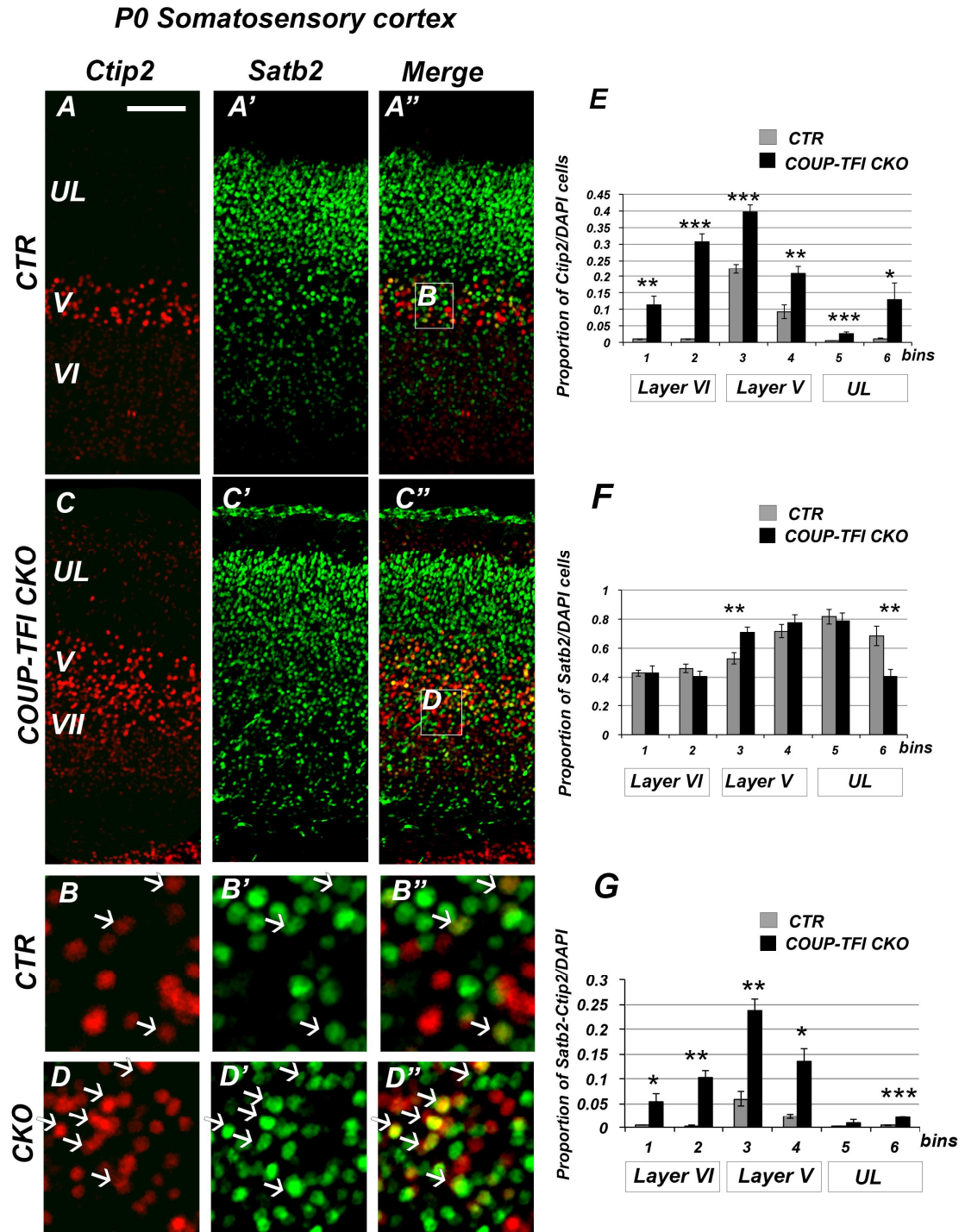


**Figure 1-Loss of COUP-TFI function leads to a drastic increase in the number of Satb2/Ctip2 Co-expressing cells in S1 Cortex.**

Coronal sections of P0 controls (A-A'') and COUP-TFI CKO (C-C'') parietal cortices immunostained for Satb2 and Ctip2. Higher magnification views of layer V (B-B'' and D-D'') indicate a higher number of double-labeled neurons in layer V of COUP-TFI CKO. Arrows indicate neurons that Co-

express both markers in controls and COUP-TFI CKO. (E-G) Quantification of the proportion of neurons expressing high levels of Ctip2 (E), Satb2 (F) and double-labeled Satb2/Ctip2 (G) per total number of cells (DAPI cells) in each bin indicate an increase in Ctip2 expressing neurons, and in Satb2/Ctip2 double-labeled neurons in layers V and VI of COUP-TFI CKO. The cortex is divided to 6 bins from layer VI to layer I, Bins 1 and 2 represent layer VI, bins 3 and 4 represent layer V, and bins 5 and 6 represent upper layers. Error bars represent SEM. Student's test, \* $P \leq 0.05$ , \*\* $P \leq 0.01$ , \*\*\* $P \leq 0.001$ . Scale bars: 100  $\mu\text{m}$  (A-A'' and C-C''). P0: postnatal day 0, CTR: controls, COUP-TFI CKO: COUP-TFI<sup>fl/fl Emx1<sup>Cre</sup></sup>, UL: upper layers, V: layer V and VI: layer VI.

## **B. Satb2/Ctip2-positive neurons are more represented in the motor/frontal area than in the somatosensory region.**

In order to understand whether double Satb2/Ctip2-positive neurons are only restricted to somatosensory cortex, I checked the distribution of Satb2 and Ctip2 proteins in the motor area of P0 cortices, a region normally characterized by high levels of Ctip2 [134] (**Figure 2A, C and E**). Interestingly, the percentage of double Satb2/Ctip2-positive cells is higher in layer V of M1 than S1 of control brains, representing 8% of counted cells (compared to  $4 \pm 0.3\%$  in the S1), whereas in layer VI the number of double positive neurons remains nearly unaltered between M1 and S1 areas ( $0.4\%$  versus  $0.35 \pm 0.01\%$ , respectively) (**Figure 1A'', B'' and G, Figure 2 A'', B'' and Figure 3 B**). Notably, even if double-positive cells are increased in the motor area of *COUP-TFI* mutant cortices compared to controls, they represent only 12% and 2% of layer V and VI neurons, respectively, thus a 1.5-fold increase in layer V (compared to a 4.5-fold increase in S1) (**Figure 2 C'', D'' and G**). These data indicate that the population of Satb2/Ctip2 positive cells is normally higher in M1 than in S1 area at P0. This trend is inverted in the absence of COUP-TFI function, the percentage of Satb2/Ctip2 positive cells in the motor area of *COUP-TFI CKO* is lower than in the “motorized” somatosensory area [134] (**Figure 3D**) indicating a difference between the “genuine” motor area and the expanded one (the “motorized” somatosensory area (mS1)). Thus, the number of double Satb2/Ctip2-positive cells varies region specifically between M1 and S1 at P0, suggesting differential expression of genes involved in their specification between motor and somatosensory areas (**Figure 3D**).

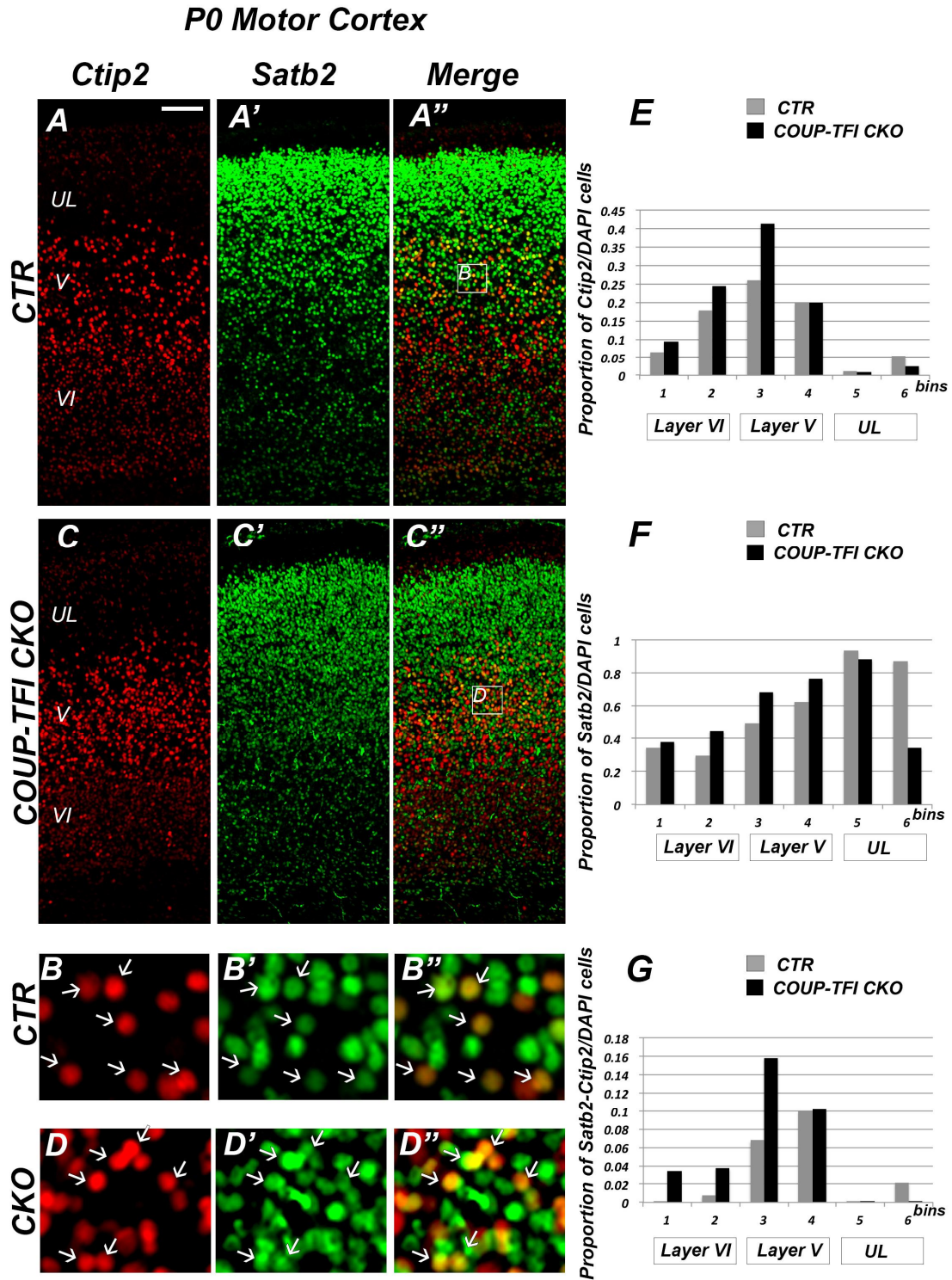


**Figure 2-High levels of Satb2/Ctip2 Coexpressing cells in the Motor Cortex.**

Coronal sections of P0 controls (A-A'') and COUP-TFI CKO (C-C'') frontal Motor cortices immunostained for Satb2 and Ctip2. Higher magnification views of layer V (B-B'' and D-D'') indicate a high number of double-labeled neurons in layer V of controls and COUP-TFI CKO. Arrows indicate

neurons that Co-express both markers in controls and COUP-TFI CKO. (E-G) Quantification of the proportion of neurons expressing high levels of Ctip2 (E), Satb2 (F) and double-labeled Satb2/Ctip2 (G) per total number of cells (DAPI cells) in each bin indicate an increase in Ctip2 expressing neurons only in lower layer V, and in Satb2/Ctip2 double-labeled neurons in layer VI and lower layer V of COUP-TFI CKO. The cortex is divided to 6 bins from layer VI to layer I, Bins 1 and 2 represent layer VI, bins 3 and 4 represent layer V, and bins 5 and 6 represent the cortical plate. Scale bars: 100  $\mu$ m (A-A'' and C-C''). Error bars are absent since the number of counted animals were n=2 (3 counted sections per animal). P0: postnatal day 0, CTR: controls, COUP-TFI CKO: COUP-TFI<sup>fl/fl Emx1<sup>Cre</sup></sup>, UL: upper layers, V: layer V and VI: layer VI.

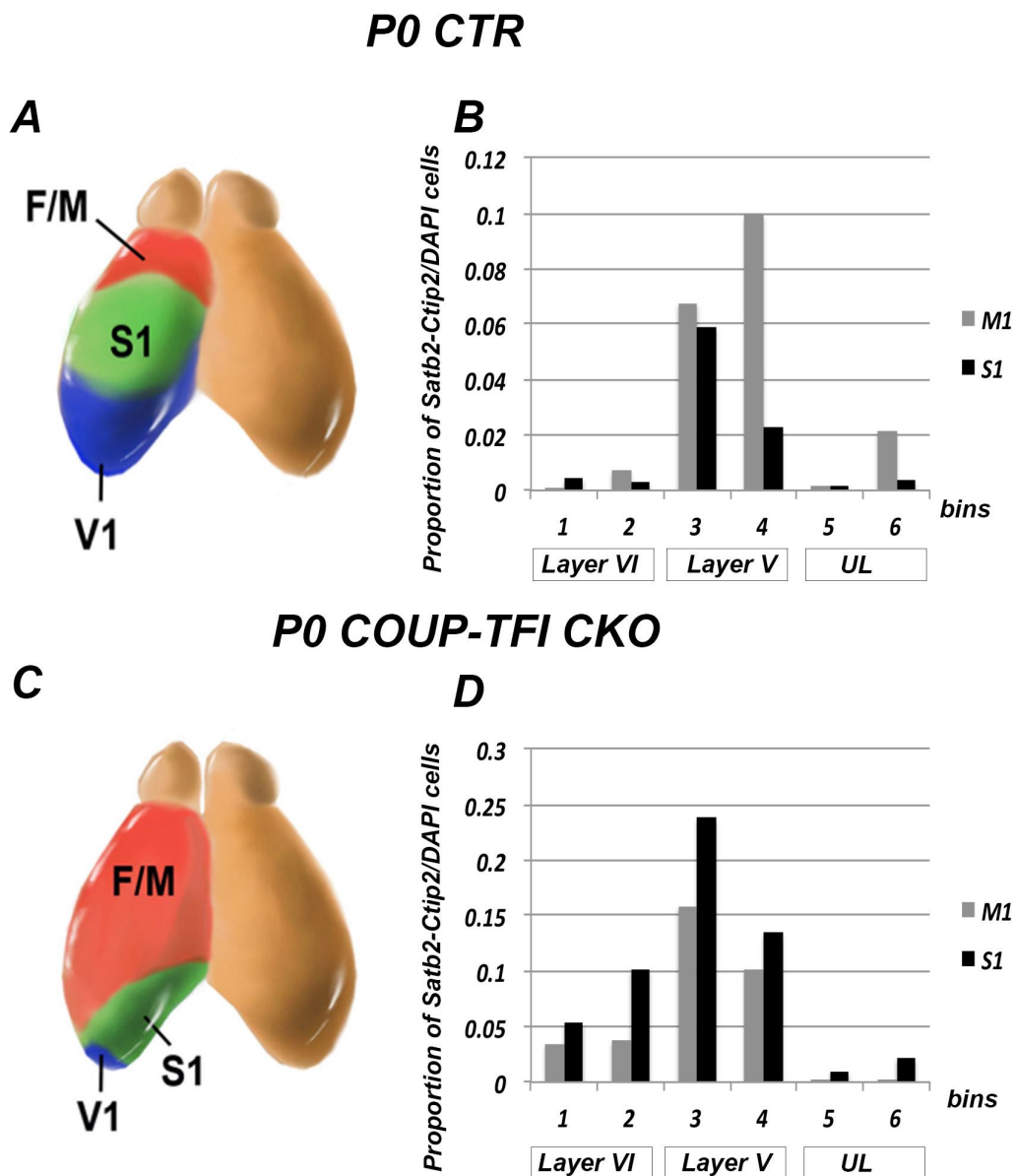


**Figure 3-Higher distribution of Satb2/Ctip2 co-expressing neurons in the Motor area of the controls and motorized somatosensory area of COUP-TFI CKO brains.**

(A and C) Schematic representation of cortical areas in P0 controls brains (A) and P0 COUP-TFI CKO brains (C) indicating the expansion of the motor area at the expense of the three reduced and caudalized sensory areas. (B and D) Graphical representation showing the distribution of Satb2/Ctip2 Co-expressing neurons in the motor (M1) versus Somatosensory (S1) areas in controls (B) and COUP-TFI CKO (D) P0 cortices indicating a higher number of Satb2/Ctip2 co-expressing neurons in M1 compared to S1 in the controls, and an inverted trend in COUP-TFI CKO cortices. The cortex is divided to 6 bins from layer VI to layer I, Bins 1 and 2 represent layer VI, bins 3 and 4 represent layer V, and bins 5 and 6 represent the cortical plate. Error bars are absent since the number of counted animals for the motor areas were n=1 (3 counted sections per animal). P0: Postnatal day 0, F/M: Frontal/Motor, M1: primary motor, S1: primary Somatosensory, V1: Primary visual, CTR: controls, COUP-TFI CKO: COUP-TFI<sup>fl/fl Emx1<sup>Cre</sup></sup>, UL: cortical plate.

### C. Tangential and radial increase of LMO4 expression in *COUP-TFI CKO* cortices

To identify the gene(s) involved in the specification of these double *Satb2/Ctip2*-expressing cells, which are more represented in motor than S1 regions in control brains, I checked for candidate genes characterized by differential expression between motor and S1 areas, which might abnormally increase in *COUP-TFI*-deficient S1 cortex. LMO4 turned out to be a good candidate since it is a region-specific gene described to be expressed in rostral/motor and caudal/visual regions of P0 cortices, but absent in the somatosensory region (**Figure 4 A**) [325]. It is also known to play a role in patterning the somatosensory barrel field [146, 325] and in establishing the subtype diversity of PNs within the rostral motor cortex [145].

I thus analyzed LMO4 expression by whole mount in situ hybridization (**Figure 4 A, A'**) and immunofluorescence experiments on control and *COUP-TFI* mutant brains (**Figure 4 B, B' and C**) and found that its levels drastically increased both tangentially and radially in the mS1 of *COUP-TFI* mutant cortices at perinatal stages. LMO4 protein is expressed in layer VI and at lower level in layer V of P0 control S1 areas (**Figure 4B**); this expression predominantly increases in layer V and part of upper layers in the mS1 of *COUP-TFI CKOs* (in layer V,  $60\pm 4.4\%$  in *COUP-TFI CKO* versus  $15\pm 2.4\%$  in controls ( $P < 0.001$ ), in layer VI,  $32\pm 2.3\%$  in *COUP-TFI CKO* versus  $26\pm 1.57\%$  in controls ( $P = 0.06$ ) and in lower part of upper layers  $51\pm 5.3\%$  in *COUP-TFI CKO* versus  $10\pm 2.8\%$  in controls ( $P < 0.001$ )) (**Figure 4 B' and C**), reminding of the increase of double *Satb2/Ctip2*-positive neurons. Thus, LMO4 increase could account for the increased number of *Satb2/Ctip2*-positive neurons in the mS1 of *COUP-TFI* mutant cortices.

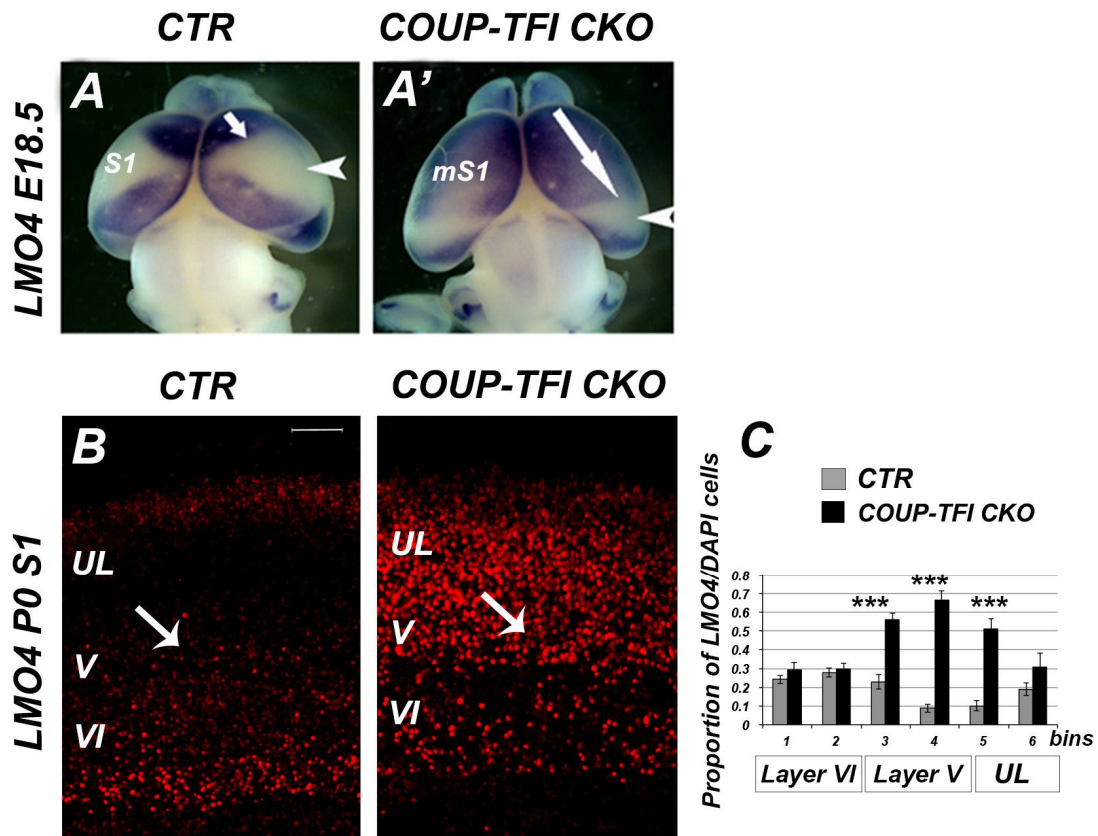


**Figure 4- Loss of COUP-TFI function leads to a tangential and radial expansion of LMO4 expression.**

(A-A'') *In situ* hybridization for LMO4 on E18.5 whole mounts of E18.5 controls (A), COUP-TFI CKO (A') brains marking the frontal/Motor (indicated by arrows) and caudal areas, while the unlabeled region corresponds to the primary somatosensory area (indicated by arrowheads). Note how LMO4 expression is expanded to the motorized somatosensory region in the absence of COUP-TFI function (A').

(B and B') Immunofluorescence against LMO4 in P0 coronal sections taken in the somatosensory area of controls (B) and motorized somatosensory area (B') of COUP-TFI CKO cortices indicating the ectopic and premature expression of LMO4 (indicated by arrows) in layer V and part of upper layers of COUP-TFI CKO cortices.

(c) Quantification of the proportion of LMO4 expressing neurons per total number of cells in each bin indicating a strong increase in LMO4 expression in layer V and part of upper layers of COUP-TFI CKO at P0.

The cortex is divided to 6 bins from layer VI to layer I, Bins 1 and 2 represent layer VI, bins 3 and 4 represent layer V, and bins 5 and 6 represent the cortical plate. Error bars represent SEM. Student's test, \*\*\*  $P \leq 0.001$ . Scale bars: 100  $\mu\text{m}$  (B and B'). E18.5: embryonic day 18.5, P0: postnatal day 0, CTR: controls, COUP-TFI CKO: COUP-TFI <sup>fl/fl</sup> Emx1 <sup>Cre</sup>, UL: upper layers, mS1: motorized somatosensory area, S1: primary somatosensory area, V: layer V and VI: layer VI.

#### **D. Progressive increase of LMO4 expression levels is correlated with the number of Satb2/Ctip2-positive neurons in the post-natal somatosensory cortex**

Previous reports have shown that LMO4 has a dynamic and region-specific expression and progressively increases with time during corticogenesis [325]. In order to follow the temporal course of LMO4 expression and, and understand how it correlates with the number and distribution of Satb2/Ctip2-positive neurons in S1, I performed immunofluorescence for LMO4 and for Satb2/Ctip2 at P0, P7 and P21 (**Figure 5 and 6**).

At P0, upper layer neurons have not completed their migration, whereas lower layer PN are fully settled, even if they are at an intermediate stage of their differentiation in which axons have not fully reached their final targets [15]. At this stage of development, LMO4 is normally expressed at low levels in layer V of the somatosensory area, and at slightly higher levels in layer VI (**Figures 4 B and 5 A**). In the absence of COUP-TFI, LMO4 expression levels increase in all cortical layers, particularly in layer V and part of upper layers (Bins 3, 4 and 5) (**Figures 4 B', C and 5 B**). Correspondingly, the number of cells expressing Satb2/Ctip2 is poorly represented in layers V and VI in control sections, but highly augmented in *COUP-TFI CKO* brains (**Figure 6 A-D'' and M**). By P7, layers V and VI neurons have more fully differentiated, and their axons innervate their respective targets [15]. At this age, LMO4 expression increases in S1 of control cortices, and seem to reach a more comparable level to the one observed in *COUP-TFI CKO* brains (**Figure 5 C and D**). However, even if the number of double Satb2/Ctip2-positive neurons gradually increases in control brains, it does not reach the percentages observed in *COUP-TFI CKO* cortices at P7 (in layer V,  $8.1\pm 1.9\%$  in controls versus  $21.7\pm 0.18\%$  in *COUP-TFI CKO* ( $P=0.004$ ), in layer VI,  $8.2\pm 2.5\%$  in the controls versus  $23.1\pm 2.4\%$  in *COUP-TFI CKO* ( $P=0.02$ ) (**Figure 6 E-H'' and N**). At P21, all cortical neurons have achieved their mature state, their axons reached their final targets, and their collaterals have been fully finished the pruning [219]. At this age almost all cortical neurons express LMO4 and no obvious differences could be observed between controls and *COUP-TFI* mutant mice (**Figure 5E and F**). Similarly, the amount of Satb2/Ctip2-positive cells in controls becomes progressively more comparable to *COUP-TFI CKO*, even if their number is still higher in the mutants (in layer V,  $8.56\pm 1.9\%$  in the controls, versus  $17.2\pm 1.48\%$  in the CKO ( $P=0.01$ ), in layer VI,  $24.7\pm 0.9\%$  in the

controls versus  $29 \pm 1.6\%$  in the CKO) (**Figure 6I- L'', O and R**). Thus, the progressive increase in LMO4 expression levels correlates with a progressive rise of Satb2/Ctip2 positive cells in lower layers.

Together these data suggest that in S1 COUP-TFI might control the timing of onset of LMO4 expression, which in turn would allow Satb2/Ctip2 co-expression in lower layer neurons. Absence of COUP-TFI might anticipate the specification of Satb2/Ctip2 positive cells due to the precocious expression of LMO4.

## Somatosensory Cortex

**CTR**                      **COUP-TFI CKO**

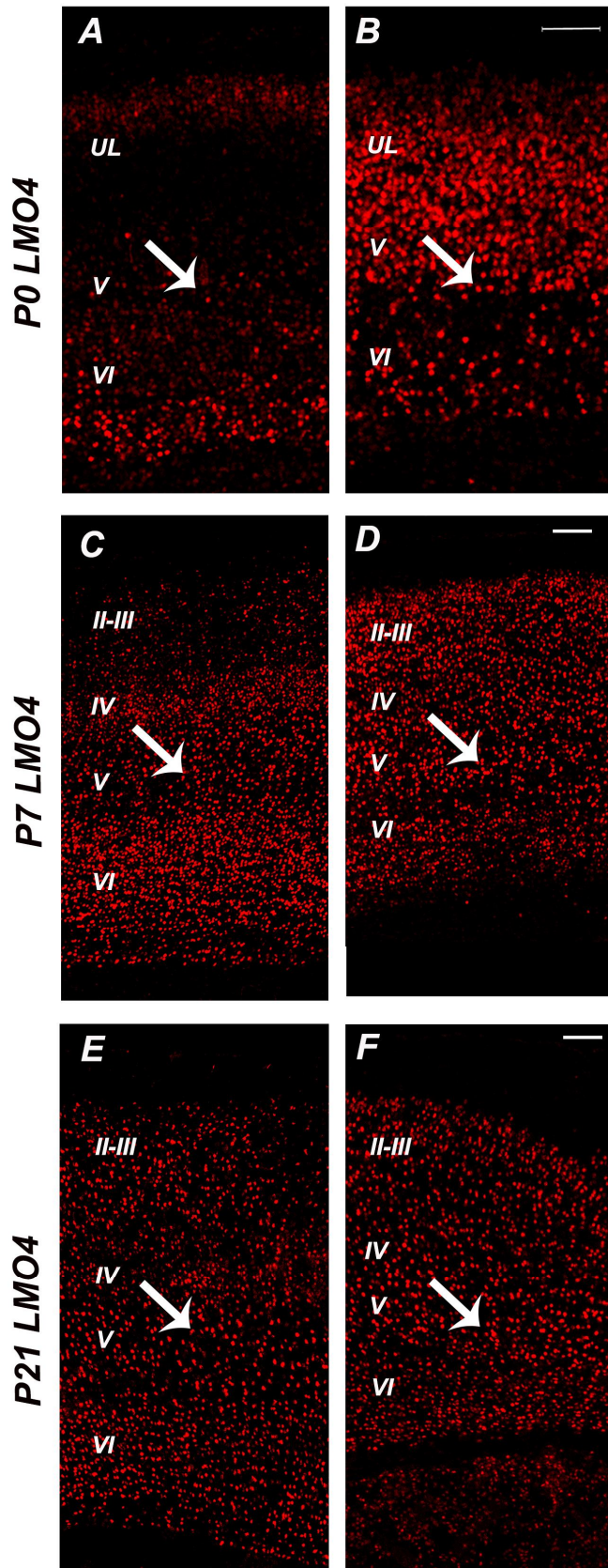


**Figure 5-Progressive increase in LMO4 expression in S1 from P0 to P7 to P21.**

(A-F) Immunofluorescence against LMO4 in coronal sections taken in the somatosensory area of controls and motorized somatosensory area of COUP-TFI CKO cortices at P0 (A-B), P7 (C-D) and P21 (E-F) indicating the progressive increase in LMO4 expression in the S1 of controls (A, C, E) from P0, to P7 to P21. The strong difference in LMO4 expression observed between controls and COUP-TFI CKO (A, B) at P0 become reduced at later ages (P7 (C and D) and P21 (E and F)). Arrows indicate LMO4 expression in layer V in WT and mutant cortices highlighting the reduced divergence with age between controls and COUP-TF CKO. Scale bars: 100  $\mu$ m. P0: postnatal day 0, CTR: controls, COUP-TFI CKO: COUP-TFI<sup>fl/fl</sup> *Emx1*<sup>Cre</sup>, UL: upper layers, II-III: layers II-III, IV: layer IV, V: layer V and VI: layer VI.



**Figure 6-Progressive increase in the proportion of Satb2/Ctip2 positive cells in S1 from P0 to P7 to P21.**

(A, C, E, G, I, K) Double immunofluorescence against Satb2 and Ctip2 and higher magnifications views (B, D, F, H, J, L) in layer V in P0, P7 and P21 parietal cortices. Arrows indicate neurons that co-express both markers in controls and COUP-TFI CKO. (M, N, O) Quantification of number of double positive cells per total of cells in each bin indicates a remarkable difference between controls and CKO at P0, a progressive increase in the proportion of Satb2/Ctip2 positive cells is observed at P7 and P21 with reduced difference between controls and mutant cortices. However, conserved and significant differences remain in the fifth and the upper sixth layer at P7 and in layer V at P21. (P, Q, R) Charts representing the trend of Satb2/Ctip2 positive cells in all cortical layers in WT and COUP-TFI CKO at P0, P7 and P21 indicating a progressive reduced divergence in the proportion of Satb2/Ctip2 positive cells with age between controls and mutant cortices.

At P0, the cortex is divided to 6 bins from layer VI to layer I, Bins 1 and 2 represent layer VI, bins 3 and 4 represent layer V, and bins 5 and 6 represent the cortical plate. At P7 and P21, the cortex is divided to 10 bins from layer VI to layer I, Bins 1, 2 and 3 represent layer VI, bins 4, 5 and 6 represent layer V, and bins 7 to 10 represent the upper layers. Error bars represent SEM. Student's test, \* $P \leq 0.05$ , \*\* $P \leq 0.01$ , \*\*\* $P \leq 0.001$ . Scale bars: 100  $\mu\text{m}$  (A, C, E, G, I, K). P0: postnatal day 0, CTR: controls, COUP-TFI CKO: COUP-TFI <sup>$\beta/\beta$  Emx1<sup>Cre</sup></sup>, UL: upper layers, II-III: layers II-III, IV: layer IV, V: layer V and VI: layer VI.

## II. A novel molecular mechanism regulating Ctip2 expression via chromatin remodeling

### A. The working hypothesis: LMO4 might interfere with the deacetylation process on the Ctip2 locus

Previous reports have shown that Satb2 binds to the Ctip2 upstream promoter region, allowing the assembly of the NURD chromatin remodeling complex on the Ctip2 locus, so that HDAC1 can deacetylate the histones at this locus converting the chromatin from an active to an inactivate state, and therefore inhibiting Ctip2 expression [150, 212]. LMO proteins function essentially as transcriptional co-regulators, mediating protein-protein interactions of various transcription factors or chromatin remodeling proteins [318-322]. LMO4 is also known to bind to HDACs and to MTA1 to modulate the expression of different genes [323, 324]; in particular, it can bind and sequester HDAC2 and allow expression of its target gene [324].

My previous data show a good correlation between the strong increase of LMO4 expression and the increase of Satb2/Ctip2 positive cells in layer V of the mS1. Therefore, I hypothesized that in the absence of COUP-TFI at P0, ectopically expressed LMO4 protein in layer V might bind to HDAC1, and possibly subtracts it from the interaction with Satb2. This would interfere with normal deacetylation of histones at the Ctip2 locus and de-repress Ctip2 expression (**Figure 7**). This mechanism could explain the increased number of double Satb2/Ctip2-positive cells in *COUP-TFI* mutant brains (**Figure 1**) in which I observed a higher number of LMO4-expressing neurons (in layer V, 60±4.4% in *COUP-TFI CKO* versus 15±2.4% in controls (P<0.001), in layer VI, 32±2.3% in *COUP-TFI CKO* versus 26±1.57% in controls (P=0.06) and in lower part of upper layers 51±5.3% in *COUP-TFI CKO* versus 10±2.8% in controls (P<0.001)) (**Figure 4**).

# THE WORKING HYPOTHESIS

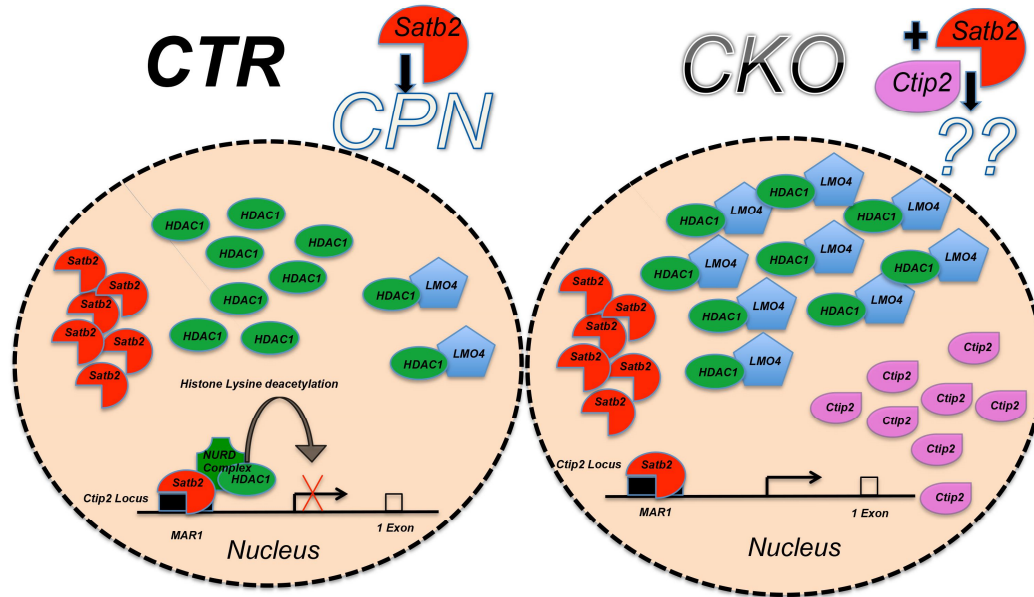


**Figure 7-LMO4 binds to HDAC1 and substracts it from Satb2 in Satb2/Ctip2 Co-expressing cells**

Schematic model explaining the molecular mechanism allowing the co-expression of Satb2 and Ctip2. In the absence of LMO4 (majority of layer V neurons in controls at P0), Satb2 binds to Ctip2 upstream promoter region, recruiting the NuRD chromatin-remodeling complex and HDAC1 to deacetylate the histones at Ctip2 locus, and represses Ctip2. In some cells in controls expressing LMO4, and the majority of layer V neurons in COUP-TFI CKO, LMO4 binds to HDAC1 and sequester it, which disturbs the formation of the NuRD complex at Ctip2 locus, and allow Ctip2 expression in LMO4/Satb2/Ctip2 positive cells. CTR: controls, CKO: COUP-TFI<sup>fl/fl Emx1<sup>Cre</sup></sup>, NuRD complex: Nucleosome remodeling and deacetylase complex, HDAC1: Histone deacetylase 1, MAR1: Matrix associated region 1, and CPN: callosal projection neurons.

## **B. Increased number of double LMO4/Satb2 and LMO4/Ctip2-positive neurons in *COUP-TFI* CKO brains**

To test this hypothesis, I first checked whether LMO4 expression increased specifically in Ctip2- and Satb2 positive neurons of P0 *COUP-TFI* CKO brains compared to controls. Double immunofluorescence revealed that the number of cells co-expressing LMO4 and Ctip2 increases particularly in layers V ( $3.20 \pm 0.4\%$  in controls versus  $21.7 \pm 1.9\%$  in *COUP-TFI* CKO,  $P=0.001$ ) and VI ( $0.36 \pm 0.02\%$  in controls versus  $9 \pm 0.3\%$  in the CKO,  $P < 0.001$ ) (**Figure 8 A-D'' and I**) of *COUP-TFI* mutant cortices. Similarly, neurons expressing simultaneously LMO4 and Satb2 (**Figure 8 E-H'' and J**) increase in layer V ( $10.7\%$  in the controls versus  $57\%$  in *COUP-TFI* CKO,  $P=0.01$ ) and in the lower part of UL in mutant brains ( $11.8 \pm 4.9\%$  in controls versus  $47.4 \pm 5.4\%$  in *COUP-TFI* CKO,  $P=0.008$ ). These data indicate that ectopic expression of LMO4 co-localizes with Satb2 and Ctip2, supporting the hypothesis of a link between LMO4 expression and Satb2/Ctip2 positive neuron specification.

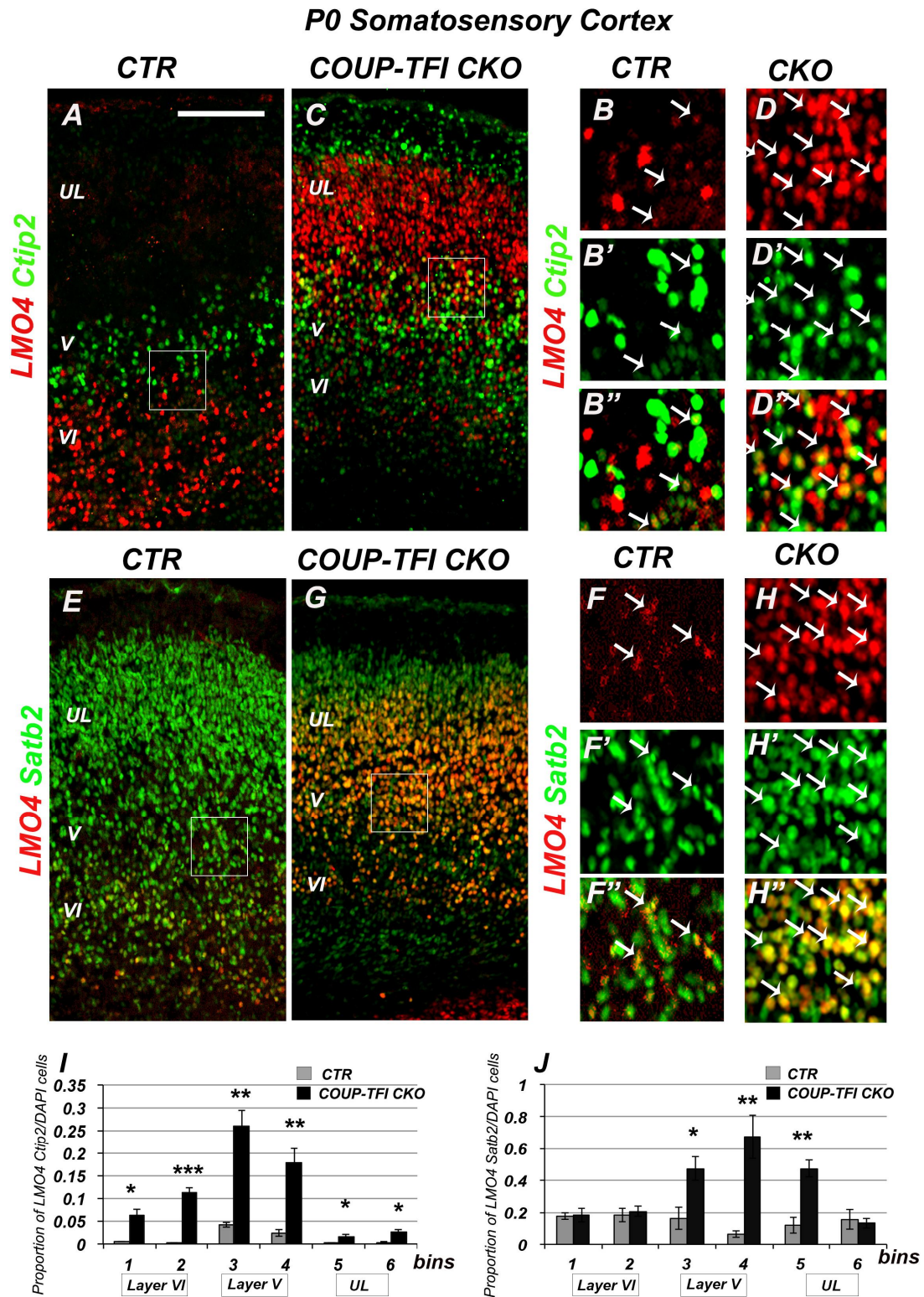


**Figure 8-Increased number of LMO4/Satb2 and LMO4/Ctip2 coexpressing cells in S1 Cortex of COUP-TFI CKO cortices.**

(A, C) Double immunofluorescence against LMO4 and Ctip2 and higher magnifications views (B and D) in layer V in P0 parietal cortices. (E, G) Double Immunofluorescence against LMO4 and Satb2 and

higher magnifications views (F and H) in layer V in P0 parietal cortices. Arrows indicate neurons that co-express both markers in controls and COUP-TFI CKO. (I, J) Quantification of number of double positive cells per total of cells in each bin indicates a remarkable increase in double labeled cells in COUP-TFI CKO compared to controls.

The cortex is divided to 6 bins from layer VI to layer I, Bins 1 and 2 represent layer VI, bins 3 and 4 represent layer V, and bins 5 and 6 represent the cortical plate. Error bars represent SEM. Student's test, \* $P \leq 0.05$ , \*\* $P \leq 0.01$ , \*\*\* $P \leq 0.001$ . Scale bars: 100  $\mu\text{m}$  (A, C, E, G). P0: postnatal day 0, CTR: controls, COUP-TFI CKO: COUP-TFI<sup>fl/fl Emx1<sup>Cre</sup></sup>, UL: upper layers, V: Layer V, and VI: layer VI.

### **C. Increased number of triple LMO4/Satb2/Ctip2-positive neurons in *COUP-TFI CKO* brains**

To further support the role of LMO4 in de-repressing Ctip2 expression, I investigated whether LMO4 was expressed in the Satb2/Ctip2-positive cells in control and *COUP-TFI CKO* cortices. By performing a triple immunofluorescence I found that the number of triple LMO4/Satb2/Ctip2-positive neurons increases in layers V and VI *COUP-TFI CKO* compared to controls (**Figure 8 A-E**). Moreover, while LMO4 is normally expressed in  $68\pm 1.7\%$  of double Satb2/Ctip2-positive cells in lower layers in S1 (**Figure 8 F**), the percentage of co-localization rises to  $92\pm 0.4\%$  in *COUP-TFI CKO* brains ( $P=0.002$ ) (**Figure 8 G**). These data indicate that LMO4 is expressed in the majority of double Satb2/Ctip2-positive cells, further suggesting its possible requirement in the specification of this cell population.

**P0 Somatosensory Cortex**

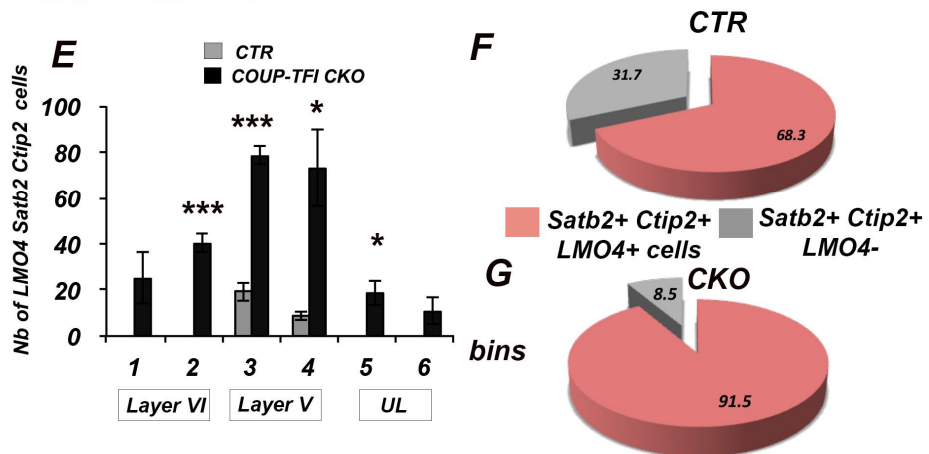
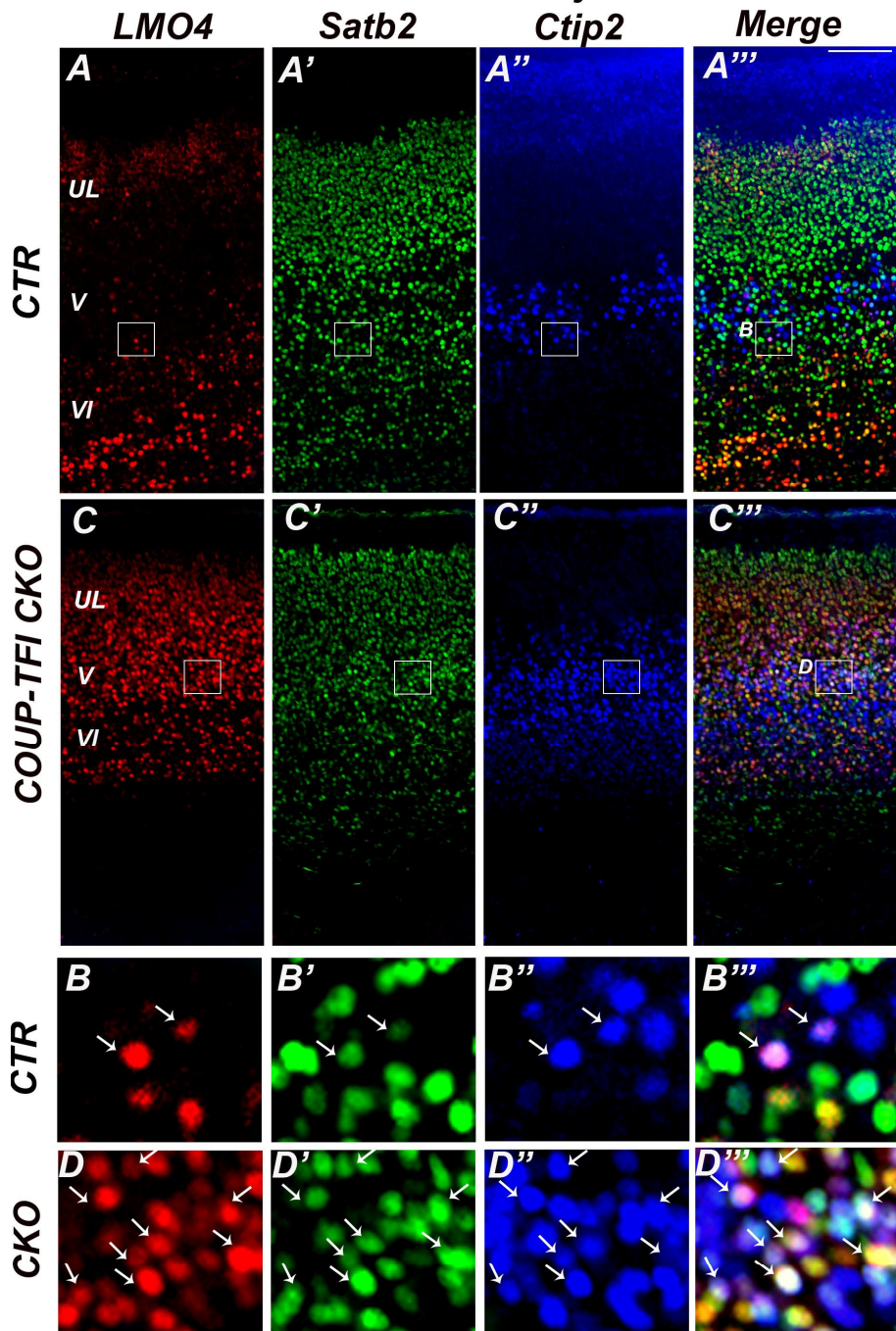


**Figure 9-Satb2/Ctip2 double-labeled cells express LMO4 in WT and COUP-TFI CKO in S1.**

(A-A''' and C-C''') Triple immunofluorescence against LMO4, Satb2 and Ctip2 and higher magnifications views (B-B''' and D-D''') in layer V of P0 parietal cortices. Arrows indicate neurons that express the three markers LMO4, Satb2 and Ctip2 in controls and COUP-TFI CKO. (E) Quantification of number of triple positive cells in a 600 $\mu$ m width indicates a remarkable increase in the number of cells expressing the three markers LMO4, Satb2 and Ctip2 in controls and *COUP-TFI CKO*. (F and G) Charts representing the percentage of Satb2/Ctip2 double-labeled neurons expressing or not LMO4 in lower layers of controls (F) and COUP-TFI CKO (G).

Error bars represent SEM. Student's test, \*P $\leq$  0.05, \*\*P $\leq$ 0.01, \*\*\*P $\leq$ 0.001. Scale bars: 100  $\mu$ m (A-A''' and C-C'''). P0: postnatal day 0, CTR: controls, COUP-TFI CKO: COUP-TFI<sup>fl/fl Emx1 Cre</sup>, UL: upper layers, V: layer V, and VI : layer VI.

#### **D. LMO4 de-represses Ctip2 transcription by binding HDAC1**

In order to directly assess whether LMO4 can bind to HDAC1 and eventually subtract it from Satb2, as proposed by my hypothesis (**Figure 7**), I immunoprecipitated nuclear proteins isolated from whole P1 cortices, using antibodies against LMO4 and Satb2. I chose P1 cortices, because at this stage a drastic difference in the percentage of double labeled Satb2/Ctip2 positive cells exists between COUP-TFI mutants and controls. Immunoblots using HDAC1 antibody showed that in controls Satb2 binds HDAC1, as previously described [150, 212]. I also found that LMO4 can interact with HDAC1 in normal conditions (**Figure 10A**). Interestingly, the interaction between LMO4 and HDAC1 drastically increases, whereas the Satb2/HDAC1 interaction strongly decreases in *COUP-TFI* mutant cortical extracts (**Figure 10A**), indicating that excess of LMO4 has subtracted part of the HDAC1 normally interacting with Satb2.

To further investigate whether this interaction affected the deacetylation of the Ctip2 locus *in vivo*, I performed a chromatin immunoprecipitation (ChIP) assay on genomic DNA extracted from control and *COUP-TFI CKO* cortices at perinatal stages. I used an antibody against HDAC1 to assess the amount of HDAC1 still bound to Ctip2 locus, and an antibody specific for the acetylated form of histone 4 (H4K12) to verify the state of the chromatin in the same locus. The interactions of HDAC1 with the complexes bound to the Ctip2 locus were detected using a semi-quantitative PCR with primers specific for MAR sequences previously analyzed in the Ctip2 upstream region [212]. The ChIP assay demonstrated a decrease in the levels of HDAC1 bound to the Ctip2 locus, and an increase in the acetylated form of histone H4 (**Figure 10B**) in COUP-TFI mutants compared to controls. Overall, these data indicate that LMO4 de-repress Ctip2 by binding HDAC1, which is no longer able to repress Ctip2 transcription. (**Figure 10 C and D**).

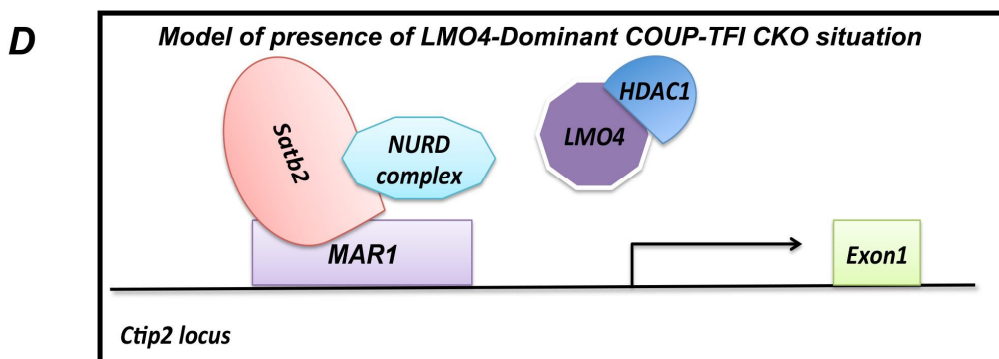
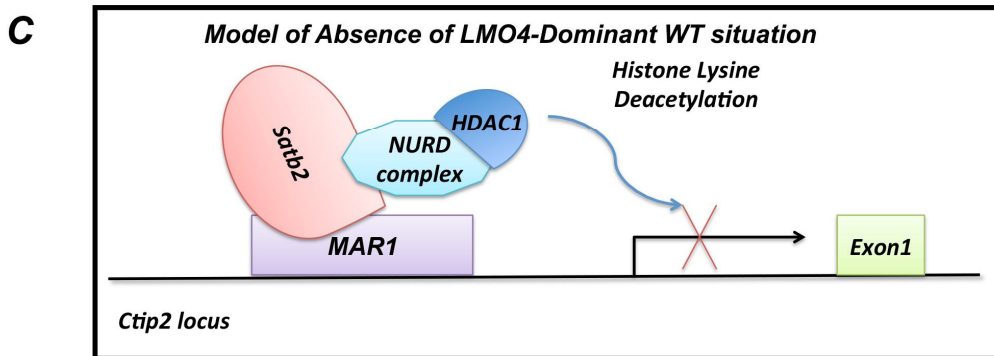
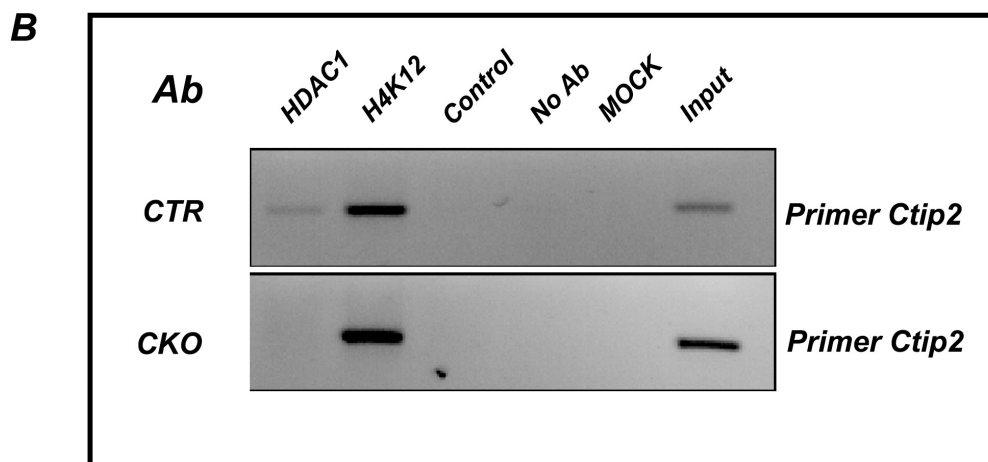
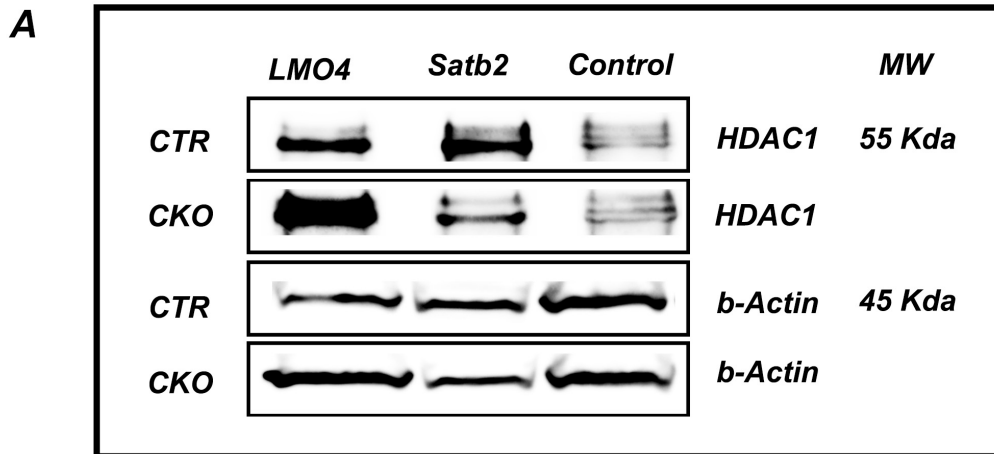


**Figure 10- LMO4 protein binds to HDAC1 and disturbs the NuRD complex on Ctip2 locus derepressing Ctip2 expression.**

(A) LMO4/HDAC1 interaction increases while Satb2/HDAC1 interaction decreases in COUP-TFI CKO compared to controls. Nuclear extracts from P0 controls and COUP-TFI CKO cortices were immunoprecipitated using either anti-LMO4 or anti-Satb2 or a control (Brdu) antibody. Following immunoprecipitation, bound and free fractions were separated on gels, and analyzed by immunoblotting using specific antibody to HDAC1 for bound fraction and  $\beta$ -actin as a control for free action. Molecular weight is shown in kDa on the right side.

(B) HDAC1 binds less to Ctip2 locus and histones become more acetylated in COUP-TFI CKO. Semiquantitative chromatin immunoprecipitation (ChIP) with Ctip2 locus DNA. ChIP assay was performed using cortices from P0 controls or COUP-TFI CKO brains. A  $\approx$  500 bp DNA fragment containing upstream part of Ctip2 DNA region (primer pair MAR1) was amplified from samples that were immunoprecipitated with anti-HDAC1, an antibody against acetylated form of the histone H4 (H4K12) and a GFP antibody, no antibody, no DNA (MOCK) and the non bound fraction of No antibody sample (input) as controls. Part (B) shows gel images of semiquantitative PCR for this ChIP.

(C) Model of the absence of LMO4, which is dominant in WT situation. Satb2 binds to Ctip2 locus and induces deacetylation of histones and inactivation of Ctip2 expression.

(D) Model of the presence of LMO4, which is dominant in COUP-TFI CKO situation. LMO4 sequesters HDAC1 disturbing the formation of the NURD complex and HDAC1 action. Histones on Ctip2 locus are more acetylated and Ctip2 expression is activated in Satb2 positive neurons.

WT: wild type, CTR: controls, CKO: COUP-TFI <sup>fl/fl</sup>Emx1<sup>cre</sup>, MW: molecular weight, P0: postnatal day 0, Ab: Antibody, MAR1: Matrix associated region 1, NURD complex: Nucleosome remodeling and deacetylase complex, H4K12: acetylated form of lysine K12 in histone 4.

### E. LMO4 binds to Ski: another component of the NuRD complex

Ski is another partner of Satb2, recruiting the histone deacetylases to the Ctip2 locus, and involved in Ctip2 inhibition at P0 [234]. In order to investigate whether LMO4 could bind to Ski, I immunoprecipitated nuclear proteins isolated from P1 cortices with antibodies against LMO4 and Satb2, as described above. Then, I immunoblotted the precipitated complexes with an antibody against Ski and found that, as for HDAC1, Satb2 interacts less with Ski in *COUP-TFI CKO* cortex extracts (**Figure 11 A**). On the contrary, the interaction of LMO4 with Ski remains unchanged (**Figure 11 A**). These data suggest that recruitment of HDAC1 to Ctip2 locus is impaired due to an absence of Ski in this locus.

Since Ski interaction was impaired, I checked whether Ski expression levels and distribution was altered in *COUP-TFI CKO* brains by comparing them to controls at P7, since my previous analyses showed that the highest percentage of Satb2/Ctip2 positive cells in lower layers is detected at this stage (**Figure 6**). Although Ski expression was altered in upper layers of mutant brains no obvious difference was detected in layer V of *COUP-TFI CKO* brains (**Figure 11 B, B' and B''**).

Next, to understand whether the increased number of Satb2/Ctip2 co-expressing neurons observed in the mutant brains could be due to the absence of Ski in double-labeled cells, I performed triple immunofluorescence with Ski, Satb2 and Ctip2 antibodies (**Figure 11 C-D'''**). Surprisingly, I found that Ski is normally expressed in 57.7% of layer V Satb2/Ctip2 co-expressing neurons in S1 of P7 cortices (**Figure 11 E**), indicating that at least in this percentage of neurons, Satb2/Ctip2 colocalization occurs *via* a Ski-independent mechanism. This process could be orchestrated, then, by LMO4, as suggested by my previous experiments.

It has been demonstrated that even in the absence of interactions with Ski and HDAC1, Satb2 remains bound to the Ctip2 promoter region [234]. In order to test whether LMO4 interferes with the assembly of the NuRD complex directly binding Satb2, or if it rather interacts independently with HDAC1 and Ski, I performed reciprocal co-immunoprecipitation between LMO4 and Satb2. Both reciprocal co-immunoprecipitation showed no protein interactions between LMO4 and Satb2 either in control or in *COUP-TFI* mutant brains (**Figure 11 A**), indicating that LMO4 probably binds and subtracts the components of the NuRD complex before their

binding to Satb2. Further ChIP experiments on Ctif2 locus are required to validate this hypothesis.

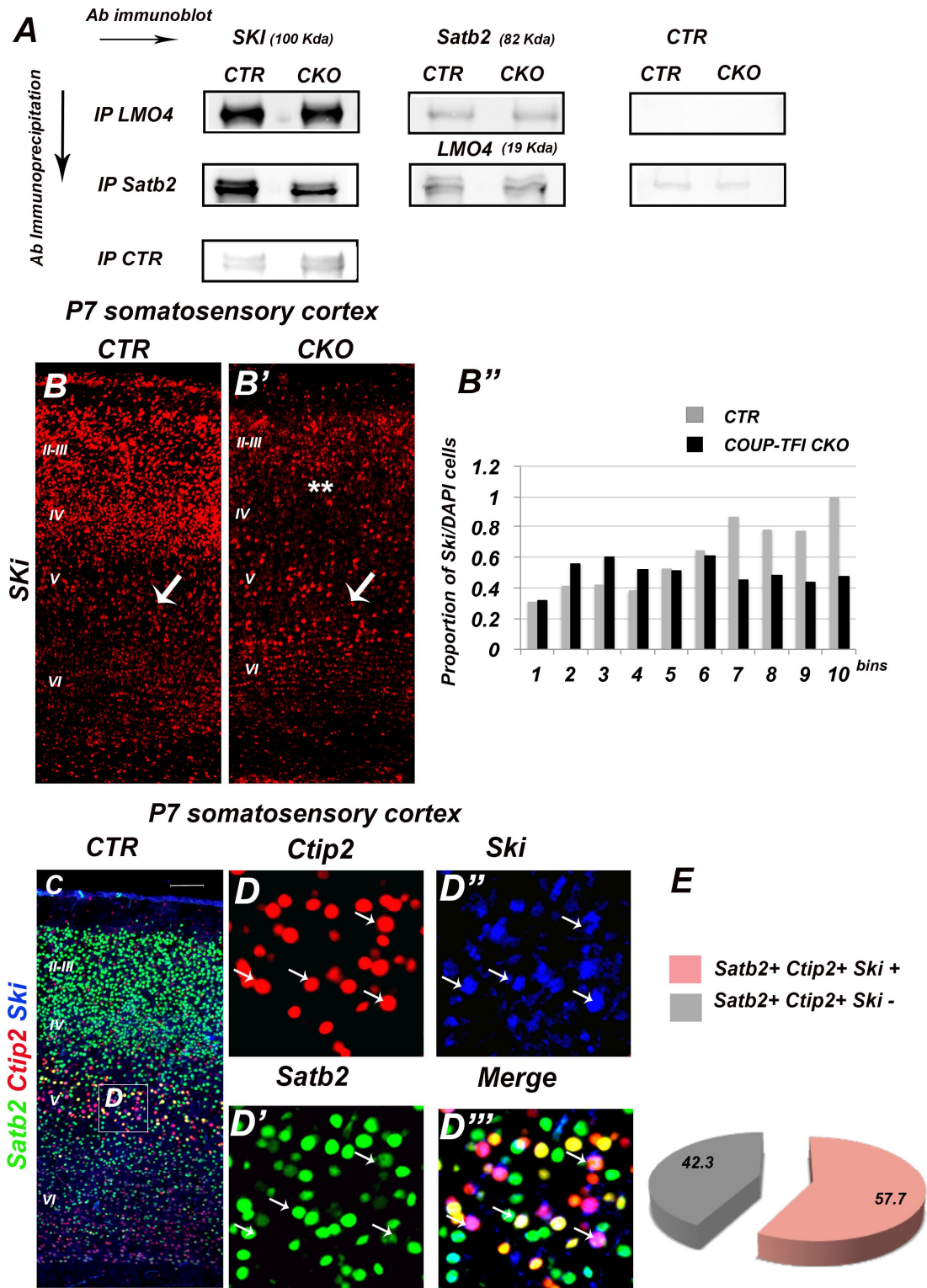


**Figure 11-LMO4 disturbs the NURD complex and derepresses Ctip2 in a Ski independent mechanism.**

(A) Satb2/Ski interaction decreases while LMO4 Ski1 remains unaltered in COUP-TFI CKO. No interaction between LMO4 and Satb2 was found in controls and mutants. Nuclear extracts from P1 controls and COUP-TFI CKO cortices were immunoprecipitated using either anti-LMO4 or anti-Satb2

or a control (Brdu) antibody. Following immunoprecipitation, bound and free fractions were separated on gels, and analyzed by immunoblotting using specific antibodies to ski, reciprocal LMO4 or Satb2 and a control antibody for bound fraction. Molecular weight is shown in kDa.

(B, B') Immunofluorescence against ski in p7 coronal sections taken in the somatosensory area of controls (B) and motorized somatosensory area (B') of COUP-TFI CKO cortices. (B'') Quantification of number of Ski positive cells per total of cells in each bin indicates a decreased Ski expression in upper layers (indicated by asteriks) while ski expression remains nearly unaltered in layers V (indicated by arrows) and VI of COUP-TFI CKO cortices. Error bars are absent since the number of counted animals were n=1 (3 counted sections per animal).

(C) Triple immunofluorescence against Ski, Satb2 and Ctip2 and higher magnifications views (D-D''') in layer V of P7 controls parietal cortices. Arrows indicate neurons that express the three markers Ski, Satb2 and Ctip2. (E) Chart representing the percentage of Satb2/Ctip2 double-labeled neurons expressing or not Ski in WT. Scale bar: 100  $\mu$ m (A-C). CTR: controls, CKO: COUP-TFI<sup>f/f</sup> Emx1<sup>Cre</sup>, P7: postnatal day 7, Ab: Antibody, and IP: immunoprecipitation.

### III. *In vivo* role of LMO4 in the specification of the Satb2/Ctip2 layer V subpopulation in the somatosensory cortex

#### A. Cortical inactivation of LMO4 affects the percentage of Satb2/Ctip2 layer V subpopulation

To directly test the *in vivo* function of LMO4 in the specification of the Satb2/Ctip2-positive neurons, I used a genetic model in which LMO4 was inactivated in all cortical neurons. We received P0 and P7 *LMO4 conditional KO* brains (*Lmo4 CKO*) obtained by crossing *LMO4 floxed* mice with an *Emx1-Cre* line, from the group of T. Sun [325]. I first used the LMO4 antibody on coronal sections of these brains and detected no LMO4 expression in the neocortex at P0, while LMO4 is still expressed in the striatum and dorsal thalamus, confirming the specificity of this cortex-specific KO (**Figure 12 A and B**). To assess whether absence of LMO4 would impinge on the number of the double Satb2/Ctip2-expressing neurons, double immunofluorescence of Satb2 and Ctip2 was performed on P7 *LMO4 CKO* brains, a stage in which a high number of Satb2/Ctip2- and Lmo4 positive cells can be normally detected in the S1 compared to P0 brains (see **Figure 5 and 6**). In the absence of LMO4 function, the number of Ctip2-positive cells in layers V and VI of S1 was decreased (in layer V,  $14.6 \pm 2.6\%$  in controls versus  $9.4 \pm 0.01\%$  in *LMO4 CKO*, in layer VI,  $14.7 \pm 2\%$  in controls versus  $2.7 \pm 0.8\%$  in *LMO4 CKO* ( $P=0.01$ ) (**Figure 12 C-D**), whereas the number of Satb2-positive cells was not increased, but even decreased in some bins indicating that Ctip2 inhibition is not due to an increase in Satb2 expression (**Figure 12 C'-H' and J**). Interestingly, the number of double Satb2/Ctip2-positive cells was also significantly decreased compared to controls (in layer V,  $8.1 \pm 1.9\%$  in controls and  $4.3 \pm 0.35\%$  in *LMO4 CKO*, in layer VI,  $8.17 \pm 1.9\%$  in controls and  $1 \pm 0.3\%$  in *LMO4 CKO*,  $P=0.05$ ) (**Figure 12 C''-H'' and K**). These data further support a key role for LMO4 in the de-repression of Ctip2 expression and therefore in the specification of Satb2/Ctip2 positive cells.

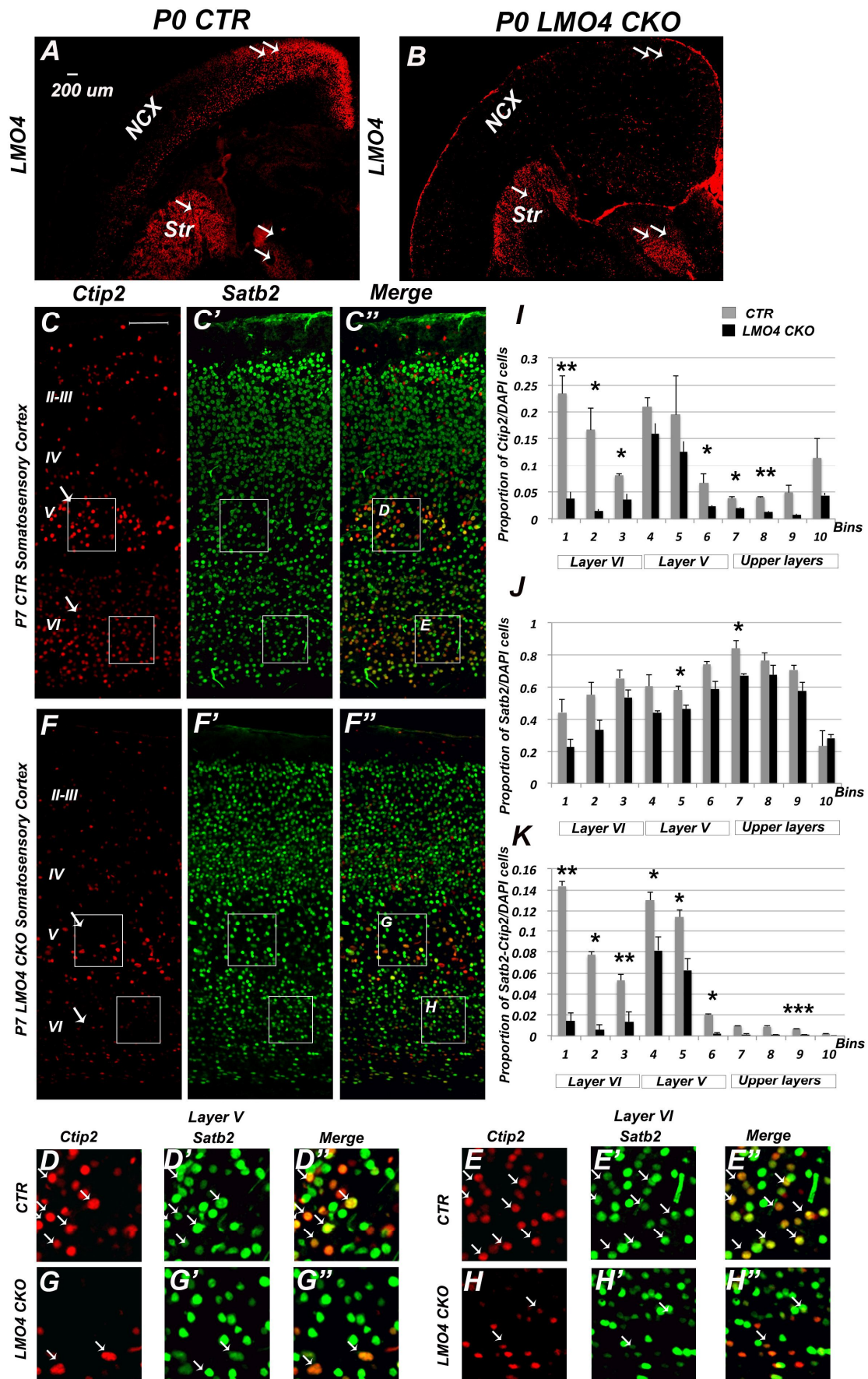


Figure 12-A strong decrease in Satb2/Ctip2 positive neurons in the absence of LMO4 function.

(A, B) Immunofluorescence against LMO4 in coronal sections of controls and LMO4 CKO brains at P0. Arrows indicate the specific ablation of LMO4 expression in the neocortex of LMO4 mutants while this expression remains similar to the controls in non-neocortical region in striatum and dorsal thalamus. (C-C'', F-F'') Double immunofluorescence against Satb2 and Ctip2 and higher magnifications views in layer V (D-D'' and G-G'') and VI (E-E'', H-H'') in P7 parietal cortices of controls and LMO4 CKO brains. Arrows indicate neurons that co-express both markers in controls and LMO4 CKO. (I, J, K) Quantification of number of Ctip2, Satb2 and double positive cells per total of cells in each bin indicates a remarkable decrease in Ctip2 and double Satb2/Ctip2 positive cells in LMO4 CKO compared to controls at P7, while the number of Satb2 positive cells does not increase, but slightly decrease in some bins. The cortex is divided to 10 bins from layer VI to layer I, Bins 1, 2 and 3 represent layer VI, bins 4, 5 and 6 represent layer V, and bins 7 to 10 represent the upper layers. Error bars represent SEM. Student's test, \* $P \leq 0.05$ , \*\* $P \leq 0.01$ , \*\*\* $P \leq 0.001$ . Scale bars: 200  $\mu\text{m}$  (A, B) and 100  $\mu\text{m}$  (C-C'' and F-F''). P0: postnatal day 0, CTR: controls, LMO4 CKO: *Lmo4* fl/fl<sup>Emx1-CRE</sup>, NCX: neocortex, Str: striatum, II-III: layers II-III, IV: layer IV, V: layer V, and VI: layer VI.

## **B. LMO4 overexpression promotes the number of double Satb2/Ctip2-positive cells in layer V**

As a complementary approach to LMO4 cortical inactivation, LMO4 was overexpressed in *wt* cortices starting from E13.5 to test whether ectopic LMO4 would increase the number of Ctip2-expressing neurons in layer V. This work was carried out in collaboration with Christian Alfano, a researcher working in the lab. We *in utero* electroporated a plasmid overexpressing LMO4 under the control of the Cdk5 promoter, which drives the expression of cloned cDNAs only in post-mitotic neurons [213]. Downstream of the polylinker this plasmid contains an IRES sequence, which allows the expression of a reporter gene (enhanced GFP, EGFP) to identify electroporated cells. From now on I will refer to the plasmid as Cdk5-LMO4-GFP. As a control, we used a cdk5-GFP plasmid [213], which was electroporated in control cortices at the same stage.

LMO4 expression was strongly upregulated in the somatosensory region of the electroporated hemisphere at P0 (**Figure 13 A-A'' and C-C''**) compared to the contralateral non-electroporated one (**Figure 13 B**), confirming the efficacy of the Cdk5-LMO4-GFP plasmid. We then tested electroporated brains at P7 (when most of cortical cells are finally settled) and found that Cdk5-GFP electroporated cells were not Satb2/Ctip2-positive, whereas a considerable number of them expressed Satb2 (**Figure 13 G-I''**). In the contrary, a remarkable number of cdk5-LMO4-GFP electroporated cells were double Satb2/Ctip2 (**Figure 13 D-F''**). Thus, overexpression of LMO4 de-represses Ctip2 in Satb2 positive cells.

However, I noticed that E13.5 Cdk5-GFP electroporated cells did not localize with any Ctip2+ cells (**Figure 13 G-I''**), even if they are supposed to be born at E13.5 [15]. This might suggest, that apical progenitors, which are the only recipient of the electroporated plasmid are not producing Ctip2+ cells anymore. This unexpected observation support the evidence that LMO4 overexpression can de-repress Ctip2 expression in Satb2 positive cells. Hence, our data further support that the enhancement of LMO4 expression from P0 to P21 progressively increases the number of Satb2/Ctip2 positive cells in lower layers.

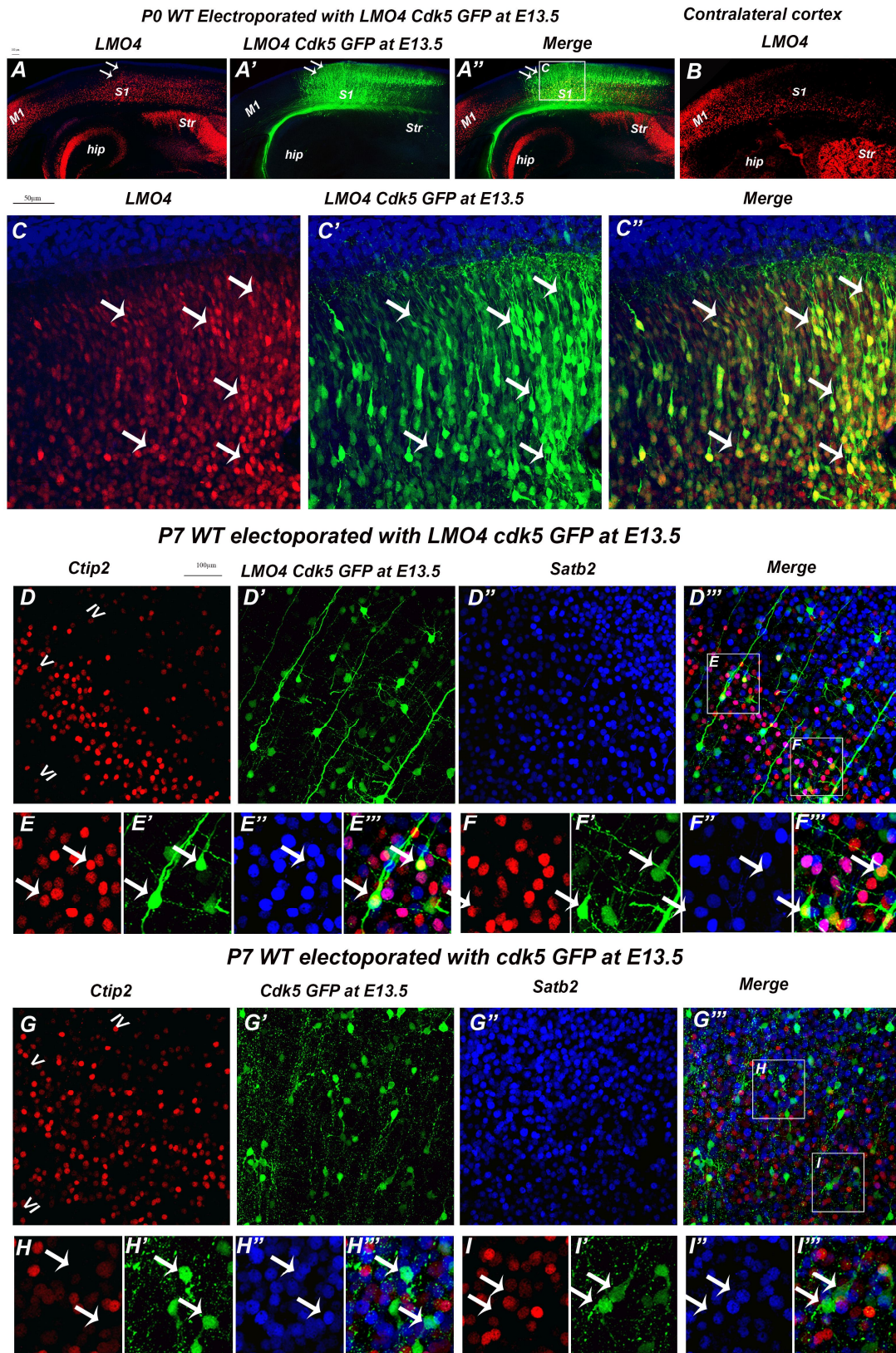


**Figure 13- LMO4 overexpression anticipates Ctip2 expression in Satb2 positive neurons.**

(A-A'' and C-F''') WT E13.5 brains were electroporated *in utero* with cdk5 LMO4 GFP expressing vectors. (A-A'') Coronal sections of electroporated brains at P0 immunostained using an antibody against LMO4 and higher magnification views (C-C'') indicate that LMO4 is strongly overexpressed

compared to contralateral non-electroporated hemisphere (B). Arrows indicate LMO4 overexpression in brains electroporated compared to their correspondent control regions.

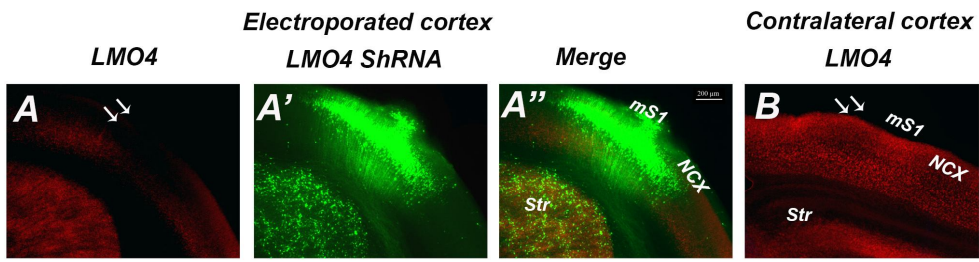
(D-I'') WT E13.5 brains were electroporated *in utero* with a control (cdk5 GFP) (G-I'') and cdk5 LMO4 GFP expressing vectors (D-F''). (D-D'' and G-G'') Coronal sections of electroporated brains at P7 immunostained using antibodies against Satb2 and Ctip2 and higher magnification views (E-E'', F-F'', H-H'' and I-I'') indicate that GFP electroporated layer V neurons do not express Satb2 and Ctip2, while a remarkable percentage of LMO4 overexpressing GFP cells are Satb2/Ctip2 positive. Arrows indicate electroporated cells with cdk5 GFP and with cdk5 LMO4 GFP.

Scale bars: 100  $\mu\text{m}$  (A-A'' and B, D-D'', and G-G''), 50  $\mu\text{m}$  (C-C''). E13.5: embryonic day 13.5, P0: postnatal day 0, WT: wild type, M1: primary motor area, S1: primary somatosensory area, Str: striatum, and hip: hippocampus.

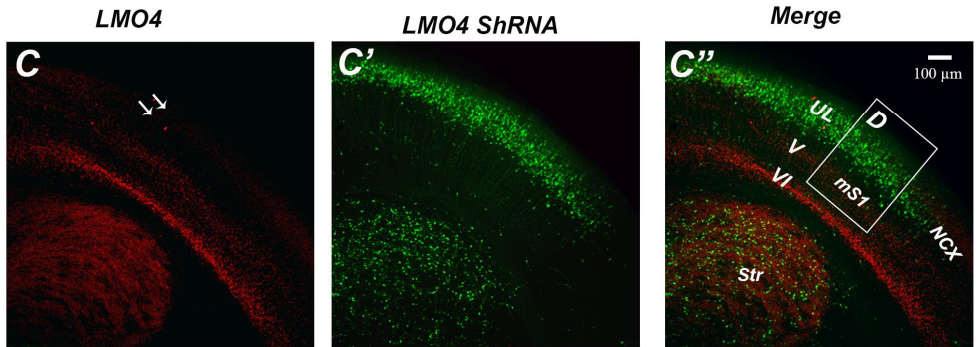
### **C. LMO4 downregulation rescues Ctip2 radial expansion in *COUP-TFI CKO* mutant cortices**

To reinforce gain-of-function data I tested whether cell-autonomous downregulation of LMO4 could repress Ctip2 expression in layer V. To this purpose, we used a construct expressing an already tested LMO4-specific *shRNA* which was kindly donated to us from HH Chen's lab [330]. We used *COUP-TFI CKO* brains in which Ctip2 expression is strongly up-regulated in lower layers. We *in utero* electroporated the *shRNA* plasmid in E13.5 mutant brains together with a GFP-expressing construct that allows distinguishing transfected cells. The efficacy and specificity of the *shRNA* construct was tested using an antibody against LMO4 on P0 *COUP-TFI CKO* brains electroporated either with the *shRNA* against LMO4 or with a "scrambled" *shRNA*, used as a control. The *LMO4-specific shRNA* strongly downregulates *LMO4* expression in the mS1 area (**Figure 14 A-A'', C-C'' and D-D''**), compared to the contralateral non-electroporated hemisphere (**Figure 14 B**) and to control electroporation with the scrambled construct (**Figure 14 E-E'', and F-F''**). Importantly, LMO4 downregulation remarkably reduces Ctip2 expression in *COUP-TFI CKO* cortices (**Figure 15 A-A'', C-C'' and E**) compared to the contralateral non-electroporated hemisphere (**Figure 15 B**) and to the control electroporation with the scrambled *shRNA* (**Figure 15 D and F**). No obvious changes were observed in the number of Satb2 expressing cells (**Figure 14 D'' and F''**), indicating that the downregulation of LMO4 has no effect on Satb2 expression. These data further support a role for LMO4 on Ctip2 transcriptional control and strongly suggests that ectopic Ctip2 expression in *COUP-TFI CKO* brains is mainly due to a transcriptional de-repression of Ctip2 by LMO4.

**P0 COUP-TFI CKO electroporated with LMO4 ShRNA at E13.5**



**P0 COUP-TFI CKO electroporated with LMO4 ShRNA at E13.5**



**P0 COUP-TFI CKO electroporated with Scrambled at E13.5**

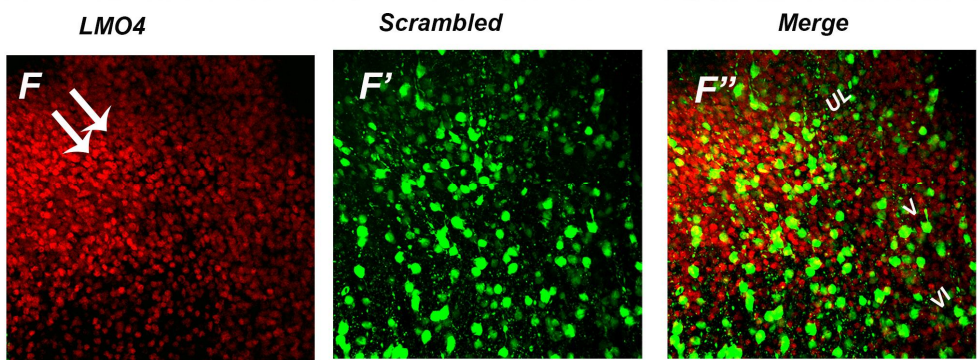
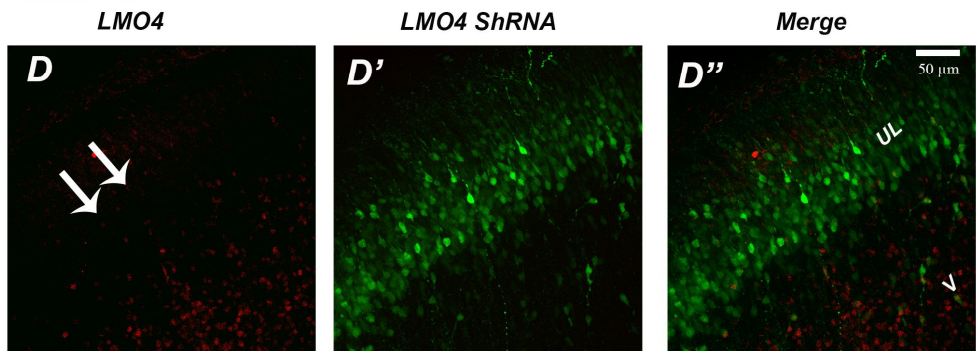
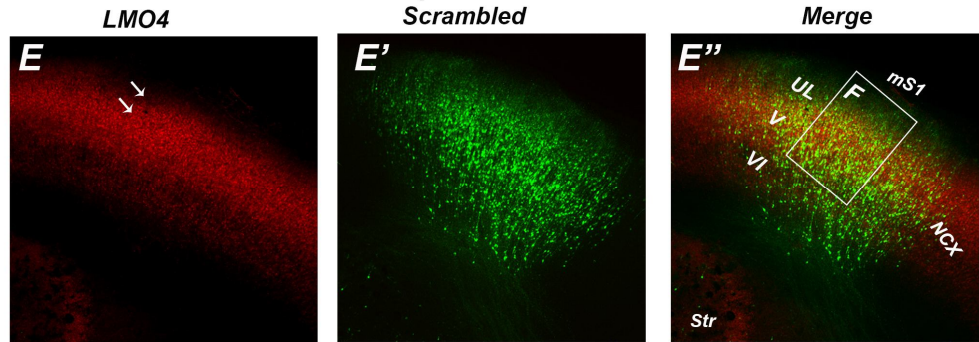
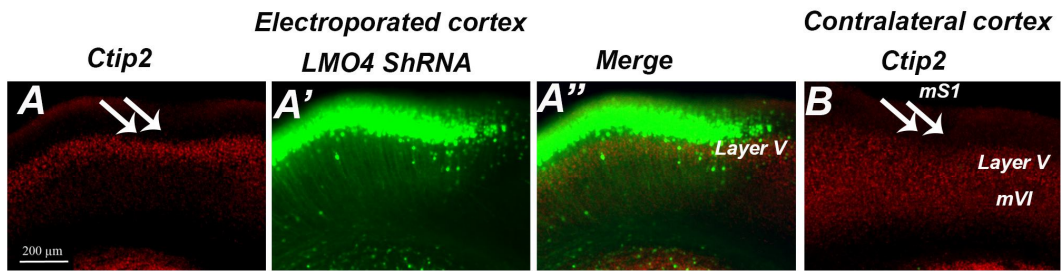


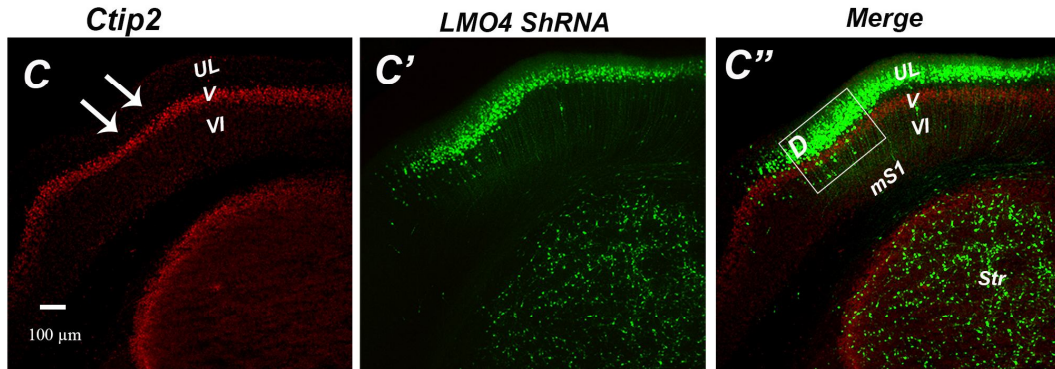
**Figure 14-Downregulation of LMO4 expression in COUP-TFI mutants using LMO4 shRNA**

(A-A'' and C-F'') COUP-TFI CKO E13.5 brains were electroporated *in utero* with a control (scrambled) and LMO4-specific shRNA-IRES GFP expressing vectors. (A-A'', C-C'', and E-E'') Coronal sections of electroporated brains at P0 immunostained using an antibody against LMO4 and higher magnification views (D-D'' and F-F'') indicate that LMO4 shRNA strongly downregulates LMO4 expression compared to contralateral non-electroporated hemisphere (B) and brains electroporated with scrambled (E-E''). Arrows indicate the downregulation of LMO4 expression in brains electroporated compared to their correspondent control regions. Error bars: 200  $\mu\text{m}$  (A-A'' and B), 100  $\mu\text{m}$  (C-C'' and E-E'') and 50  $\mu\text{m}$  (D-D'' and F-F''). E13.5: embryonic day 13.5, P0: postnatal day 0, COUP-TFI CKO: COUP-TFI<sup>f/f Emx1 Cre</sup>, NCX: neocortex, Str: striatum, mS1: motorized S1, UL: upper layers, V: layer V and VI: layer VI.

**P0 COUP-TFI CKO electroporated with LMO4 ShRNA at E13.5**



**P0 COUP-TFI CKO electroporated with LMO4 ShRNA at E13.5**



**P0 COUP-TFI CKO electroporated with Scrambled at E13.5**

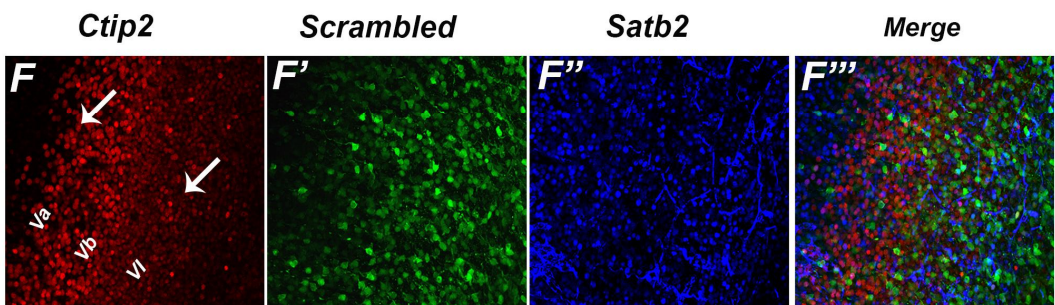
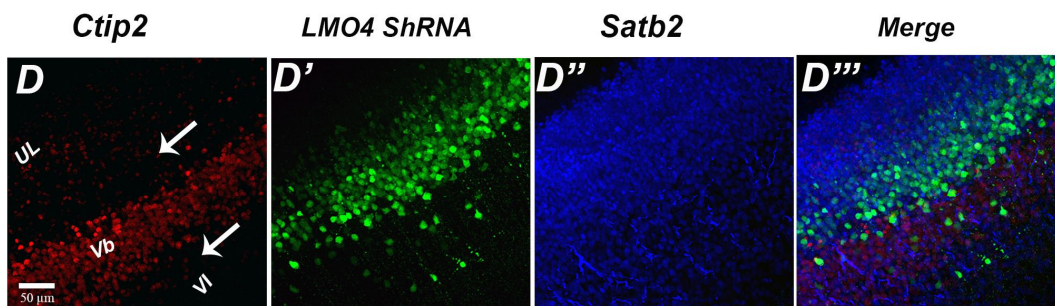
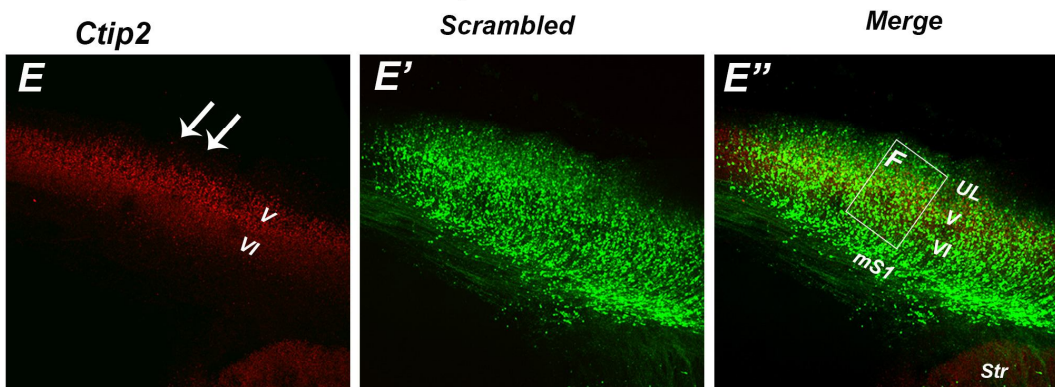


**Figure 15- Downregulation of LMO4 expression reduces Ctip2 expression in COUP-TFI mutants**

(A-A'' and C-F''') COUP-TFI CKO E13.5 brains were electroporated *in utero* with a control (scrambled) (E-E'') and LMO4-specific shRNA-IRES GFP expressing vectors. (A-A'', C-C'') Coronal sections of electroporated brains at P0 immunostained using an antibody against Ctip2 and higher magnification views for Ctip2 and Satb2 (D-D''' and F-F''') indicate that LMO4 downregulation strongly decreases Ctip2 expression compared to contralateral non-electroporated hemisphere (B) and brains electroporated with scrambled, while Satb2 expression remains unaltered. Arrows indicate the downregulation of Ctip2 expression in brains electroporated compared to their correspondent control regions. Error bars: 200  $\mu\text{m}$  (A-A'' and B), 100  $\mu\text{m}$  (C-C'' and E-E'') and 50  $\mu\text{m}$  (D-D''' and F-F'''). E13.5: embryonic day 13.5, P0: postnatal day 0, COUP-TFI CKO: COUP-TFI<sup>f/f Emx1 Cre</sup>, Str: striatum, mS1: motorized S1, UL: upper layers, V: layer V, Va: upper layer V, Vb: lower layer V and VI: layer VI.

## **IV. Molecular, morphological, hodological and electrophysiological properties of the Satb2/Ctip2 layer V neuronal population**

### **A. Molecular characterization of the double Satb2/Ctip2-positive layer V neurons unravels two major subpopulations**

Next, since Satb2/Ctip2-expressing neurons in S1 layer V were poorly if not at all characterized, I began a molecular analysis of this population using antibodies against known transcriptional regulators of distinct subpopulations of cortical projection neurons. This last part of my work was carried out mainly on *wt* cortices since my aim was to design a profile of Satb2/Ctip2-positive cells in normal conditions. As previously mentioned, Bhlhb5 is strongly expressed in cortico-spinal motor neurons (CSMN) of sensorimotor cortex and corticotectal PN of the visual cortex [144], whereas LMO4 is expressed in more divergent subpopulations, such as cortico-brainstem motor neurons (CBMN) in layer Va of the motor cortex, callosal PN (CPN), backward projection neurons and dual callosal or subcerebral/backward projection neurons; however, it appears completely excluded from CSMNs [145]. The transcription factor Sox5 is expressed by the major classes of corticofugal projection neurons (CFuPNs) (subplate, corticothalamic and all subcerebral subtypes), but not by corticocortical CPNs [166, 217]. Finally the transcription factor Er81 (also named Etv1), a member of the Ets family, is of particular interest for my analysis, since it is expressed throughout layer V in both CPNs and SCPNs in rat brains [348].

Triple immunofluorescence for Satb2, Ctip2 and alternatively one of these molecular markers (LMO4, Bhlhb5, Sox5 or Er81) were performed on *wt* cortices at P7, a stage where layer V PN are almost fully differentiated. My counting revealed that among the Satb2/Ctip2 co-expressing neurons in layer V, a percentage of 90% are LMO4-positive (**Figure 16 A-B''' and I**), 86% are Bhlhb5-positive (**Figure 16 C-D''' and J**), 74% are Er81-positive (**Figure 16 E-F''' and K**), and 81% are Sox5 positive (**Figure 16 G-H''' and L**). These results suggested that Satb2/Ctip2 positive cells may be constituted, by different SCPN expressing Sox5 and Bhlhb5 and CPN most probably expressing LMO4 and Er81 in S1 cortex.

**P7 WT Somatosensory Cortex**

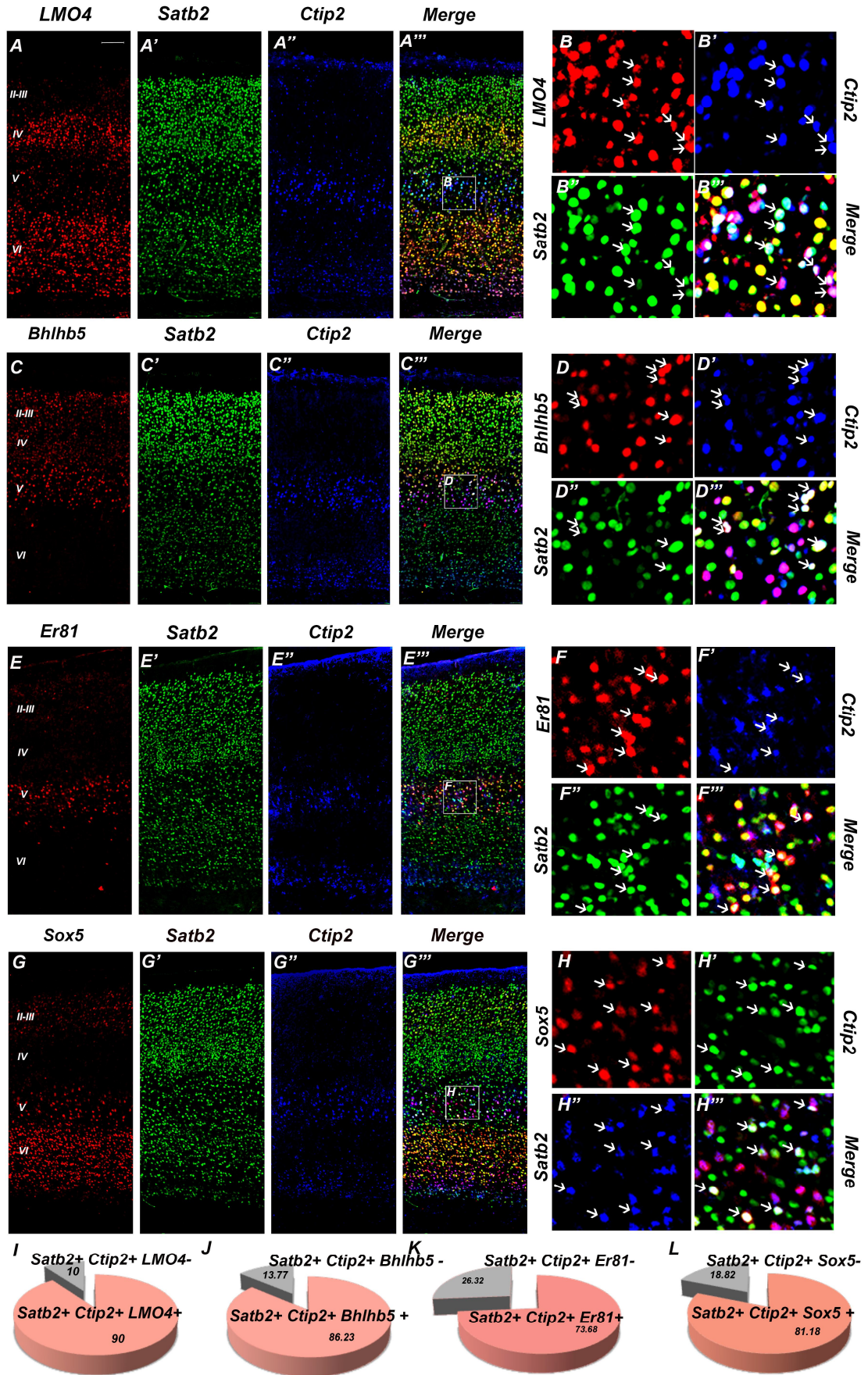


**Figure 16-Molecular markers characterizing the Satb2/Ctip2 positive neurons.**

(A-A''') Triple immunofluorescence against LMO4, Satb2 and Ctip2 and higher magnifications views (B-B''') in layer V of P7 WT parietal cortices. Arrows indicate neurons that express the three markers LMO4, Satb2 and Ctip2. (I) Chart representing the percentage of Layer V Satb2/Ctip2 double-labeled neurons expressing or not LMO4.

(C-C''') Triple immunofluorescence against Bhlhb5, Satb2 and Ctip2 and higher magnifications views (D-D''') in layer V of P7 WT parietal cortices. Arrows indicate neurons that express the three markers Bhlhb5, Satb2 and Ctip2. (J) Chart representing the percentage of layer V Satb2/Ctip2 double-labeled neurons expressing or not Bhlhb5.

(E-E''') Triple immunofluorescence against Er81, Satb2 and Ctip2 and higher magnifications views (F-F''') in layer V of P7 WT parietal cortices. Arrows indicate neurons that express the three markers Er81, Satb2 and Ctip2. (K) Chart representing the percentage of layer V Satb2/Ctip2 double-labeled neurons expressing or not Er81.

(G-G''') Triple immunofluorescence against Sox5, Satb2 and Ctip2 and higher magnifications views (H-H''') in layer V of P7 WT parietal cortices. Arrows indicate neurons that express the three markers Sox5, Satb2 and Ctip2. (L) Chart representing the percentage of layer V Satb2/Ctip2 double-labeled neurons expressing or not Sox5.

Scale bars: 100  $\mu$ m (A-A''', C-C''', E-E''' and G-G'''). P7: postnatal day 7, WT: Wild type, II-III: layers II-III, IV: layer IV, V: layer V and VI: layer VI.

## B. Satb2/Ctip2-positive neurons in layer V project to subcerebral and callosal targets

Projection neurons in the neocortex can be classified based on their projection patterns; for example, callosal neurons send their axons to the contralateral hemisphere within the cerebral cortex, while corticofugal projection neurons send their axons to targets outside the cortex. The choice between these two trajectories is based on the specific combination of mitotic and post-mitotic molecular events that ultimately lead to specific PN responses to different axon guidance molecules during their differentiation process [260]. Satb2/Ctip2 co-expressing neurons are an ambiguous cell population expressing two mutually exclusive transcriptional regulators, Satb2 and Ctip2, one known to specify callosal identity (Satb2) and the other involved in the establishment of SCPN connectivity (Ctip2).

To investigate the connectivity of Satb2/Ctip2-positive neurons we performed fluorescent retrograde labeling experiments between P2 and P3 *wt* pups in collaboration with Denis Jabaudon, our collaborator from the University of Geneva (Switzerland). Cholera toxin subunit B (CTB) conjugated with Alexa Fluor fluorophores [349] is a highly efficient molecule to retrograde label vital neurons and was injected both in callosal and/or subcerebral targets. CTB 488 (green) was injected in the somatosensory area to label callosal PNs of the contralateral hemisphere (**Figure 17 A'', F-G''**), whereas CTB 555 (red) was injected separately in two different subcerebral targets: either in the cervical spinal cord to label CSMNs (**Figure 17 A', D-E''**), or in the rostral pons region to label all subcerebral projection neurons (SCPN) including CSMN, whose axons transit through this region before reaching the spinal cord, and CBMN projecting locally [349] (**Figure 17 A, B-C''**). In some cases (**Figure 17 M-N''**) we used red and green CTB-coated beads, which allow a more detailed analysis of co-localization after simultaneous injection of fluorophores in subcerebral and cortical targets [350]. Injected brains were collected at P7 and I analyzed the somatosensory area in coronal sections. Here, I present results from *wt* pups since, as mentioned above, our analysis was essentially aimed to define Satb2/Ctip2-positive cells in normal conditions.

Double immunofluorescence for Satb2 and Ctip2 on P7 coronal sections showed a remarkable co-localization of Satb2 and Ctip2, in both SCPN- (**Figure 17 B-C''**) and CPN- (**Figure 17F-G''**) retrogradely-labeled neurons in the S1 area.

Interestingly, while the totality of labeled CSMN expresses Ctip2, they never co-express Satb2 and Ctip2 (**Figure 17 D-E''**). These data suggest that double Satb2/Ctip2-positive neurons project either through the corpus callosum to the contralateral hemisphere, or to the brainstem, or to both.

To distinguish between these different possibilities, we co-injected CTB-coated beads in the pons and in S1 of *wt* pups at P2 and P3. In collected brains at P7, I found no co-labeling in layer V neurons (**Figure 17 H-I''**). Retrogradely-labeled neurons are either callosal or subcerebral, but not both, indicating that S1 Satb2/Ctip2 co-expressing layer V neurons are composed at least by two distinct subpopulations, one with dominant callosal features projecting through the corpus callosum to the contralateral hemisphere and another with dominant subcerebral features projecting to the brainstem, but not to the spinal cord. However, at this stage of analysis we cannot exclude either that these cell populations project to other targets, or that callosal neurons co-expressing Satb2 and Ctip2 have different features with respect to single Satb2 expressing CPN in upper layers. New tracing experiments aimed to verify if these neuronal populations project also to other subcortical (e.g. striatum) or intracortical (rostral/caudal areas) targets are ongoing.

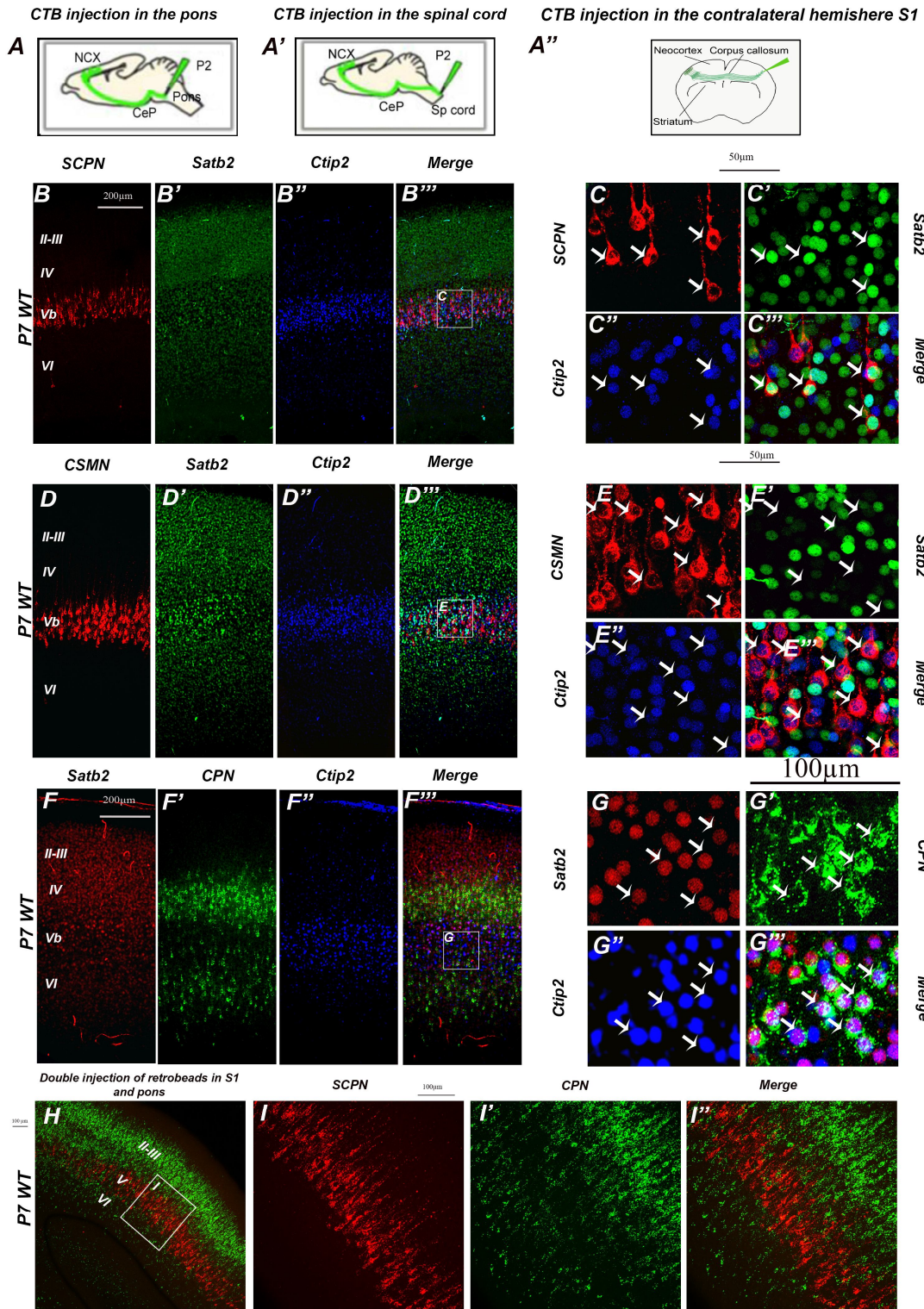


**Figure 17-Satb2 Ctip2 positive cells project to brainstem or callosally to contralateral hemisphere.**

(A-A'') Schematics of labeling paradigms to label subcerebral, corticospinal and callosal projection neurons.

(B) Retrogradely labeled coronal sections taken in the somatosensory area of P7 WT brains, with CTB 555 (red) injected in the pons labeling broad class of subcerebral PN (SCPN): Corticobrainstem and corticospinal projection neurons.

(D) Retrogradely labeled coronal sections taken in the somatosensory area of P7 WT brains, with CTB 555 (red) injected in the spinal cord labeling corticospinal motor neurons (CSMN).

(F) Retrogradely labeled coronal sections taken in the somatosensory area of P7 WT brains, with CTB 488 (green) injected in the somatosensory area, labeling callosal neurons in the contralateral hemisphere (F).

(B-B''') Sections containing retrogradely labeled SCPN (including corticobrainstem and corticospinal neurons) are immunostained for Satb2 and Ctip2 and higher magnification views (C-C''') indicating that a remarkable percentage of labeled SCPN are Satb2/Ctip2 positive. Arrows indicate SCPN coexpressing Satb2 and Ctip2.

(D-D''') Sections containing retrogradely labeled CSMN are immunostained for Satb2 and Ctip2 and higher magnification views (E-E''') indicating that CSMN do never express both Satb2 and Ctip2. Arrows indicate CSMN expressing only Ctip2 but not Satb2.

(F-F''') Sections containing retrogradely labeled callosal projection neurons are immunostained for Satb2 and Ctip2 and higher magnification views (G-G''') indicating that a remarkable percentage of labeled callosal neurons are Satb2/Ctip2 positive. Arrows indicate callosal neurons coexpressing Satb2 and Ctip2.

(H) Red and green retrobeads were injected in the pons and somatosensory cortex respectively and higher magnification view (I-I'') indicating that layer V callosal and subcerebral neurons do never colocalize, layer Vb neurons can be either callosal either subcerebral but never both.

Scale bars: 200  $\mu\text{m}$  (B-B''', D-D''', and G-G'''), 100  $\mu\text{m}$  (G-G'' and M-N'') and 50  $\mu\text{m}$  (C-C''' and E-E'''). CTB: Cholera toxin subunit B, S1: primary somatosensory, P7: postnatal day 7, WT: wild type, CeP: cerebral peduncle, NCX: neocortex, sp cord: Spinal cord, SCPN: subcerebral projection neurons, CSMN: corticospinal motor neurons, CPN: callosal projection neurons, II-III: layers II-III, IV: layer IV, V: layer V and VI: layer VI.

Retrograde labeling showed that *Satb2/Ctip2* co-expressing neurons are corticobrainstem but not corticospinal PN. However, my data showed that 70% of *Satb2/Ctip2* double labeled cells are also *Bhlhb5* positive. It has been reported that *Bhlhb5* is mainly expressed in CSMN and involved in their specification, whereas *LMO4* is involved in CBMN specification and excluded from CSMN [144, 145]. In order to assess whether *Satb2/Ctip2* positive cells expressing *Bhlhb5* are also CBMN, I performed double immunofluorescence for *LMO4* and *Bhlhb5* on retrogradely labeled coronal sections of *wt* S1 cortices. These immunofluorescence demonstrate that all CSMN are positive for *Bhlhb5* but not for *LMO4* (**Figure 18 C-D**”). In contrast, SCPN are either positive for *LMO4*, or *Bhlhb5* or double positive for *LMO4* and *Bhlhb5*. Since *LMO4* is excluded by CSMN, SCPN expressing both *LMO4* and *Bhlhb5* must be CBMN (**Figure 18 A-B**”). Thus, *Satb2/Ctip2* positive corticobrainstem PNs can be either *LMO4* positive or *LMO4/Bhlhb5* positive further confirming the previous molecular characterization of this cell population.

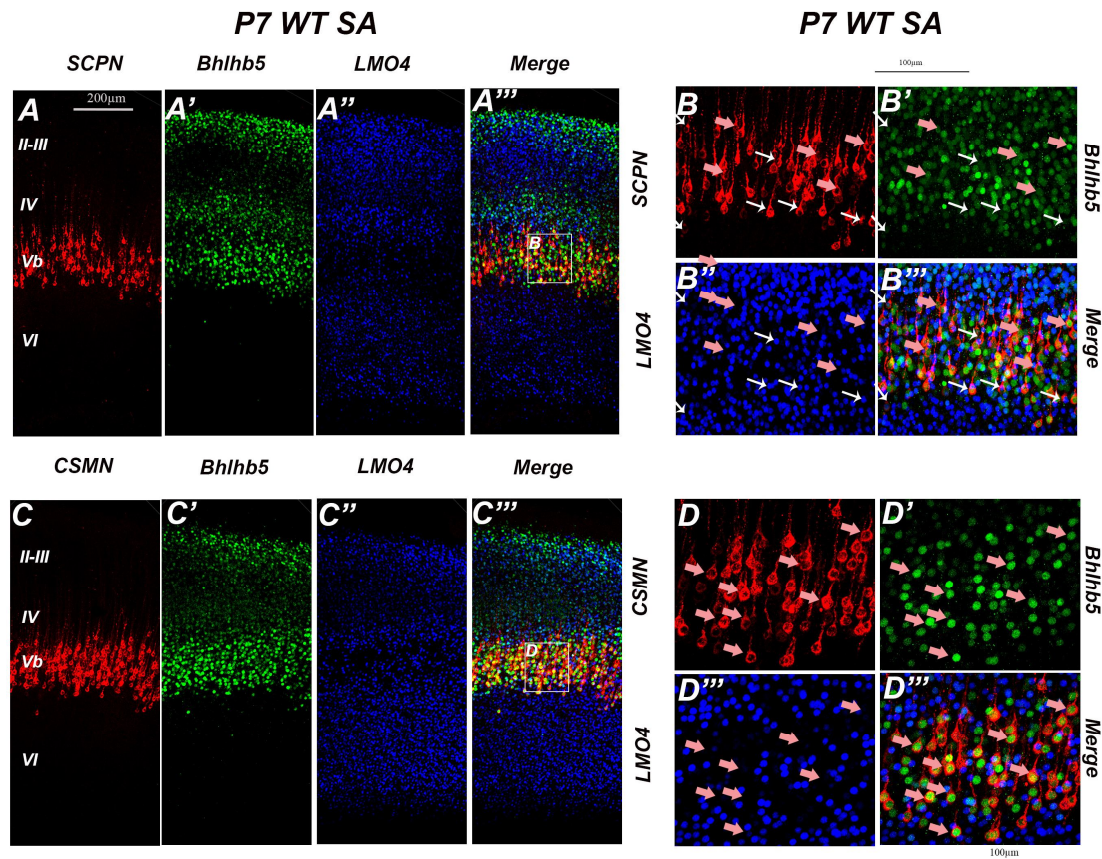


**Figure 18-Corticobrainstem neurons express LMO4 while corticospinal express Bhlhb5 instead.**

(A-A''') Retrogradely labeled coronal sections taken in the somatosensory area of P7 WT with CTB 555 (red) injected in the pons labeling broad class of subcerebral PN (SCPN): Corticobrainstem and corticospinal projection neurons. Sections containing retrogradely labeled SCPN (including corticobrainstem and corticospinal neurons) are immunostained for LMO4 and Bhlhb5 and higher magnification views (B-B''') indicating that a remarkable percentage of labeled SCPN are LMO4 positive or Bhlhb5 positive or both. White arrows indicate SCPN expressing LMO4; pink arrows indicate SCPN expressing Bhlhb5.

(C-C''') Retrogradely labeled coronal sections taken in the somatosensory area of P7 WT brains, with CTB 555 (red) injected in the spinal cord labeling corticospinal motor neurons (CSMN). Sections containing retrogradely labeled CSMN are immunostained for LMO4 and Bhlhb5 and higher magnification views (D-D''') indicating that CSMN do never express LMO4 but rather they are all Bhlhb5 positive. Pink arrows indicate CSMN expressing only Bhlhb5.

Scale bars: 200 µm (A-A''', C-C'''), 100 µm (B-B''', D-D'''). P7: Postnatal day 7, WT: wild type, SA: somatosensory area, SCPN: subcerebral projection neurons, CSMN: corticospinal motor neurons, II-III: layers II-III, IV: layer IV, V: layer V, and VI: layer VI.

In order to associate to the two sub-populations of Satb2/Ctip2 co-expressing neurons, the analyzed molecular markers, immunofluorescence against LMO4, Bhlhb5, Sox5 and Er81 were performed in retrogradely double labeled callosal and SCPN coronal sections of P7 *wt* cortices taken in S1. LMO4 was expressed by both callosal and subcerebral PNs (**Figure 19 A-C''**). However, Er81 was expressed only by CPNs (**Figure 19 D-F''**). On the other hand, Sox5 and Bhlhb5 were expressed exclusively by SCPN, while they were both excluded from layer V callosal neurons (**Figure 20**). Thus, association of retrograde labeling with subtype specific genes confirmed that the two sub-populations of Satb2/Ctip2 co-expressing neurons express specifically distinct molecular markers, with callosal sub-population expressing LMO4 and Er81, and corticobrainstem cell population expressing Sox5 and Bhlhb5.

**P7 WT with Red beads injection in the pons  
and green beads injection in S1**

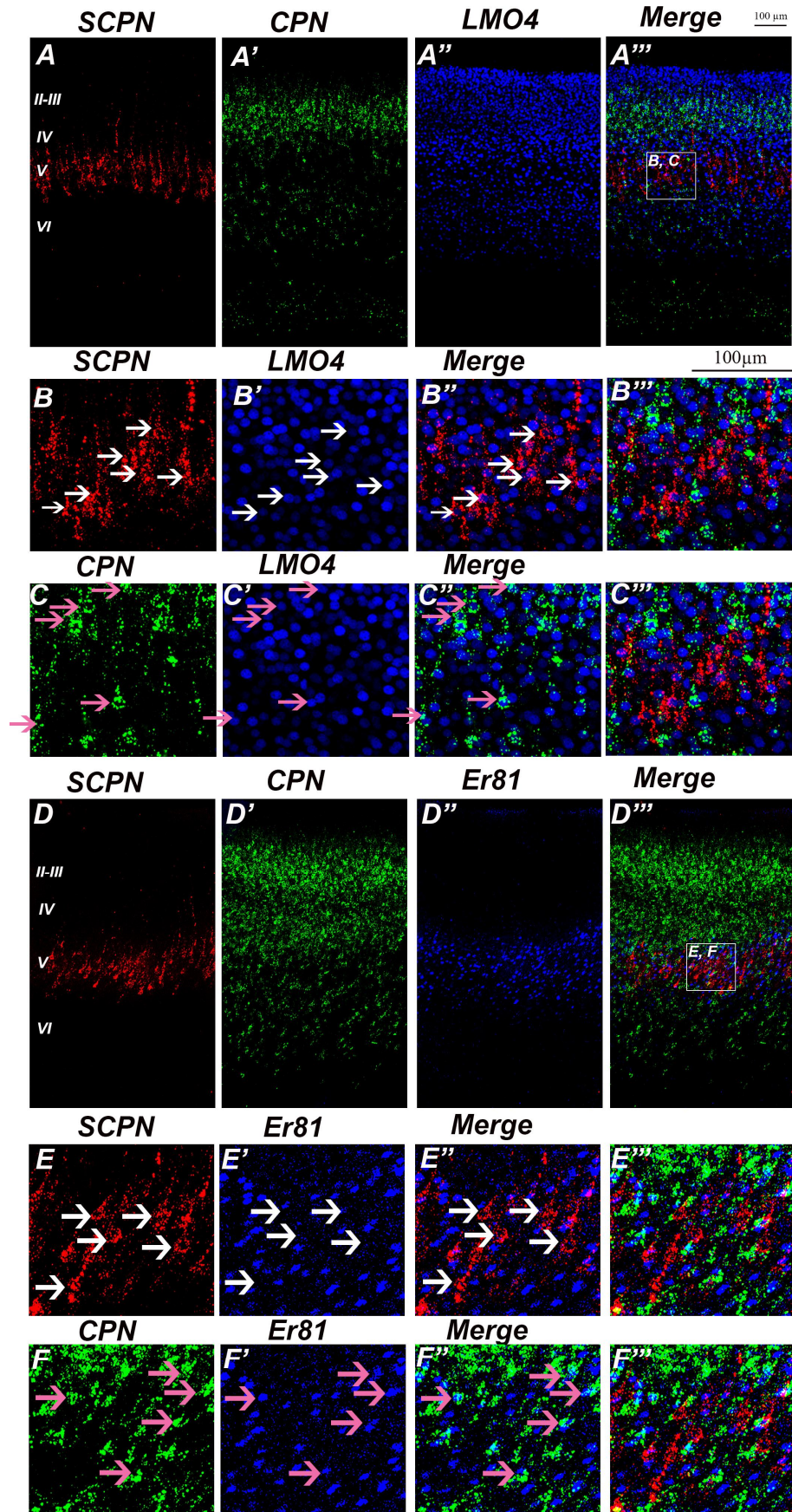


**Figure 19- LMO4 is expressed by CPN and SCPN, while Er81 is layer V callosal specific gene.**

(A-A''', D-D''') Retrogradely double-labeled coronal sections taken in the somatosensory area of P7 WT with red and green beads injected in the pons and the somatosensory area respectively labeling broad class of subcerebral PN (SCPN): Corticobrainstem and corticospinal projection neurons, and callosal PN (CPN) in the contralateral hemisphere.

(A-A''') Sections containing retrogradely labeled SCPN (including corticobrainstem and corticospinal neurons) and CPN are immunostained for LMO4 and higher magnification views (B-B''', C-C''') indicating that a remarkable percentage of labeled SCPN and CPN are LMO4 positive. Arrows indicate SCPN or CPN expressing LMO4.

(D-D''') Sections containing retrogradely labeled SCPN (including corticobrainstem and corticospinal neurons) and CPN are immunostained for Er81 and higher magnification views (E-E''', F-F''') indicating that a remarkable percentage of labeled CPN are Er81 positive, however SCPN are Er81 negative. White arrows indicate CPN expressing Er81, and pink arrows indicate SCPN Er81 negative. Scale bar: 100  $\mu$ m. P7: Postnatal day 7, WT: wild type, S1: Primary somatosensory area, CPN: callosal projection neurons, SCPN: subcerebral projection neurons, II-III: layers II-III, IV: layer IV, V: layer V, and VI: layer VI.

**P7 WT with Red beads injection in the pons  
and green beads injection in S1**

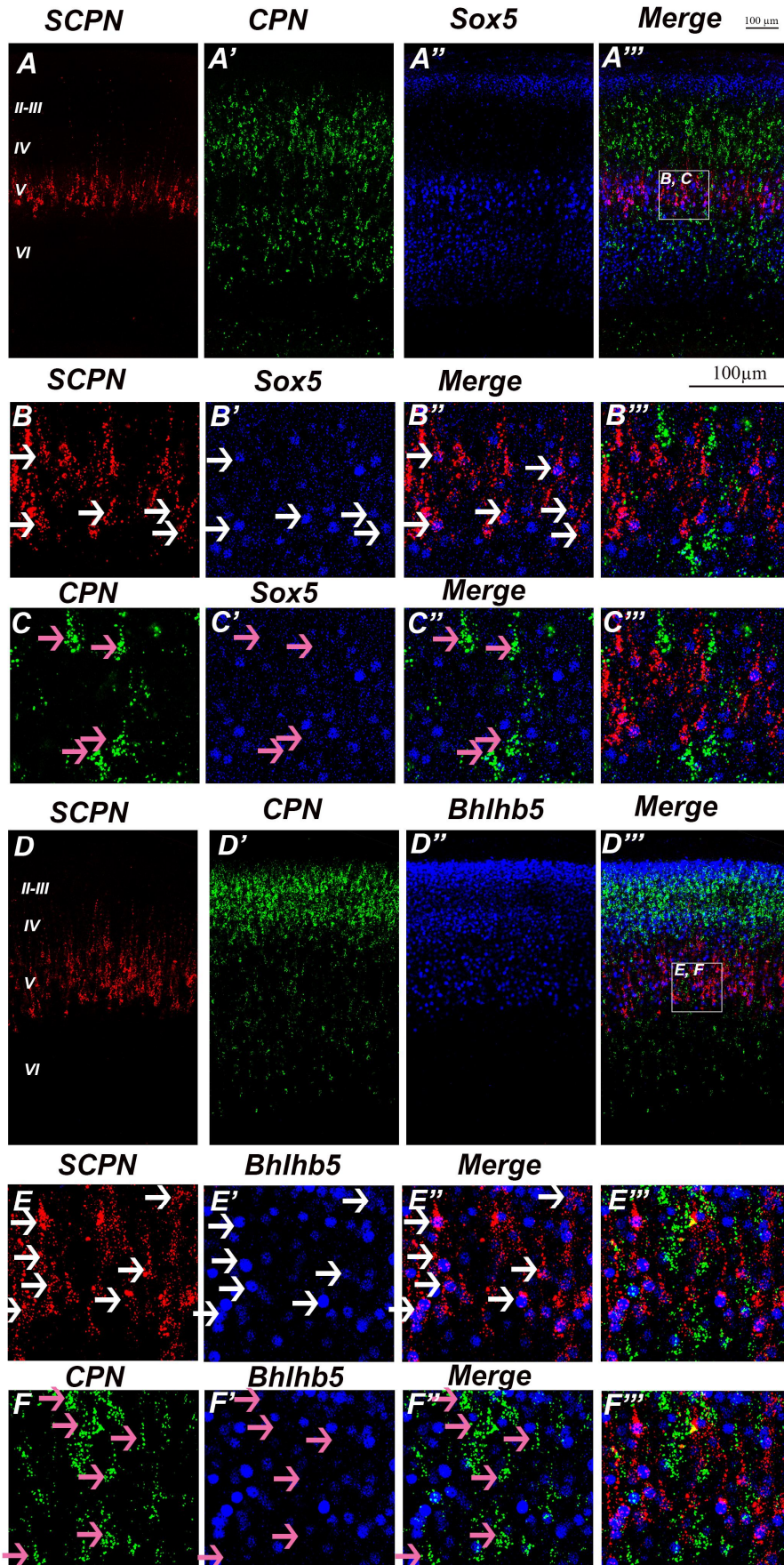


**Figure 20- Sox5 and Bhlhb5: layer V SCPN specific genes.**

(A-A''', D-D''') Retrogradely double-labeled coronal sections taken in the somatosensory area of P7 WT with red and green beads injected in the pons and the somatosensory area respectively labeling broad class of subcerebral PN (SCP<sub>N</sub>): Corticobrainstem and corticospinal projection neurons and callosal PN (CPN) in the contralateral hemisphere.

(A-A''') Sections containing retrogradely labeled SCP<sub>N</sub> (including corticobrainstem and corticospinal neurons) and CPN are immunostained for Sox5 and higher magnification views (B-B''', C-C''') indicating that all SCP<sub>N</sub> are Sox5 positive, while Sox5 is excluded from all CPN. White arrows indicate SCP<sub>N</sub> expressing Sox5, and pink arrows indicate CPN Sox5 negative.

(D-D''') Sections containing retrogradely labeled SCP<sub>N</sub> (including corticobrainstem and corticospinal neurons) and CPN are immunostained for Bhlhb5 and higher magnification views (E-E''', F-F''') indicating that a remarkable percentage of labeled SCP<sub>N</sub> are Bhlhb5 positive, however layer CPN are Bhlhb5 negative. White arrows indicate SCP<sub>N</sub> expressing Bhlhb5, and pink arrows indicate CPN Bhlhb5 negative.

Scale bar: 100  $\mu$ m. P7: Postnatal day 7, WT: wild type, S1: Primary somatosensory area, CPN: callosal projection neurons, SCP<sub>N</sub>: subcerebral projection neurons, II-III: layers II-III, IV: layer IV, V: layer V, and VI: layer VI.

### C. Morphological analysis confirms differences between single and double Satb2/Ctip2-positive layer V neurons

Morphological diversity has been observed between several subtypes of layer V neurons in different species [347, 351, 352]. Thus, to further investigate whether double Satb2/Ctip2-expressing neurons could also exhibit morphological differences with respect to other layer V subpopulations (single Ctip2 or Satb2 positive neurons). I used a transgenic line expressing the reporter gene YFP under the Thy1 promoter [345]. In this line, YFP is expressed mainly in the soma, dendrites and axons of layer Vb cortical neurons from P14 onwards [353]. Immunostaining for Satb2 and Ctip2 was thus performed on P21 YFP-positive coronal sections, and confocal images were taken in the somatosensory area at different magnifications to highlight any morphological features in the soma shape, apical and secondary dendrites of layer V neurons (**Figure 21A**).

Morphological analysis of the soma shape of layer V YFP-positive neurons reveals differences in soma size, geometrical morphology, distribution of secondary dendrites, and angles between these dendrites. Thanks to these differences and to the immunoreactivity for Satb2 and Ctip2, I classified YFP-positive neurons into three main shapes: double Satb2/Ctip2 co-expressing neurons (shape I), single Ctip2 (shape II) and single Satb2 (shape III) positive neurons (**Figure 21 A-G**).

A deeper analysis of the soma shape and distribution of dendrites was performed using the Sholl analysis, which is a method of quantitative analysis commonly used to analyze the morphological characteristics of neurons [354] (**Figure 22 A**). To perform this analysis I used a freely available plug-in based on the ImageJ software that automatically creates a series of concentric circles around the center of a neuronal arbor (dendritic or axonal), and quantifies how many times the arbor intersects the circumference of these circles (**Figure 22 B**). The algorithm then generates a curve representing the logarithm of the number of intersections divided by the surface ( $\text{Log } N/S$ ) of each created circle in function of the logarithm of the radius ( $\text{Log } R$ ) of each circle (**Figure 22 C**). Such a curve typically represents neuronal morphology. By applying the Sholl analysis, three distinct morphologies came out among the YFP-positive neurons, corresponding to Satb2/Ctip2, single Ctip2 and single Satb2 positive cells.

Moreover, analysis of YFP-labeled apical dendrites aimed to identify further morphological differences, such as apical dendrite thickness, bifurcation point of the apical dendrite (**Figure 23 B**), apical tuft complexity and other parameters (**Figure 23 A, B**) is ongoing. In collaboration with *mathematicians* of the Morpheme team at the iBV, we are currently generating a software that would automatically detect morphological differences among layer V neurons and classify them according to different parameters, such as sphericity and volume of the soma, number of secondary dendrites, their diameters and angles between them, distance to the bifurcation point of the apical dendrite, distance from the soma center to the pia, and complexity of the apical tuft.

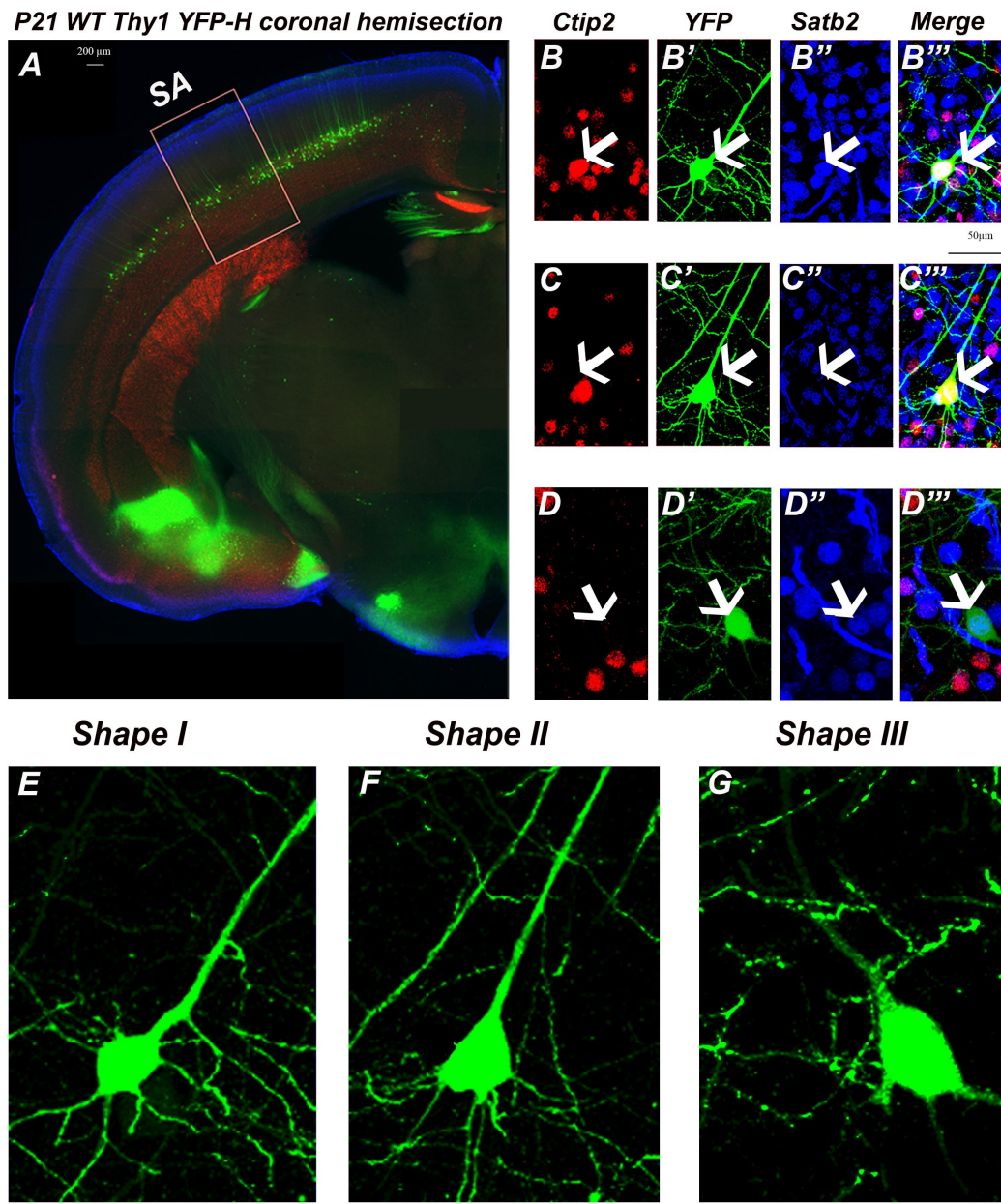


**Figure 21-Morphological differences in soma shape among Satb2/Ctip2 co-expressing neurons and single Satb2 or Ctip2 positive neurons.**

(A) Coronal hemisection of P21 WT Thy1-YFP-H brains, labeling with YFP layer V cortical neurons, immunostained for Ctip2 (Red) and satb2 (shown only in higher magnification) indicating the position of YFP labeled neurons, in layer Vb. (B-D''') Higher magnifications views in layer V in the somatosensory area revealing 3 neuronal population: Double Satb2/Ctip2 co-expressing neurons (B-B'''), single Ctip2 positive neurons (C-C''') and Single Satb2 positive neurons (D-D'''). Arrows indicate YFP neurons with their molecular code (Double Satb2/Ctip2, single Ctip2 or single Satb2 positive neurons).

(E-G) Higher magnifications for the three detected different shapes showing differences in the morphology of the soma between Double Satb2/Ctip2 co-expressing neurons (Shape I) (E), single Ctip2 positive neurons (Shape II) (F) and Single Satb2 positive neurons (Shape III) (G).

Scale bars: 200  $\mu\text{m}$  (A), 50  $\mu\text{m}$  (B-G). P21: postnatal day 21, WT: Wild type, and YFP: yellow fluorescent protein.

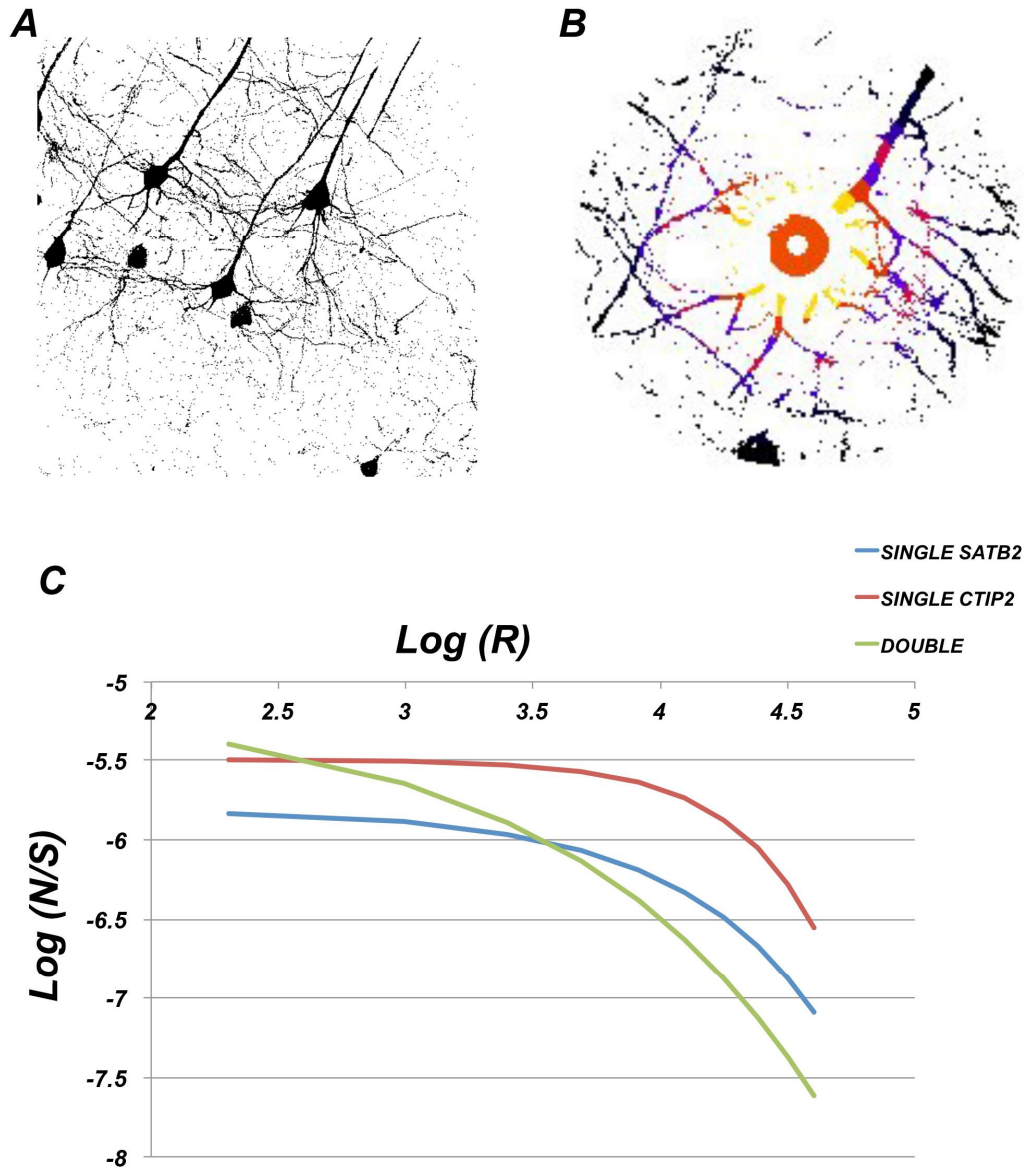


**Figure 22-Three shapes for different molecular codes detected by Sholl analysis.**

(A) Binary imaged neuron for high magnification YFP layer V neurons taken in the somatosensory area. (B) Concentric circles created around the center of the imaged neuron that intersects with its dendrites. (C) Sholl analysis representative curves representing the log of N/S in function of log (R), obtained from the analysis of neurons with three different molecular codes, double Satb2 Ctip2 co-expressing neurons, single Ctip2 and single Satb2 positive neurons, showing differences in morphologies between these 3 populations. Log: logarithm, N: number of intersections, S: surface of the circle and R: Radius of the circle.

**P21 WT thy1-YFP-H SA**

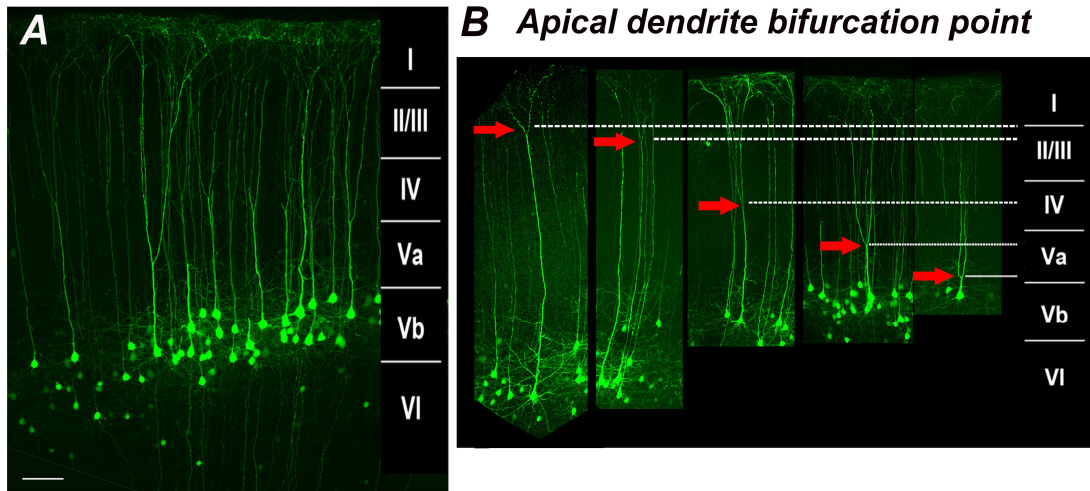


**Figure 23-Apical dendrite morphology; another parameter distinguishing different shapes among layer V cortical neurons.**

(A) Image of the somatosensory area of a P21 WT Thy1-YFP-H brains, labeling with YFP layer V cortical neurons, their axons, apical dendrite reaching the layer I, and secondary dendrites. (B) Different layer V YFP labeled neurons with their apical dendrites. Arrows and dashed lines indicate bifurcation point of apical dendrites revealing positional laminar differences of its primary branching in different cortical layers. Scale bar: 100  $\mu$ m (A, B).

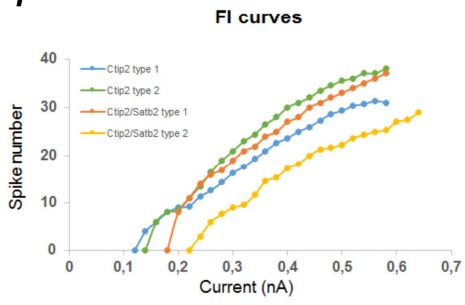
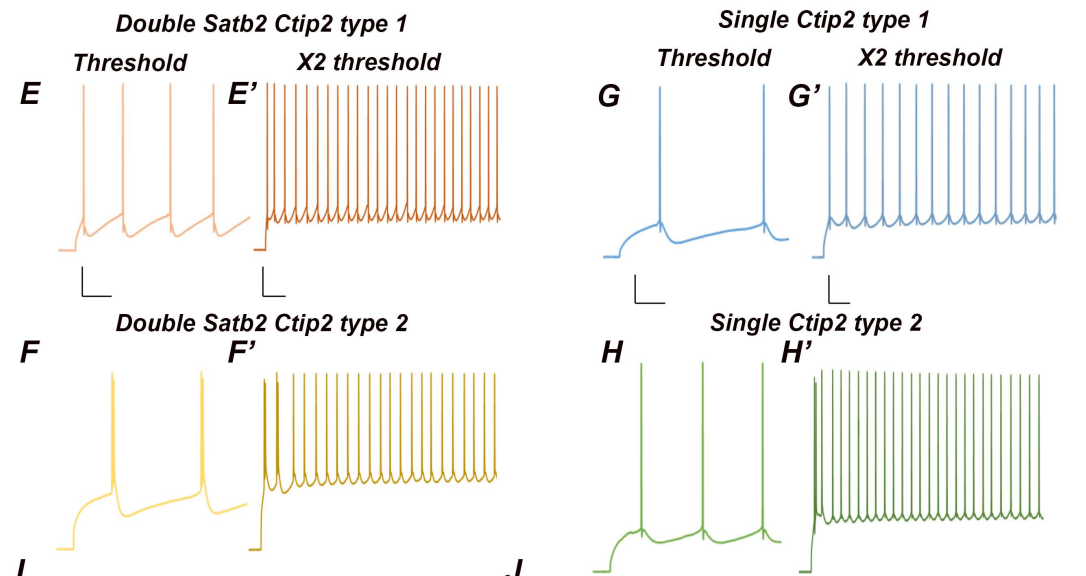
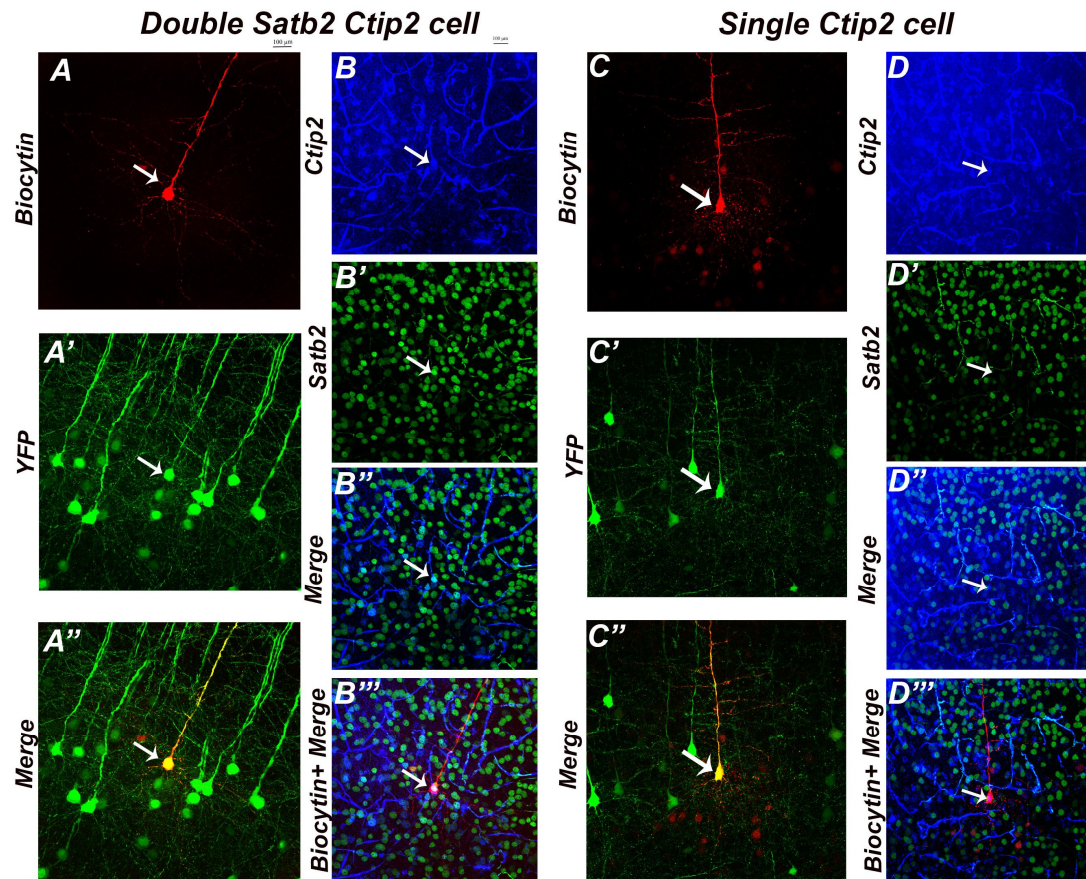
#### **D. Distinct electrophysiological properties of double Satb2/Ctip2-positive neurons in layer V**

I finally asked whether this population of cells coexpressing Satb2 and Ctip2 had characteristic membrane and firing properties, and whether further differences could exist between the two identified subpopulations. With the help of Céline Nicolas, a researcher working in G. Sandoz's lab at the iBV, we studied by whole cell patch-clamp recordings the neuronal intrinsic membrane and firing properties of YFP+ layer V neurons from the Thy1-YFP-H mouse line. Intrinsic properties of layer V neurons were studied by inhibiting cell-cell synaptic activity in the presence of ionotropic glutamate and GABA receptors antagonists (APV, DNQX and picrotoxin). The results were compared between double Satb2/Ctip2 and single Ctip2-expressing YFP+ neurons. Clamped cells were injected with biocytin during recordings, which allows correlating their electrophysiological activity to their morphological and molecular properties (**Figure 24 A-D''**).

Analysis of cell behavior in response to depolarizing current injections in function of their molecular code, allowed dividing the recorded cells into four populations: two populations of Satb2/Ctip2 co-expressing neurons (**Fig 24 A-B''**), and two populations of single Ctip2 expressing neurons (**Figure 24 C-D''**). We found that at their resting membrane potentials, all cell subtypes fail to fire spontaneously. However, in response to depolarizing current injections, Satb2/Ctip2 type 2 and single Ctip2 type 1 fire an initial doublet, whereas Satb2/Ctip2 (type 1) fire a quadruplet and single Ctip2 type 2 a triplet (**Figure 24 E-H**). This initial firing is followed by a particularly long, large-amplitude AHP (After Hyperpolarization) (**Figure 24 J**), while DAP (Depolarizing afterhyperpolarization) is higher in Satb2/Ctip2 (type 1) compared to the other three sub-populations (**Figure 24 J**). After this phase of adaptation, the neurons fall into regular trains of action potentials (**Figure 24 E'-H'**) that exhibited different spike frequency adaptation.

Interestingly, quantification of the spike frequency adaptation and of the FI (Firing current) curve show that Satb2/Ctip2 type 2 neurons are very different from the other three subpopulations. The firing frequency of single Ctip2 type 1 and 2 and double Satb2/Ctip2 type 1 remain nearly constant, as demonstrated by their high adaptation ratio; however, the extent of adaptation of double Satb2/Ctip2 type 2 is much larger (very small adaptation ratio) and clearly different from the other three

subpopulations (**Figure 24 J**). In response to a series of depolarizing currents, the three subpopulations show relatively uniform mean firing rates. The slopes of their FI curves are larger than those of the Satb2/Ctip2 (type 2) subpopulation (**Figure 24 I, J**). These results indicate that the two sub-populations of Satb2/Ctip2 positive neurons have distinct firing properties, the first subpopulation of Satb2/Ctip2 positive neurons (type 1) shows intrinsic electrical activity similar to single Ctip2 positive neurons, whereas Satb2/Ctip2 type 2 positive cells showed remarkably intrinsic electrophysiological distinct features.



**J**

Cell parameters	Ctip2+		Ctip2+/Satb2+	
	Type 1	Type 2	Type 1	Type 2
Initial burst interval at x2 threshold	47.23	5.50	27.90	3.90
Initial burst interval at threshold	267.17	168.90	111.30	4.23
Adaptation ratio (1st/last)	0.85	0.15	0.83	0.09
Adaptation ratio (3d/last)	1.22	1.07	1.30	0.11
FI slope	123.16	113.13	95.00	61.90
fAHP	14.61	12.31	17.21	14.20
DAP	3.35	3.76	10.19	3.69
Rs (peak)	109.00	104.50	92.00	66.50

Figure 24-Electrophysiological properties of Satb2/Ctip2 co-expressing neurons.

(A-A'', C-C'') whole-cell patch clamp performed on layer V YFP+ pyramidal cells from Thy1-YFP-H mouse line from P21-P30, and biocytin injection during recording indicates analyzed neurons after texas red avidin revelation. (B-B'', D-D'') Higher magnification views for GFP-biocytin labeled and analyzed neurons immunostained with antibodies against Satb2 and Ctip2 reveal different populations of cells co-expressing Satb2 and Ctip2, or single Ctip2 neurons.

(E-J) In response to depolarizing current injections, layer V analyzed pyramidal neurons exhibit an initial doublet, triplet, or quadruplet followed by trains of action potentials (E-J) with different spike frequency adaptation. Different electrophysiological parameters including initial burst interval, FI curves, adaptation ratio, FI slope, fAHP, DAP and Rs peak (I, J) revealed two different subpopulations among Satb2/Ctip2 positive neurons and two different populations among single Ctip2 positive neurons. The first subpopulation of Satb2/Ctip2 positive neurons (type 1) shows intrinsic electrical activity similar to single Ctip2 positive neurons. Type 2 Satb2/Ctip2 positive cells, instead, shows remarkably different features. FI: firing current, fAHP: fast afterhyperpolarization, DAP: depolarizing afterhyperpolarization, Rs: resistance.

## *Chapter 4: Discussion*

---

## **I. Satb2/Ctip2 co-expression: not a transient state but a permanent cell population.**

The impressive ability of the neocortex to process information relies on the accurate establishment of neuronal connections. The expression of Satb2 or Ctip2 in cortical neurons triggers mutually exclusive genetic programs leading to their final connectivity [150, 212, 355]. Ctip2 imprints a corticofugal fate to neocortical projection neurons and is involved in the fasciculation and appropriate targeting of their axons [66]. In contrast, Satb2 is a key determinant for callosal projection neurons, since its deletion results in the absence of the corpus callosum, misrouting of callosal axons towards the internal capsule and spinal cord, and ectopic upregulation of Ctip2 in presumptive callosal neurons [150, 212].

It was previously stated that the refinement of subtype identity is a progressive mechanism. While mature lower-layer neurons exhibit strikingly specific patterns of gene expression and axonal projection, newly postmitotic neurons often extensively co-express transcription factors that later become restricted to different subtypes and temporarily innervate aspecific targets [150, 203, 217, 229, 333, 356]. For instance, between E12.4 and E14.5, neurons in the cortical plate co-express high levels of Ctip2 and TBR1/FOG2, which later resolve into SCPN and CThPN respectively. Similarly, at E13.5, lower layer neurons briefly co-express Ctip2 and Satb2, which become over time restricted to SCPN and CPN respectively [150].

On the contrary my data show that the co-expression of two transcription factors, Satb2 and Ctip2, normally restricted to callosal versus subcerebral PNs respectively, does not represent a transient state lasting only the few days needed for post-mitotic refinement. It represents, indeed, a definitive and permanent molecular feature maintained after final differentiation and pruning events (at P21), therefore defining a cell population showing a specific morphology, connectivity and electrical activity.

## **II. Satb2/Ctip2 co-expressing neurons: a previously uncharacterized cell population.**

It is well reported that Satb2 normally represses Ctip2 expression in the cerebral cortex, leading to a sharp distinction between callosal and sub-cerebral

projection neuron subtypes [150, 212]. Nevertheless, different reports briefly mentioned the presence of a small number of double Ctip2/Satb2 co-expressing neurons in lower layers [150, 212, 234, 260], in which Satb2 seemed to be expressed at very low levels [212]. It was also stated that a few Satb2-positive neurons failed to downregulate Ctip2 in deep cortical layers [260], however these Satb2 positive cells were never seen projecting to the spinal cord [212]. The authors proposed that these Satb2/Ctip2 positive cells were lacking Ski expression necessary to inhibit Ctip2, and that these Satb2<sup>+</sup>/Ctip2<sup>+</sup>/Ski<sup>-</sup> cells were most likely non-callosal neurons [234, 260].

Beside these minor comments in the above-mentioned papers, to my knowledge, no other studies have thoroughly described this population of double Satb2/Ctip2 co-expressing neurons. Differently from what was reported in these previous studies, my data reveal a non-irrelevant population of neurons co-expressing both Satb2 and Ctip2 at high levels in lower layers, and a key role for LMO4 in this process. I provide a molecular mechanism responsible for the de-repression of Ctip2, which allows Satb2 and Ctip2 co-expression in a sub-population of lower layer neurons. Moreover, I characterized major features of this previously uncharacterized cell population, including its connectivity, electrophysiological and morphological characteristics, as well as their specific molecular profile.

### **III. Ectopic and precocious expression of LMO4 in COUP-TFI CKO.**

#### **A. LMO4 allows Ctip2 expression in Satb2-positive cells of COUP-TFI CKO brains**

LMO4 is normally highly expressed in frontal and occipital regions of *wt* cortices at P0, while it is expressed only at low levels in layers V and VI of the parietal cortex (**Figure 4 A**). This expression increases with time to reach high levels at P7 (**Figure 5**). In the absence of COUP-TFI function, LMO4 expression is prematurely increased in all cortical layers of the motorized S1 (**Figure 4 A' and B'**), indicating a direct or indirect control of LMO4 transcription by COUP-TFI. COUP-TFI presumably represses LMO4 expression at early postnatal stages, most probably not in a direct way since our preliminary ChIP experiments failed to unravel a direct binding of

COUP-TFI on LMO4 regulatory regions (*data not shown*). Alternatively, LMO4 expression might be controlled by an activity dependent mechanism. Accordingly, I report a strong increase in LMO4 expression in *wt* conditions in the S1 at P7, a stage when the barrel field is refined by activity. This would suggest that Calcium activity not only regulate LMO4 function, as previously shown [146], but also regulate its expression. Moreover, COUP-TFI has been recently described to regulate dopaminergic interneuron specification in the olfactory bulb through an activity-dependent mechanism involving the expression of the immediate-early gene *Zif268* (previously known as *Egr1*) [357]. Thus, it is conceivable that COUP-TFI might modulate LMO4 expression levels by controlling expression of activity-dependent genes in S1 cortex. The lab is at present testing this hypothesis.

LMO4 premature expression leads to an increased number of double Satb2/Ctip2-positive neurons in COUP-TFI mutants, allowing their co-expression in layers V and VI (**Figure 1**). However, Satb2 and Ctip2 do not normally co-localize in layer VI of P0 S1, neither in upper layers of *COUP-TFI CKOs*, albeit high LMO4 and Satb2 expression levels in these neurons (**Figure 8 E-H' and J**). This suggests that beside the chromatin remodeling machinery controlled by the NuRD complex on the Ctip2 locus, another independent mechanism that modulates Ctip2 expression might exist. We hypothesize that this alternative mechanism might be under the control of *Fezf2*, which is directly and/or indirectly required in activating Ctip2 expression in lower layers [211, 229]. Ctip2 is not expressed in *Fezf2 null* mutant mice [211, 229] and *Fezf2* is up-regulated in layer VI of COUP-TFI mutants, while it is absent in upper layers [134]. Finally, previous studies have demonstrated that ectopic expression of *Fezf2* in progenitors, post-mitotic neurons or into striatum ectopically activates Ctip2 and promotes features of subcerebral neuronal projections [65, 66, 213]. Thus, it is very plausible that the strong up-regulation of Ctip2 in lower layers of COUP-TFI mutant brains (**Figure 1 C and E**) might be due not only to the ectopic expression of LMO4, which primarily accounts for the increase of Satb2/Ctip2 co-expression, but also to the up-regulation of *Fezf2* expression in layers V and VI. This would also explain the lack of Ctip2 expression in the upper layers of *COUP-TFI CKO* although high levels of Lmo4 in the S1 area (**Figure 9**).

My triple immunofluorescence data revealed that LMO4 is normally expressed in  $68\pm 1.7\%$  of double Satb2/Ctip2 at P0, and in  $92\pm 0.4\%$  of Satb2/Ctip2-positive cells in layer V neurons of *COUP-TFI* mutants (**Figure 9 F and G**). This

confirms that the presence of LMO4 in the majority of layer V Satb2/Ctip2-positive cells is required in the specification of this neuronal population. However, LMO4 is absent in  $32\pm 1.7\%$  of Satb2/Ctip2-positive cells in controls, and in  $8\pm 0.4\%$  of them in COUP-TFI CKO. Thus, it is possible that another mechanism, independent from LMO4, is responsible for the specification of this complementary percentage, particularly in controls, whereas this complementary mechanism seems to have a minor effect in *COUP-TFI CKO* brains.

Contrary to LMO4, Ski expression is required for Ctip2 inhibition by Satb2. Ski is expressed in 57.7% of Satb2/Ctip2 positive cells in layer V and absent in 42.3% of them (**Figure 11 E**). Thus, it is likely that in double-positive neurons where LMO4 is not expressed, absence of Ski fails to inhibit Ctip2 transcription, leading thus to Satb2 and Ctip2 co-localization. In the cells where both, LMO4 and Ski are expressed, presence of Ski is not sufficient to interfere with LMO4 function and de-repress Ctip2. In summary, at least two independent epigenetic mechanisms might exist in the Ctip2 transcriptional control, which is dependent on the delicate balance between Ski and LMO4.

## **B. LMO4 binds to HDAC1 and de-represses Ctip2**

In physiologic conditions, LMO4 interacts with several kinds of proteins, and modulate transcriptional activity of target genes. LMO4 was found to bind *in vivo* to the ER $\alpha$  and recruit the member of the NuRD complex MTA1 and HDACs leading to transcriptional repression of ER $\alpha$  target genes [323]. Moreover, LMO4 can also associate with HDAC2, sequester it and thus enhance the activity of Stat3 in mouse cortical neurons [324].

In this study, I showed that LMO4 binds to HDAC1 and prevents it to interact with Satb2, leading to a decrease in the levels of HDAC1 bound to the Ctip2 locus and to an increased histone “acetylation”, which maintains the locus in an active transcriptional state (**Figure 10**). Thus, LMO4 competes with Satb2 in the transcriptional control of Ctip2 allowing the co-expression of Satb2 and Ctip2 in lower layer neurons. At P0, LMO4 is expressed only in few layer V neurons and this would explain why only  $4 \pm 0.3\%$  of layer V neurons co-expresses Satb2 and Ctip2 at this stage. However, in *COUP-TFI CKO*, LMO4 is prematurely and ectopically

expressed at high levels in lower layers, allowing a high and efficient de-repression of Ctip2 and giving rise to a higher percentage of double-labeled cells ( $18\pm 1.8\%$  of layer V and  $8\pm 0.5\%$  of layer VI neurons) (**Figure 1**).

Ski was also identified as a Satb2 partner, which recruits HDAC1 at the Ctip2 locus enabling the formation of the NuRD complex and Ctip2 transcriptional repression. My data revealed that LMO4 not only binds and subtract HDAC1 from Satb2, but that it also binds to Ski (**Figure 11 A**). Satb2 interaction with these two molecules decreases in the presence of high levels of LMO4, such as in the case of *COUP-TFI CKO* brains. Therefore, LMO4 perturbs the formation of the NuRD complex at Ctip2 locus. My data show that Satb2 and LMO4 proteins fail to interact either in controls or in COUP-TFI mutants (**Figure 11 A**). Since, Satb2 still remains bound to Ctip2 upstream regulatory regions in the absence of interaction with Ski and HDAC1[234], the action of LMO4 might happen before the NuRD complex assembles at the Ctip2 locus, and not on the locus itself, further explaining the decrease of Satb2 interactions with HDAC1 and Ski. Therefore, LMO4 does not only perturb the action of the NuRD complex, but it even disturbs its assembly on the Ctip2 locus.

My co-immunoprecipitation data showed also that, even though LMO4 subtracts HDAC1 from Satb2, LMO4 interaction with Ski does not appreciably change between controls and mutants, as for HDAC1 (**Figure 11 A**). This may be explained by the strong decrease in Ski expression in upper layers of COUP-TFI mutants (**Figure 11 B-B''**). Our nuclear extracts, indeed, derive from the whole cortex and not only from lower layers. Thus, although the interaction with LMO4 increases, Ski levels decrease in upper layers of *COUP-TFI CKO brains*, so that its interaction with LMO4 is apparently unchanged, while that with Satb2 is strongly decreased.

#### **IV. Areal and temporal distribution of Satb2/Ctip2 positive neurons in S1 cortex**

Previous reports [325] and this study have shown that LMO4 has a regional and temporal specific expression pattern in the developing neocortex being highly expressed in the motor and visual areas at P0 (**Figure 5**). I have showed that the distribution of Satb2/Ctip2 co-expressing neurons and that of Lmo4-expressing follow a similar trend (**Figure 6**). Indeed, the percentage of Satb2/Ctip2 co-expressing neurons in layer V of the motor area represents twice the percentage observed in S1

(**Figures 2 and 3**). Interestingly, both LMO4 expression and the percentage of Satb2/Ctip2-positive neurons progressively increase in layers V and VI of S1 after P0 (**Figures 5 and 6**). My triple immunofluorescence LMO4/Satb2/Ctip2 at P0 and P7 (Figures 9 and 16 A-B''' and I) directly proof that LMO4 is normally expressed in the majority of double Satb2/Ctip2-expressing neurons over time. Moreover, my gain- and loss-of-function experiments in which we directly manipulated LMO4 expression in S1 (see below) strongly support this evidence.

## A. LMO4 Gain- and loss-of-function

### 1. **The majority, but not the totality of Satb2/Ctip2 co-expressing neurons decrease in the absence of LMO4 in layer V, unraveling a complementary compensatory mechanism**

My data show that Ctip2 expression strongly decreases in layers V and VI in S1 of *LMO4 CKO* cortices (**Figure 12 F and I**). Even more interestingly, the percentage of double Satb2/Ctip2 co-expressing neurons drastically decreases in layers V (1.9 fold decrease) and VI (8 fold decrease) of *LMO4* mutants (**Figure 12 F'' and K**). Furthermore, although the total population of Satb2/Ctip2-positive cells showed a 3.5-fold decrease, Satb2 expression did not increase and even slightly decreased in some bins of *LMO4 CKO* cortices (**Figure 12 F' and J**). This confirms that the lack of Satb2/Ctip2-positive cells in mutant cortices is due to a higher repression of Ctip2 in Satb2 positive cells rather than to a mis-specification of subcerebral Ctip2-positive PNs.

However, despite the absence of LMO4 (in *LMO4 CKO*), the number of Satb2/Ctip2 co-expressing neurons shows only 1.9 fold decrease in layer V (**Figure 12 F'' and K**). This implies, as previously mentioned, the presence of a complementary mechanism, which is independent from LMO4 and also required in specifying the Satb2/Ctip2 co-expressing population. Given this relatively high remaining percentage of Satb2/Ctip2 co-expressing neurons in *LMO4* mutants, it would be interesting to verify whether *Fezf2* and *Ski* expression levels, which may underlie complementary mechanisms, are changed.

In contrast to layer V, layer VI Satb2/Ctip2 co-expressing neurons were absent in P0 wt cortices, whereas at P7 they were around around  $8.2 \pm 2.5\%$  of the total layer VI neuronal population (**Figure 6**). Only  $1 \pm 0.3\%$  of layer VI neurons Satb2/Ctip2-

positive remained in layer VI of *LMO4* mutants (**Figure 12 F'' and K**), suggesting that the complementary mechanism favoring *Satb2/Ctip2* co-expression in layer V is less active in layer VI. Therefore, I propose that the specification of layer VI *Satb2/Ctip2* co-expressing neurons, which appear at P7 together with the increase in *LMO4* expression, is primarily dependent on *LMO4*.

## 2. **Downregulation of *LMO4* is sufficient to reduce the expansion of *Ctip2* expression in layer V of COUP-TFI mutant S1 cortices.**

Absence of COUP-TFI induces a clear radial expansion of *Ctip2*-positive neurons in layer V of S1, which reproduces the distribution of subcerebral projection neurons observed in motor/frontal areas [134]. My study strikingly showed that downregulating *LMO4* expression by *in utero* electroporating an *shRNA* construct against *LMO4*, strongly decreases *Ctip2* expression in the mS1 area of *COUP-TFI CKO* cortices (**Figure 15 A, C and D**), whereas *Satb2* expression remains unchanged (**Figure 15 D'' and F''**). Interestingly, *Ctip2* expression is completely down-regulated in layer Va. Since not all *Ctip2* positive cells are also *Satb2* positive, *Ctip2* is ablated from *Satb2* positive and negative cells. These data indicate that *LMO4* not only de-represses *Ctip2*, but also promotes its expression by other mechanisms.

Moreover, *Ctip2* expression disappears from layer VI of COUP-TFI mutants after, even if layer VI neurons do not express the *LMO4 shRNA* electroporated at E13.5. Two hypotheses could explain this observation. First, *LMO4* could regulate *Ctip2* expression by “extrinsic” mechanisms, through regulation of diffusible signaling molecules (as it was shown for *Sip1* [358]), negatively regulating *Ctip2* expression in layer VI. Another plausible explanation involves impairment in neuronal migration. A defect in migration was previously reported in COUP-TFI mutant cortices [341]. Thus *Ctip2* positive cells in layer VIa could represent a delayed migration of a layer V neuronal population (**Figure 15 E**). Accordingly, electroporation of scrambled construct shows a defective migration of *Ctip2* positive cells, which are spread along the radial extent of the cortex (**Figure 15 E'**). *LMO4 shRNA* unexpectedly rescues the migration of delayed cells, and simultaneously down-regulates *Ctip2* expression in these cells (**Figure 15 C-C''**). This hypothesis seems plausible since *LMO4* has been reported to facilitate *Ngn2* mediated radial migration [326]. Interestingly, it was

shown that migratory defects observed in COUP-TFI mutants depend on dysregulation of Rnd2, which is a downstream target of Ngn2 during radial neuronal migration.

### 3. **LMO4 overexpression anticipates the birth of Satb2/Ctip2 co-expressing neurons.**

Complementary to the previous approach, *in utero* electroporation of a post-mitotic expressing *LMO4* construct in E13.5 *wt* brains, strongly up-regulated *LMO4* expression in the S1 of P0 brains, where normally *LMO4* is weakly expressed. As previously mentioned electroporation of a control GFP-expressing plasmid failed to target Ctip2-expressing neurons, indicating a probable earlier birthdate of Ctip2- and Satb2/Ctip2-positive cells. However, a remarkable percentage of the GFP-positive cells were Satb2 positive (**Figure 13 G-I''**). Thus, absence of GFP positive neurons expressing Ctip2 (alone or with Satb2) at P7 in control electroporated cells implies that these cells might be born earlier than E13.5. This apparent discrepancy compared to previous birthdating analyses [15] might be explained by technical limits inherent to the electroporation method. Indeed, ventricle-injected DNA can be electroporated only in progenitors surrounding the ventricular surface (apical progenitors), while BrdU molecules can label both apical and intermediate progenitors. These data suggest, interestingly, that at E13.5 apical progenitors do not produce anymore Ctip2 positive cells, while intermediate progenitors continue to amplify this neuronal population. Moreover, this unexpected result confirmed that *Lmo4* acts by de-repression of Ctip2 expression in Satb2 expressing cells.

*Lmo4* overexpression, indeed, induced Satb2/Ctip2 co-expression in a population of cells that in control electroporations expressed solely Satb2 (**Figure 13 D-F''**). This seems very plausible, since Satb2/Ctip2 co-expressing neurons are a population that increases over time, together with the increase in *LMO4* expression. My data show that the percentage of Satb2/Ctip2 co-expressing neurons increases from  $4 \pm 0.3\%$  at P0 to  $8.1 \pm 1.9\%$  at P7 in layer V neurons, and from  $0.35 \pm 0.01\%$  at P0 to  $8.2 \pm 2.5\%$  at P7 in layer VI neurons (**Figure 6**). The number of double Satb2/Ctip2-expressing neurons increases even more after P7, a stage where normally cortical neurons are fully committed, suggesting late specification of this cell population. Thus, *LMO4* overexpression at E13.5 leads to an anticipated specification of Satb2/Ctip2 co-expressing neurons among the Satb2-positive cell population,

similarly to what observed in *COUP-TFI* mutant P0 cortices. Thus, LMO4 overexpression at E13.5 in already born *Satb2*-positive cells (as shown in electroporated control cells) most probably de-represses *Ctip2* in these cells and gives rise to *Satb2/Ctip2* co-expressing neurons at an earlier developmental stage.

## **V. Two distinct cell populations differing in their axonal projection, molecular code, morphological and electrophysiological properties**

Since the double *Satb2/Ctip2*-expressing population was not characterized so far, we decided to further investigate its properties in terms of connectivity, molecular code, morphology and electrophysiology. Our comprehensive studies, which included connectivity, electrophysiological, molecular and preliminary morphological analyses, brought to similar conclusions: *Satb2/Ctip2* co-expressing cells do not constitute a temporary population of neurons with hybrid callosal/subcerebral features and can be subdivided at least in two distinct sub-populations. One major sub-population with subcerebral characteristics, projecting to the pons and mainly expressing *Bhlhb5* and *Sox5* in addition to LMO4 and another minor sub-population, mainly expressing LMO4 and *Er81*, but not *Bhlhb5* and *Sox5*, and projecting across the corpus callosum to the contralateral hemisphere.

### **A. Molecular Characterization**

The analysis of regulatory genes expressed in layer V PNs (i.e. LMO4, *Bhlhb5*, *Sox5* and *Er81*), based on subtype specific expression patterns and functional roles, allowed me to subdivide *Satb2/Ctip2*-positive cells into two sub-populations. *Bhlhb5* is strongly expressed in CSMN of sensorimotor cortex and corticotectal PN of the occipital cortex [144]. LMO4 is highly expressed in CBMN in layer Va of the motor cortex, in CPN, in backward projection neurons and in dual callosal or subcerebral/backward projection neurons, however, it is completely excluded from CSMNs [145]. The transcription factor *Sox5* is expressed by the major classes of CFuPNs (subplate, corticothalamic and all subcerebral subtypes) but not by corticocortical CPNs, and it controls the sequential generation of these subtypes by its

own progressive downregulation [166, 217]. Finally the transcription factor Er81 is expressed throughout layer V in both CPNs and SCPNs in the rat cortex [348].

Thus, since Satb2/Ctip2 neurons expressed all these subtype-specific genes with different percentages, I divided this cell population into two major sub-populations: one with subcerebral characteristics expressing Sox5 and Bhlhb5, which are known to be involved in corticofugal and CSMN respectively, and the other with callosal properties and expressing LMO4 and Er81, but not Bhlhb5 and Sox5 (**Figure 16**), and which seems to be less represented than the subcerebral one.

My molecular analysis on retrogradely-labeled callosal and subcerebral PNs revealed that LMO4, which is expressed in almost all Satb2/Ctip2 co-expressing neurons, is expressed by both CPNs and SCPNs, whereas Er81 is expressed only by layer V callosal neurons. Differently, Sox5 and Bhlhb5 are expressed only by SCPN, and excluded from layer V callosal neurons. In summary, combining retrograde labeling with molecular analysis, my data revealed that Satb2/Ctip2 co-expressing neurons can be classified into two major cell sub-populations, a callosal sub-population expressing LMO4 and Er81 and another subcerebral sub-population expressing Sox5, Bhlhb5 and LMO4 (**Figures 19 and 20**).

## **B. Connectivity**

My data demonstrate that Satb2 and Ctip2 co-expression does not give rise to one hybrid cell population projecting both intracortically and subcerebrally, but rather to two distinct sub-populations projecting either to the contralateral cortex (CPN) or to the brainstem (cortico-brainstem PNs, CBPN) (**Figure 17**). My analyses on retrogradely labeled brains showed that cortico-spinal motor neurons (CSMN) express Bhlhb5 but not LMO4 as previously described [145]. In contrast, cells labeled by CTB injection in the rostral pontine region can be either LMO4 or double LMO4/Bhlhb5 positive. This is not surprising since injection of the tracer in this brainstem region will label not only CBPNs but also CSMNs whose axons are *en route* to the spinal cord. However, two points should be discussed in this issue. First, it has been previously shown that LMO4 and Bhlhb5 have a complementary expression pattern [145], however it is important to note that my data revealed that LMO4 and Bhlhb5 also co-localize in a remarkable percentage of layer V neurons,

including *Satb2/Ctip2* positive cortico-brainstem neurons (**Figure 18**). Second, *Bhlhb5* confers cortico-spinal identity [144], whereas in the absence of LMO4 function, SCPN in layer Va of the rostral motor cortex project to the spinal cord instead of the brainstem [145]. Thus, present data support previous evidence and suggest a scenario in which LMO4 determines cortico-brainstem fate in the somatosensory cortex by either limiting SCPN axonal pathfinding to the brainstem or favoring the pruning of aspecific connectivity to the spinal cord.

Moreover, layer V PNs can also send their axons and/or collaterals to the striatum [204]. Corticostriatal PNs can be of intratelencephalic (IT) type sending their axons to the contralateral striatum, or pyramidal tract (PT) type sending their axons to the ipsilateral striatum. However, corticostriatal PNs can be either IT or PT but never both [204]. Thus, it is not plausible that *Satb2/Ctip2* co-expressing neurons, even though they co-express callosal and subcerebral specific genes, project to both targets. Whether they do also project to the striatum is still under investigation in the lab.

The choice of *Satb2/Ctip2* co-expressing neurons to send axonal projections to the brainstem or to the corpus callosum depends probably on the expression of other neuronal identity modulators. The expression of *Er81* versus *Sox5* and *Bhlhb5* could be a potential molecular mechanism, since *Er81* expression seems to be exclusive to CPN sub-population of *Satb2/Ctip2* co-expressing neurons in the S1, while *Sox5* and *Bhlhb5* expression are confined to the cortico-brainstem sub-population of *Satb2/Ctip2*-positive cells. Other downstream targets of *Satb2* and *Ctip2* could be also involved, particularly axon guidance molecules. *Unc5C* and *DCC* are downstream effectors of *Satb2* and *Ctip2* in the choice of callosal versus subcerebral fate in lower layer neurons [260]. *Unc5C* and *DCC* are negatively regulated by *Satb2* and *Ctip2*, respectively. High levels of *Unc5C* and low levels of *DCC* are required to project axons to the corpus callosum. In contrast, high levels of *DCC* and low levels of *Unc5C* are required to project axons sub-cerebrally [260]. Thus, in *Satb2/Ctip2* co-expressing neurons the expression of a third transcription regulator, *Er81* or *Bhlhb5/Sox5*, would probably be a key event to ultimately decide which axon molecule is predominantly expressed. I plan in the future to assess the expression of *DCC*, *Unc5C* and other guidance molecules in double *Satb2/Ctip2*-expressing neurons.

LMO4 establishes subtypes projection neurons diversity within the rostral motor cortex. In the absence of LMO4 function, the molecular identity of subcerebral and callosal projection neurons in the rostral motor cortex is affected and projection

neurons lose their specific connectivity [145]. My molecular analysis shows that LMO4 is expressed in almost all *Satb2/Ctip2* co-expressing neurons at P7. Moreover, immunostaining on retrogradely-labeled callosal and subcerebral projection neurons revealed the presence of LMO4 in both of them. Thus, it seems plausible that, rather than directly contribute to the subdivision of *Satb2/Ctip2*-positive cells, *Lmo4* performs two important tasks: it promotes layer V CPN and CBPN identity at the expenses of CSMN identity, and creates the right conditions for the expression of other regulators (such as *Er81*, *Sox5*, and *Bhlhb5*), which likely contribute to the specification of *Satb2/Ctip2* sub-types.

Overall, these data indicate that LMO4, in cooperation with other transcriptional regulators, segregates *Satb2/Ctip2* positive neurons into two distinct sub-populations, which might regulate axon guidance molecules to direct their axonal projections toward the corpus callosum or the brainstem.

### C. Electrophysiology

Physiologically, two major classes of pyramidal neurons, based on differences in their intrinsic firing properties, have been described in layer V: intrinsically bursting neurons that fire bursts of action potentials in response to depolarizing current injection, and regular spiking cells that fire trains of single action potentials [359, 360]. However, analyses of additional parameters, including spike frequency adaptation and afterpolarizations [361-364], have revealed a rich diversity of layer V pyramidal cells.

Previous findings have shown that layer V neurons in the somatosensory cortex projecting to different targets, have distinct physiological properties. Intrinsic membrane and firing properties of cortico-thalamic and cortico-trigeminal neurons differ from those of callosal and cortico-striatal neurons [347]. Similarly, cortico-brainstem and cortico-spinal projection neurons can be distinguished by their specific physiological properties [365-367], indicating that cortical neurons with different subcortical targets are electrically distinct from each other.

Our electrophysiological studies suggest that the *Satb2/Ctip2 type 2* cells are most likely the callosal sub-population of *Satb2/Ctip2* co-expressing neurons (**Figure 24**). This sub-population has very different firing and membrane properties, most importantly a much larger adaptation, compared to the other three subpopulations: the

double *Satb2/Ctip2 type 1* cells, and two other two populations expressing only *Ctip2* (single *Ctip2 type 1*, and single *Ctip2 type 2*). These latter two populations show higher similarities and, since my analysis showed no single *Ctip2*-positive cells projecting to the corpus callosum, they may all be constituted by SCPN. Thus, the *Satb2/Ctip2 type 1* neurons, which show similar electrical features, could correspond to the sub-cerebral projecting sub-population of *Satb2/Ctip2*-positive cells. Nonetheless, physiological differences exist also among these 3 sub-populations (**Figure 24**), which is very plausible since they project to different targets. To ultimately confirm the identity of these four cell populations and distinguish the callosal from the subcerebral sub-population *Satb2/Ctip2*-positive cells, I will use the molecular factors described above.

The differences in intrinsic firing properties observed in distinct subtypes of cortical projection neurons may reflect differences in the readout of cortical activity that they transmit to their targets. Cortical excitatory neurons provide massive recurrent excitation onto other excitatory neurons, therefore amplifying their feedforward signals [368, 369]. In addition to inputs from inhibitory neurons, strong spike frequency adaptation of cortical excitatory neurons, including callosal neurons, may be essential for stabilizing the network and preventing runaway excitation. Instead, little spike frequency adaptation observed in subcerebral projection neurons, which is also a hallmark of cortico-spinal neurons, have been suggested to be important for maintaining rhythmic firing in these cells [370, 371], which is required for such long-range targets (brainstem and spinal cord).

#### **D. Morphology**

Layer V pyramidal neuron populations projecting to different targets show distinct morphological features. Differences in the length and thickness of the apical dendrite, the laminar position of their bifurcation points, and width of apical tuft were found between callosal, cortico-thalamic, cortico-trigeminal and cortico-striatal layer V neurons in the somatosensory cortex [347], indicating that morphological differences most probably have an effect on the function of a neuron. Interestingly, morphology and electrophysiological properties are very tightly linked parameters. For instance, intrinsically bursting cells have thick apical dendrites, whereas regular spiking cells

have thinner apical dendrites [372]. Moreover, membrane capacitance of a neuron is proportional to its soma area and architecture [373].

My analysis associates morphological and electrophysiological differences of layer V neurons to their molecular code, which is a very novel and relevant analysis that will further help understanding PNs diversity within the cerebral cortex. Our morphological data, although preliminary, showed differences in soma shape between Satb2/Ctip2 co-expressing neurons, and single Ctip2 or Satb2 positive neurons, including soma area and distribution of secondary dendrites, angles between the secondary dendrites, and sphericity of the soma (**Figures 21 and 22**). Moreover, we found some clear differences in apical dendrite morphology (**Figure 23**) between different populations and sub-populations of neurons within each molecular code, including apical dendrite bifurcation point, thickness, length, and apical tuft. All these data are in phase of elaboration by Morpheme mathematicians, which are creating algorithms to allow automatic detection of morphological differences and correlate them with the observed molecular code. Preliminary analysis subdivided Satb2/Ctip2 co-expressing neurons into two main populations further confirming data obtained from retrograde labeling, molecular markers and electrophysiological analyses.

These morphological traits will help in revealing differences in the electrophysiological activity and function of these neurons: associating these morphological differences with retrograde labeling, analysis of molecular markers and biocytin reconstructions will further help in grouping the characteristics of these two sub-populations of Satb2/Ctip2 co-expressing neurons.

## *Chapter V- Conclusion*

---

In conclusion, this work has characterized a previously unknown cell population, co-expressing mutually exclusive callosal versus subcerebral transcriptional regulators, and analysed its molecular, hodological, morphological and electrophysiological properties. Importantly, my study demonstrates that the co-expression of callosal and subcerebral neuronal markers does not only characterize early phases of neuronal specification, as previously described, but also defines distinct mature neuronal subpopulations with different areal-specific features and developmental timing in the mammalian neocortex.

Satb2/Ctip2 co-expressing neurons have a precise regional and temporal distribution in layer V and VI of the somatosensory and motor cortex. At postnatal day 0 (P0), these neurons are just a minor population in the somatosensory cortex, while they are highly represented in the motor cortex. From P0 onwards, Satb2/Ctip2 co-expressing neurons progressively increase in the somatosensory cortex together with the increase of LMO4, a transcriptional regulator that I demonstrated to be strongly involved in the specification of this cell population.

Satb2 inhibits Ctip2 by recruiting the chromatin remodeling NuRD complex to Ctip2 locus and, thus, allowing HDAC1 to deacetylate nearby histones and turn the chromatin to an inactive state. My data demonstrate that LMO4 is a main actor in the development of Satb2/Ctip2 co-expressing neurons and acts by de-repressing Ctip2 expression in Satb2-positive neurons. LMO4 binds and sequesters HDAC1 and Ski, another member of the NuRD complex, perturbing the assembly of this machinery on the Ctip2 locus.

Beside the biochemical approach, I have been able to confirm the key role of LMO4 in specifying layer V Satb2/Ctip2 co-expressing neurons *in vivo* by manipulating LMO4 expression levels starting from E13.5 old embryos. While downregulation of LMO4 diminishes the number of double Satb2/Ctip2-positive neurons in somatosensory cortex, overexpression of LMO4 derepresses Ctip2 expression in Satb2-positive cells, which normally do not co-express these two factors. In addition, in LMO4 mutant mice, both the percentage of Ctip2 and that of Satb2/Ctip2 co-expressing neurons are decreased, and conversely in COUP-TFI mutant cortices, in which LMO4 is prematurely expressed in S1, the specification of Satb2/Ctip2 co-expressing neurons is anticipated and their number is increased.

Since these double Satb2/Ctip2 co-expressing neurons were not described so far, I used several complementary approaches, including double and triple

immunostaining with a battery of molecular markers specific to different layer V PN populations, retrograde labeling combined with molecular marker analysis, and morphological and electrophysiological analyses to characterize their cellular and molecular properties. My data clearly show that this “hybrid” population co-expressing *Satb2* and *Ctip2* gives rise to two distinct PN sub-populations. One population with callosal properties, projecting through the corpus callosum to the contralateral hemisphere and expressing *LMO4* and *Er81*, and the other with subcerebral properties, projecting to the brainstem and expressing *LMO4*, *Sox5* and *Bhlhb5*.

Finally, electrophysiological and morphological analyses confirmed the existence of two sub-populations of *Satb2/Ctip2* co-expressing neurons with different membrane and firing properties, and distinct morphologies, including differences in soma shape, distribution of secondary dendrites and apical dendrite characteristics.

## *Future Perspectives*

---

## **I. To combine the morphological and electrophysiological properties with molecular markers characterizing the two sub-populations of Satb2/Ctip2 co-expressing neurons**

To finalize the characterization of the double Satb2/Ctip2 co-expressing neurons I first need to combine the use of molecular markers that allow me to distinguish the callosal sub-population from the subcerebral one, with the morphological and electrophysiological data. In particular, I need to apply the automatized morphometric algorithm, as soon as it will be available, to subdivide the different morphologies identified among YFP-positive layer V neurons and biocytin-injected recorded neurons in specific classes. Then, I will cross these data with molecular and hodological ones to identify the different sub-types of Satb2/Ctip2 co-expressing neurons present in layer V of the S1.

In addition, applying retrograde labeling on the Thy1-YFP brains, which we have used for the morphological and electrophysiological studies, could be useful to properly integrate our multidisciplinary approach and couple the two different sub-populations with their specific morphologies and electrophysiological properties. In this way, I could repeat the immunostaining of the different molecular markers (LMO4, Bhlhb5, Er81 and Sox5) on YFP brains and directly correlate the morphologically different two sub-populations of Satb2/Ctip2 co-expressing neurons to their specific molecular code.

## **II. To directly investigate the role of LMO4 on the subtype diversity and axonal projections of cortico-brainstem projection neurons**

By retrograde labeling *LMO4 CKO* brains, or alternatively, *LMO4 shRNA in utero* electroporated brains, I could evaluate whether LMO4 ablation would affect the connectivity of the 2 identified sub-populations of Satb2/Ctip2 co-expressing neurons.

Similarly, retrograde labeling experiments on LMO4 GFP-overexpressing brains, or brains electroporated with *LMO4 shRNA*, or GFP-electroporated *LMO4 CKO* brains at E13.5 would be required to evaluate whether LMO4 really limits axonal projection at the level of the pons. Alternatively, electroporation of a GFP-

expressing construct in different cortical regions of the gain-and loss-of-function models would help to follow the trajectories of GFP-positive axon and identify final targets of the two major subclasses of Satb2/Ctip2 co-expressing neurons.

Finally, further chromatin immunoprecipitation and co-immunoprecipitation experiments on nuclear and cytoplasmic targets would be required in order to better understand the whole molecular mechanism of Ctip2 de-repression driven by LMO4.

### **III. Further molecular and functional characterization of Satb2/Ctip2 co-expressing neurons**

FACS sorting of Satb2/Ctip2 co-expressing neurons, and RNA extraction from sorted cells would help to identify specific genes highly expressed by the Satb2/Ctip2-positive cells. This may help in identifying the axon guidance molecules and understanding how they direct the two pathways, callosal versus subcerebral, of the two main sub-populations of Satb2/Ctip2 co-expressing neurons. This would be an interesting additional step in our understanding of how different cortical neuron subpopulations reach their final targets during corticogenesis. Moreover, RNAseq on sorted cells could help to discover new important markers of layer V neurons, which could help in the classification of this neuronal population.

More functional and electrophysiological characterization of the Satb2/Ctip2 co-expressing neurons would be required to understand how this cell population accounts for the overall behaviour and the organization of functional circuits in the mammalian brain. Creating mutant mice with a substantial loss or an over-production of Satb2/Ctip2 positive cells would be an interesting and indispensable approach to this aim. Indeed, although LMO4 and COUP-TFI mutants show, respectively, a decrease and a strong increase in the number of Satb2/Ctip2-positive cells, their phenotypes involve many different neuronal subtypes impeding a clear functional or behavioural analysis. On the contrary, the intersectional approach would be a powerful instrument, in future, to ablate Satb2 and Ctip2 expression only in cells co-expressing these genes and to analyse the impact of their impaired specification on mice behaviour.

# References

---

1. Rubenstein, J.L., et al., *Regionalization of the prosencephalic neural plate*. Annu Rev Neurosci, 1998. **21**: p. 445-77.
2. Aboitiz, F., *Genetic and developmental homology in amniote brains. Toward conciliating radical views of brain evolution*. Brain Res Bull, 2011. **84**(2): p. 125-36.
3. Aboitiz, F., D. Morales, and J. Montiel, *The evolutionary origin of the mammalian isocortex: towards an integrated developmental and functional approach*. Behav Brain Sci, 2003. **26**(5): p. 535-52; discussion 552-85.
4. Super, H. and H.B. Uylings, *The early differentiation of the neocortex: a hypothesis on neocortical evolution*. Cereb Cortex, 2001. **11**(12): p. 1101-9.
5. Krubitzer, L. and J. Kaas, *The evolution of the neocortex in mammals: how is phenotypic diversity generated?* Curr Opin Neurobiol, 2005. **15**(4): p. 444-53.
6. Kaas, J.H., *Neocortex in early mammals and its subsequent variations*. Ann N Y Acad Sci, 2011. **1225**: p. 28-36.
7. Puelles, L., *Pallio-pallial tangential migrations and growth signaling: new scenario for cortical evolution?* Brain Behav Evol, 2011. **78**(1): p. 108-27.
8. Alfano, C. and M. Studer, *Neocortical arealization: evolution, mechanisms, and open questions*. Dev Neurobiol, 2013. **73**(6): p. 411-47.
9. O'Leary, D.D. and Y. Nakagawa, *Patterning centers, regulatory genes and extrinsic mechanisms controlling arealization of the neocortex*. Curr Opin Neurobiol, 2002. **12**(1): p. 14-25.
10. Rash, B.G. and E.A. Grove, *Area and layer patterning in the developing cerebral cortex*. Curr Opin Neurobiol, 2006. **16**(1): p. 25-34.
11. Sur, M. and J.L. Rubenstein, *Patterning and plasticity of the cerebral cortex*. Science, 2005. **310**(5749): p. 805-10.
12. Geng, X. and G. Oliver, *Pathogenesis of holoprosencephaly*. J Clin Invest, 2009. **119**(6): p. 1403-13.
13. O'Leary, D.D., S.J. Chou, and S. Sahara, *Area patterning of the mammalian cortex*. Neuron, 2007. **56**(2): p. 252-69.
14. Rakic, P., *Neuronal migration and contact guidance in the primate telencephalon*. Postgrad Med J, 1978. **54 Suppl 1**: p. 25-40.
15. Molyneaux, B.J., et al., *Neuronal subtype specification in the cerebral cortex*. Nat Rev Neurosci, 2007. **8**(6): p. 427-37.
16. Molnar, Z., et al., *Mechanisms controlling the guidance of thalamocortical axons through the embryonic forebrain*. Eur J Neurosci, 2012. **35**(10): p. 1573-85.
17. Clasca, F., P. Rubio-Garrido, and D. Jabaudon, *Unveiling the diversity of thalamocortical neuron subtypes*. Eur J Neurosci, 2012. **35**(10): p. 1524-32.
18. Grant, E., A. Hoerder-Suabedissen, and Z. Molnar, *Development of the corticothalamic projections*. Front Neurosci, 2012. **6**: p. 53.

19. Strick, P.L. and P. Sterling, *Synaptic termination of afferents from the ventrolateral nucleus of the thalamus in the cat motor cortex. A light and electron microscopy study.* J Comp Neurol, 1974. **153**(1): p. 77-106.
20. Jones, E.G., *Lamination and differential distribution of thalamic afferents within the sensory-motor cortex of the squirrel monkey.* J Comp Neurol, 1975. **160**(2): p. 167-203.
21. Donoghue, J.P. and S.P. Wise, *The motor cortex of the rat: cytoarchitecture and microstimulation mapping.* J Comp Neurol, 1982. **212**(1): p. 76-88.
22. Tan, X. and S.H. Shi, *Neocortical neurogenesis and neuronal migration.* Wiley Interdiscip Rev Dev Biol, 2013. **2**(4): p. 443-59.
23. Halassa, M.M. and P.G. Haydon, *Integrated brain circuits: astrocytic networks modulate neuronal activity and behavior.* Annu Rev Physiol, 2010. **72**: p. 335-55.
24. Perea, G., M. Navarrete, and A. Araque, *Tripartite synapses: astrocytes process and control synaptic information.* Trends Neurosci, 2009. **32**(8): p. 421-31.
25. Lin, S.C. and D.E. Bergles, *Synaptic signaling between GABAergic interneurons and oligodendrocyte precursor cells in the hippocampus.* Nat Neurosci, 2004. **7**(1): p. 24-32.
26. Lopez-Bendito, G. and Z. Molnar, *Thalamocortical development: how are we going to get there?* Nat Rev Neurosci, 2003. **4**(4): p. 276-89.
27. Haubensak, W., et al., *Neurons arise in the basal neuroepithelium of the early mammalian telencephalon: a major site of neurogenesis.* Proc Natl Acad Sci U S A, 2004. **101**(9): p. 3196-201.
28. Williams, B.P. and J. Price, *Evidence for multiple precursor cell types in the embryonic rat cerebral cortex.* Neuron, 1995. **14**(6): p. 1181-8.
29. Bentivoglio, M. and P. Mazzarello, *The history of radial glia.* Brain Res Bull, 1999. **49**(5): p. 305-15.
30. Cameron, R.S. and P. Rakic, *Glial cell lineage in the cerebral cortex: a review and synthesis.* Glia, 1991. **4**(2): p. 124-37.
31. Noctor, S.C., et al., *Neurons derived from radial glial cells establish radial units in neocortex.* Nature, 2001. **409**(6821): p. 714-20.
32. Miyata, T., et al., *Asymmetric inheritance of radial glial fibers by cortical neurons.* Neuron, 2001. **31**(5): p. 727-41.
33. Wang, X., et al., *A new subtype of progenitor cell in the mouse embryonic neocortex.* Nat Neurosci, 2011. **14**(5): p. 555-61.
34. Reillo, I. and V. Borrell, *Germinal zones in the developing cerebral cortex of ferret: ontogeny, cell cycle kinetics, and diversity of progenitors.* Cereb Cortex, 2012. **22**(9): p. 2039-54.
35. Fietz, S.A., et al., *OSVZ progenitors of human and ferret neocortex are epithelial-like and expand by integrin signaling.* Nat Neurosci, 2010. **13**(6): p. 690-9.
36. Noctor, S.C., et al., *Cortical neurons arise in symmetric and asymmetric division zones and migrate through specific phases.* Nat Neurosci, 2004. **7**(2): p. 136-44.
37. Wu, S.X., et al., *Pyramidal neurons of upper cortical layers generated by NEX-positive progenitor cells in the subventricular zone.* Proc Natl Acad Sci U S A, 2005. **102**(47): p. 17172-7.

38. Kowalczyk, T., et al., *Intermediate neuronal progenitors (basal progenitors) produce pyramidal-projection neurons for all layers of cerebral cortex*. Cereb Cortex, 2009. **19**(10): p. 2439-50.
39. Greig, L.C., et al., *Molecular logic of neocortical projection neuron specification, development and diversity*. Nat Rev Neurosci, 2013. **14**(11): p. 755-69.
40. Martinez-Cerdeno, V., S.C. Noctor, and A.R. Kriegstein, *The role of intermediate progenitor cells in the evolutionary expansion of the cerebral cortex*. Cereb Cortex, 2006. **16 Suppl 1**: p. i152-61.
41. Hansen, D.V., et al., *Neurogenic radial glia in the outer subventricular zone of human neocortex*. Nature, 2010. **464**(7288): p. 554-561.
42. Kelava, I., et al., *Abundant occurrence of basal radial glia in the subventricular zone of embryonic neocortex of a lissencephalic primate, the common marmoset *Callithrix jacchus**. Cereb Cortex, 2012. **22**(2): p. 469-81.
43. Shitamukai, A., D. Konno, and F. Matsuzaki, *Oblique radial glial divisions in the developing mouse neocortex induce self-renewing progenitors outside the germinal zone that resemble primate outer subventricular zone progenitors*. J Neurosci, 2011. **31**(10): p. 3683-95.
44. Gal, J.S., et al., *Molecular and morphological heterogeneity of neural precursors in the mouse neocortical proliferative zones*. J Neurosci, 2006. **26**(3): p. 1045-56.
45. Stancik, E.K., et al., *Heterogeneity in ventricular zone neural precursors contributes to neuronal fate diversity in the postnatal neocortex*. J Neurosci, 2010. **30**(20): p. 7028-36.
46. Marin-Padilla, M., *Dual origin of the mammalian neocortex and evolution of the cortical plate*. Anat Embryol (Berl), 1978. **152**(2): p. 109-26.
47. Raedler, E. and A. Raedler, *Autoradiographic study of early neurogenesis in rat neocortex*. Anat Embryol (Berl), 1978. **154**(3): p. 267-84.
48. Luskin, M.B. and C.J. Shatz, *Studies of the earliest generated cells of the cat's visual cortex: cogeneration of subplate and marginal zones*. J Neurosci, 1985. **5**(4): p. 1062-75.
49. Rakic, P., *Neurons in rhesus monkey visual cortex: systematic relation between time of origin and eventual disposition*. Science, 1974. **183**(4123): p. 425-7.
50. Miyata, T., et al., *Asymmetric production of surface-dividing and non-surface-dividing cortical progenitor cells*. Development, 2004. **131**(13): p. 3133-45.
51. Nadarajah, B., et al., *Ventricle-directed migration in the developing cerebral cortex*. Nat Neurosci, 2002. **5**(3): p. 218-24.
52. Nadarajah, B., et al., *Two modes of radial migration in early development of the cerebral cortex*. Nat Neurosci, 2001. **4**(2): p. 143-50.
53. LoTurco, J.J. and J. Bai, *The multipolar stage and disruptions in neuronal migration*. Trends Neurosci, 2006. **29**(7): p. 407-13.
54. Tabata, H. and K. Nakajima, *Multipolar migration: the third mode of radial neuronal migration in the developing cerebral cortex*. J Neurosci, 2003. **23**(31): p. 9996-10001.
55. Rakic, P., *Mode of cell migration to the superficial layers of fetal monkey neocortex*. J Comp Neurol, 1972. **145**(1): p. 61-83.

56. McConnell, S.K., *Fates of visual cortical neurons in the ferret after isochronic and heterochronic transplantation*. J Neurosci, 1988. **8**(3): p. 945-74.
57. McConnell, S.K. and C.E. Kaznowski, *Cell cycle dependence of laminar determination in developing neocortex*. Science, 1991. **254**(5029): p. 282-5.
58. Frantz, G.D. and S.K. McConnell, *Restriction of late cerebral cortical progenitors to an upper-layer fate*. Neuron, 1996. **17**(1): p. 55-61.
59. Luskin, M.B., A.L. Pearlman, and J.R. Sanes, *Cell lineage in the cerebral cortex of the mouse studied in vivo and in vitro with a recombinant retrovirus*. Neuron, 1988. **1**(8): p. 635-47.
60. Walsh, C. and C.L. Cepko, *Clonally related cortical cells show several migration patterns*. Science, 1988. **241**(4871): p. 1342-5.
61. Price, J. and L. Thurlow, *Cell lineage in the rat cerebral cortex: a study using retroviral-mediated gene transfer*. Development, 1988. **104**(3): p. 473-82.
62. Reid, C.B., I. Liang, and C. Walsh, *Systematic widespread clonal organization in cerebral cortex*. Neuron, 1995. **15**(2): p. 299-310.
63. Inoue, K., et al., *Fez1 is layer-specifically expressed in the adult mouse neocortex*. Eur J Neurosci, 2004. **20**(11): p. 2909-16.
64. Hirata, T., et al., *Zinc finger gene fez-like functions in the formation of subplate neurons and thalamocortical axons*. Dev Dyn, 2004. **230**(3): p. 546-56.
65. Molyneaux, B.J., et al., *Fez1 is required for the birth and specification of corticospinal motor neurons*. Neuron, 2005. **47**(6): p. 817-31.
66. Arlotta, P., et al., *Neuronal subtype-specific genes that control corticospinal motor neuron development in vivo*. Neuron, 2005. **45**(2): p. 207-21.
67. Chen, J.G., et al., *Zfp312 is required for subcortical axonal projections and dendritic morphology of deep-layer pyramidal neurons of the cerebral cortex*. Proc Natl Acad Sci U S A, 2005. **102**(49): p. 17792-7.
68. Nieto, M., et al., *Expression of Cux-1 and Cux-2 in the subventricular zone and upper layers II-IV of the cerebral cortex*. J Comp Neurol, 2004. **479**(2): p. 168-80.
69. Zimmer, C., et al., *Dynamics of Cux2 expression suggests that an early pool of SVZ precursors is fated to become upper cortical layer neurons*. Cereb Cortex, 2004. **14**(12): p. 1408-20.
70. Molyneaux, B.J., et al., *Novel subtype-specific genes identify distinct subpopulations of callosal projection neurons*. J Neurosci, 2009. **29**(39): p. 12343-54.
71. Franco, S.J., et al., *Fate-restricted neural progenitors in the mammalian cerebral cortex*. Science, 2012. **337**(6095): p. 746-9.
72. Guo, C., et al., *Fezf2 expression identifies a multipotent progenitor for neocortical projection neurons, astrocytes, and oligodendrocytes*. Neuron, 2013. **80**(5): p. 1167-74.
73. Li, J. and E.S. Anton, *Rnd-ing up RhoA activity to link neurogenesis with steps in neuronal migration*. Dev Cell, 2011. **20**(4): p. 409-10.
74. O'Leary, D.D. and S. Sahara, *Genetic regulation of arealization of the neocortex*. Curr Opin Neurobiol, 2008. **18**(1): p. 90-100.

75. Van der Loos, H. and T.A. Woolsey, *Somatosensory cortex: structural alterations following early injury to sense organs*. *Science*, 1973. **179**(4071): p. 395-8.
76. O'Leary, D.D., *Do cortical areas emerge from a protocortex?* *Trends Neurosci*, 1989. **12**(10): p. 400-6.
77. Rakic, P., *Specification of cerebral cortical areas*. *Science*, 1988. **241**(4862): p. 170-6.
78. Maruoka, Y., et al., *Comparison of the expression of three highly related genes, Fgf8, Fgf17 and Fgf18, in the mouse embryo*. *Mech Dev*, 1998. **74**(1-2): p. 175-7.
79. Garel, S., K.J. Huffman, and J.L. Rubenstein, *Molecular regionalization of the neocortex is disrupted in Fgf8 hypomorphic mutants*. *Development*, 2003. **130**(9): p. 1903-14.
80. Storm, E.E., et al., *Dose-dependent functions of Fgf8 in regulating telencephalic patterning centers*. *Development*, 2006. **133**(9): p. 1831-44.
81. Fukuchi-Shimogori, T. and E.A. Grove, *Neocortex patterning by the secreted signaling molecule FGF8*. *Science*, 2001. **294**(5544): p. 1071-4.
82. Cholfin, J.A. and J.L. Rubenstein, *Patterning of frontal cortex subdivisions by Fgf17*. *Proc Natl Acad Sci U S A*, 2007. **104**(18): p. 7652-7.
83. Toyoda, R., et al., *FGF8 acts as a classic diffusible morphogen to pattern the neocortex*. *Development*, 2010. **137**(20): p. 3439-48.
84. Grove, E.A., et al., *The hem of the embryonic cerebral cortex is defined by the expression of multiple Wnt genes and is compromised in Gli3-deficient mice*. *Development*, 1998. **125**(12): p. 2315-25.
85. Aoto, K., et al., *Mouse GLI3 regulates Fgf8 expression and apoptosis in the developing neural tube, face, and limb bud*. *Dev Biol*, 2002. **251**(2): p. 320-32.
86. Kuschel, S., U. Ruther, and T. Theil, *A disrupted balance between Bmp/Wnt and Fgf signaling underlies the ventralization of the Gli3 mutant telencephalon*. *Dev Biol*, 2003. **260**(2): p. 484-95.
87. Anderson, R.M., et al., *Chordin and noggin promote organizing centers of forebrain development in the mouse*. *Development*, 2002. **129**(21): p. 4975-87.
88. Crossley, P.H., et al., *Coordinate expression of Fgf8, Otx2, Bmp4, and Shh in the rostral prosencephalon during development of the telencephalic and optic vesicles*. *Neuroscience*, 2001. **108**(2): p. 183-206.
89. Ohkubo, Y., C. Chiang, and J.L. Rubenstein, *Coordinate regulation and synergistic actions of BMP4, SHH and FGF8 in the rostral prosencephalon regulate morphogenesis of the telencephalic and optic vesicles*. *Neuroscience*, 2002. **111**(1): p. 1-17.
90. Panman, L., et al., *Differential regulation of gene expression in the digit forming area of the mouse limb bud by SHH and gremlin 1/FGF-mediated epithelial-mesenchymal signalling*. *Development*, 2006. **133**(17): p. 3419-28.
91. Piccolo, S., et al., *Dorsoventral patterning in Xenopus: inhibition of ventral signals by direct binding of chordin to BMP-4*. *Cell*, 1996. **86**(4): p. 589-98.
92. Shimamura, K., et al., *Longitudinal organization of the anterior neural plate and neural tube*. *Development*, 1995. **121**(12): p. 3923-33.

93. Shimogori, T., et al., *Embryonic signaling centers expressing BMP, WNT and FGF proteins interact to pattern the cerebral cortex*. *Development*, 2004. **131**(22): p. 5639-47.
94. Sousa, V.H. and G. Fishell, *Sonic hedgehog functions through dynamic changes in temporal competence in the developing forebrain*. *Curr Opin Genet Dev*, 2010. **20**(4): p. 391-9.
95. Zimmerman, L.B., J.M. De Jesus-Escobar, and R.M. Harland, *The Spemann organizer signal noggin binds and inactivates bone morphogenetic protein 4*. *Cell*, 1996. **86**(4): p. 599-606.
96. Furuta, Y., D.W. Piston, and B.L. Hogan, *Bone morphogenetic proteins (BMPs) as regulators of dorsal forebrain development*. *Development*, 1997. **124**(11): p. 2203-12.
97. Caronia-Brown, G., et al., *The cortical hem regulates the size and patterning of neocortex*. *Development*, 2014. **141**(14): p. 2855-65.
98. Zhao, Y., et al., *Control of hippocampal morphogenesis and neuronal differentiation by the LIM homeobox gene Lhx5*. *Science*, 1999. **284**(5417): p. 1155-8.
99. Monuki, E.S., F.D. Porter, and C.A. Walsh, *Patterning of the dorsal telencephalon and cerebral cortex by a roof plate-Lhx2 pathway*. *Neuron*, 2001. **32**(4): p. 591-604.
100. Bulchand, S., et al., *LIM-homeodomain gene Lhx2 regulates the formation of the cortical hem*. *Mech Dev*, 2001. **100**(2): p. 165-75.
101. Porter, F.D., et al., *Lhx2, a LIM homeobox gene, is required for eye, forebrain, and definitive erythrocyte development*. *Development*, 1997. **124**(15): p. 2935-44.
102. Mangale, V.S., et al., *Lhx2 selector activity specifies cortical identity and suppresses hippocampal organizer fate*. *Science*, 2008. **319**(5861): p. 304-9.
103. Kim, A.S., et al., *Pax-6 regulates expression of SFRP-2 and Wnt-7b in the developing CNS*. *J Neurosci*, 2001. **21**(5): p. RC132.
104. Assimacopoulos, S., E.A. Grove, and C.W. Ragsdale, *Identification of a Pax6-dependent epidermal growth factor family signaling source at the lateral edge of the embryonic cerebral cortex*. *J Neurosci*, 2003. **23**(16): p. 6399-403.
105. Chiang, C., et al., *Cyclopia and defective axial patterning in mice lacking Sonic hedgehog gene function*. *Nature*, 1996. **383**(6599): p. 407-13.
106. Dahmane, N. and A. Ruiz i Altaba, *Sonic hedgehog regulates the growth and patterning of the cerebellum*. *Development*, 1999. **126**(14): p. 3089-100.
107. Sahara, S., et al., *Sp8 exhibits reciprocal induction with Fgf8 but has an opposing effect on anterior-posterior cortical area patterning*. *Neural Dev*, 2007. **2**: p. 10.
108. Treichel, D., et al., *mBtd is required to maintain signaling during murine limb development*. *Genes Dev*, 2003. **17**(21): p. 2630-5.
109. Zembrzycki, A., et al., *Genetic interplay between the transcription factors Sp8 and Emx2 in the patterning of the forebrain*. *Neural Dev*, 2007. **2**: p. 8.
110. Borello, U., et al., *Sp8 and COUP-TF1 reciprocally regulate patterning and Fgf signaling in cortical progenitors*. *Cereb Cortex*, 2014. **24**(6): p. 1409-21.

111. Bishop, K.M., G. Goudreau, and D.D. O'Leary, *Regulation of area identity in the mammalian neocortex by Emx2 and Pax6*. *Science*, 2000. **288**(5464): p. 344-9.
112. Mallamaci, A., et al., *Area identity shifts in the early cerebral cortex of Emx2<sup>-/-</sup> mutant mice*. *Nat Neurosci*, 2000. **3**(7): p. 679-86.
113. Asami, M., et al., *The role of Pax6 in regulating the orientation and mode of cell division of progenitors in the mouse cerebral cortex*. *Development*, 2011. **138**(23): p. 5067-78.
114. Georgala, P.A., C.B. Carr, and D.J. Price, *The role of Pax6 in forebrain development*. *Dev Neurobiol*, 2011. **71**(8): p. 690-709.
115. Sansom, S.N., et al., *The level of the transcription factor Pax6 is essential for controlling the balance between neural stem cell self-renewal and neurogenesis*. *PLoS Genet*, 2009. **5**(6): p. e1000511.
116. Bishop, K.M., J.L. Rubenstein, and D.D. O'Leary, *Distinct actions of Emx1, Emx2, and Pax6 in regulating the specification of areas in the developing neocortex*. *J Neurosci*, 2002. **22**(17): p. 7627-38.
117. Li, H., K.M. Bishop, and D.D. O'Leary, *Potential target genes of EMX2 include Odz/Ten-M and other gene families with implications for cortical patterning*. *Mol Cell Neurosci*, 2006. **33**(2): p. 136-49.
118. Muzio, L., et al., *Emx2 and Pax6 control regionalization of the pre-neuronogenic cortical primordium*. *Cereb Cortex*, 2002. **12**(2): p. 129-39.
119. Berger, J., et al., *Conditional activation of Pax6 in the developing cortex of transgenic mice causes progenitor apoptosis*. *Development*, 2007. **134**(7): p. 1311-22.
120. Manuel, M., et al., *Controlled overexpression of Pax6 in vivo negatively autoregulates the Pax6 locus, causing cell-autonomous defects of late cortical progenitor proliferation with little effect on cortical arealization*. *Development*, 2007. **134**(3): p. 545-55.
121. Pinon, M.C., et al., *Altered molecular regionalization and normal thalamocortical connections in cortex-specific Pax6 knock-out mice*. *J Neurosci*, 2008. **28**(35): p. 8724-34.
122. Mallamaci, A., et al., *The lack of Emx2 causes impairment of Reelin signaling and defects of neuronal migration in the developing cerebral cortex*. *J Neurosci*, 2000. **20**(3): p. 1109-18.
123. Hamasaki, T., et al., *EMX2 regulates sizes and positioning of the primary sensory and motor areas in neocortex by direct specification of cortical progenitors*. *Neuron*, 2004. **43**(3): p. 359-72.
124. Cholfin, J.A. and J.L. Rubenstein, *Frontal cortex subdivision patterning is coordinately regulated by Fgf8, Fgf17, and Emx2*. *J Comp Neurol*, 2008. **509**(2): p. 144-55.
125. Leingartner, A., et al., *Cortical area size dictates performance at modality-specific behaviors*. *Proc Natl Acad Sci U S A*, 2007. **104**(10): p. 4153-8.
126. Ladias, J.A., et al., *Transcriptional regulation of human apolipoprotein genes ApoB, ApoCIII, and ApoAII by members of the steroid hormone receptor superfamily HNF-4, ARP-1, EAR-2, and EAR-3*. *J Biol Chem*, 1992. **267**(22): p. 15849-60.
127. Paulweber, B., et al., *Identification of a negative regulatory region 5' of the human apolipoprotein B promoter*. *J Biol Chem*, 1991. **266**(32): p. 21956-61.

128. Rottman, J.N., et al., *A retinoic acid-responsive element in the apolipoprotein AI gene distinguishes between two different retinoic acid response pathways*. Mol Cell Biol, 1991. **11**(7): p. 3814-20.
129. Widom, R.L., et al., *Synergistic interactions between transcription factors control expression of the apolipoprotein AI gene in liver cells*. Mol Cell Biol, 1991. **11**(2): p. 677-87.
130. Widom, R.L., M. Rhee, and S.K. Karathanasis, *Repression by ARP-1 sensitizes apolipoprotein AI gene responsiveness to RXR alpha and retinoic acid*. Mol Cell Biol, 1992. **12**(8): p. 3380-9.
131. Lu, X.P., G. Salbert, and M. Pfahl, *An evolutionary conserved COUP-TF binding element in a neural-specific gene and COUP-TF expression patterns support a major role for COUP-TF in neural development*. Mol Endocrinol, 1994. **8**(12): p. 1774-88.
132. Power, S.C. and S. Cereghini, *Positive regulation of the vHNF1 promoter by the orphan receptors COUP-TF1/Ear3 and COUP-TFII/Arp1*. Mol Cell Biol, 1996. **16**(3): p. 778-91.
133. Hall, R.K., F.M. Sladek, and D.K. Granner, *The orphan receptors COUP-TF and HNF-4 serve as accessory factors required for induction of phosphoenolpyruvate carboxykinase gene transcription by glucocorticoids*. Proc Natl Acad Sci U S A, 1995. **92**(2): p. 412-6.
134. Tomassy, G.S., et al., *Area-specific temporal control of corticospinal motor neuron differentiation by COUP-TFI*. Proc Natl Acad Sci U S A, 2010. **107**(8): p. 3576-81.
135. Dye, C.A., H. El Shawa, and K.J. Huffman, *A lifespan analysis of intraneocortical connections and gene expression in the mouse II*. Cereb Cortex, 2011. **21**(6): p. 1331-50.
136. Dye, C.A., H. El Shawa, and K.J. Huffman, *A lifespan analysis of intraneocortical connections and gene expression in the mouse I*. Cereb Cortex, 2011. **21**(6): p. 1311-30.
137. Zhou, C., et al., *The nuclear orphan receptor COUP-TFI is required for differentiation of subplate neurons and guidance of thalamocortical axons*. Neuron, 1999. **24**(4): p. 847-59.
138. Zhou, C., S.Y. Tsai, and M.J. Tsai, *COUP-TFI: an intrinsic factor for early regionalization of the neocortex*. Genes Dev, 2001. **15**(16): p. 2054-9.
139. Qiu, Y., et al., *Spatiotemporal expression patterns of chicken ovalbumin upstream promoter-transcription factors in the developing mouse central nervous system: evidence for a role in segmental patterning of the diencephalon*. Proc Natl Acad Sci U S A, 1994. **91**(10): p. 4451-5.
140. Armentano, M., et al., *COUP-TFI regulates the balance of cortical patterning between frontal/motor and sensory areas*. Nat Neurosci, 2007. **10**(10): p. 1277-86.
141. Faedo, A., U. Borello, and J.L. Rubenstein, *Repression of Fgf signaling by sprouty1-2 regulates cortical patterning in two distinct regions and times*. J Neurosci, 2010. **30**(11): p. 4015-23.
142. Faedo, A., et al., *COUP-TFI coordinates cortical patterning, neurogenesis, and laminar fate and modulates MAPK/ERK, AKT, and beta-catenin signaling*. Cereb Cortex, 2008. **18**(9): p. 2117-31.

143. Bedogni, F., et al., *Tbr1 regulates regional and laminar identity of postmitotic neurons in developing neocortex*. Proc Natl Acad Sci U S A, 2010. **107**(29): p. 13129-34.
144. Joshi, P.S., et al., *Bhlhb5 regulates the postmitotic acquisition of area identities in layers II-V of the developing neocortex*. Neuron, 2008. **60**(2): p. 258-72.
145. Cederquist, G.Y., et al., *Lmo4 establishes rostral motor cortex projection neuron subtype diversity*. J Neurosci, 2013. **33**(15): p. 6321-32.
146. Kashani, A.H., et al., *Calcium activation of the LMO4 transcription complex and its role in the patterning of thalamocortical connections*. J Neurosci, 2006. **26**(32): p. 8398-408.
147. Aboitiz, F. and J. Montiel, *One hundred million years of interhemispheric communication: the history of the corpus callosum*. Braz J Med Biol Res, 2003. **36**(4): p. 409-20.
148. Fame, R.M., J.L. MacDonald, and J.D. Macklis, *Development, specification, and diversity of callosal projection neurons*. Trends Neurosci, 2011. **34**(1): p. 41-50.
149. Leyva-Diaz, E. and G. Lopez-Bendito, *In and out from the cortex: development of major forebrain connections*. Neuroscience, 2013. **254**: p. 26-44.
150. Alcamo, E.A., et al., *Satb2 regulates callosal projection neuron identity in the developing cerebral cortex*. Neuron, 2008. **57**(3): p. 364-77.
151. Minshew, N.J. and D.L. Williams, *The new neurobiology of autism: cortex, connectivity, and neuronal organization*. Arch Neurol, 2007. **64**(7): p. 945-50.
152. Herbert, M.R. and T. Kenet, *Brain abnormalities in language disorders and in autism*. Pediatr Clin North Am, 2007. **54**(3): p. 563-83, vii.
153. McAlonan, G.M., et al., *Differential effects on white-matter systems in high-functioning autism and Asperger's syndrome*. Psychol Med, 2009. **39**(11): p. 1885-93.
154. Freitag, C.M., et al., *Total brain volume and corpus callosum size in medication-naive adolescents and young adults with autism spectrum disorder*. Biol Psychiatry, 2009. **66**(4): p. 316-9.
155. Vidal, C.N., et al., *Mapping corpus callosum deficits in autism: an index of aberrant cortical connectivity*. Biol Psychiatry, 2006. **60**(3): p. 218-25.
156. Egaas, B., E. Courchesne, and O. Saitoh, *Reduced size of corpus callosum in autism*. Arch Neurol, 1995. **52**(8): p. 794-801.
157. Angevine, J.B., Jr. and R.L. Sidman, *Autoradiographic study of cell migration during histogenesis of cerebral cortex in the mouse*. Nature, 1961. **192**: p. 766-8.
158. Tarabykin, V., et al., *Cortical upper layer neurons derive from the subventricular zone as indicated by Svet1 gene expression*. Development, 2001. **128**(11): p. 1983-93.
159. Yorke, C.H., Jr. and V.S. Caviness, Jr., *Interhemispheric neocortical connections of the corpus callosum in the normal mouse: a study based on anterograde and retrograde methods*. J Comp Neurol, 1975. **164**(2): p. 233-45.

160. Mitchell, B.D. and J.D. Macklis, *Large-scale maintenance of dual projections by callosal and frontal cortical projection neurons in adult mice*. J Comp Neurol, 2005. **482**(1): p. 17-32.
161. Wilson, C.J., *Morphology and synaptic connections of crossed corticostriatal neurons in the rat*. J Comp Neurol, 1987. **263**(4): p. 567-80.
162. Cauller, L.J., B. Clancy, and B.W. Connors, *Backward cortical projections to primary somatosensory cortex in rats extend long horizontal axons in layer I*. J Comp Neurol, 1998. **390**(2): p. 297-310.
163. Petreanu, L., et al., *Channelrhodopsin-2-assisted circuit mapping of long-range callosal projections*. Nat Neurosci, 2007. **10**(5): p. 663-8.
164. Mizuno, H., T. Hirano, and Y. Tagawa, *Evidence for activity-dependent cortical wiring: formation of interhemispheric connections in neonatal mouse visual cortex requires projection neuron activity*. J Neurosci, 2007. **27**(25): p. 6760-70.
165. Innocenti, G.M. and D.J. Price, *Exuberance in the development of cortical networks*. Nat Rev Neurosci, 2005. **6**(12): p. 955-65.
166. Lai, T., et al., *SOX5 controls the sequential generation of distinct corticofugal neuron subtypes*. Neuron, 2008. **57**(2): p. 232-47.
167. Gupta, A., L.H. Tsai, and A. Wynshaw-Boris, *Life is a journey: a genetic look at neocortical development*. Nat Rev Genet, 2002. **3**(5): p. 342-55.
168. Allendoerfer, K.L. and C.J. Shatz, *The subplate, a transient neocortical structure: its role in the development of connections between thalamus and cortex*. Annu Rev Neurosci, 1994. **17**: p. 185-218.
169. McConnell, S.K., A. Ghosh, and C.J. Shatz, *Subplate neurons pioneer the first axon pathway from the cerebral cortex*. Science, 1989. **245**(4921): p. 978-82.
170. Deng, J. and A.J. Elberger, *Corticothalamic and thalamocortical pathfinding in the mouse: dependence on intermediate targets and guidance axis*. Anat Embryol (Berl), 2003. **207**(3): p. 177-92.
171. Caviness, V.S., Jr. and D.O. Frost, *Tangential organization of thalamic projections to the neocortex in the mouse*. J Comp Neurol, 1980. **194**(2): p. 335-67.
172. Sherman, S.M. and R.W. Guillery, *On the actions that one nerve cell can have on another: distinguishing "drivers" from "modulators"*. Proc Natl Acad Sci U S A, 1998. **95**(12): p. 7121-6.
173. Auladell, C., et al., *The early development of thalamocortical and corticothalamic projections in the mouse*. Anat Embryol (Berl), 2000. **201**(3): p. 169-79.
174. Price, D.J., et al., *The development of cortical connections*. Eur J Neurosci, 2006. **23**(4): p. 910-20.
175. Guillery, R.W., *Patterns of fiber degeneration in the dorsal lateral geniculate nucleus of the cat following lesions in the visual cortex*. J Comp Neurol, 1967. **130**(3): p. 197-221.
176. Jones, E.G. and T.P. Powell, *The projection of the somatic sensory cortex upon the thalamus in the cat*. Brain Res, 1968. **10**(3): p. 369-91.
177. Diamond, I.T., E.G. Jones, and T.P. Powell, *The projection of the auditory cortex upon the diencephalon and brain stem in the cat*. Brain Res, 1969. **15**(2): p. 305-40.

178. Hoogland, P.V., E. Welker, and H. Van der Loos, *Organization of the projections from barrel cortex to thalamus in mice studied with Phaseolus vulgaris-leucoagglutinin and HRP*. Exp Brain Res, 1987. **68**(1): p. 73-87.
179. Guillery, R.W., *Anatomical evidence concerning the role of the thalamus in corticocortical communication: a brief review*. J Anat, 1995. **187 ( Pt 3)**: p. 583-92.
180. Jones, L., et al., *Pax6 is required for the normal development of the forebrain axonal connections*. Development, 2002. **129**(21): p. 5041-52.
181. Sherman, S.M. and R.W. Guillery, *The role of the thalamus in the flow of information to the cortex*. Philos Trans R Soc Lond B Biol Sci, 2002. **357**(1428): p. 1695-708.
182. O'Leary, D.D. and S.E. Koester, *Development of projection neuron types, axon pathways, and patterned connections of the mammalian cortex*. Neuron, 1993. **10**(6): p. 991-1006.
183. O'Leary, D.D. and T. Terashima, *Cortical axons branch to multiple subcortical targets by interstitial axon budding: implications for target recognition and "waiting periods"*. Neuron, 1988. **1**(10): p. 901-10.
184. Schreyer, D.J. and E.H. Jones, *Topographic sequence of outgrowth of corticospinal axons in the rat: a study using retrograde axonal labeling with Fast blue*. Brain Res, 1988. **466**(1): p. 89-101.
185. Jones, E.G., D.J. Schreyer, and S.P. Wise, *Growth and maturation of the rat corticospinal tract*. Prog Brain Res, 1982. **57**: p. 361-79.
186. Terashima, T., *Anatomy, development and lesion-induced plasticity of rodent corticospinal tract*. Neurosci Res, 1995. **22**(2): p. 139-61.
187. Brosamle, C. and M.E. Schwab, *Cells of origin, course, and termination patterns of the ventral, uncrossed component of the mature rat corticospinal tract*. J Comp Neurol, 1997. **386**(2): p. 293-303.
188. Brosamle, C. and M.E. Schwab, *Ipsilateral, ventral corticospinal tract of the adult rat: ultrastructure, myelination and synaptic connections*. J Neurocytol, 2000. **29**(7): p. 499-507.
189. Joosten, E.A., et al., *Postnatal development of the ipsilateral corticospinal component in rat spinal cord: a light and electron microscopic anterograde HRP study*. J Comp Neurol, 1992. **326**(1): p. 133-46.
190. Schreyer, D.J. and E.G. Jones, *Growth and target finding by axons of the corticospinal tract in prenatal and postnatal rats*. Neuroscience, 1982. **7**(8): p. 1837-53.
191. Stanfield, B.B., *The development of the corticospinal projection*. Prog Neurobiol, 1992. **38**(2): p. 169-202.
192. Pennartz, C.M., et al., *Corticostriatal Interactions during Learning, Memory Processing, and Decision Making*. J Neurosci, 2009. **29**(41): p. 12831-8.
193. Reiner, A., et al., *Corticostriatal projection neurons - dichotomous types and dichotomous functions*. Front Neuroanat, 2010. **4**: p. 142.
194. Shepherd, G.M., *Corticostriatal connectivity and its role in disease*. Nat Rev Neurosci, 2013. **14**(4): p. 278-91.
195. Albright, A.L., *Spasticity and movement disorders in cerebral palsy*. J Child Neurol, 1996. **11 Suppl 1**: p. S1-4.
196. Martin, L.J., et al., *Primary sensory and forebrain motor systems in the newborn brain are preferentially damaged by hypoxia-ischemia*. J Comp Neurol, 1997. **377**(2): p. 262-85.

197. Reading, S.A., et al., *Functional brain changes in presymptomatic Huntington's disease*. *Ann Neurol*, 2004. **55**(6): p. 879-83.
198. Rosas, H.D., et al., *Regional and progressive thinning of the cortical ribbon in Huntington's disease*. *Neurology*, 2002. **58**(5): p. 695-701.
199. Sieradzan, K.A. and D.M. Mann, *The selective vulnerability of nerve cells in Huntington's disease*. *Neuropathol Appl Neurobiol*, 2001. **27**(1): p. 1-21.
200. Sotrel, A., et al., *Morphometric analysis of the prefrontal cortex in Huntington's disease*. *Neurology*, 1991. **41**(7): p. 1117-23.
201. Stephens, B., et al., *Evidence of a breakdown of corticostriatal connections in Parkinson's disease*. *Neuroscience*, 2005. **132**(3): p. 741-54.
202. Vonsattel, J.P., et al., *Neuropathological classification of Huntington's disease*. *J Neuropathol Exp Neurol*, 1985. **44**(6): p. 559-77.
203. Sohur, U.S., et al., *Anatomic and molecular development of corticostriatal projection neurons in mice*. *Cereb Cortex*, 2014. **24**(2): p. 293-303.
204. Molnar, Z. and A.F. Cheung, *Towards the classification of subpopulations of layer V pyramidal projection neurons*. *Neurosci Res*, 2006. **55**(2): p. 105-15.
205. Wilson, C.J., *Postsynaptic potentials evoked in spiny neostriatal projection neurons by stimulation of ipsilateral and contralateral neocortex*. *Brain Res*, 1986. **367**(1-2): p. 201-13.
206. Bauswein, E., C. Fromm, and A. Preuss, *Corticostriatal cells in comparison with pyramidal tract neurons: contrasting properties in the behaving monkey*. *Brain Res*, 1989. **493**(1): p. 198-203.
207. Cowan, R.L. and C.J. Wilson, *Spontaneous firing patterns and axonal projections of single corticostriatal neurons in the rat medial agranular cortex*. *J Neurophysiol*, 1994. **71**(1): p. 17-32.
208. Turner, R.S. and M.R. DeLong, *Corticostriatal activity in primary motor cortex of the macaque*. *J Neurosci*, 2000. **20**(18): p. 7096-108.
209. Beloozerova, I.N., et al., *Activity of different classes of neurons of the motor cortex during postural corrections*. *J Neurosci*, 2003. **23**(21): p. 7844-53.
210. Chen, B., L.R. Schaevitz, and S.K. McConnell, *Fez1 regulates the differentiation and axon targeting of layer 5 subcortical projection neurons in cerebral cortex*. *Proc Natl Acad Sci U S A*, 2005. **102**(47): p. 17184-9.
211. Chen, B., et al., *The Fezf2-Ctip2 genetic pathway regulates the fate choice of subcortical projection neurons in the developing cerebral cortex*. *Proc Natl Acad Sci U S A*, 2008. **105**(32): p. 11382-7.
212. Britanova, O., et al., *Satb2 is a postmitotic determinant for upper-layer neuron specification in the neocortex*. *Neuron*, 2008. **57**(3): p. 378-92.
213. Rouaux, C. and P. Arlotta, *Direct lineage reprogramming of post-mitotic callosal neurons into corticofugal neurons in vivo*. *Nat Cell Biol*, 2013. **15**(2): p. 214-21.
214. Avram, D., et al., *Isolation of a novel family of C(2)H(2) zinc finger proteins implicated in transcriptional repression mediated by chicken ovalbumin upstream promoter transcription factor (COUP-TF) orphan nuclear receptors*. *J Biol Chem*, 2000. **275**(14): p. 10315-22.
215. Senawong, T., et al., *Involvement of the histone deacetylase SIRT1 in chicken ovalbumin upstream promoter transcription factor (COUP-TF)-interacting protein 2-mediated transcriptional repression*. *J Biol Chem*, 2003. **278**(44): p. 43041-50.

216. Arlotta, P., et al., *Ctip2 controls the differentiation of medium spiny neurons and the establishment of the cellular architecture of the striatum*. J Neurosci, 2008. **28**(3): p. 622-32.
217. Kwan, K.Y., et al., *SOX5 postmitotically regulates migration, postmigratory differentiation, and projections of subplate and deep-layer neocortical neurons*. Proc Natl Acad Sci U S A, 2008. **105**(41): p. 16021-6.
218. Shim, S., et al., *Cis-regulatory control of corticospinal system development and evolution*. Nature, 2012. **486**(7401): p. 74-9.
219. Weimann, J.M., et al., *Cortical neurons require Otx1 for the refinement of exuberant axonal projections to subcortical targets*. Neuron, 1999. **24**(4): p. 819-31.
220. Frantz, G.D., et al., *Otx1 and Otx2 define layers and regions in developing cerebral cortex and cerebellum*. J Neurosci, 1994. **14**(10): p. 5725-40.
221. Hevner, R.F., et al., *Tbr1 regulates differentiation of the preplate and layer 6*. Neuron, 2001. **29**(2): p. 353-66.
222. Bulfone, A., et al., *An olfactory sensory map develops in the absence of normal projection neurons or GABAergic interneurons*. Neuron, 1998. **21**(6): p. 1273-82.
223. McKenna, W.L., et al., *Tbr1 and Fezf2 regulate alternate corticofugal neuronal identities during neocortical development*. J Neurosci, 2011. **31**(2): p. 549-64.
224. Han, W., et al., *TBR1 directly represses Fezf2 to control the laminar origin and development of the corticospinal tract*. Proc Natl Acad Sci U S A, 2011. **108**(7): p. 3041-6.
225. Koester, S.E. and D.D. O'Leary, *Connectional distinction between callosal and subcortically projecting cortical neurons is determined prior to axon extension*. Dev Biol, 1993. **160**(1): p. 1-14.
226. Szemes, M., et al., *Isolation and characterization of SATB2, a novel AT-rich DNA binding protein expressed in development- and cell-specific manner in the rat brain*. Neurochem Res, 2006. **31**(2): p. 237-46.
227. Britanova, O., et al., *Novel transcription factor Satb2 interacts with matrix attachment region DNA elements in a tissue-specific manner and demonstrates cell-type-dependent expression in the developing mouse CNS*. Eur J Neurosci, 2005. **21**(3): p. 658-68.
228. Dobрева, G., J. Dambacher, and R. Grosschedl, *SUMO modification of a novel MAR-binding protein, SATB2, modulates immunoglobulin mu gene expression*. Genes Dev, 2003. **17**(24): p. 3048-61.
229. Srinivasan, K., et al., *A network of genetic repression and derepression specifies projection fates in the developing neocortex*. Proc Natl Acad Sci U S A, 2012. **109**(47): p. 19071-8.
230. Cai, S., H.J. Han, and T. Kohwi-Shigematsu, *Tissue-specific nuclear architecture and gene expression regulated by SATB1*. Nat Genet, 2003. **34**(1): p. 42-51.
231. Jenuwein, T., et al., *Extension of chromatin accessibility by nuclear matrix attachment regions*. Nature, 1997. **385**(6613): p. 269-72.
232. Gyorgy, A.B., et al., *SATB2 interacts with chromatin-remodeling molecules in differentiating cortical neurons*. Eur J Neurosci, 2008. **27**(4): p. 865-73.

233. Xue, Y., et al., *NURD, a novel complex with both ATP-dependent chromatin-remodeling and histone deacetylase activities*. Mol Cell, 1998. **2**(6): p. 851-61.
234. Baranek, C., et al., *Protooncogene Ski cooperates with the chromatin-remodeling factor Satb2 in specifying callosal neurons*. Proc Natl Acad Sci U S A, 2012. **109**(9): p. 3546-51.
235. Sugitani, Y., et al., *Brn-1 and Brn-2 share crucial roles in the production and positioning of mouse neocortical neurons*. Genes Dev, 2002. **16**(14): p. 1760-5.
236. McEvilly, R.J., et al., *Transcriptional regulation of cortical neuron migration by POU domain factors*. Science, 2002. **295**(5559): p. 1528-32.
237. Cubelos, B., et al., *Cux-2 controls the proliferation of neuronal intermediate precursors of the cortical subventricular zone*. Cereb Cortex, 2008. **18**(8): p. 1758-70.
238. Polleux, F., et al., *Patterning of cortical efferent projections by semaphorin-neuropilin interactions*. Science, 1998. **282**(5395): p. 1904-6.
239. Zhao, H., et al., *A molecular mechanism that regulates medially oriented axonal growth of upper layer neurons in the developing neocortex*. J Comp Neurol, 2011. **519**(5): p. 834-48.
240. Silver, J., et al., *Axonal guidance during development of the great cerebral commissures: descriptive and experimental studies, in vivo, on the role of preformed glial pathways*. J Comp Neurol, 1982. **210**(1): p. 10-29.
241. Koester, S.E. and D.D. O'Leary, *Axons of early generated neurons in cingulate cortex pioneer the corpus callosum*. J Neurosci, 1994. **14**(11 Pt 1): p. 6608-20.
242. Ozaki, H.S. and D. Wahlsten, *Timing and origin of the first cortical axons to project through the corpus callosum and the subsequent emergence of callosal projection cells in mouse*. J Comp Neurol, 1998. **400**(2): p. 197-206.
243. Rash, B.G. and L.J. Richards, *A role for cingulate pioneering axons in the development of the corpus callosum*. J Comp Neurol, 2001. **434**(2): p. 147-57.
244. Piper, M., et al., *Neuropilin 1-Sema signaling regulates crossing of cingulate pioneering axons during development of the corpus callosum*. Cereb Cortex, 2009. **19 Suppl 1**: p. i11-21.
245. Norris, C.R. and K. Kalil, *Guidance of callosal axons by radial glia in the developing cerebral cortex*. J Neurosci, 1991. **11**(11): p. 3481-92.
246. Hatanaka, Y., et al., *Distinct roles of neuropilin 1 signaling for radial and tangential extension of callosal axons*. J Comp Neurol, 2009. **514**(3): p. 215-25.
247. Fothergill, T., et al., *Netrin-DCC signaling regulates corpus callosum formation through attraction of pioneering axons and by modulating Slit2-mediated repulsion*. Cereb Cortex, 2014. **24**(5): p. 1138-51.
248. Gu, C., et al., *Neuropilin-1 conveys semaphorin and VEGF signaling during neural and cardiovascular development*. Dev Cell, 2003. **5**(1): p. 45-57.
249. Serafini, T., et al., *Netrin-1 is required for commissural axon guidance in the developing vertebrate nervous system*. Cell, 1996. **87**(6): p. 1001-14.

250. Niquille, M., et al., *Transient neuronal populations are required to guide callosal axons: a role for semaphorin 3C*. PLoS Biol, 2009. **7**(10): p. e1000230.
251. Mendes, S.W., M. Henkemeyer, and D.J. Liebl, *Multiple Eph receptors and B-class ephrins regulate midline crossing of corpus callosum fibers in the developing mouse forebrain*. J Neurosci, 2006. **26**(3): p. 882-92.
252. Shu, T. and L.J. Richards, *Cortical axon guidance by the glial wedge during the development of the corpus callosum*. J Neurosci, 2001. **21**(8): p. 2749-58.
253. Shu, T., et al., *Slit2 guides both precrossing and postcrossing callosal axons at the midline in vivo*. J Neurosci, 2003. **23**(22): p. 8176-84.
254. Bagri, A., et al., *Slit proteins prevent midline crossing and determine the dorsoventral position of major axonal pathways in the mammalian forebrain*. Neuron, 2002. **33**(2): p. 233-48.
255. Islam, S.M., et al., *Draxin, a repulsive guidance protein for spinal cord and forebrain commissures*. Science, 2009. **323**(5912): p. 388-93.
256. Keeble, T.R., et al., *The Wnt receptor Ryk is required for Wnt5a-mediated axon guidance on the contralateral side of the corpus callosum*. J Neurosci, 2006. **26**(21): p. 5840-8.
257. Lopez-Bendito, G., et al., *Robo1 and Robo2 cooperate to control the guidance of major axonal tracts in the mammalian forebrain*. J Neurosci, 2007. **27**(13): p. 3395-407.
258. Marillat, V., et al., *Spatiotemporal expression patterns of slit and robo genes in the rat brain*. J Comp Neurol, 2002. **442**(2): p. 130-55.
259. Koralek, K.A. and H.P. Killackey, *Callosal projections in rat somatosensory cortex are altered by early removal of afferent input*. Proc Natl Acad Sci U S A, 1990. **87**(4): p. 1396-400.
260. Srivatsa, S., et al., *Unc5C and DCC act downstream of Ctip2 and Satb2 and contribute to corpus callosum formation*. Nat Commun, 2014. **5**: p. 3708.
261. Fazeli, A., et al., *Phenotype of mice lacking functional Deleted in colorectal cancer (Dcc) gene*. Nature, 1997. **386**(6627): p. 796-804.
262. Hedgecock, E.M., J.G. Culotti, and D.H. Hall, *The unc-5, unc-6, and unc-40 genes guide circumferential migrations of pioneer axons and mesodermal cells on the epidermis in C. elegans*. Neuron, 1990. **4**(1): p. 61-85.
263. Hamelin, M., et al., *Expression of the UNC-5 guidance receptor in the touch neurons of C. elegans steers their axons dorsally*. Nature, 1993. **364**(6435): p. 327-30.
264. Colamarino, S.A. and M. Tessier-Lavigne, *The axonal chemoattractant netrin-1 is also a chemorepellent for trochlear motor axons*. Cell, 1995. **81**(4): p. 621-9.
265. Bagnard, D., et al., *Semaphorins act as attractive and repulsive guidance signals during the development of cortical projections*. Development, 1998. **125**(24): p. 5043-53.
266. Castellani, V., et al., *Analysis of the L1-deficient mouse phenotype reveals cross-talk between Sema3A and L1 signaling pathways in axonal guidance*. Neuron, 2000. **27**(2): p. 237-49.
267. Castellani, V., *The function of neuropilin/L1 complex*. Adv Exp Med Biol, 2002. **515**: p. 91-102.

268. Metin, C., et al., *A role for netrin-1 in the guidance of cortical efferents*. *Development*, 1997. **124**(24): p. 5063-74.
269. Richards, L.J., et al., *Directed growth of early cortical axons is influenced by a chemoattractant released from an intermediate target*. *J Neurosci*, 1997. **17**(7): p. 2445-58.
270. Finger, J.H., et al., *The netrin 1 receptors *Unc5h3* and *Dcc* are necessary at multiple choice points for the guidance of corticospinal tract axons*. *J Neurosci*, 2002. **22**(23): p. 10346-56.
271. Joosten, E.A., *An ultrastructural double-labelling method: immunohistochemical localization of cell adhesion molecule L1 on HRP-labelled developing corticospinal tract axons in the rat*. *Histochemistry*, 1990. **94**(6): p. 645-51.
272. Joosten, E.A., A.A. Gribnau, and T.G. Gorgels, *Immunoelectron microscopic localization of cell adhesion molecule L1 in developing rat pyramidal tract*. *Neuroscience*, 1990. **38**(3): p. 675-86.
273. Cohen, S. and M.E. Greenberg, *Communication between the synapse and the nucleus in neuronal development, plasticity, and disease*. *Annu Rev Cell Dev Biol*, 2008. **24**: p. 183-209.
274. Rolf, B., et al., *Pathfinding errors of corticospinal axons in neural cell adhesion molecule-deficient mice*. *J Neurosci*, 2002. **22**(19): p. 8357-62.
275. Canty, A.J. and M. Murphy, *Molecular mechanisms of axon guidance in the developing corticospinal tract*. *Prog Neurobiol*, 2008. **85**(2): p. 214-35.
276. Faulkner, R.L., et al., *Dorsal turning of motor corticospinal axons at the pyramidal decussation requires plexin signaling*. *Neural Dev*, 2008. **3**: p. 21.
277. Runker, A.E., et al., *Semaphorin-6A controls guidance of corticospinal tract axons at multiple choice points*. *Neural Dev*, 2008. **3**: p. 34.
278. Liu, Y., et al., *Ryk-mediated Wnt repulsion regulates posterior-directed growth of corticospinal tract*. *Nat Neurosci*, 2005. **8**(9): p. 1151-9.
279. Ozdinler, P.H. and J.D. Macklis, *IGF-I specifically enhances axon outgrowth of corticospinal motor neurons*. *Nat Neurosci*, 2006. **9**(11): p. 1371-81.
280. Dottori, M., et al., *EphA4 (Sek1) receptor tyrosine kinase is required for the development of the corticospinal tract*. *Proc Natl Acad Sci U S A*, 1998. **95**(22): p. 13248-53.
281. Coonan, J.R., et al., *Development and reorganization of corticospinal projections in EphA4 deficient mice*. *J Comp Neurol*, 2001. **436**(2): p. 248-62.
282. Englund, C., et al., *Pax6, Tbr2, and Tbr1 are expressed sequentially by radial glia, intermediate progenitor cells, and postmitotic neurons in developing neocortex*. *J Neurosci*, 2005. **25**(1): p. 247-51.
283. Bedogni, F., et al., *Autism susceptibility candidate 2 (*Auts2*) encodes a nuclear protein expressed in developing brain regions implicated in autism neuropathology*. *Gene Expr Patterns*, 2010. **10**(1): p. 9-15.
284. Sultana, R., et al., *Identification of a novel gene on chromosome 7q11.2 interrupted by a translocation breakpoint in a pair of autistic twins*. *Genomics*, 2002. **80**(2): p. 129-34.
285. Deane, J.E., et al., *Tandem LIM domains provide synergistic binding in the *LMO4:Ldb1* complex*. *EMBO J*, 2004. **23**(18): p. 3589-98.
286. Dawid, I.B., R. Toyama, and M. Taira, *LIM domain proteins*. *C R Acad Sci III*, 1995. **318**(3): p. 295-306.

287. Sanchez-Garcia, I. and T.H. Rabbitts, *The LIM domain: a new structural motif found in zinc-finger-like proteins*. Trends Genet, 1994. **10**(9): p. 315-20.
288. Bach, I., *The LIM domain: regulation by association*. Mech Dev, 2000. **91**(1-2): p. 5-17.
289. Dawid, I.B., J.J. Breen, and R. Toyama, *LIM domains: multiple roles as adapters and functional modifiers in protein interactions*. Trends Genet, 1998. **14**(4): p. 156-62.
290. Jurata, L.W. and G.N. Gill, *Structure and function of LIM domains*. Curr Top Microbiol Immunol, 1998. **228**: p. 75-113.
291. Matthews, J.B., et al., *Identification of a LIM domain-containing gene in the Cyathostominae*. Vet Parasitol, 2008. **154**(1-2): p. 82-93.
292. Heberlein, U., et al., *Drosophila, a genetic model system to study cocaine-related behaviors: a review with focus on LIM-only proteins*. Neuropharmacology, 2009. **56 Suppl 1**: p. 97-106.
293. Patterson, L.J., et al., *The transcription factors Sc1 and Lmo2 act together during development of the hemangioblast in zebrafish*. Blood, 2007. **109**(6): p. 2389-98.
294. McCollum, C.W., et al., *A zebrafish LMO4 ortholog limits the size of the forebrain and eyes through negative regulation of six3b and rx3*. Dev Biol, 2007. **309**(2): p. 373-85.
295. Retaux, S. and I. Bachy, *A short history of LIM domains (1993-2002): from protein interaction to degradation*. Mol Neurobiol, 2002. **26**(2-3): p. 269-81.
296. Kenny, D.A., et al., *Identification and characterization of LMO4, an LMO gene with a novel pattern of expression during embryogenesis*. Proc Natl Acad Sci U S A, 1998. **95**(19): p. 11257-62.
297. Sugihara, T.M., et al., *Mouse deformed epidermal autoregulatory factor 1 recruits a LIM domain factor, LMO-4, and CLIM coregulators*. Proc Natl Acad Sci U S A, 1998. **95**(26): p. 15418-23.
298. Racevskis, J., et al., *Molecular cloning of LMO41, a new human LIM domain gene*. Biochim Biophys Acta, 1999. **1445**(1): p. 148-53.
299. Joshi, K., et al., *LMO4 controls the balance between excitatory and inhibitory spinal V2 interneurons*. Neuron, 2009. **61**(6): p. 839-51.
300. Milan, M. and S.M. Cohen, *Regulation of LIM homeodomain activity in vivo: a tetramer of dLDB and apterous confers activity and capacity for regulation by dLMO*. Mol Cell, 1999. **4**(2): p. 267-73.
301. Milan, M., F.J. Diaz-Benjumea, and S.M. Cohen, *Beadex encodes an LMO protein that regulates Apterous LIM-homeodomain activity in Drosophila wing development: a model for LMO oncogene function*. Genes Dev, 1998. **12**(18): p. 2912-20.
302. Song, M.R., et al., *Islet-to-LMO stoichiometries control the function of transcription complexes that specify motor neuron and V2a interneuron identity*. Development, 2009. **136**(17): p. 2923-32.
303. Thaler, J.P., et al., *LIM factor Lhx3 contributes to the specification of motor neuron and interneuron identity through cell-type-specific protein-protein interactions*. Cell, 2002. **110**(2): p. 237-49.

304. Wadman, I., et al., *Specific in vivo association between the bHLH and LIM proteins implicated in human T cell leukemia*. EMBO J, 1994. **13**(20): p. 4831-9.
305. Wadman, I.A., et al., *The LIM-only protein Lmo2 is a bridging molecule assembling an erythroid, DNA-binding complex which includes the TAL1, E47, GATA-1 and Ldb1/NLI proteins*. EMBO J, 1997. **16**(11): p. 3145-57.
306. Sang, M., et al., *LIM-domain-only proteins: multifunctional nuclear transcription coregulators that interacts with diverse proteins*. Mol Biol Rep, 2014. **41**(2): p. 1067-73.
307. Deng, M., et al., *Requirement for Lmo4 in the vestibular morphogenesis of mouse inner ear*. Dev Biol, 2010. **338**(1): p. 38-49.
308. Hahm, K., et al., *Defective neural tube closure and anteroposterior patterning in mice lacking the LIM protein LMO4 or its interacting partner Deaf-1*. Mol Cell Biol, 2004. **24**(5): p. 2074-82.
309. Lee, S.K., et al., *The LIM domain-only protein LMO4 is required for neural tube closure*. Mol Cell Neurosci, 2005. **28**(2): p. 205-14.
310. Sum, E.Y., et al., *Overexpression of LMO4 induces mammary hyperplasia, promotes cell invasion, and is a predictor of poor outcome in breast cancer*. Proc Natl Acad Sci U S A, 2005. **102**(21): p. 7659-64.
311. Tse, E., et al., *Null mutation of the Lmo4 gene or a combined null mutation of the Lmo1/Lmo3 genes causes perinatal lethality, and Lmo4 controls neural tube development in mice*. Mol Cell Biol, 2004. **24**(5): p. 2063-73.
312. Wang, N., et al., *The LIM-only factor LMO4 regulates expression of the BMP7 gene through an HDAC2-dependent mechanism, and controls cell proliferation and apoptosis of mammary epithelial cells*. Oncogene, 2007. **26**(44): p. 6431-41.
313. Visvader, J.E., et al., *The LIM domain gene LMO4 inhibits differentiation of mammary epithelial cells in vitro and is overexpressed in breast cancer*. Proc Natl Acad Sci U S A, 2001. **98**(25): p. 14452-7.
314. Mizunuma, H., et al., *The LIM-only protein, LMO4, and the LIM domain-binding protein, LDB1, expression in squamous cell carcinomas of the oral cavity*. Br J Cancer, 2003. **88**(10): p. 1543-8.
315. Mousses, S., et al., *Clinical validation of candidate genes associated with prostate cancer progression in the CWR22 model system using tissue microarrays*. Cancer Res, 2002. **62**(5): p. 1256-60.
316. Wang, N., et al., *Expression of an engrailed-LMO4 fusion protein in mammary epithelial cells inhibits mammary gland development in mice*. Oncogene, 2004. **23**(8): p. 1507-13.
317. Sum, E.Y., et al., *The LIM domain protein LMO4 interacts with the cofactor CtIP and the tumor suppressor BRCA1 and inhibits BRCA1 activity*. J Biol Chem, 2002. **277**(10): p. 7849-56.
318. Manetopoulos, C., et al., *The LIM-only protein LMO4 modulates the transcriptional activity of HEN1*. Biochem Biophys Res Commun, 2003. **307**(4): p. 891-9.
319. Begley, C.G., et al., *Molecular characterization of NSCL, a gene encoding a helix-loop-helix protein expressed in the developing nervous system*. Proc Natl Acad Sci U S A, 1992. **89**(1): p. 38-42.

320. Schaffar, G., et al., *LIM-only protein 4 interacts directly with the repulsive guidance molecule A receptor Neogenin*. J Neurochem, 2008. **107**(2): p. 418-31.
321. Novotny-Diermayr, V., et al., *Modulation of the interleukin-6 receptor subunit glycoprotein 130 complex and its signaling by LMO4 interaction*. J Biol Chem, 2005. **280**(13): p. 12747-57.
322. Michell, A.C., et al., *A novel role for transcription factor Lmo4 in thymus development through genetic interaction with Cited2*. Dev Dyn, 2010. **239**(7): p. 1988-94.
323. Singh, R.R., et al., *Negative regulation of estrogen receptor alpha transactivation functions by LIM domain only 4 protein*. Cancer Res, 2005. **65**(22): p. 10594-601.
324. Gomez-Smith, M., et al., *LIM domain only 4 protein promotes granulocyte colony-stimulating factor-induced signaling in neurons*. Cell Mol Life Sci, 2010. **67**(6): p. 949-57.
325. Huang, Z., et al., *Transcription factor Lmo4 defines the shape of functional areas in developing cortices and regulates sensorimotor control*. Dev Biol, 2009. **327**(1): p. 132-42.
326. Asprer, J.S., et al., *LMO4 functions as a co-activator of neurogenin 2 in the developing cortex*. Development, 2011. **138**(13): p. 2823-32.
327. Bertrand, N., D.S. Castro, and F. Guillemot, *Proneural genes and the specification of neural cell types*. Nat Rev Neurosci, 2002. **3**(7): p. 517-30.
328. Ross, S.E., M.E. Greenberg, and C.D. Stiles, *Basic helix-loop-helix factors in cortical development*. Neuron, 2003. **39**(1): p. 13-25.
329. Heng, J.I., et al., *Neurogenin 2 controls cortical neuron migration through regulation of Rnd2*. Nature, 2008. **455**(7209): p. 114-8.
330. Qin, Z., et al., *LIM domain only 4 (LMO4) regulates calcium-induced calcium release and synaptic plasticity in the hippocampus*. J Neurosci, 2012. **32**(12): p. 4271-83.
331. Zaman, T., et al., *LMO4 is essential for paraventricular hypothalamic neuronal activity and calcium channel expression to prevent hyperphagia*. J Neurosci, 2014. **34**(1): p. 140-8.
332. Iwasato, T., et al., *NMDA receptor-dependent refinement of somatotopic maps*. Neuron, 1997. **19**(6): p. 1201-10.
333. Azim, E., et al., *Lmo4 and Clim1 progressively delineate cortical projection neuron subtypes during development*. Cereb Cortex, 2009. **19 Suppl 1**: p. i62-9.
334. Naka, H., et al., *Requirement for COUP-TFI and II in the temporal specification of neural stem cells in CNS development*. Nat Neurosci, 2008. **11**(9): p. 1014-23.
335. Meloche, S. and J. Pouyssegur, *The ERK1/2 mitogen-activated protein kinase pathway as a master regulator of the G1- to S-phase transition*. Oncogene, 2007. **26**(22): p. 3227-39.
336. Megason, S.G. and A.P. McMahon, *A mitogen gradient of dorsal midline Wnts organizes growth in the CNS*. Development, 2002. **129**(9): p. 2087-98.
337. Dehay, C. and H. Kennedy, *Cell-cycle control and cortical development*. Nat Rev Neurosci, 2007. **8**(6): p. 438-50.

338. Armentano, M., et al., *COUP-TFI is required for the formation of commissural projections in the forebrain by regulating axonal growth*. Development, 2006. **133**(21): p. 4151-62.
339. Molnar, Z., et al., *Comparative aspects of cerebral cortical development*. Eur J Neurosci, 2006. **23**(4): p. 921-34.
340. Nakamura, K., et al., *In vivo function of Rnd2 in the development of neocortical pyramidal neurons*. Neurosci Res, 2006. **54**(2): p. 149-53.
341. Alfano, C., et al., *COUP-TFI promotes radial migration and proper morphology of callosal projection neurons by repressing Rnd2 expression*. Development, 2011. **138**(21): p. 4685-97.
342. Liu, Q., N.D. Dwyer, and D.D. O'Leary, *Differential expression of COUP-TFI, CHL1, and two novel genes in developing neocortex identified by differential display PCR*. J Neurosci, 2000. **20**(20): p. 7682-90.
343. Tripodi, M., et al., *The COUP-TF nuclear receptors regulate cell migration in the mammalian basal forebrain*. Development, 2004. **131**(24): p. 6119-29.
344. Polleux, F., et al., *Pre- and post-mitotic events contribute to the progressive acquisition of area-specific connectional fate in the neocortex*. Cereb Cortex, 2001. **11**(11): p. 1027-39.
345. Feng, G., et al., *Imaging neuronal subsets in transgenic mice expressing multiple spectral variants of GFP*. Neuron, 2000. **28**(1): p. 41-51.
346. Saito, T. and N. Nakatsuji, *Efficient gene transfer into the embryonic mouse brain using in vivo electroporation*. Dev Biol, 2001. **240**(1): p. 237-46.
347. Hattox, A.M. and S.B. Nelson, *Layer V neurons in mouse cortex projecting to different targets have distinct physiological properties*. J Neurophysiol, 2007. **98**(6): p. 3330-40.
348. Yoneshima, H., et al., *Er81 is expressed in a subpopulation of layer 5 neurons in rodent and primate neocortices*. Neuroscience, 2006. **137**(2): p. 401-12.
349. Conte, W.L., H. Kamishina, and R.L. Reep, *Multiple neuroanatomical tract-tracing using fluorescent Alexa Fluor conjugates of cholera toxin subunit B in rats*. Nat Protoc, 2009. **4**(8): p. 1157-66.
350. Dugas, J.C., et al., *A novel purification method for CNS projection neurons leads to the identification of brain vascular cells as a source of trophic support for corticospinal motor neurons*. J Neurosci, 2008. **28**(33): p. 8294-305.
351. Deschenes, M., A. Labelle, and P. Landry, *Morphological characterization of slow and fast pyramidal tract cells in the cat*. Brain Res, 1979. **178**(2-3): p. 251-74.
352. Spain, W.J., P.C. Schwindt, and W.E. Crill, *Post-inhibitory excitation and inhibition in layer V pyramidal neurones from cat sensorimotor cortex*. J Physiol, 1991. **434**: p. 609-26.
353. Porrero, C., et al., *Mapping of fluorescent protein-expressing neurons and axon pathways in adult and developing Thy1-eYFP-H transgenic mice*. Brain Res, 2010. **1345**: p. 59-72.
354. Binley, K.E., et al., *Sholl analysis: a quantitative comparison of semi-automated methods*. J Neurosci Methods, 2014. **225**: p. 65-70.
355. Lickiss, T., et al., *Examining the relationship between early axon growth and transcription factor expression in the developing cerebral cortex*. J Anat, 2012. **220**(3): p. 201-11.

356. Deck, M., et al., *Pathfinding of corticothalamic axons relies on a rendezvous with thalamic projections*. *Neuron*, 2013. **77**(3): p. 472-84.
357. Bovetti, S., et al., *COUP-TFI controls activity-dependent tyrosine hydroxylase expression in adult dopaminergic olfactory bulb interneurons*. *Development*, 2013. **140**(24): p. 4850-9.
358. Seuntjens, E., et al., *Sip1 regulates sequential fate decisions by feedback signaling from postmitotic neurons to progenitors*. *Nat Neurosci*, 2009. **12**(11): p. 1373-80.
359. Connors, B.W., M.J. Gutnick, and D.A. Prince, *Electrophysiological properties of neocortical neurons in vitro*. *J Neurophysiol*, 1982. **48**(6): p. 1302-20.
360. McCormick, D.A., et al., *Comparative electrophysiology of pyramidal and sparsely spiny stellate neurons of the neocortex*. *J Neurophysiol*, 1985. **54**(4): p. 782-806.
361. Agmon, A. and B.W. Connors, *Correlation between intrinsic firing patterns and thalamocortical synaptic responses of neurons in mouse barrel cortex*. *J Neurosci*, 1992. **12**(1): p. 319-29.
362. Gottlieb, J.P. and A. Keller, *Intrinsic circuitry and physiological properties of pyramidal neurons in rat barrel cortex*. *Exp Brain Res*, 1997. **115**(1): p. 47-60.
363. Kang, Y. and F. Kayano, *Electrophysiological and morphological characteristics of layer VI pyramidal cells in the cat motor cortex*. *J Neurophysiol*, 1994. **72**(2): p. 578-91.
364. Tsiola, A., et al., *Quantitative morphologic classification of layer 5 neurons from mouse primary visual cortex*. *J Comp Neurol*, 2003. **461**(4): p. 415-28.
365. Tseng, G.F. and D.A. Prince, *Heterogeneity of rat corticospinal neurons*. *J Comp Neurol*, 1993. **335**(1): p. 92-108.
366. Rumberger, A., et al., *Correlation of electrophysiology, morphology, and functions in corticotectal and corticopretectal projection neurons in rat visual cortex*. *Exp Brain Res*, 1998. **119**(3): p. 375-90.
367. Wang, Z. and D.A. McCormick, *Control of firing mode of corticotectal and corticopontine layer V burst-generating neurons by norepinephrine, acetylcholine, and 1S,3R-ACPD*. *J Neurosci*, 1993. **13**(5): p. 2199-216.
368. Kisvarday, Z.F., et al., *Synaptic targets of HRP-filled layer III pyramidal cells in the cat striate cortex*. *Exp Brain Res*, 1986. **64**(3): p. 541-52.
369. Douglas, R.J., et al., *Recurrent excitation in neocortical circuits*. *Science*, 1995. **269**(5226): p. 981-5.
370. Schwindt, P.C. and W.E. Crill, *Factors influencing motoneuron rhythmic firing: results from a voltage-clamp study*. *J Neurophysiol*, 1982. **48**(4): p. 875-90.
371. Schwindt, P.C., et al., *Multiple potassium conductances and their functions in neurons from cat sensorimotor cortex in vitro*. *J Neurophysiol*, 1988. **59**(2): p. 424-49.
372. Chagnac-Amitai, Y., H.J. Luhmann, and D.A. Prince, *Burst generating and regular spiking layer 5 pyramidal neurons of rat neocortex have different morphological features*. *J Comp Neurol*, 1990. **296**(4): p. 598-613.
373. Golowasch, J., et al., *Membrane capacitance measurements revisited: dependence of capacitance value on measurement method in nonisopotential neurons*. *J Neurophysiol*, 2009. **102**(4): p. 2161-75.